Hard x-ray and standing-wave excitation as probes of bulk properties and buried layers and interfaces: applications to spintronic systems and strongly correlated oxides

Chuck Fadley
Dept. of Physics, UC Davis
and
Materials Sciences Division
Lawrence Berkeley National Laboratory

Supported by:
DOE: LBNL Materials Sciences Division
ARO-MURI: “Emergent Phenomena at Mott Interfaces”
Jülich Research Center

Seminar at the University of Rome Three
June 30, 2011

Hard x-ray and standing-wave excitation as probes of bulk properties and buried layers and interfaces: applications to spintronic systems and strongly correlated oxides

The Advanced Light Source

Experiments **Sample synthesis** **Theory/Modeling**

A.Gray[1,2], C. Papp[1,2,*], B. Balke[1,2,+], A. Kaiser[1,2,], S. Ueda[3,4], Y. Yamashita[3,4], K. Kobayashi[3,4], M. Gorgoi[5], S.-H. Yang[6], L. Plucinski[7], S. Döring[8], U. Berges[8], M. Huijben[9,10], D. Buergler[7], J. Minar[12], J. Braun[12], H. Ebert[12], E. Rotenberg[11], A. Bostwick[11], B.C. Sell[1,2,#], M. W. West[2], M. Press[2,] F. Salmassi[2], J.B. Kortright[2], E. Gullikson[2], S.S.P. Parkin[6], A. Gloskovskii[13], W. Drube[13], F. Kronast[5], C. Westphal[8], C.M. Schneider[7], R. Ramesh[2,9], J. Son[14], S. Stemmer[14], A. Janotti[14,], C. Van der Welle[14,] and C.S. Fadley[1,2]

----

[1]Physics, UC Davis; [2]Mat. Sci. Div., LBNL; [3]SPring8; [4]NIMS; [5]HZB-BESSY Berlin; [6]IBM Almaden; [7]Research Center Jűlich; [8]Physics, Tech. Univ. Dortmund; Physics; [9]Mat. Sci., UC Berkeley; [10]Univ. of Twente; [11]ALS, LBNL; [12]Physical Chem., Univ. Munich; [13] Hasylab, Hamburg; [14]UC Santa Barbara; Present addresses: [*]Univ. Erlangen, [+]Univ. Mainz; [#]Otterbein Coll.

Julich Research Center

Emergent Phenomena at Mott Interfaces - Multidisciplinary University Research Initiative

Outline

Photoemission: Some limitations, some new directions

6-8 keV

Hard x-ray photoemission of interesting bulk materials→core and valence spectra:
half-metallic/colossal magnetoresistive $La_{0.67}Sr_{0.33}MnO_3$
semiconducting CrAl alloy
metal-to-insulator transition in thin-film $LaNiO_3$

3.2 & 6 keV

Angle-resolved hard x-ray photoemission→HXPD: Kikuchi-band modeling, and HARPES for: W, GaAs & the magnetic semiconductor (Ga,Mn)As

833 & 6 keV

Standing-wave photoemission combining soft and hard x-rays, depth-resolved composition, densities of states and ARPES, and magnetization:
$SrTiO_3/La_{2/3}Sr_{1/3}MnO_3$ multilayer
Fe/MgO tunnel junction

500-700 eV

Standing-waves in a photoelectron microscope, adding the third dimension:
multilayers and microdots

Conclusions and Future Outlook

Outline

Photoemission: Some limitations, some new directions

6-8 keV

Hard x-ray photoemission of interesting bulk materials→core and valence spectra:
half-metallic/colossal magnetoresistive $La_{0.67}Sr_{0.33}MnO_3$
semiconducting CrAl alloy
metal-to-insulator transition in thin-film $LaNiO_3$

3.2 & 6 keV

Angle-resolved hard x-ray photoemission→HXPD: Kikuchi-band modeling, and HARPES for: W, GaAs & the magnetic semiconductor (Ga,Mn)As

833 & 6 keV

Standing-wave photoemission combining soft and hard x-rays, depth-resolved composition, densities of states and ARPES, and magnetization:
$SrTiO_3/La_{2/3}Sr_{1/3}MnO_3$ multilayer
Fe/MgO tunnel junction

500-700 eV

Standing-waves in a photoelectron microscope, adding the third dimension:
multilayers and microdots

Conclusions and Future Outlook

Photoemission: Some limitations, some new directions

Core photoemission→XPS, X-ray photoelectron diffraction-XPD,…
Valence photoemission→UPS, SXPS
Higher energy a/o temperature→Densities of states-DOSs
Lower energy a/o temperature→Band mapping, Angle-resolved photoemission-ARPES
are very powerful techniques, but they:

- **are sometimes too strongly influenced by surface effects, if bulk or buried layer/interface properties are to be studied**

- **may not be able to selectively and quantitatively see buried-layer and interface properties**

Two ways to address these limitations:

- **use harder x-ray excitation (HAXPES, HXPS) for deeper probing: core (HXPD) and valence DOSs or hard x-ray ARPES ("HARPES")**

- **use soft and hard x-ray standing waves to selectively look below the surface, including depth-resolved ARPES**

X-ray photoemission: some key elements

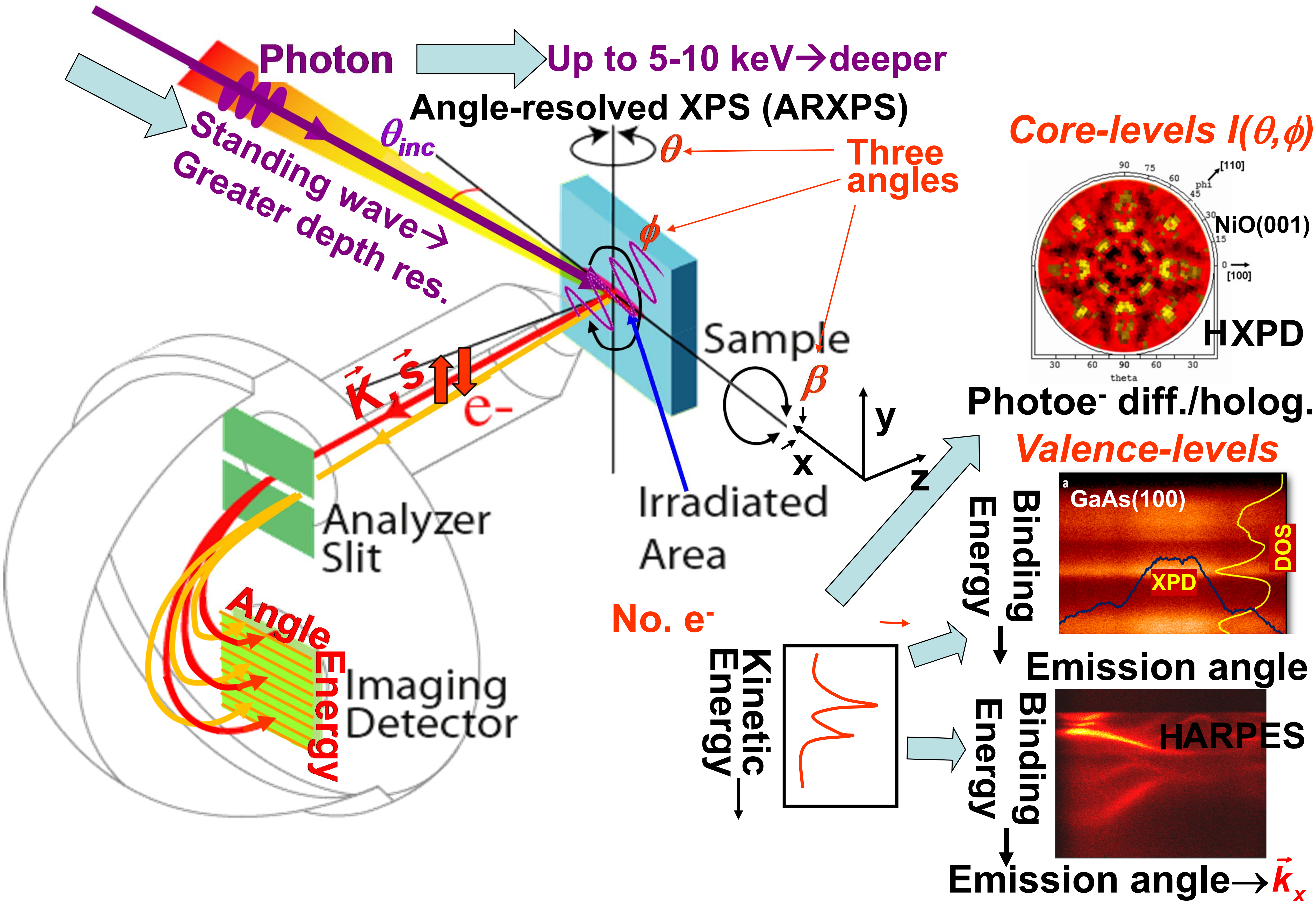

Why do we want to go to 5-10 keV in XPS?

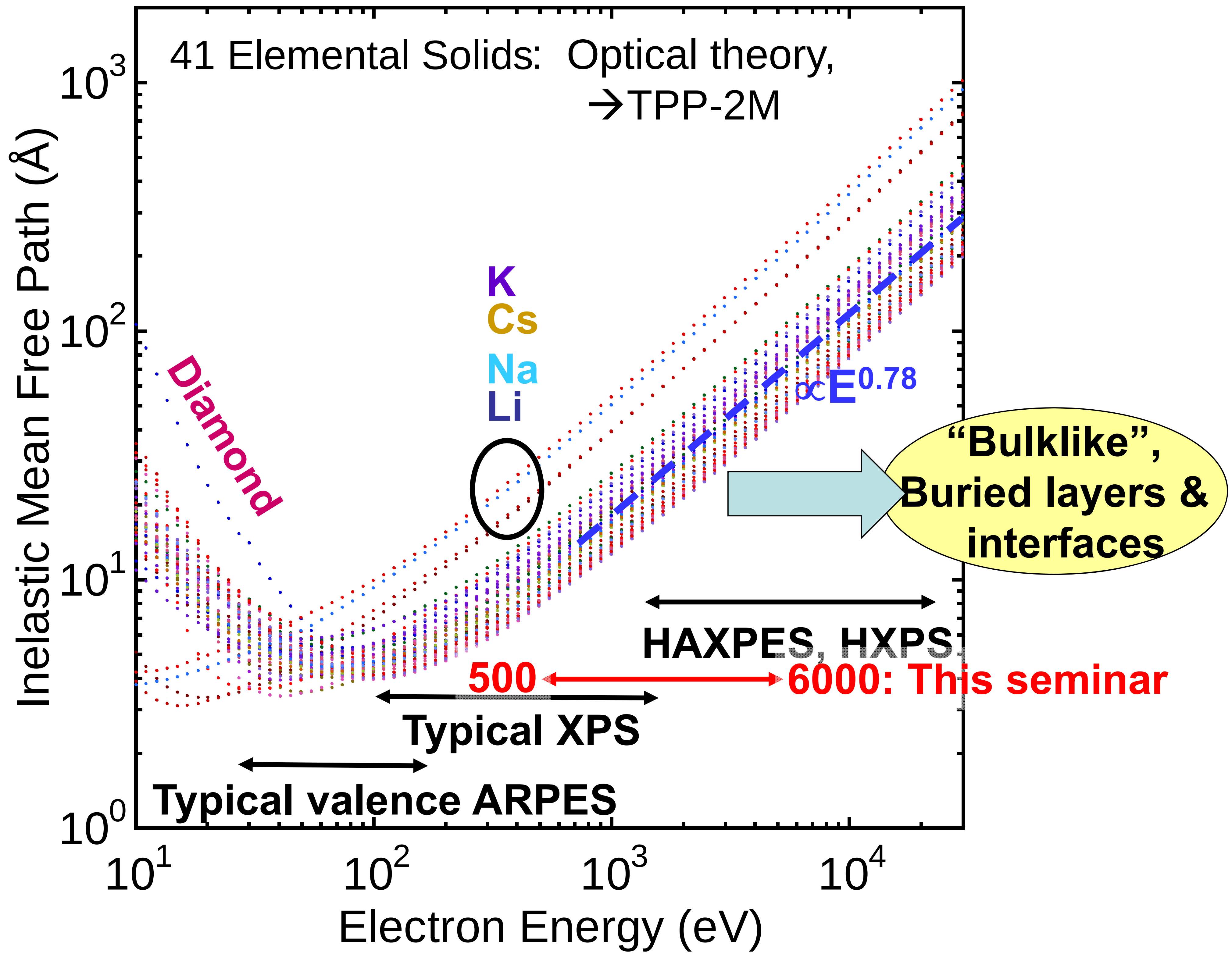

Tanuma, Powell, Penn, Surf. and Interf. Anal. 43, 689 (2011)

Hard x-ray photoemission—plusses and minusses

•**Plusses**

•More bulk sensitive spectra → a versatile tool for any new material or multilayer nanostructure

•Inelastic background less important & Augers more widely spread, less overlap

•Less radiation damage

•Easier interpretation of angle-resolved data → surface and bulk information

•Easier quantitative analysis via core spectra

•New "bulk fingerprint" satellite effects seen in both core and valence spectra

•Magnetic circular and linear dichroism and spin-resolved spectra for magnetic systems

•Bulk DOS info. at highest energies and temperatures

or

•3d "bulk" band mapping ARPES capability with cryocooling

• Hard x-ray photoelectron diffraction promising: dopants, lattice distortions

•Strong reflectivity and standing wave effects for depth-resolved properties

•Higher pressures possible in ambient pressure experiments, even windowed cell

Minusses

•Cross sections low, need special undulatorbeamline/spectrometer combinations—several solutions→ 1 micron focus and 10 meV resolution

•Intensity calculations must allow for photon wave vector, other non-dipole effects, but easy

•High *n,* low-ℓ cross section components strongly favored, but in VB they can be more involved in transport

•Resolution not as good as VUV PS, but as good/better than SX PS, and down to 50 meV overall, even lower, good enough for many applications

•Phonon effects reduce capability for ARPES at higher energies/temperatures

•Recoil energy limits resolution, esp. for lighter elements; complex systematics, depending on local bond distances/phonon frequencies→Doppler spectroscopy?

Photoemission: Some limitations, some new directions

Core photoemission→XPS, X-ray photoelectron diffraction-XPD,…
Valence photoemission→UPS, SXPS
Higher energy a/o temperature→Densities of states-DOSs
Lower energy a/o temperature→Band mapping, Angle-resolved photoemission-ARPES
are very powerful techniques, but they:

- **are sometimes too strongly influenced by surface effects, if bulk or buried layer/interface properties are to be studied**

- **may not be able to selectively and quantitatively see buried-layer and interface properties**

Two ways to address these limitations:

- **use harder x-ray excitation (HAXPES, HXPS) for deeper probing: core (HXPD) and valence DOSs or hard x-ray ARPES ("HARPES")**

- **use soft and hard x-ray standing waves to selectively look below the surface, including depth-resolved ARPES**

Standing wave formation in reflection from a surface, or single-crystal Bragg planes, or a multilayer mirror

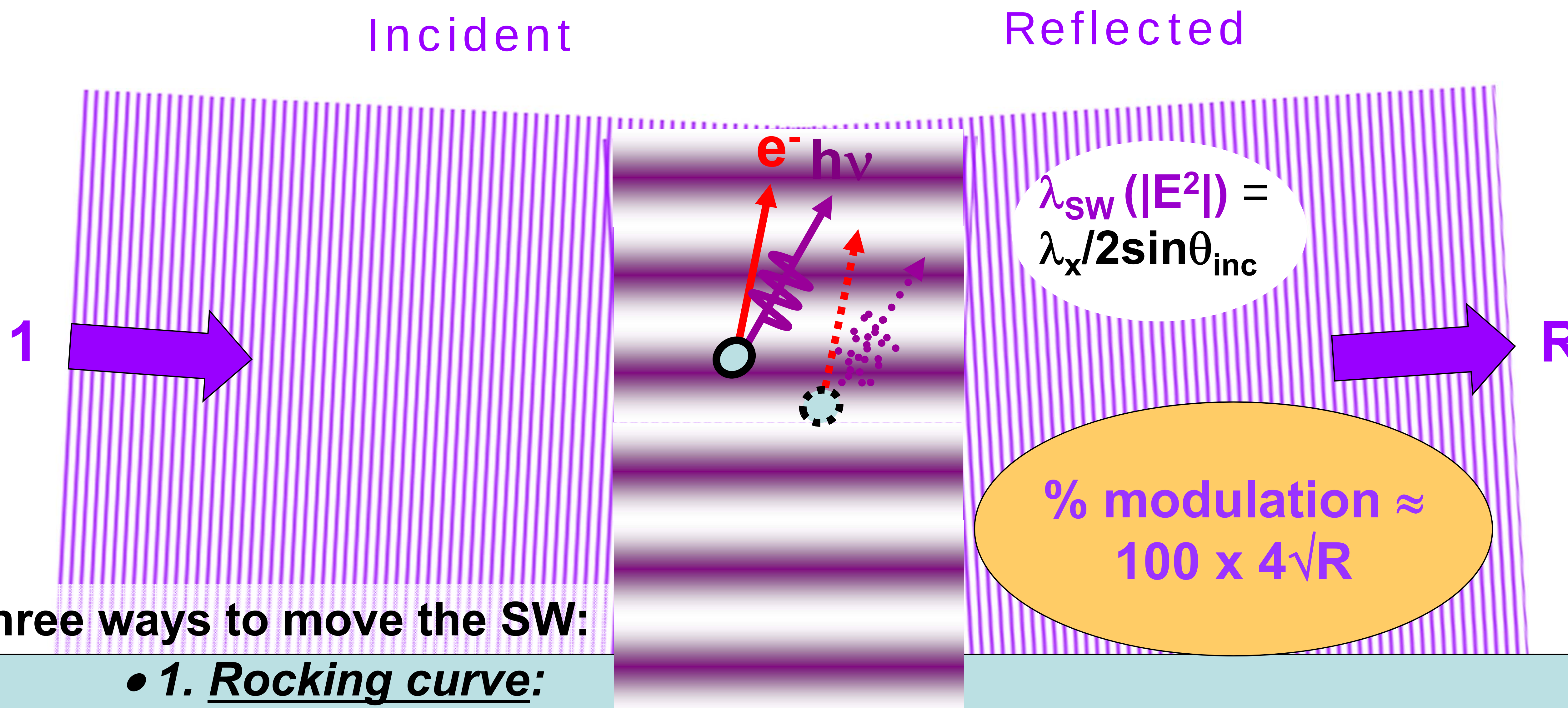

Three ways to move the SW:

- ***1. Rocking curve:***

$$I(\theta_{inc}) \propto 1 + R(\theta_{inc}) + 2\sqrt{R(\theta_{inc})}\, f \cos[\varphi(\theta_{inc}) - 2\pi P]$$

- ***2. Photon energy scan:***

$$I(h\nu) \propto 1 + R(h\nu) + 2\sqrt{R(h\nu)}\, f \cos[\varphi(h\nu) - 2\pi P]$$

with: f = coherent fraction of atoms, P = phase of coherent-atom/layer position

- ***3. Phase scan with wedge-shaped sample ("Swedge" method):***

C.S.F., Journal of Electron Spectroscopy and Related Phenomena 178–179 (2010) 2–32

Outline

Photoemission: Some limitations, some new directions

6-8 keV

Hard x-ray photoemission of interesting bulk materials→core and valence spectra:

half-metallic/colossal magnetoresistive $La_{0.67}Sr_{0.33}MnO_3$

semiconducting CrAl alloy

metal-to-insulator transition in thin-film $LaNiO_3$

3.2 & 6 keV

Angle-resolved hard x-ray photoemission→HXPD: Kikuchi-band modeling, and HARPES for: W, GaAs & the magnetic semiconductor (Ga,Mn)As

833 & 6 keV

Standing-wave photoemission combining soft and hard x-rays, depth-resolved composition, densities of states and ARPES, and magnetization:

$SrTiO_3/La_{2/3}Sr_{1/3}MnO_3$ multilayer

Fe/MgO tunnel junction

500-700 eV

Standing-waves in a photoelectron microscope, adding the third dimension:

multilayers and microdots

Conclusions and Future Outlook

X-ray photoemission: some key elements

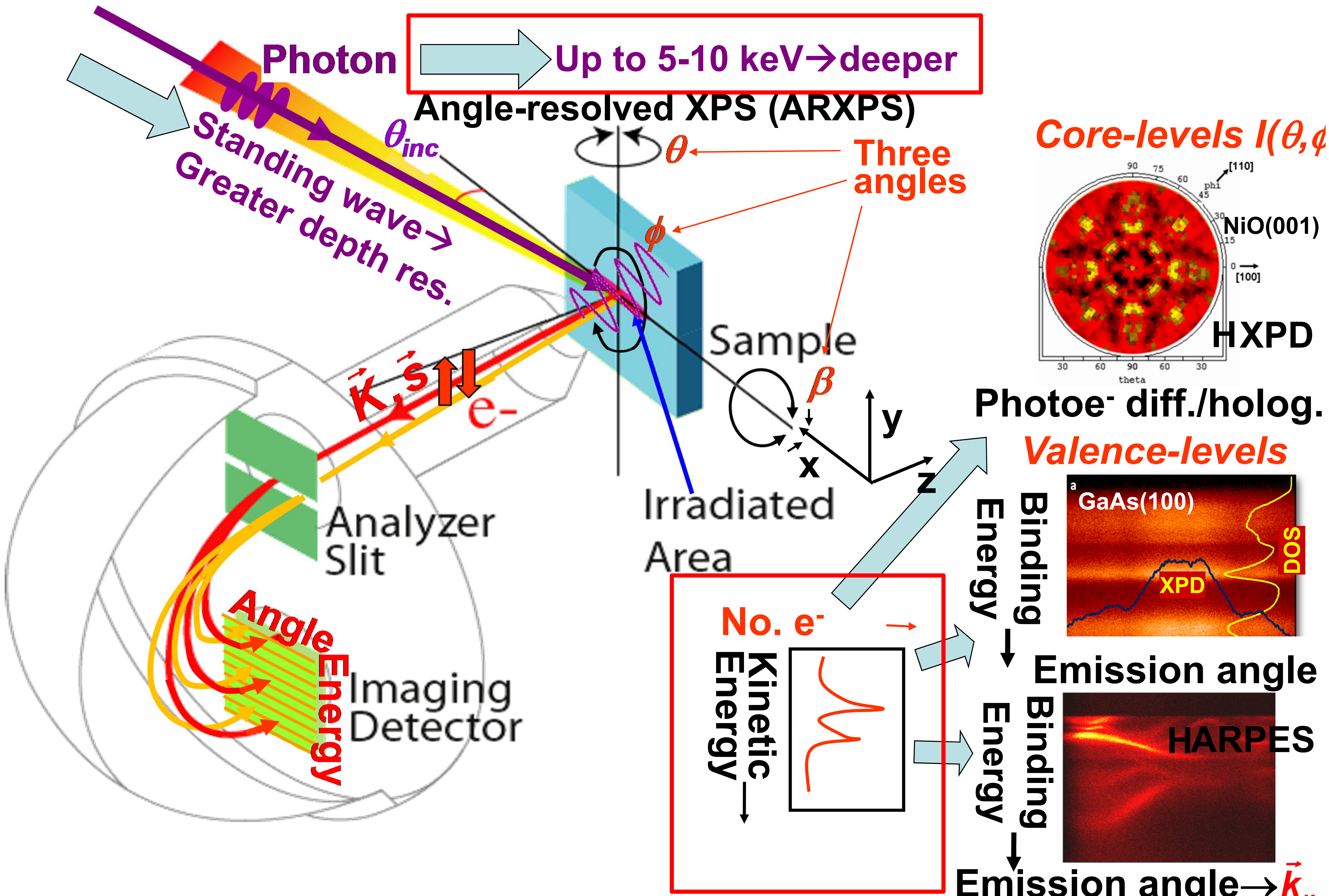

Hard x-ray photoemission--Quantitative analysis of peak intensities using theoretical cross sections: $La_{0.7}Sr_{0.3}MnO_3$, $h\nu$ = 7700 eV

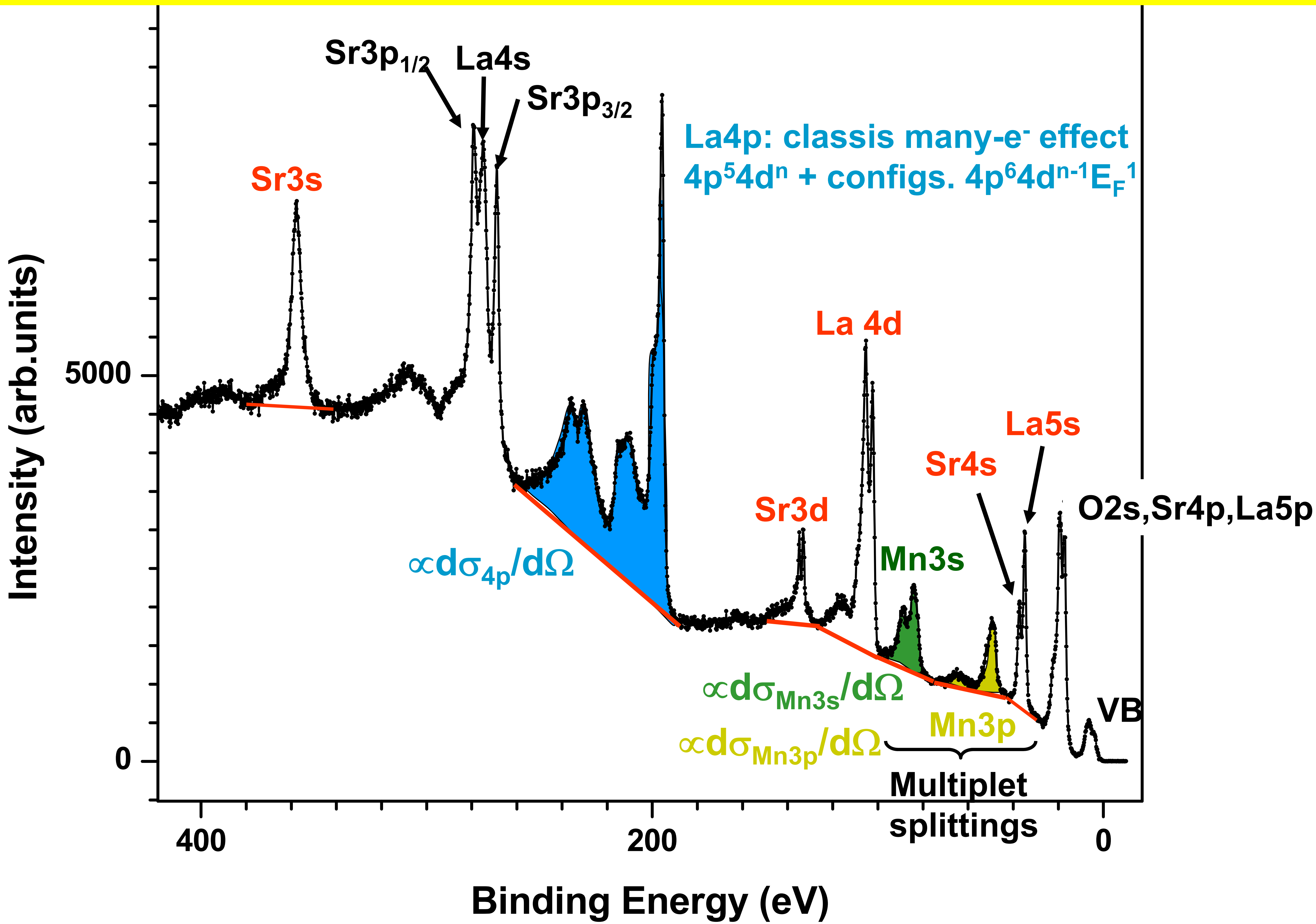

Offi et al., PRB 77, 174422 ('08)-ESRF

Quantitative analysis of peak intensities using theoretical cross sections (Scofield): $La_{0.7}Sr_{0.3}MnO_3$, hν = 7700 eV

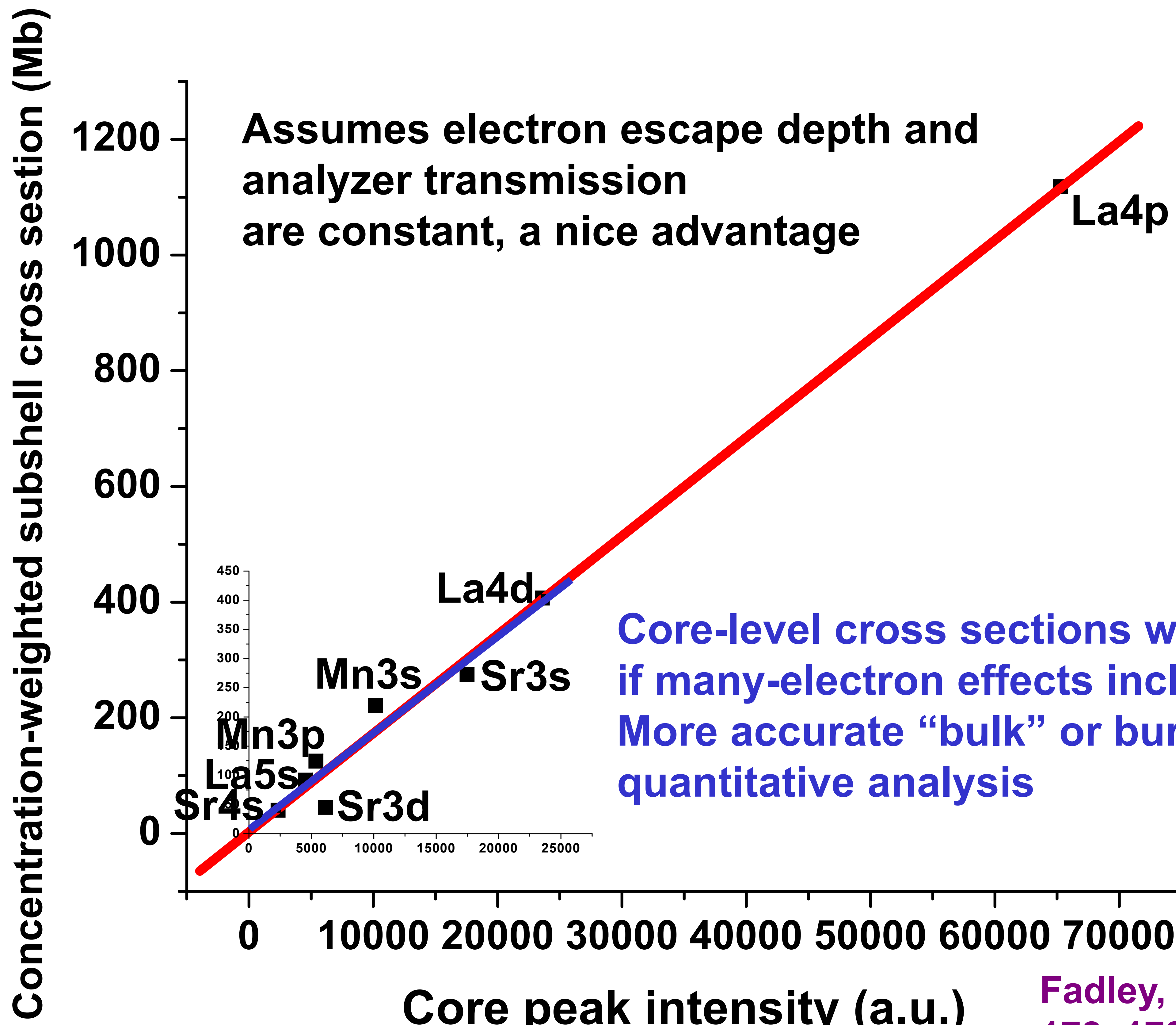

Core-level cross sections work very well, if many-electron effects included→ More accurate "bulk" or buried layer quantitative analysis

Fadley, J. Electr. Spect. 178–179 (2010) 2–32

Mn magnetic moment change: bulk or surface effect?
Compare soft and hard x-ray data
Temperature dependence of Mn2p spectra: $La_{0.7}Sr_{0.3}MnO_3$

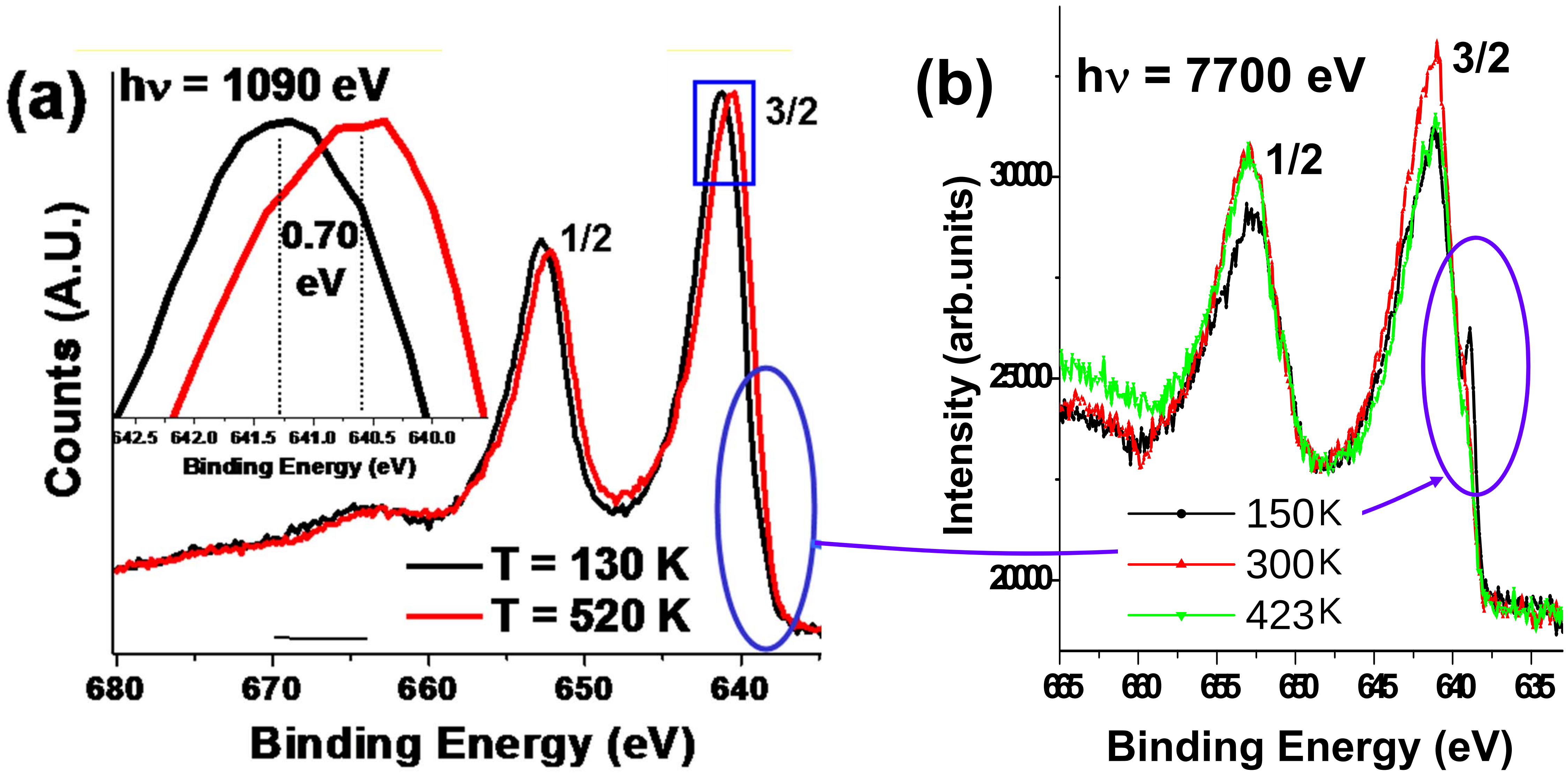

Mean depth: ~1 nm

Mean depth: ~8 nm

→Suggests bulk electronic structure not reached until ca. 8 nm depth

Offi et al., PRB 77, 174422 ('08))-ESRF

Electronic Structure of Strained Manganite Thin Films with Room Temperature Ferromagnetism Investigated by Hard X-ray Photoemission Spectroscopy: $La_{0.85}Ba_{0.15}MnO_3$

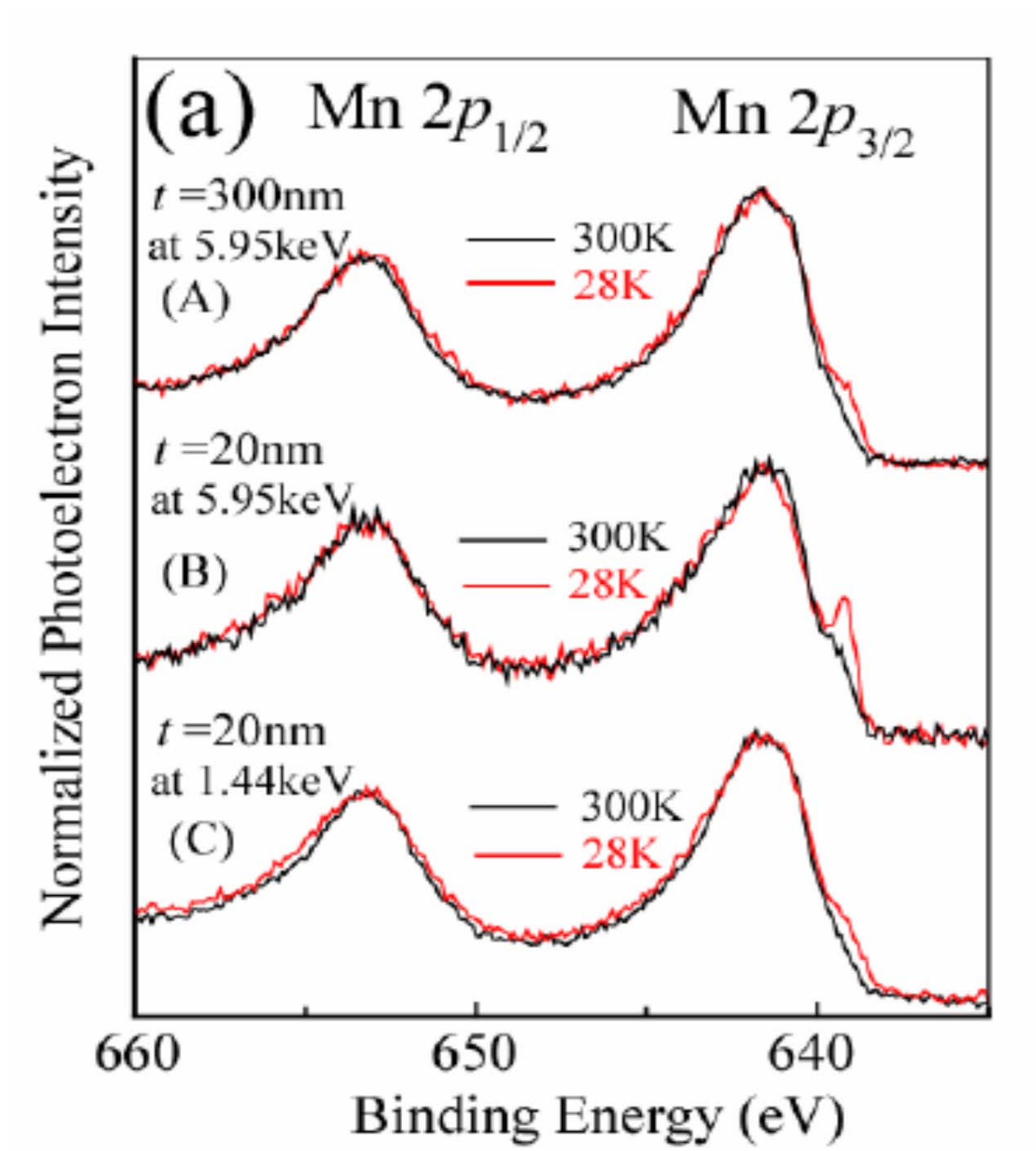

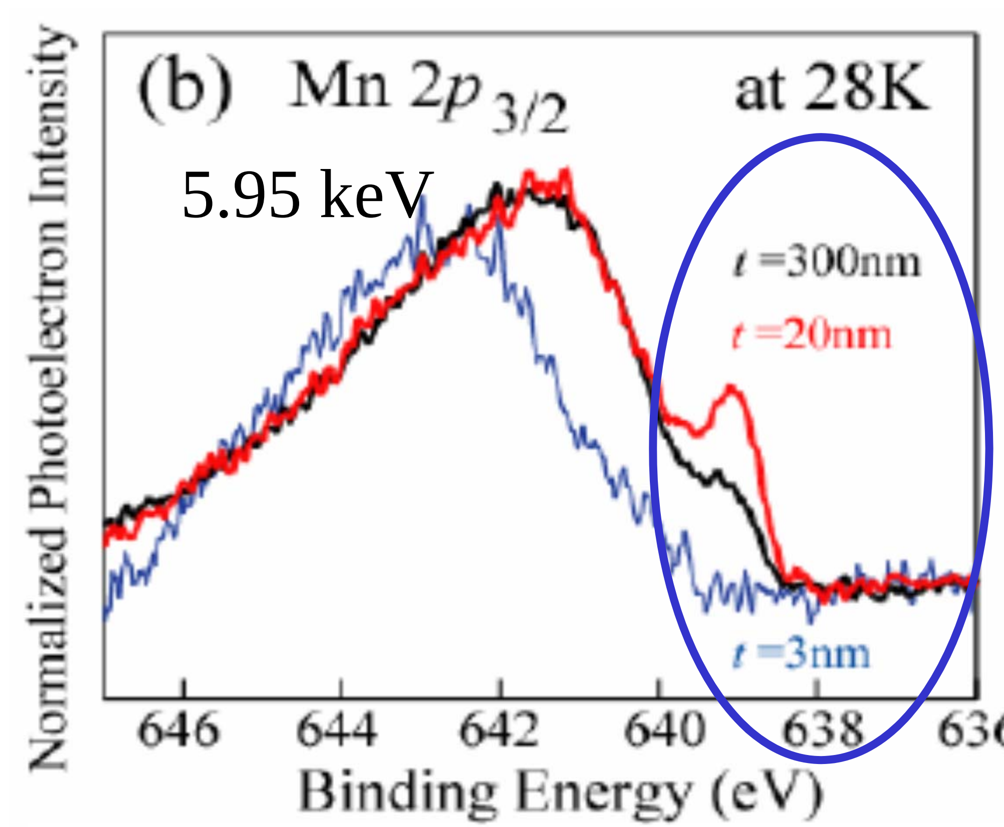

Strain/Magnetism-associated screening feature

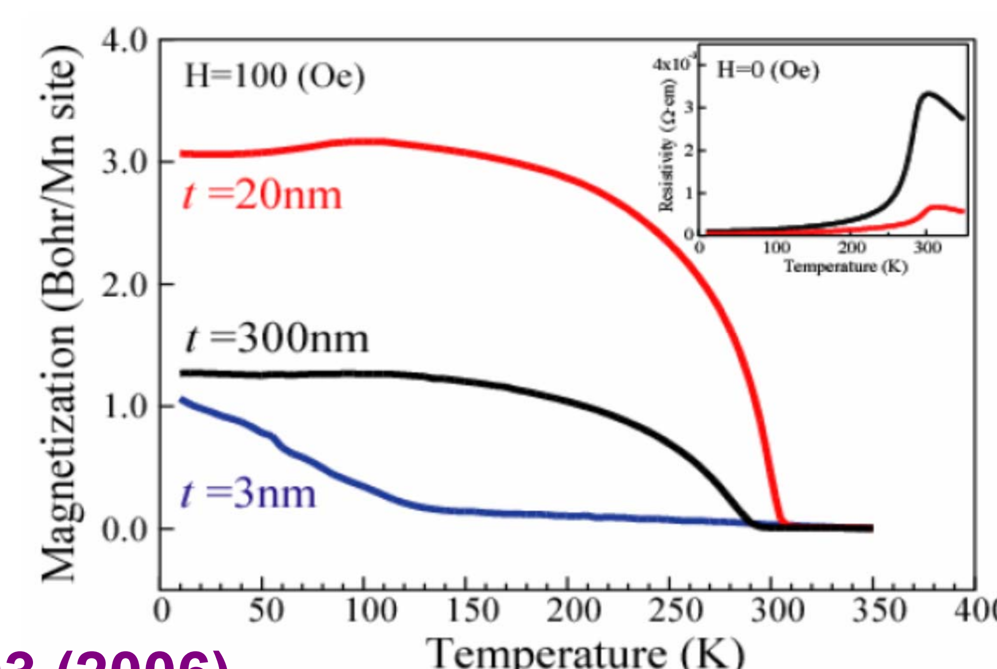

Tanaka et al., Spring8, Phys. Rev. B 73, 094403 (2006)

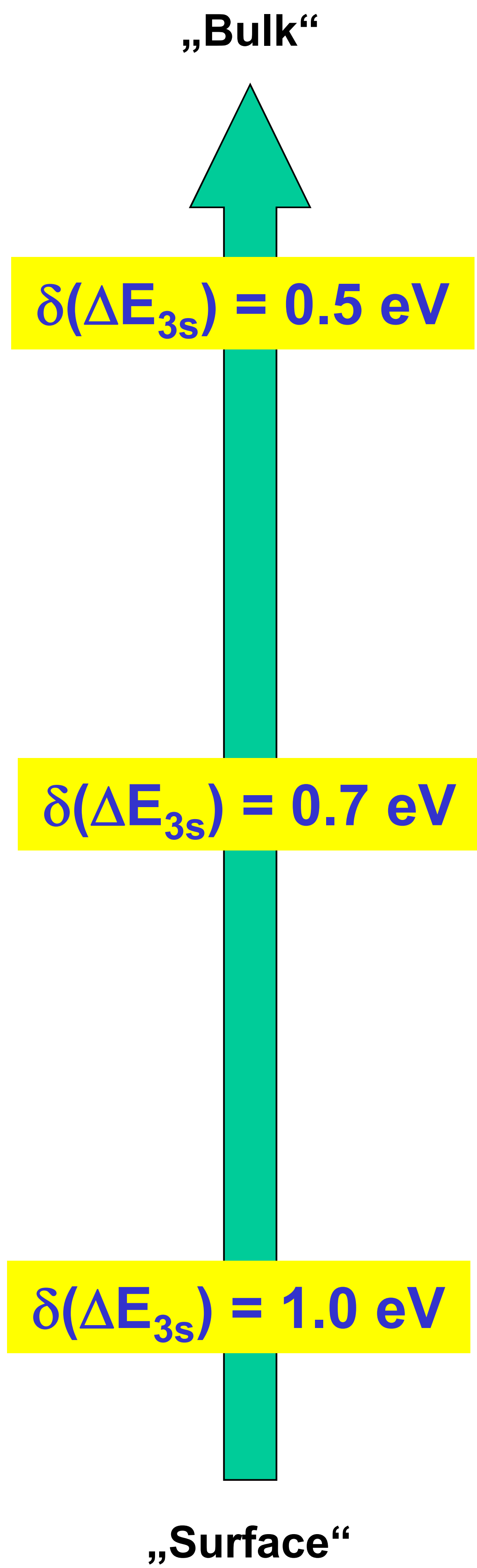

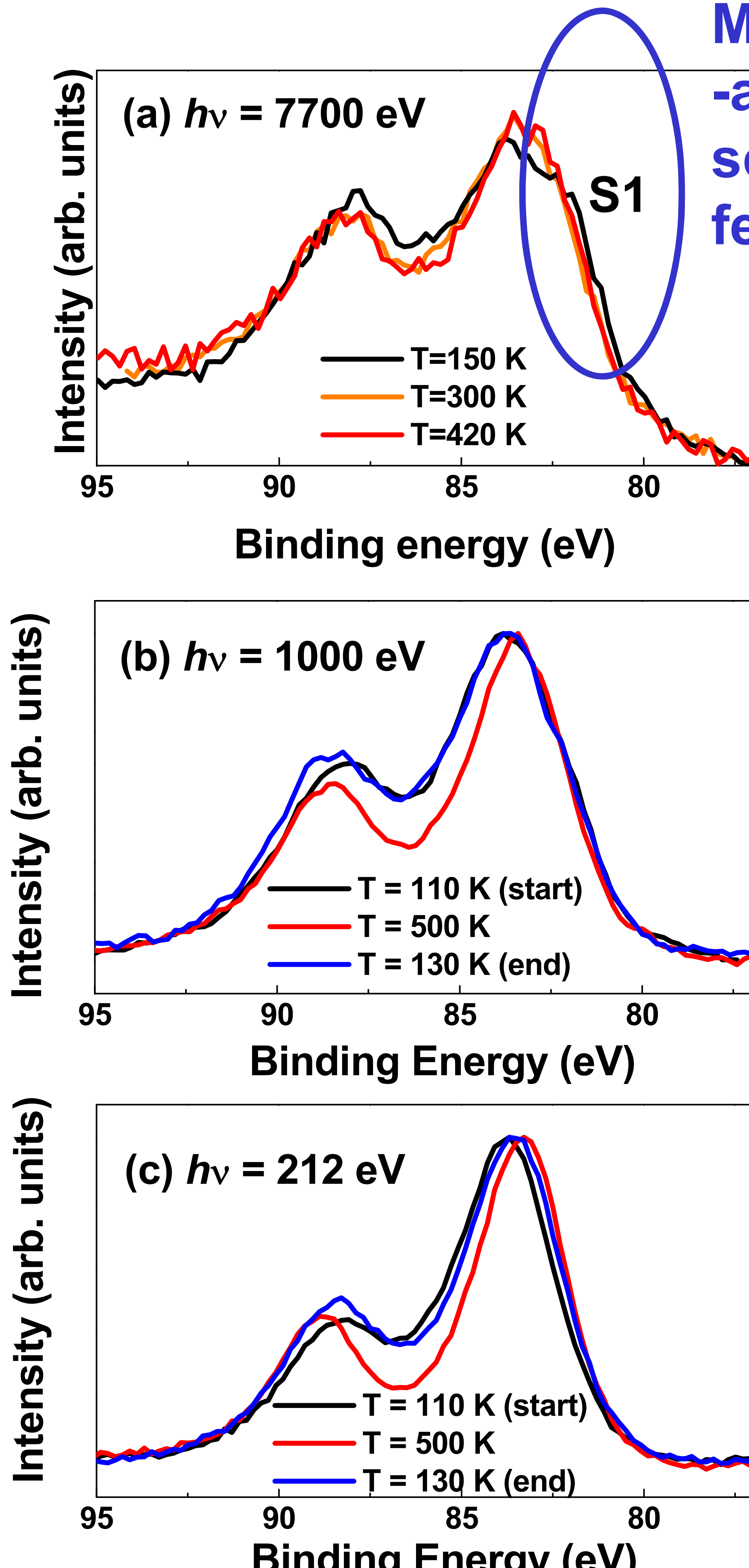

Magnetism -associated screening feature

Change in Mn 3s splitting (magnetic moment) is smaller for higher energy excitation, but still exists:
suggests stronger effect near surface,
but some depth penetration

Offi et al., PRB 77, 174422 (‘08))-ESRF

Presence of "bulk" magnetism-associated screening features on on both Mn 3s and 3p features

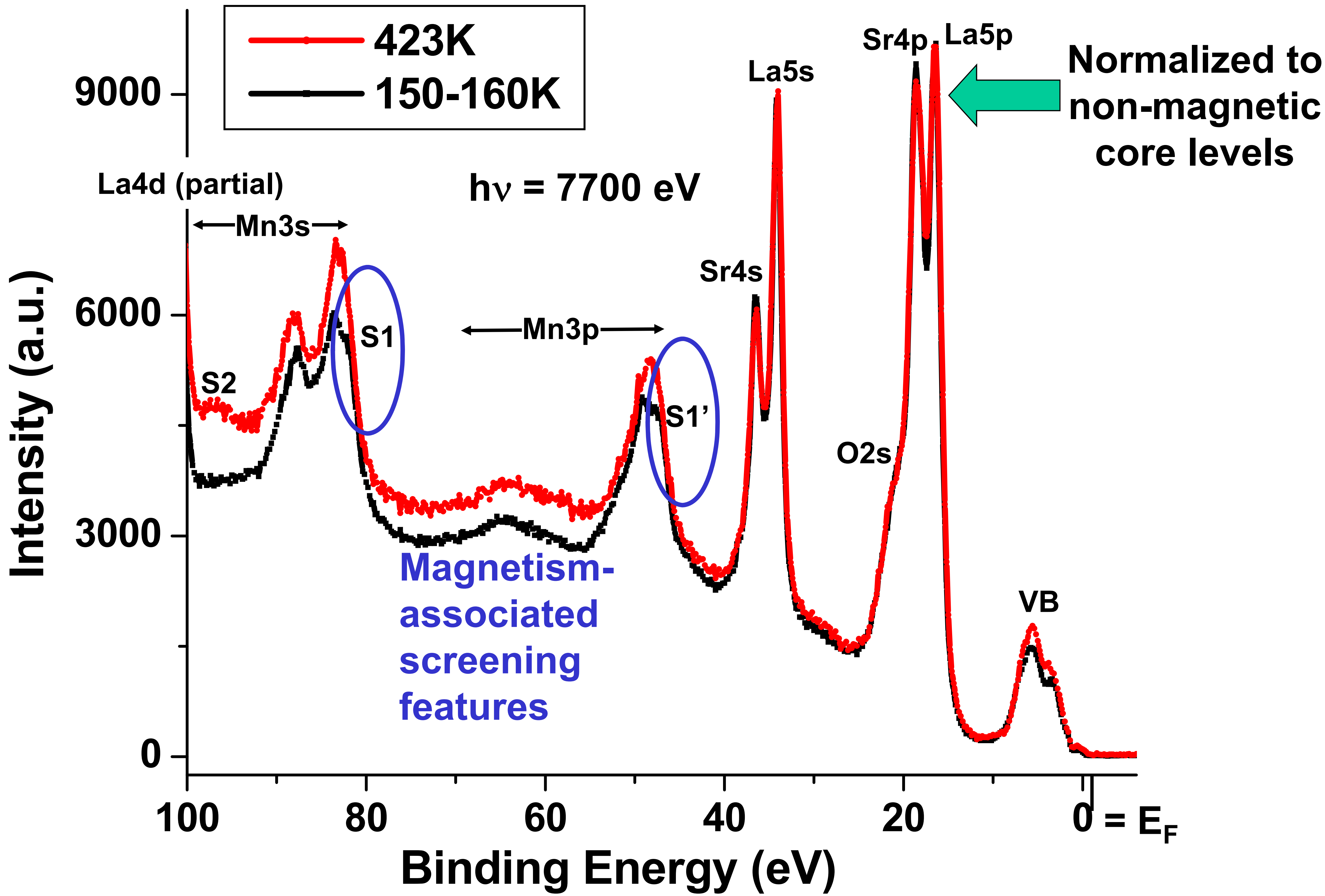

Offi et al., PRB 77, 174422 ('08)-ESRF

Derivation of density-of-states information from core-normalized HXPS valence-band spectra

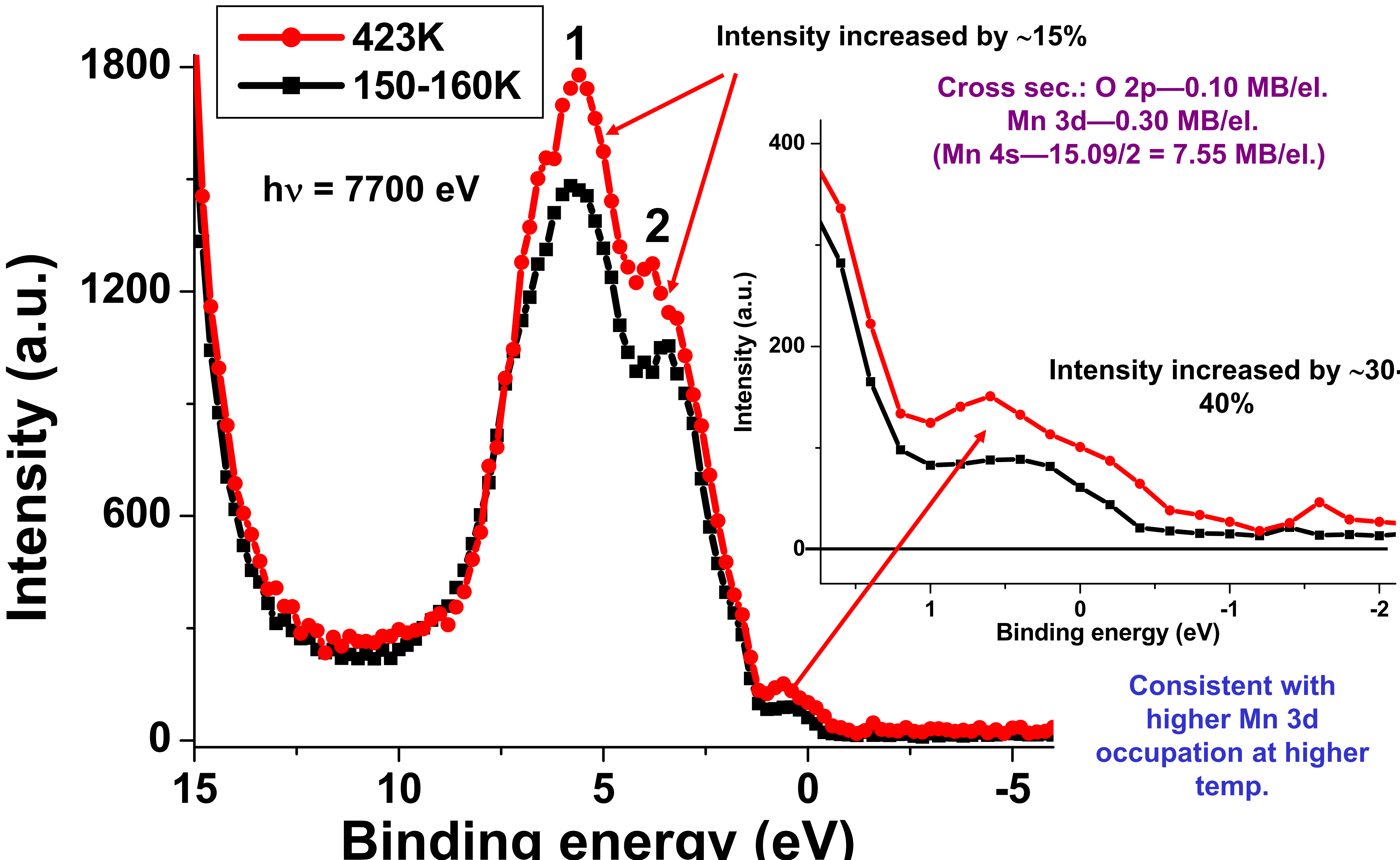

Consistent with higher Mn 3d occupation at higher temp.

Offi et al., PRB 77, 174422 ('08)-ESRF

Outline

Photoemission: Some limitations, some new directions

6-8 keV

Hard x-ray photoemission of interesting bulk materials→core and valence spectra:
half-metallic/colossal magnetoresistive $La_{0.67}Sr_{0.33}MnO_3$
semiconducting CrAl alloy
metal-to-insulator transition in thin-film $LaNiO_3$

3.2 & 6 keV

Angle-resolved hard x-ray photoemission→HXPD: Kikuchi-band modeling, and HARPES for: W, GaAs & the magnetic semiconductor (Ga,Mn)As

833 & 6 keV

Standing-wave photoemission combining soft and hard x-rays, depth-resolved composition, densities of states and ARPES, and magnetization:
$SrTiO_3/La_{2/3}Sr_{1/3}MnO_3$ multilayer
Fe/MgO tunnel junction

500-700 eV

Standing-waves in a photoelectron microscope, adding the third dimension:
multilayers and microdots

Conclusions and Future Outlook

Band Gap and Electronic Structure of an Epitaxial, Semiconducting $Cr_{0.80}Al_{0.20}$ Thin Film

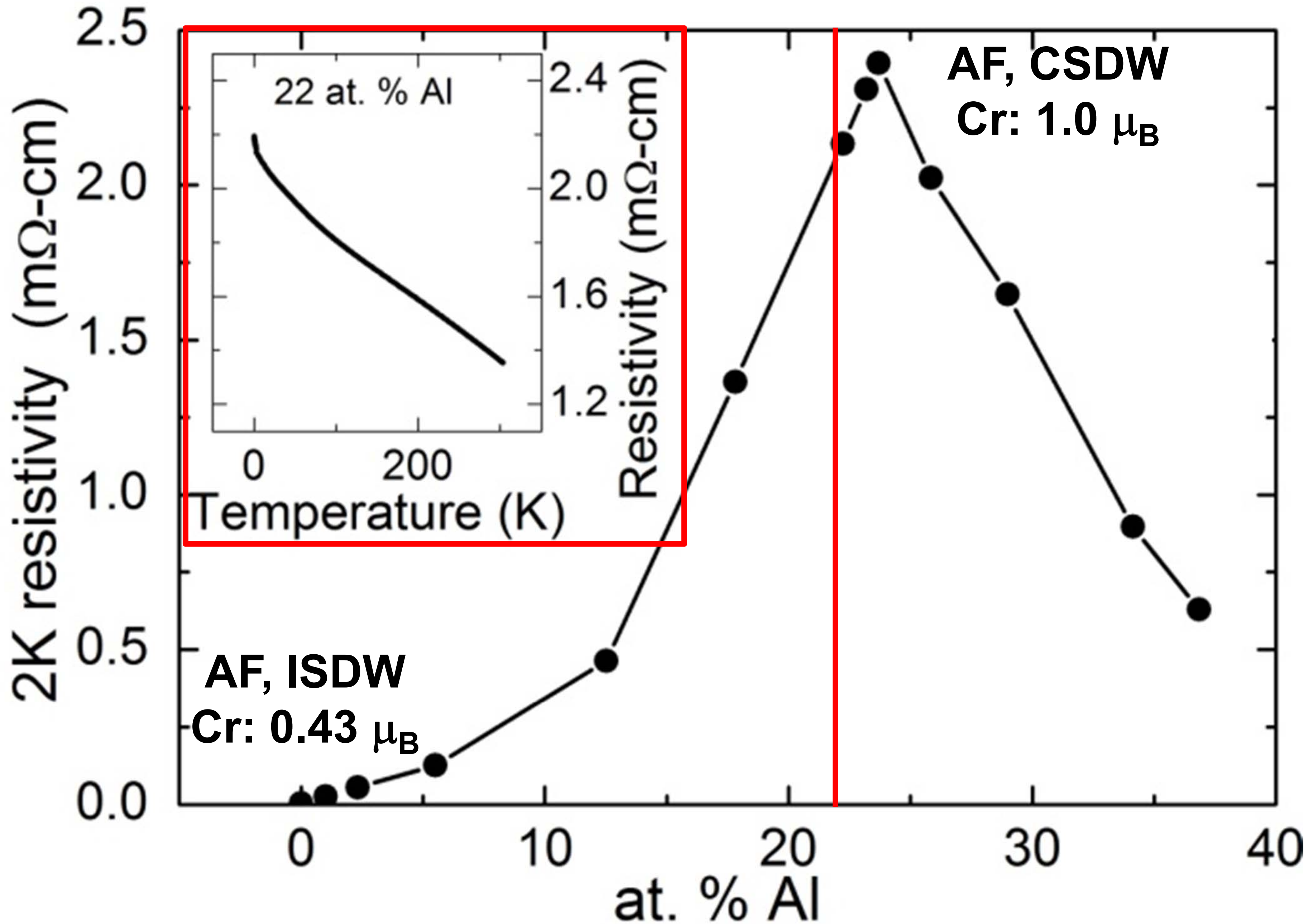

Resistivity of $Cr_{1-x}Al_x$ thin films vs. concentration at 2 K.
Inset: Resistivity of $Cr_{0.78}Al_{0.22}$ vs. temperature.
What happens to the electronic structure?

Boekelheide, Gray, et al., PRL 105, 236404 (2010)-SPring8

Cr and Epitaxial, Semiconducting $Cr_{0.80}Al_{0.20}$ Thin Films: Core and Valence Spectra (DOS limit)

Broad survey

Cr 3s multiplets

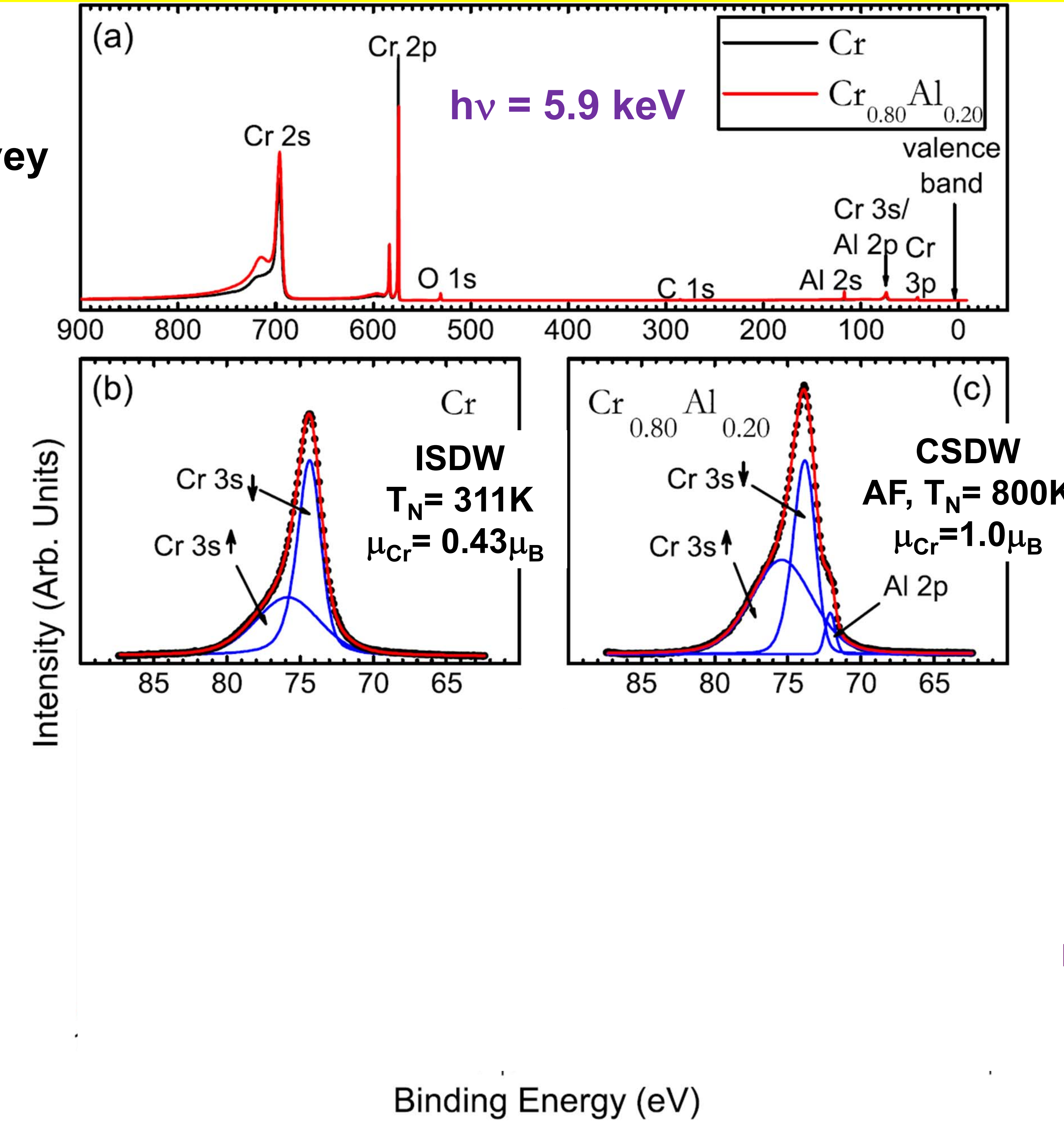

Boekelheide, Gray, et al., PRL 105, 236404 (2010)-SPring8

VALENCE-BAND PHOTOELECTRON INTENSITIES: DOS LIMIT

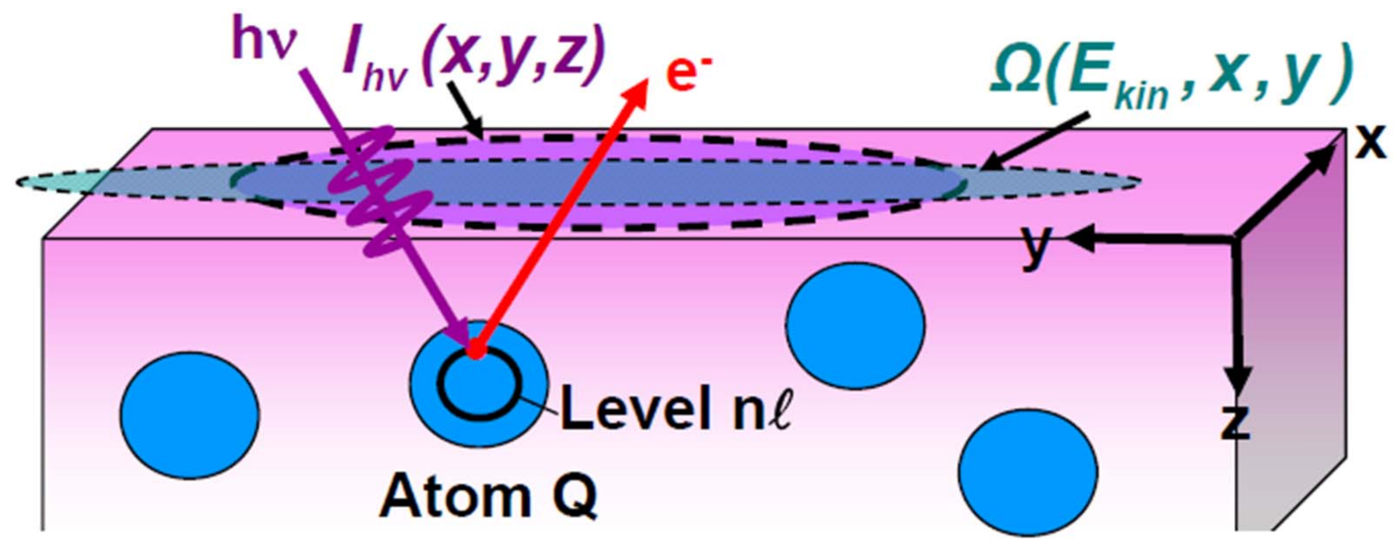

$$I(E_{kin}, Qn\ell) =$$

$$C' \int_0^\infty I_{hv}(x,y,z)\rho_{Qn\ell}(E_b,x,y,z)\frac{d\sigma_{Qn\ell}(hv)}{d\Omega}\exp\left[-\frac{z}{\Lambda_e(E_{kin})\sin\theta}\right]\Omega(E_{kin},x,y)\,dxdydz$$

$I_{hv}(x,y,z)$ = *x-ray flux*

$\rho_{Qn\ell}(E_b,x,y,z)$ = *density of states, projected onto* $Qn\ell$ *character*

$\frac{d\sigma_{Qn\ell}(hv)}{d\Omega}$ = *differential photoelectric cross section for subshell* $Qn\ell$

$\Lambda_e(E_{kin})$ = *energy-dependent inelastic attenuation length*

$\rightarrow$ *Mean Emission Depth*

$\Omega(E_{kin}, x, y)$ = *energy-dependent spectrometer acceptance solid angle*

Cr and Epitaxial, Semiconducting $Cr_{0.80}Al_{0.20}$ Thin Films: Core and Valence Spectra (DOS limit)

Broad survey

Cr 3s multiplets

Valence Spectra: Expt. and Cross-Section Weighted LDA theory

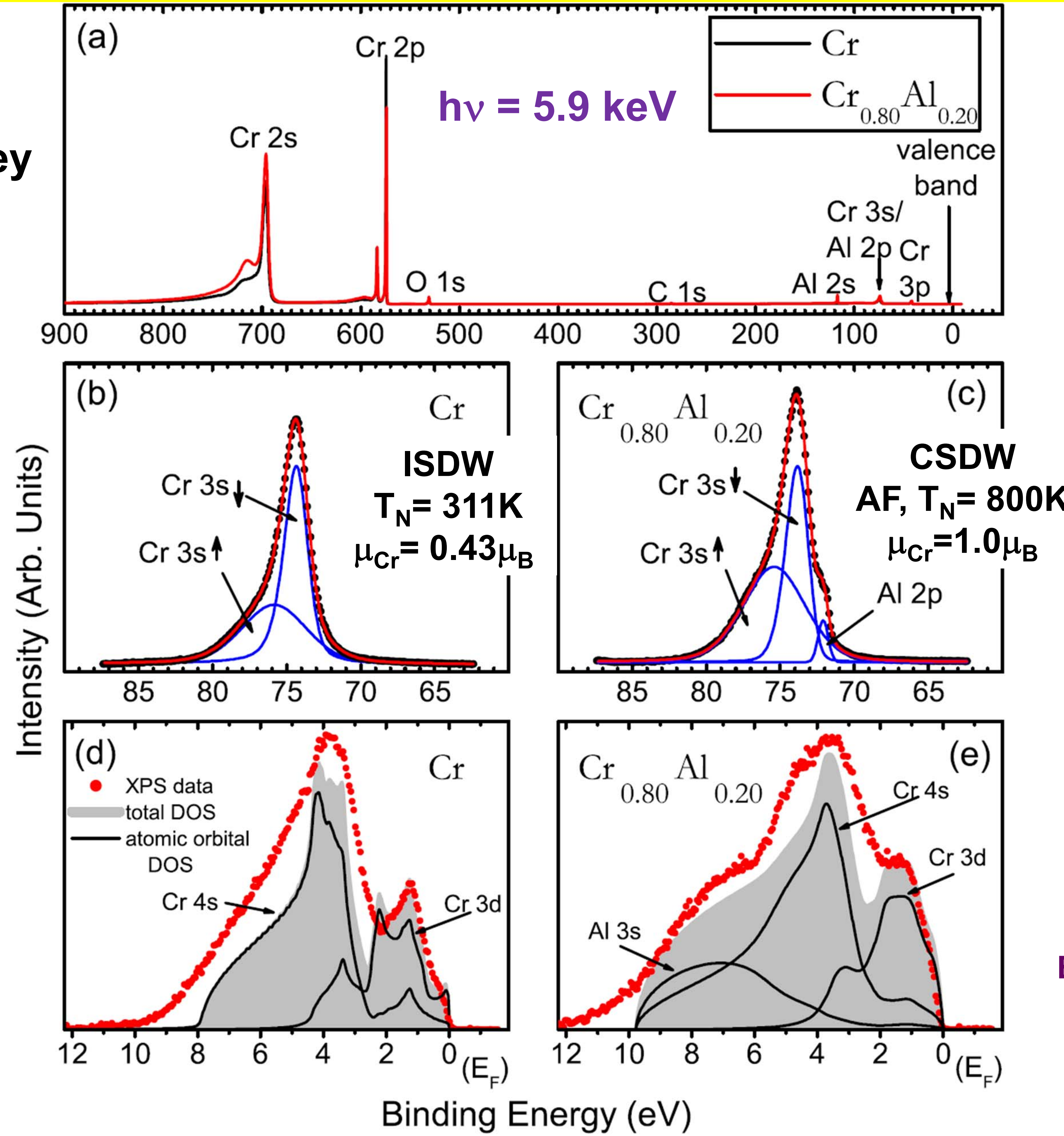

Boekelheide, Gray, et al., PRL 105, 236404 (2010)-SPring8

Cr and Epitaxial, Semiconducting $Cr_{0.80}Al_{0.20}$ Thin Films: Valence Spectra (DOS limit), compared to Au standard

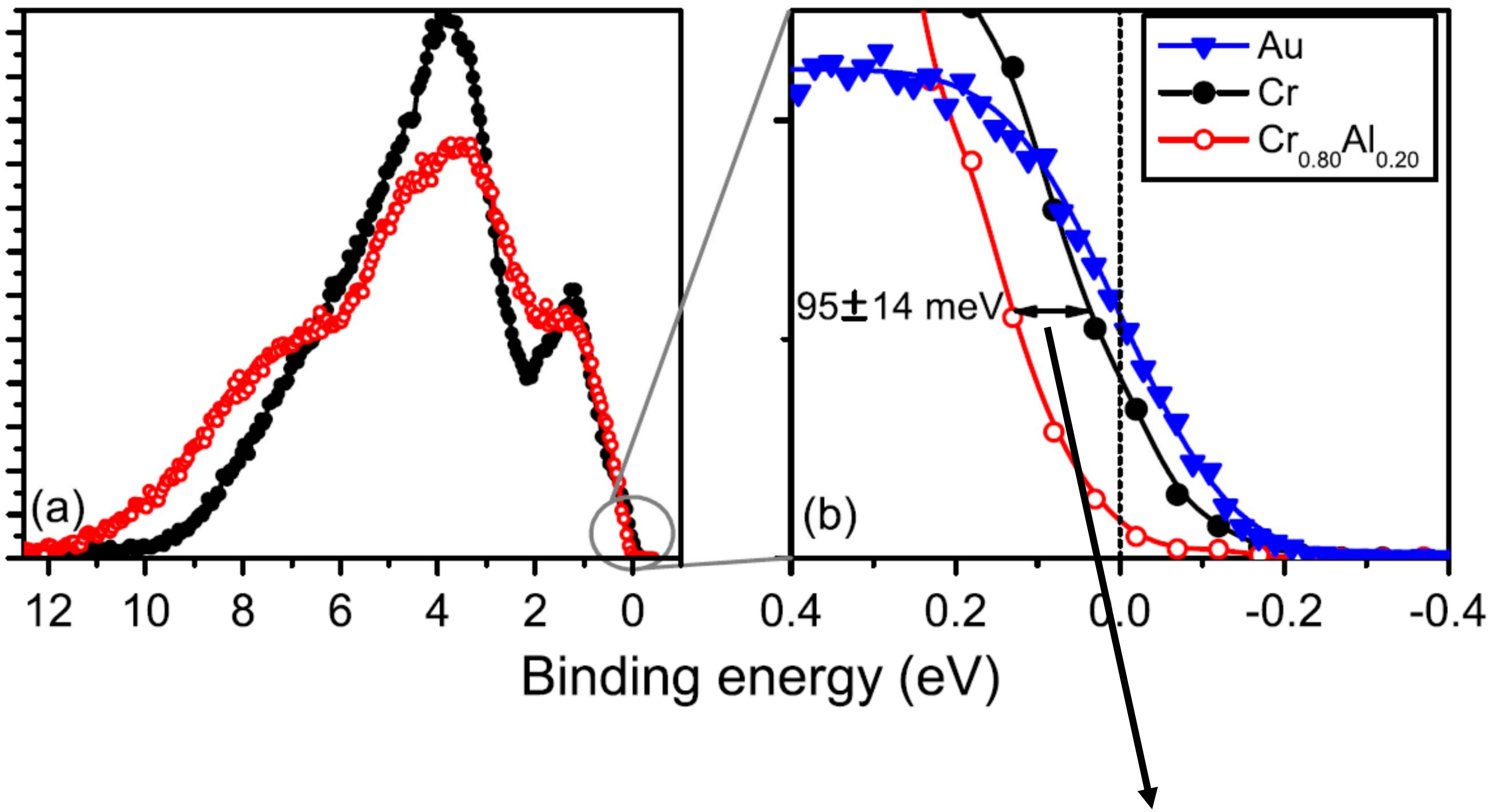

Opening of semiconducting gap

Boekelheide, Gray, et al., PRL 105, 236404 (2010)-SPring8

Cr and Epitaxial, Semiconducting $Cr_{0.80}Al_{0.20}$ Thin Films: LDA theory, with CPA approximation

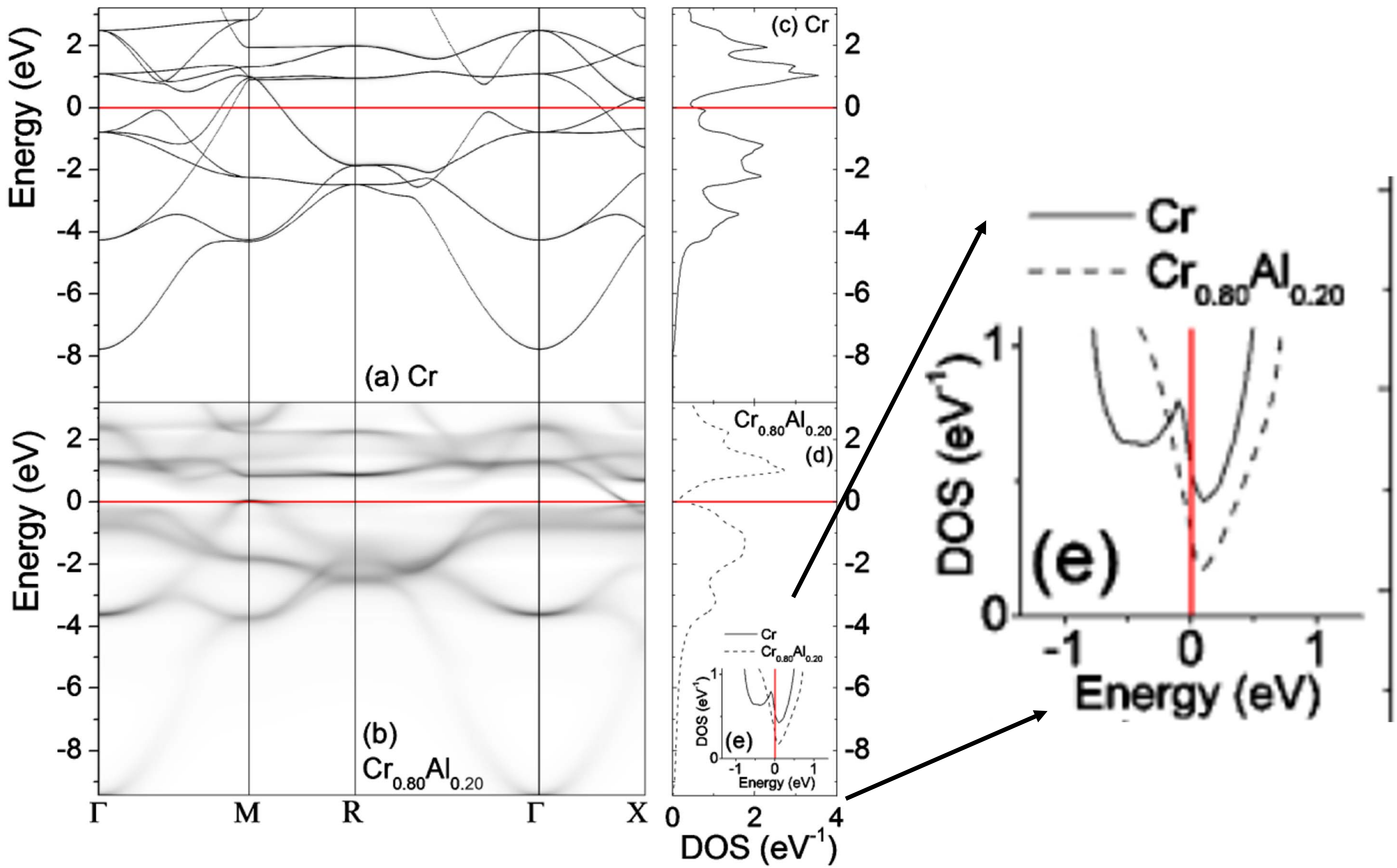

Boekelheide, Gray, et al., PRL 105, 236404 (2010)—Theory, D. Stewart, Cornell

Outline

Photoemission: Some limitations, some new directions

6-8 keV

Hard x-ray photoemission of interesting bulk materials→core and valence spectra:
half-metallic/colossal magnetoresistive $La_{0.67}Sr_{0.33}MnO_3$
semiconducting CrAl alloy
metal-to-insulator transition in thin-film $LaNiO_3$

3.2 & 6 keV

Angle-resolved hard x-ray photoemission→HXPD: Kikuchi-band modeling, and HARPES for: W, GaAs & the magnetic semiconductor (Ga,Mn)As

833 & 6 keV

Standing-wave photoemission combining soft and hard x-rays, depth-resolved composition, densities of states and ARPES, and magnetization:
$SrTiO_3/La_{2/3}Sr_{1/3}MnO_3$ multilayer
Fe/MgO tunnel junction

500-700 eV

Standing-waves in a photoelectron microscope, adding the third dimension:
multilayers and microdots

Conclusions and Future Outlook

$LaNiO_3$ Thin films: Insulator-to-Metal Transition Induced by Strain

Epitaxial layers with TEM thickness det'n.
(Junwoo Son, James LeBeau)

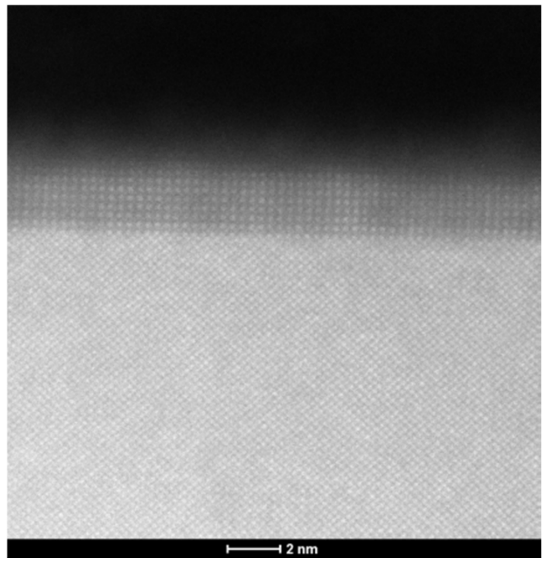

LNO/LSAT
~ 7 unit cells = 2.7 nm

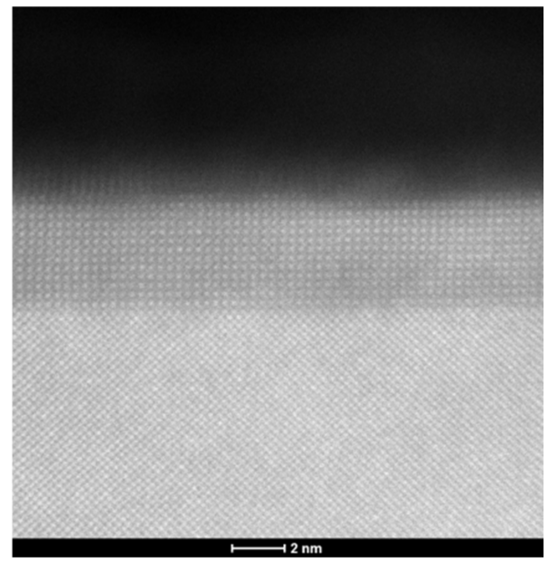

LNO/LSAT
~ 12 unit cells = 4.6 nm

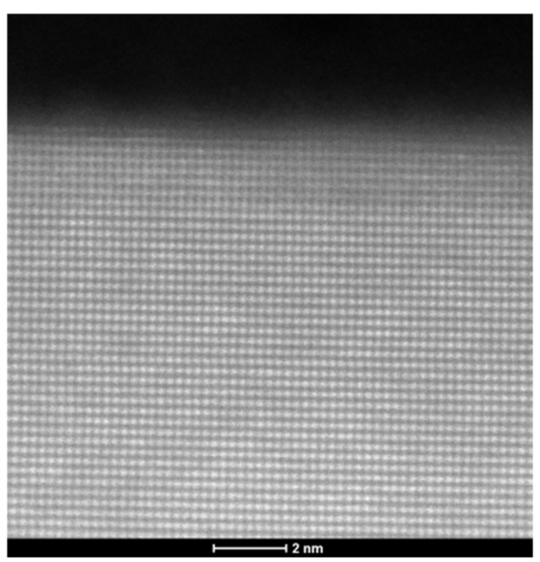

LNO/LAO
~ 7 unit cells = 2.8 nm

Eight samples

LNO/LAO Thickness (nm)	LNO/LSAT Thickness (nm)
2.8	2.7
4.2	4.6
11.1	10.7
17.6	16.0

Conductivity (Stemmer, Allen et al.)

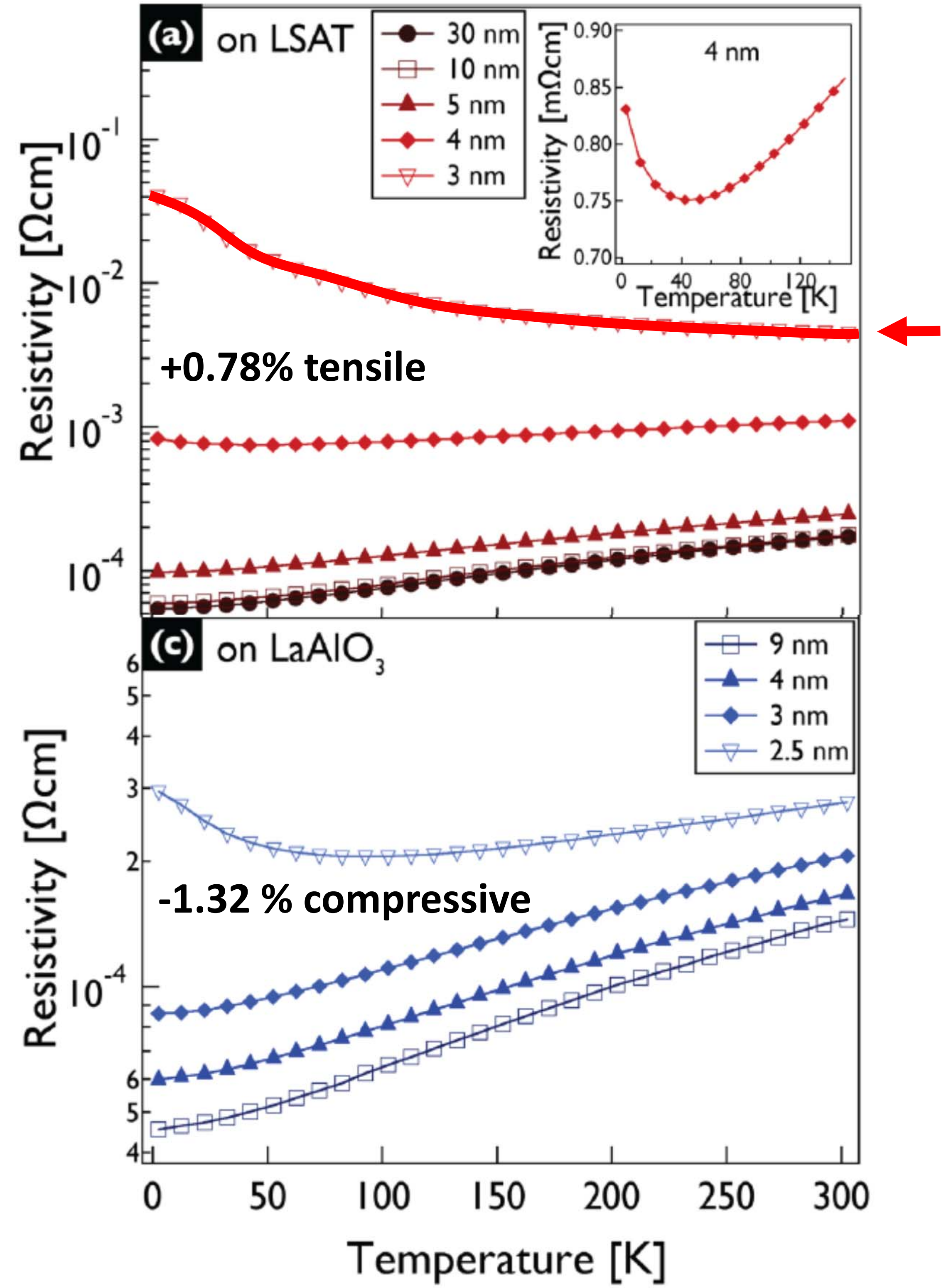

Gray, Janotti, et al., Phys. Rev. B, to appear-SPring8

Son et al., Appl. Phys. Lett. 96, 062114 (2010); 97, 202109 2010

LNO: Prior soft x-ray photoemission→ What's expected with soft→hard x-rays?

Photon energy of 800 eV

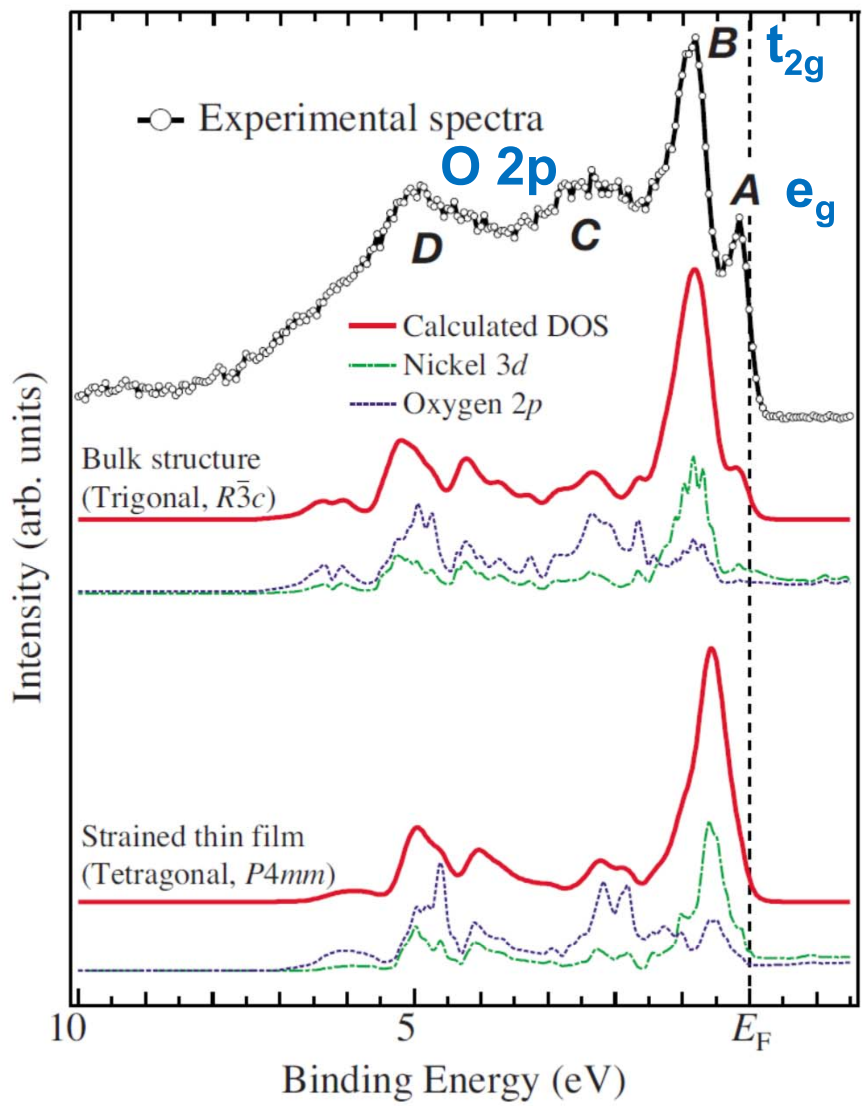

FIG. 4. (Color online) Comparison between experimental PES spectra and calculated DOS for $LaNiO_3$ bulk crystal and strained films.

Horiba et al., PHYSICAL REVIEW B **76**, 155104 (2007)

Atomic photoelectric cross sections/electron

Level	Photon energy: 80 eV	800 eV	1.0 keV	2.0 keV	6.0 keV
Ni 3d ($8 e^-$)	7.9E6/ 8 = 1.91	4.9E4/ 8 = 11.13	21654.9/ 8 = 10.17	1838.9/ 8 = 10.30	23.5/ 8 = 9.26
O 2p ($4 e^-$)	2.06E6/ 4 = 1.00	2200/ 4 = 1.00	1065.14/ 4 = 1.00	89.30/ 4 = 1.00	1.27/ 4 =1.00

Yeh, Lindau; Scofield

Simple model says:
Ni 3d dominant from soft to hard x-ray energies

Gray, Janotti, et al., Phys. Rev. B, to appear-SPring8

Broad Hard X-ray Photoemission (HAXPES) Survey: High Binding Energies, LNO (2.8 nm) on LAO

$h\nu$ = 5950.27 eV
Θ = 2.0°

LNO on LAO -1.32 % compressive strain
LNO on LSAT +0.78% tensile strain

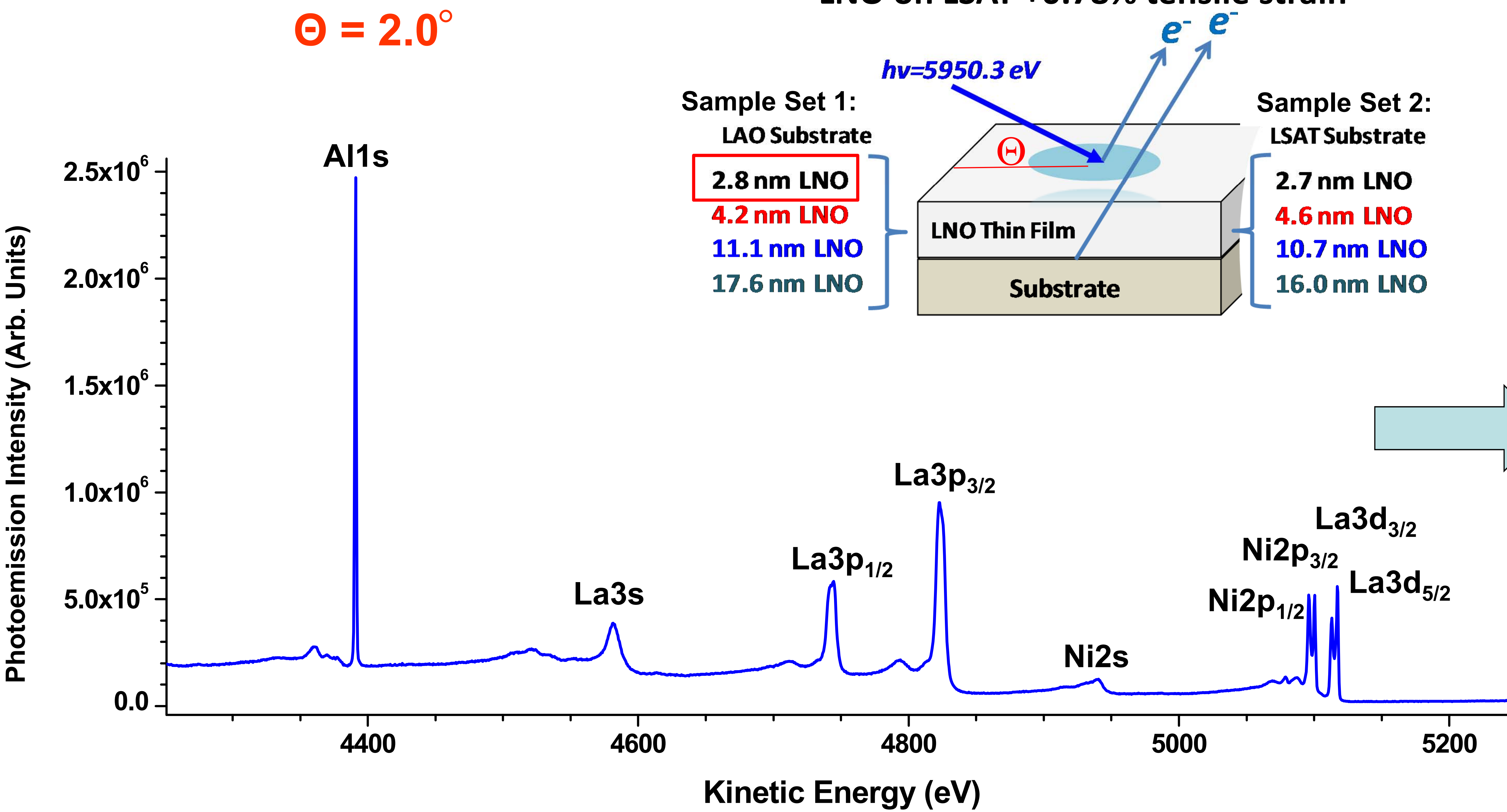

Gray, Janotti, et al., Phys. Rev. B, to appear-SPring8

Typical Broad HAXPES Survey: Low Binding Energies, LNO (2.8 nm) on LAO

LNO on LAO -1.32 % compressive strain
LNO on LSAT +0.78% tensile strain

h*v* = 5950.27 eV
Θ = 2.0°

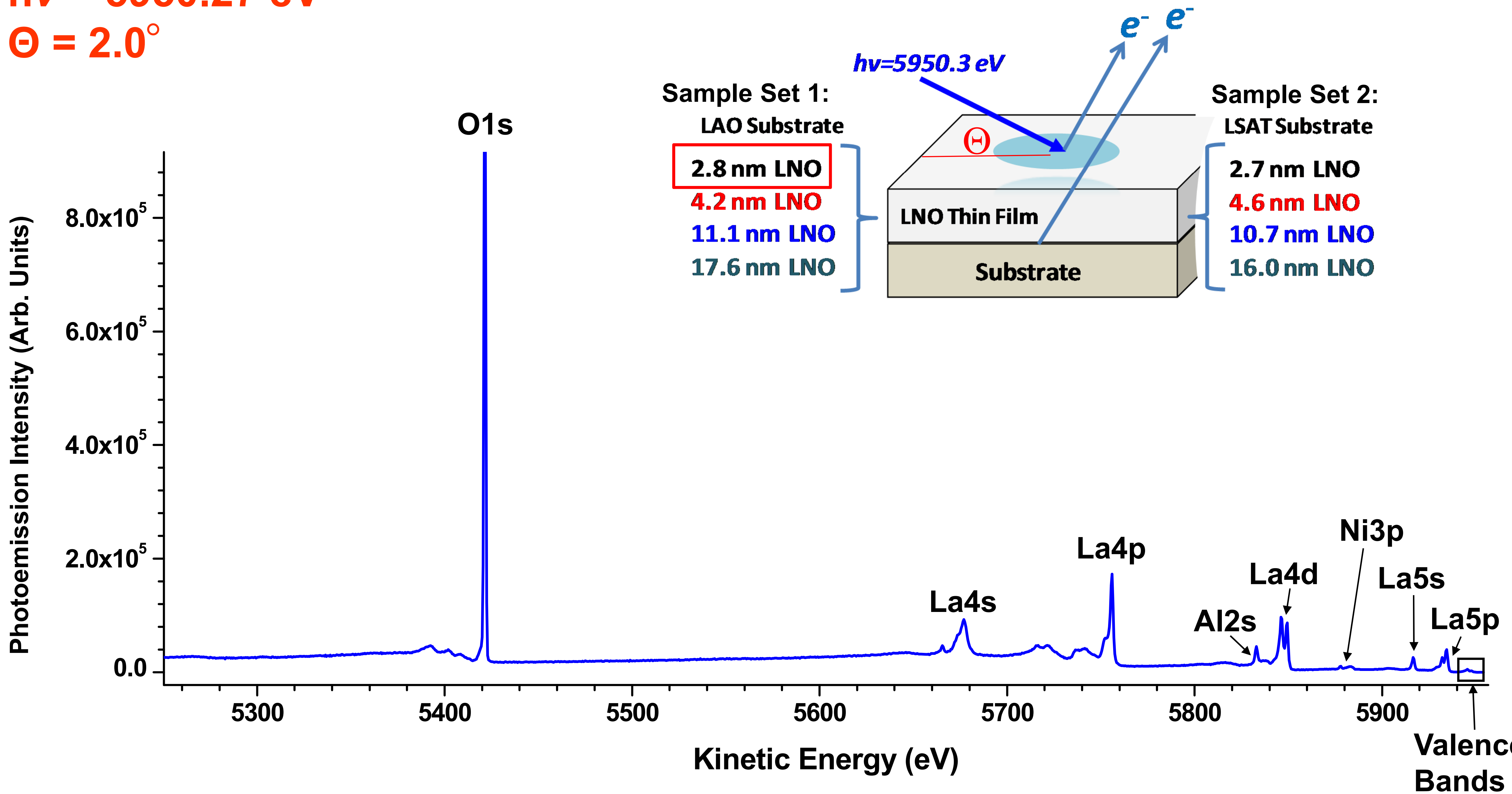

Gray, Janotti, et al., Phys. Rev. B, to appear-SPring8

Substrate Core Level HAXPES Intensities: LNO/LAO

Core peaks originating from the substrate lose intensity as the overlayer thickness becomes larger: $I_{substrate} \propto e^{-t/\Lambda_{EAL,LNO}}$

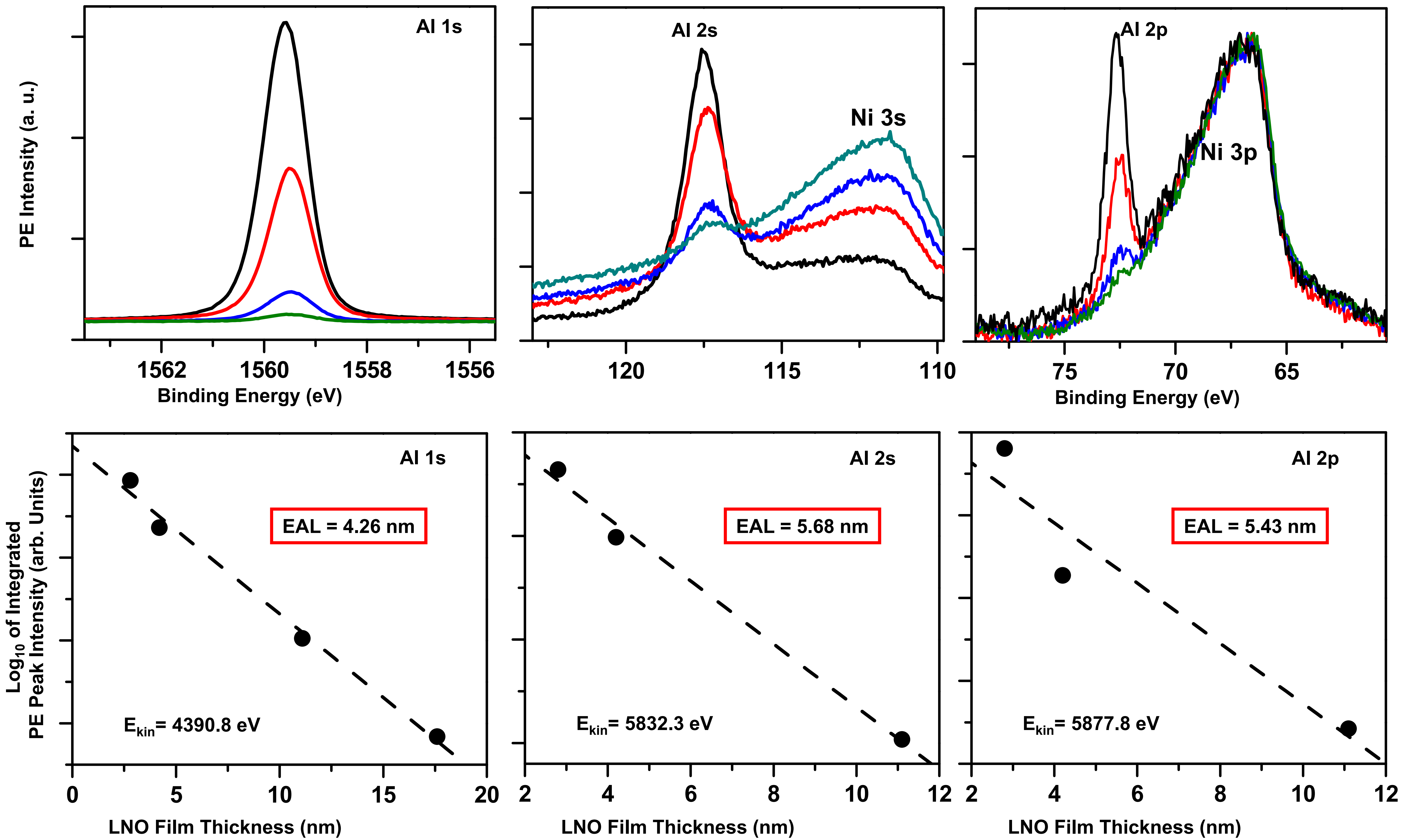

Effective Attenuation Lengths (EALs) from Core-Level HAXPES

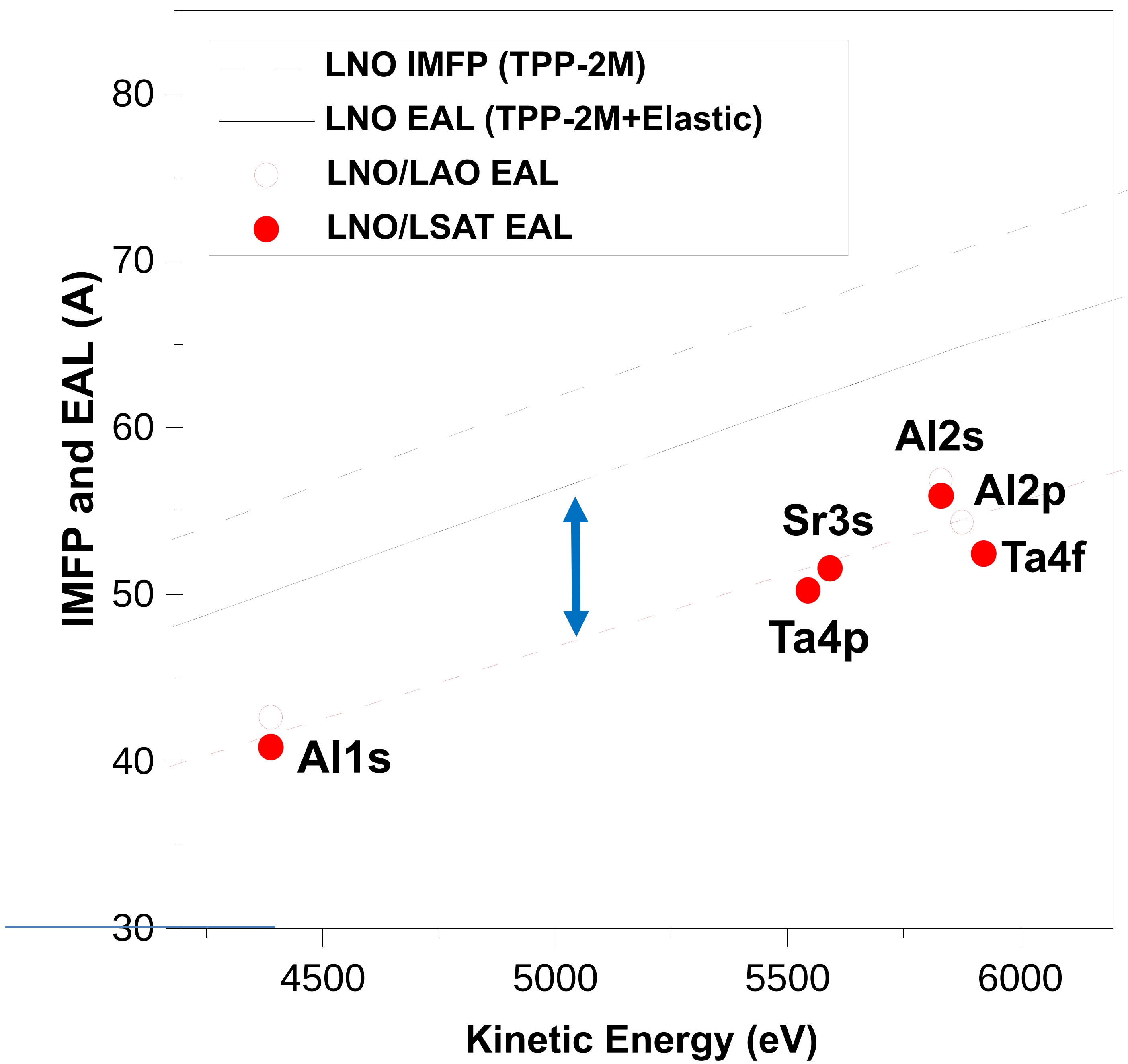

- **Measurement of substrate peak intensity dependence on overlayer thickness → effective attenuation lengths EAL**
- **LNO EALs from both substrates are in agreement with each other to ~5-10%**
- **EALs within 20% of the semi-empirical TPP-2M formula if corrected for elastic scattering**
- **Remaining experiment/theory discrepancy may be due to lack of resonant absorption edges in theory – not considered previously**

Gray, Janotti, et al., Phys. Rev. B, to appear-SPring8

Effective Attenuation Lengths (EALs) from Core-Level HAXPES

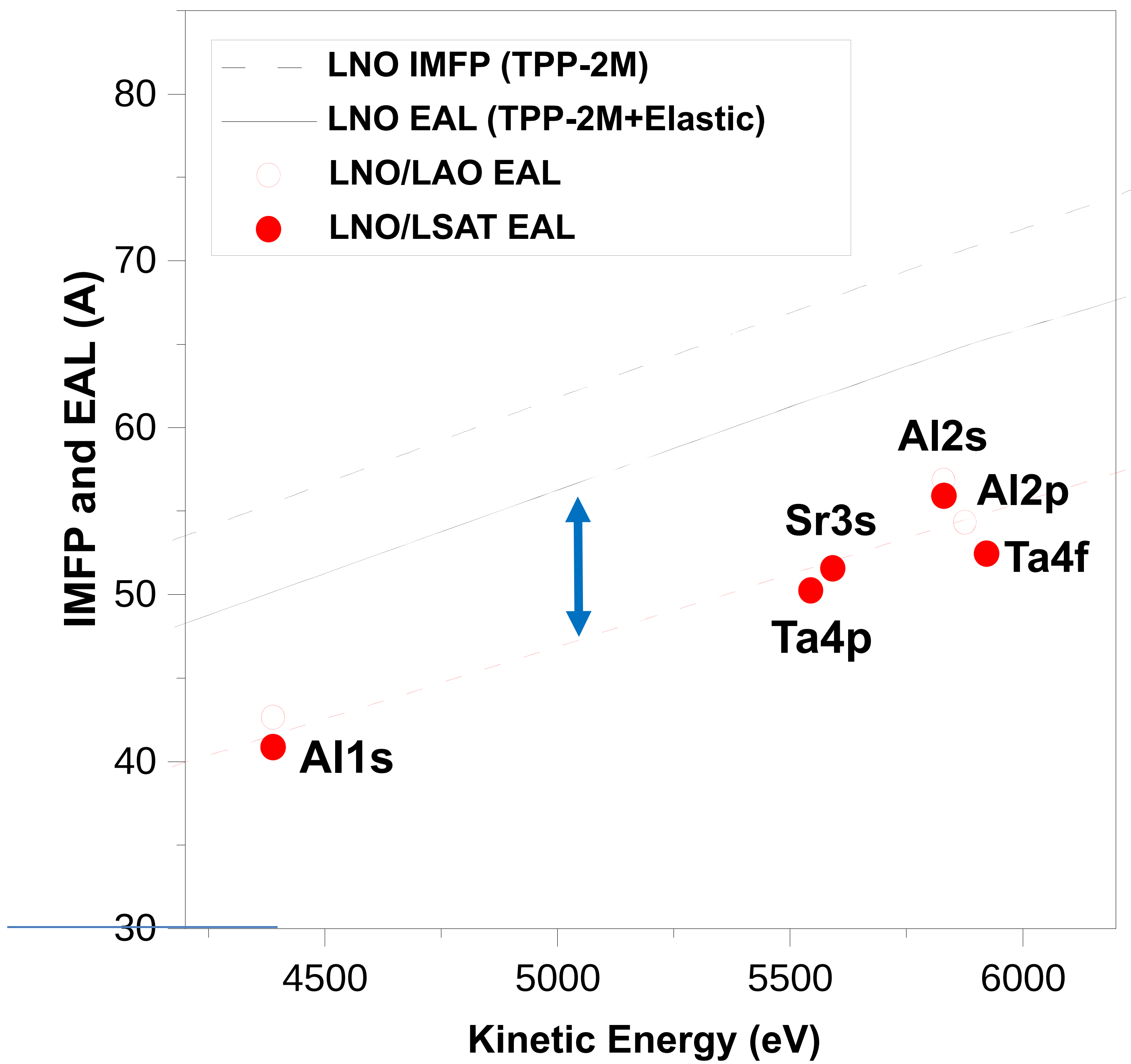

- Measurement of substrate peak intensity dependence on overlayer thickness → effective attenuation lengths EAL
- LNO EALs from both substrates are in agreement with each other to ~5-10%
- EALs within 20% of the semi-empirical TPP-2M formula if corrected for elastic scattering
- Remaining experiment/theory discrepancy may be due to lack of resonant absorption edges in theory – not considered previously

Gray, Janotti, et al., Phys. Rev. B, to appear-SPring8

Effective Attenuation Lengths (EALs) from Core-Level HAXPES

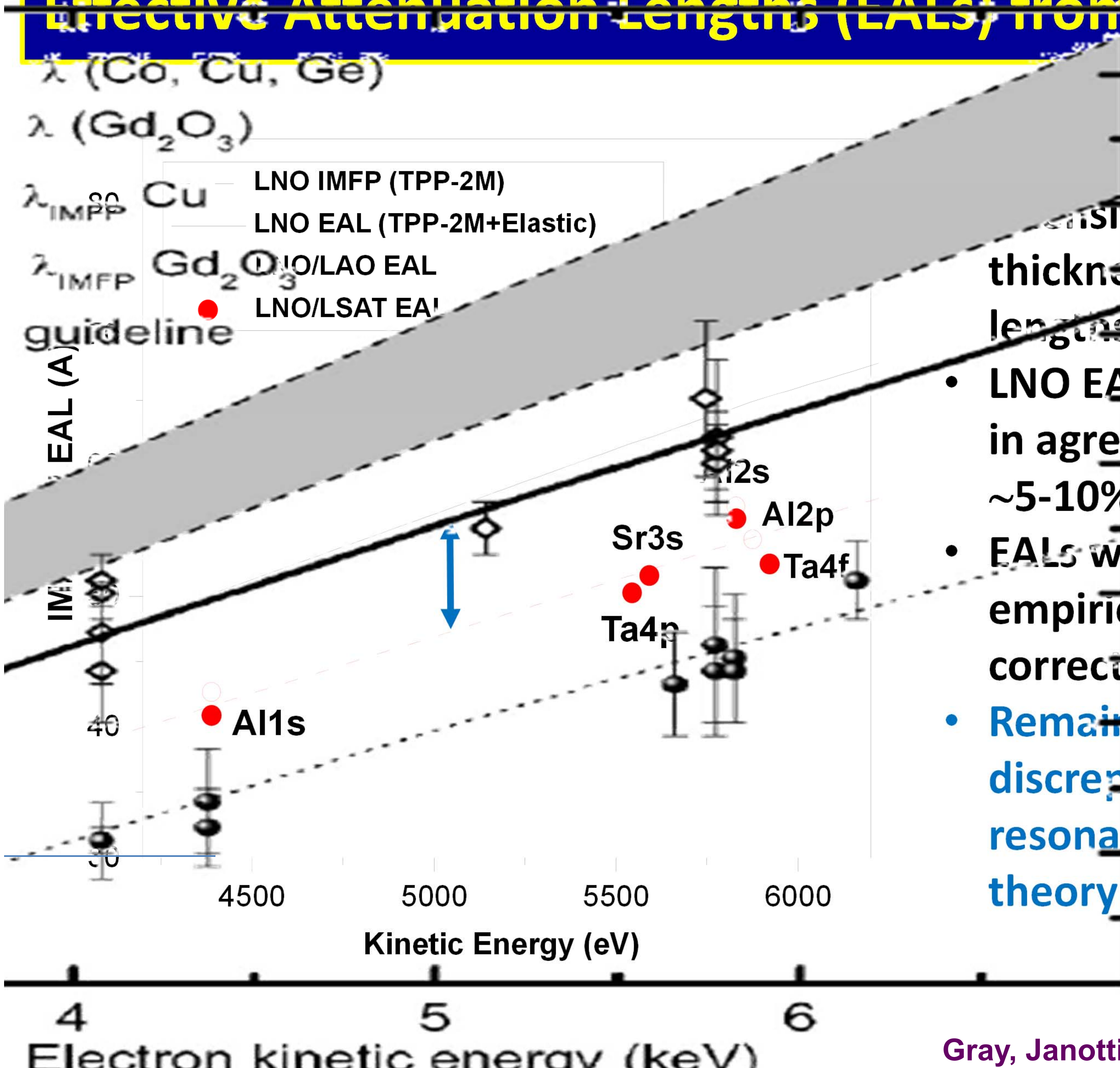

- …rement of substrate peak …sity dependence on overlayer thickness → effective attenuation lengths EAL
- LNO EALs from both substrates are in agreement with each other to ~5-10%
- EALs within 20% of the semi-empirical TPP-2M formula if corrected for elastic scattering
- Remaining experiment/theory discrepancy may be due to lack of resonant absorption edges in theory – not considered previously

Gray, Janotti, et al., Phys. Rev. B, to appear-SPring8

Overlay of Fig. 7 from Sacchi et al., PRB 71, 155117 (2005)—
Gd_2O_3, another RE-containing compound like LNO, ~20% lower

LNO and substrates: thickness-dependent density of states

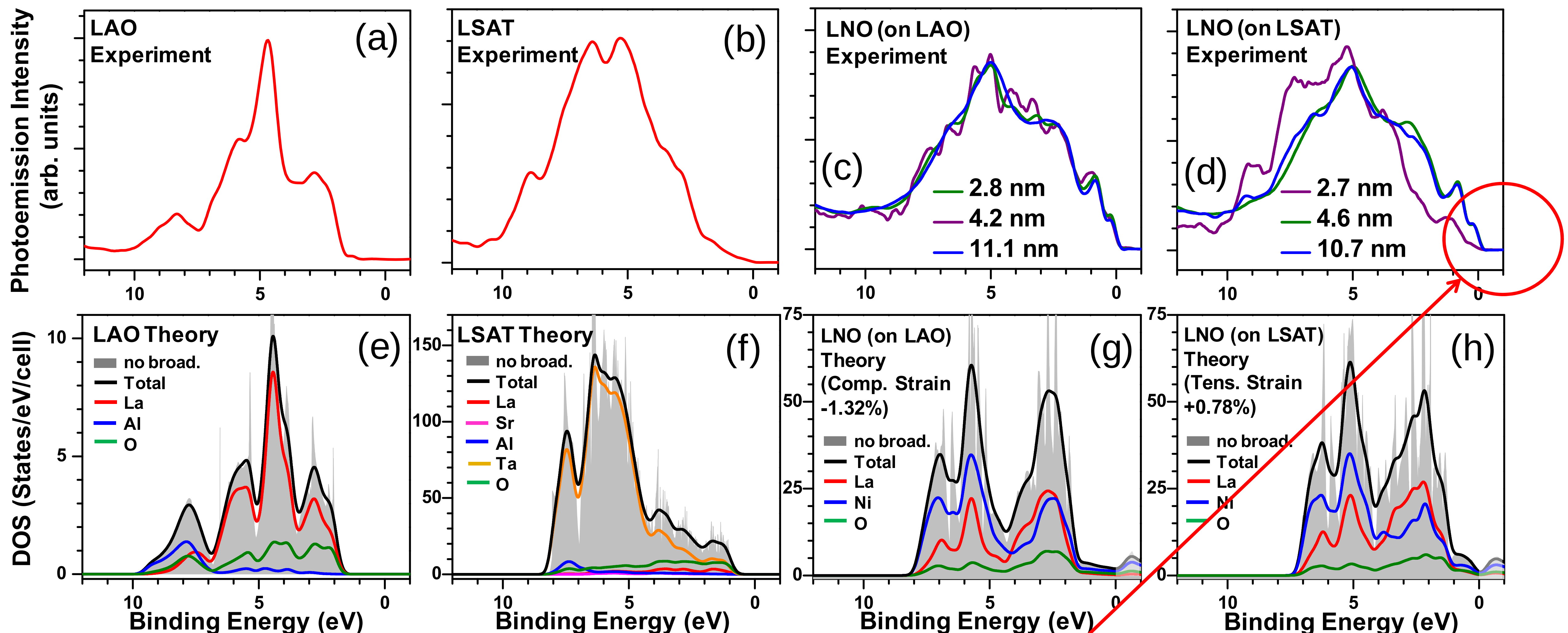

- **Decomposition of valence spectra into film and substrate DOS using EALs and**

  $$I_t = (1-\exp(-t/l_{EAL}))I_{film,t} + \exp(-t/l_{EAL})\, I_{subst,t}$$

- **DOS for thinnest 2.7 nm LNO film on LSAT differs from others, with greater effect for LSAT substrate that is consistent with conductivity results (Stemmer et al.)**
- **Similar result for 1.7 nm LNO on LAO from XPS at 1.5 keV (H. Wadati, G. A. Sawatzky)**
- **Theory with hybrid functional does well for LAO & LSAT, not so well for strained bulklike LNO (Janotti and Van der Welle)**

Gray, Janotti, et al., to be published

$LaNiO_3$ Thin films: Insulator-to-Metal Transition-Soft X-ray PS

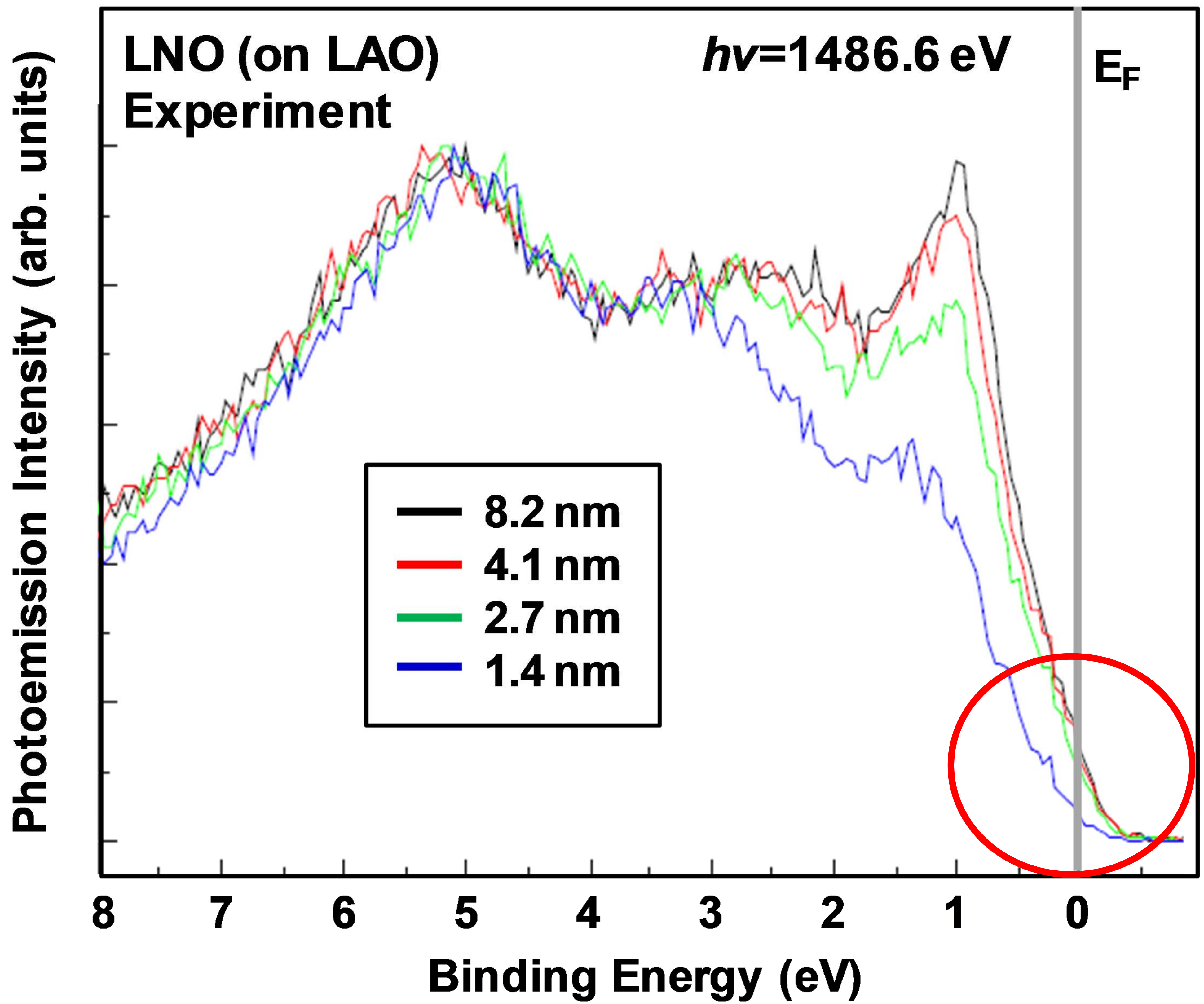

R. Sutarto, H. Wadati, G. A. Sawatzky, Canadian Light Source

$LaNiO_3$ Thin films: Insulator-to-Metal Transition Induced by Strain a/o Interface Effects

Epitaxial layers with TEM thickness det'n.
(Junwoo Son, James LeBeau)

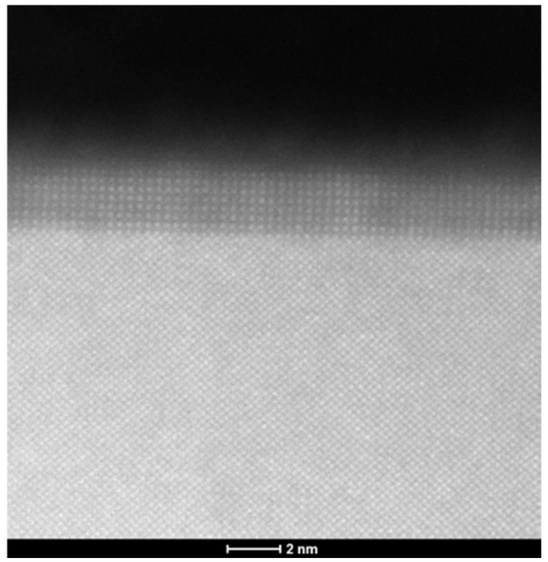

LNO/LSAT
~ 7 unit cells = 2.7 nm

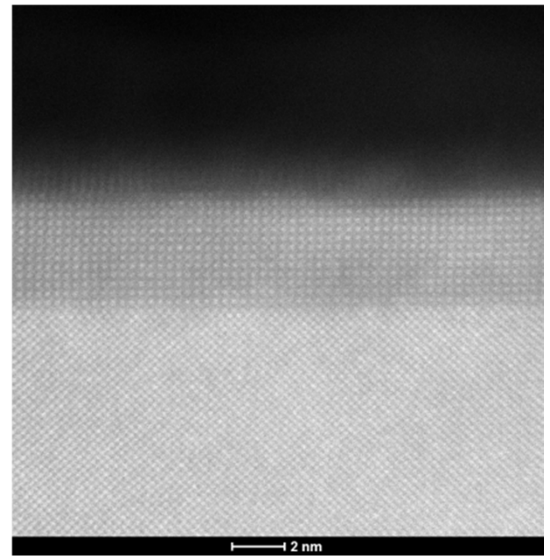

LNO/LSAT
~ 12 unit cells = 4.6 nm

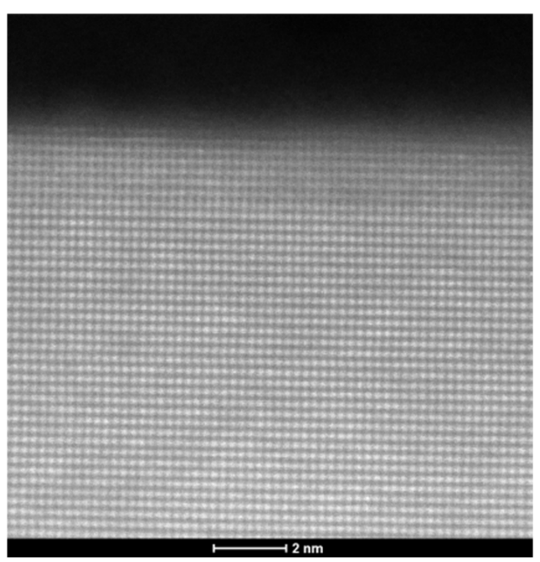

LNO/LAO
~ 7 unit cells = 2.8 nm

Eight samples

LNO/LAO Thickness (nm)	LNO/LSAT Thickness (nm)
2.8	2.7
4.2	4.6
11.1	10.7
17.6	16.0

Conductivity (Stemmer, Allen et al.)

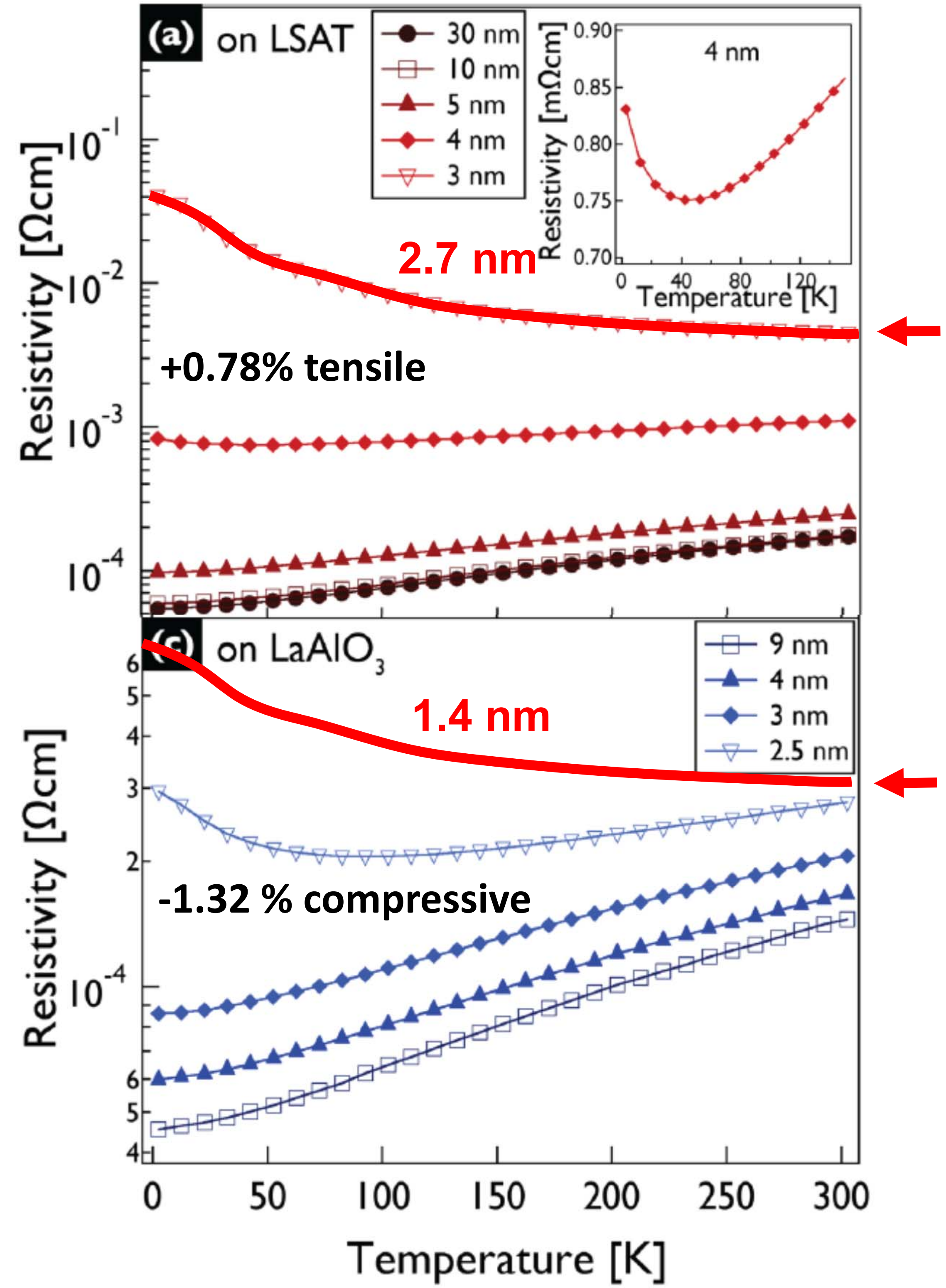

Gray, Janotti, et al., Phys. Rev. B, to appear-SPring8 Son et al., Appl. Phys. Lett. 96, 062114 (2010); 97, 202109 (2010)

Outline

Photoemission: Some limitations, some new directions

6-8 keV

Hard x-ray photoemission of interesting bulk materials→core and valence spectra:
half-metallic/colossal magnetoresistive $La_{0.67}Sr_{0.33}MnO_3$
semiconducting CrAl alloy
metal-to-insulator transition in thin-film $LaNiO_3$

3.2 & 6 keV

Angle-resolved hard x-ray photoemission→HXPD: Kikuchi-band modeling, and HARPES for: W, GaAs & the magnetic semiconductor (Ga,Mn)As

833 & 6 keV

Standing-wave photoemission combining soft and hard x-rays, depth-resolved composition, densities of states and ARPES, and magnetization:
$SrTiO_3/La_{2/3}Sr_{1/3}MnO_3$ multilayer
Fe/MgO tunnel junction

500-700 eV

Standing-waves in a photoelectron microscope, adding the third dimension:
multilayers and microdots

Conclusions and Future Outlook

X-ray photoemission: some key elements

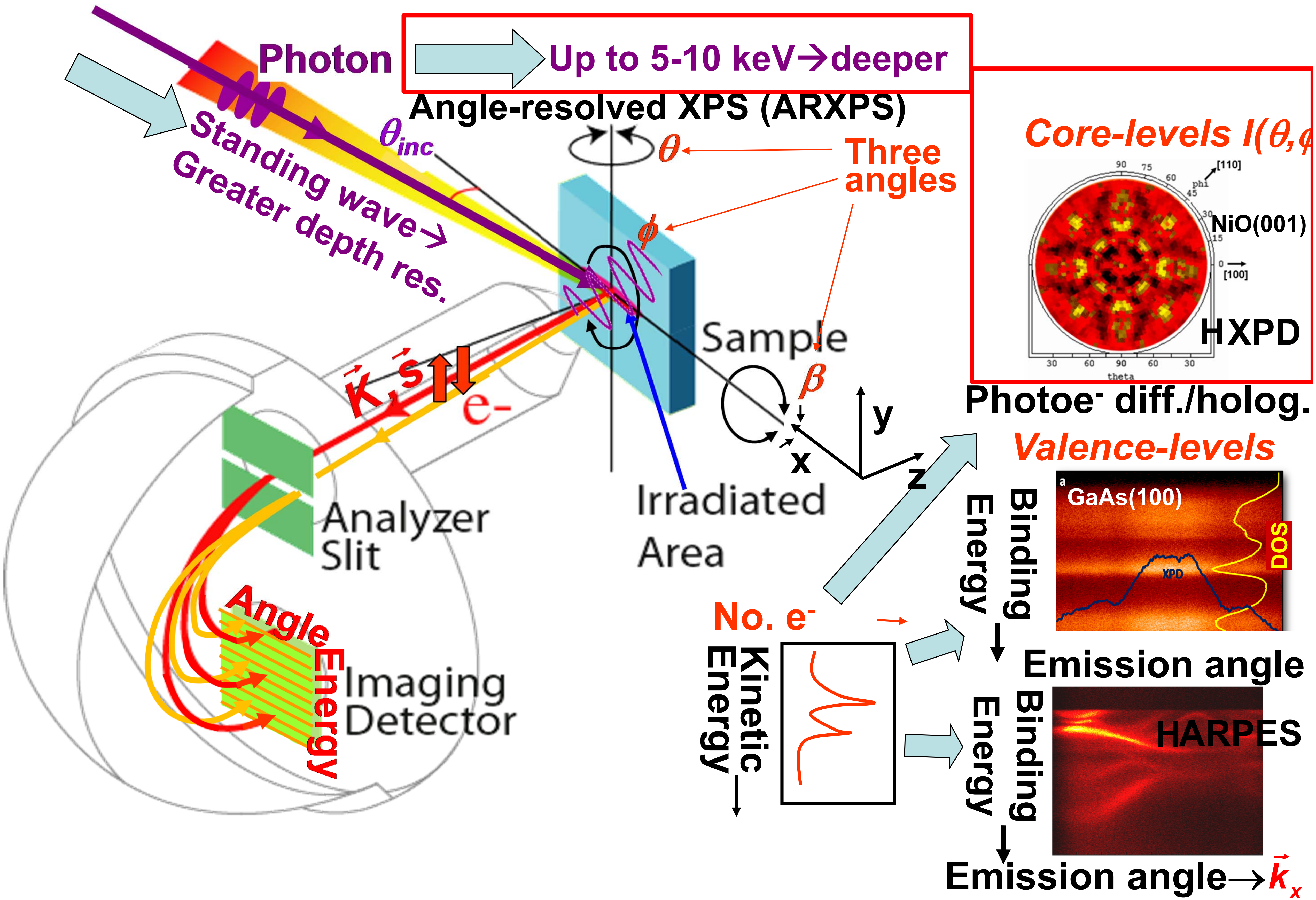

Photoelectron diffraction with hard x-ray excitation: 1000 eV→10,000 eV, the first theoretical study

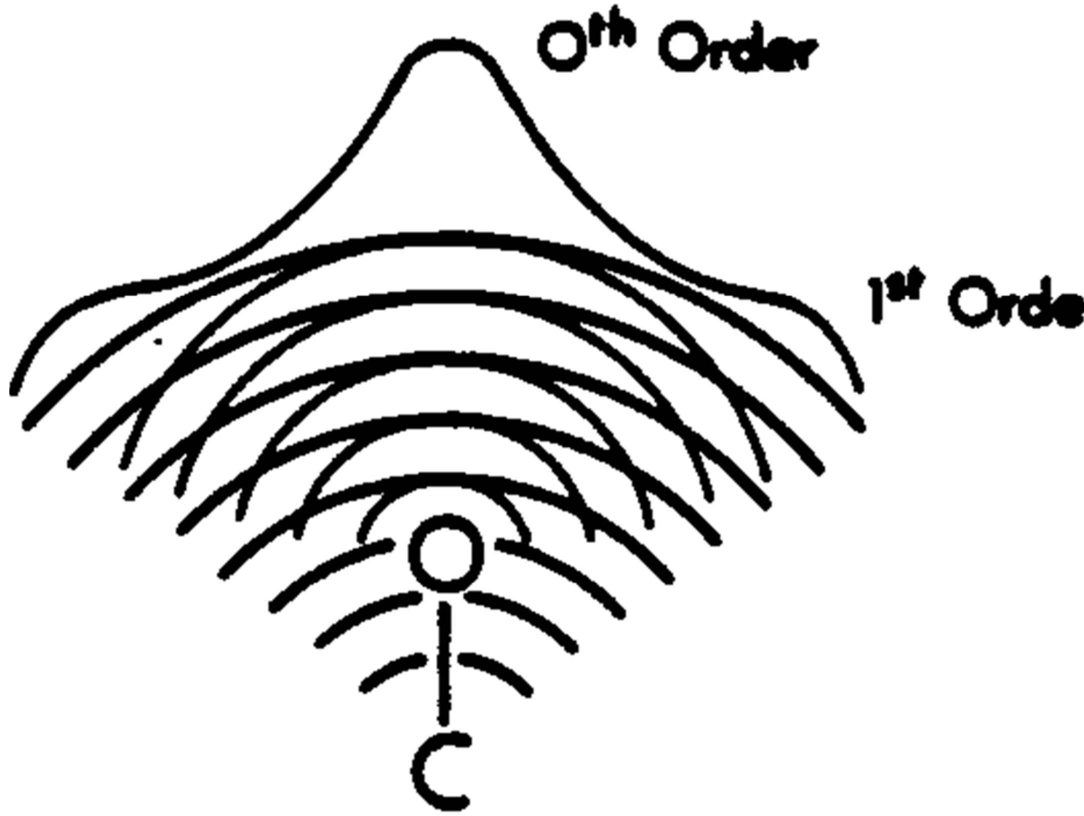

No vibration

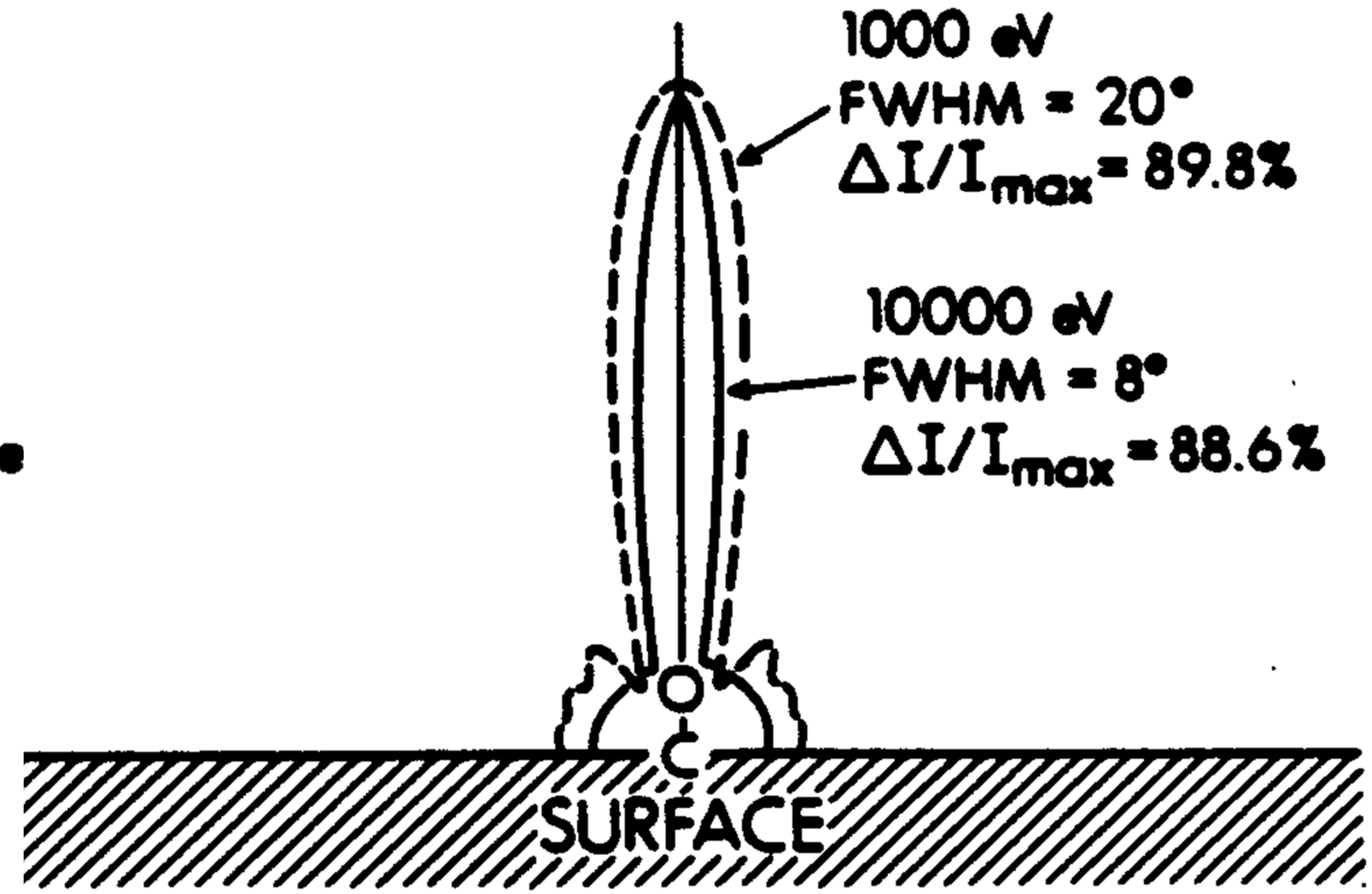

Qualitative expectations:
Forward scattering peak strengths f(0) ~ constant
Overall scattering cross section $\sigma = \int f d\Omega$ decreases

K.A. Thompson and C.F.
J. Elect. Spect. 33, 29 ('84)

Hard X-Ray Photoelectron Diffraction: Basic Systematics and Modeling

The scattering of photoelectrons from localized sources can be described in real space (multiple scattering cluster) and reciprocal space (dynamical theory of electron diffraction)

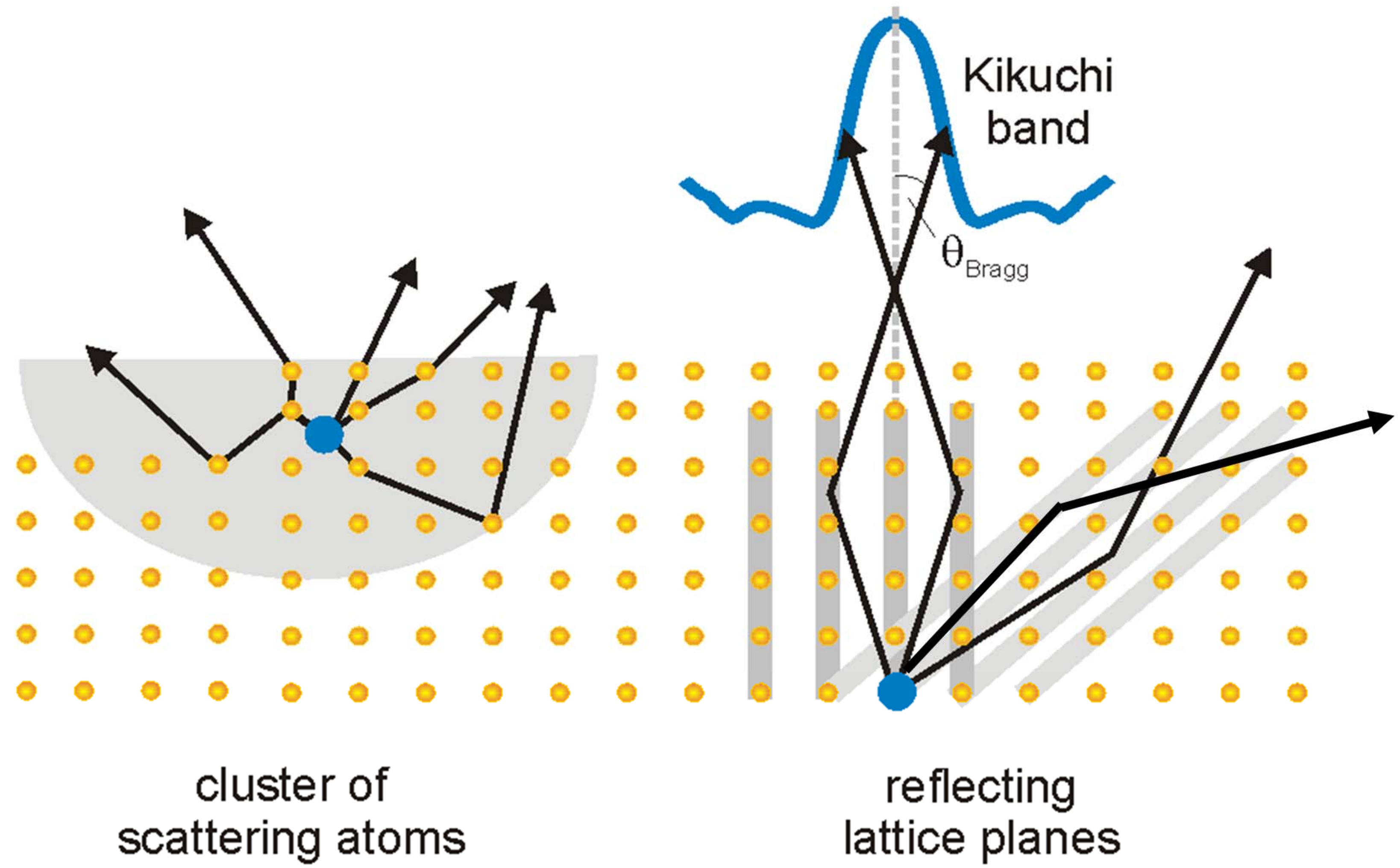

A.Winkelmann, J. Garcia de Abajo, C.F., Journal of Physics 10 (2008) 113002

Photoelectron Diffraction with soft and hard x-ray excitation: two viewpoints, expt. vs. theory

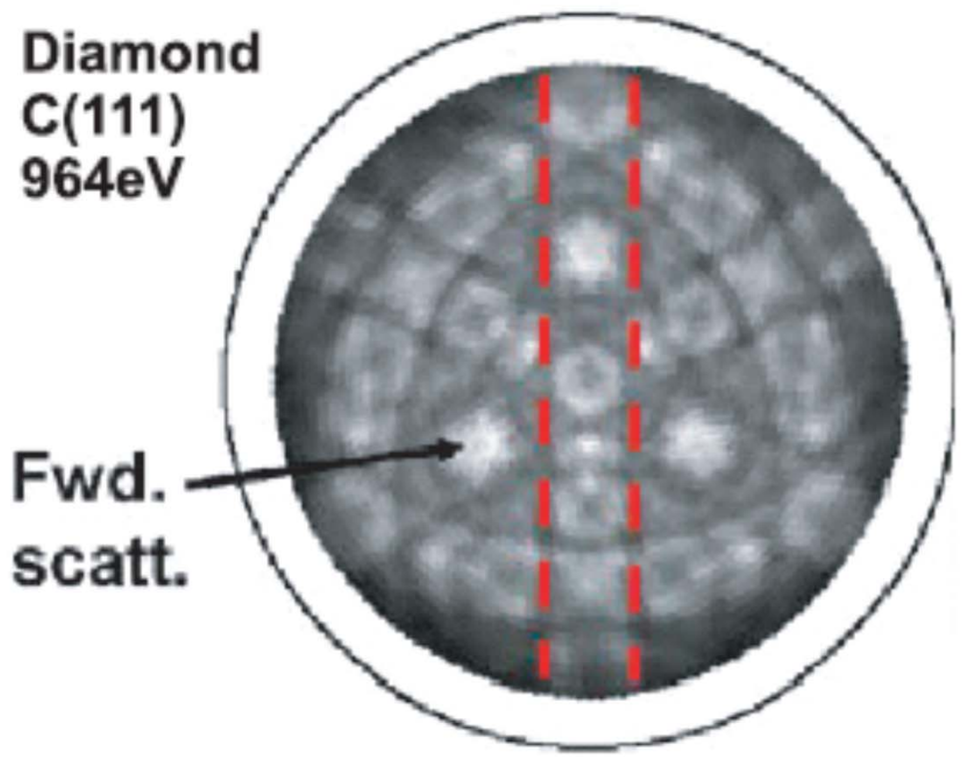

(a) experiment

Osterwalder et al.,
Surf. Sci. 312, 131 (1994)

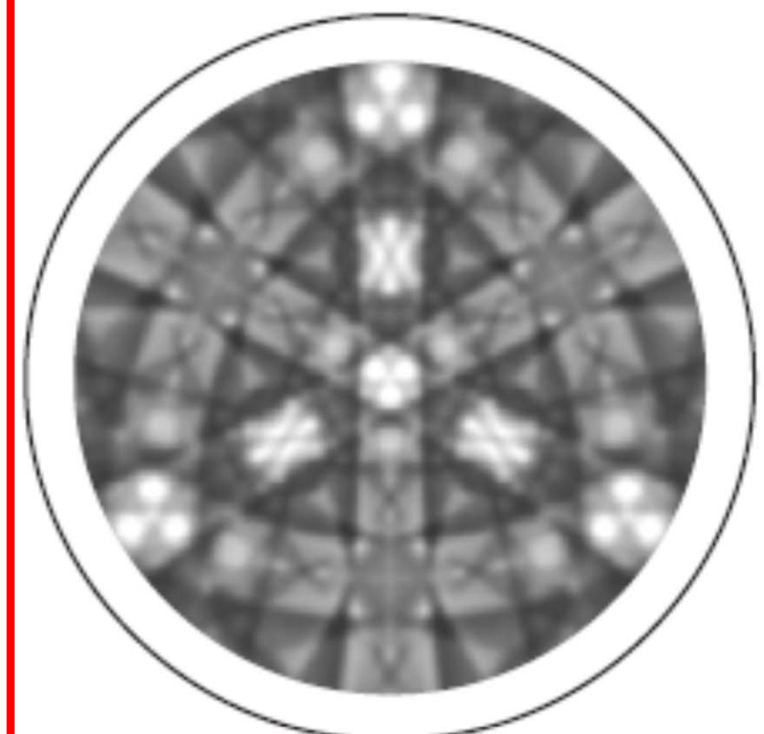

(b) dynamical simulation

Kikuchi-band approach

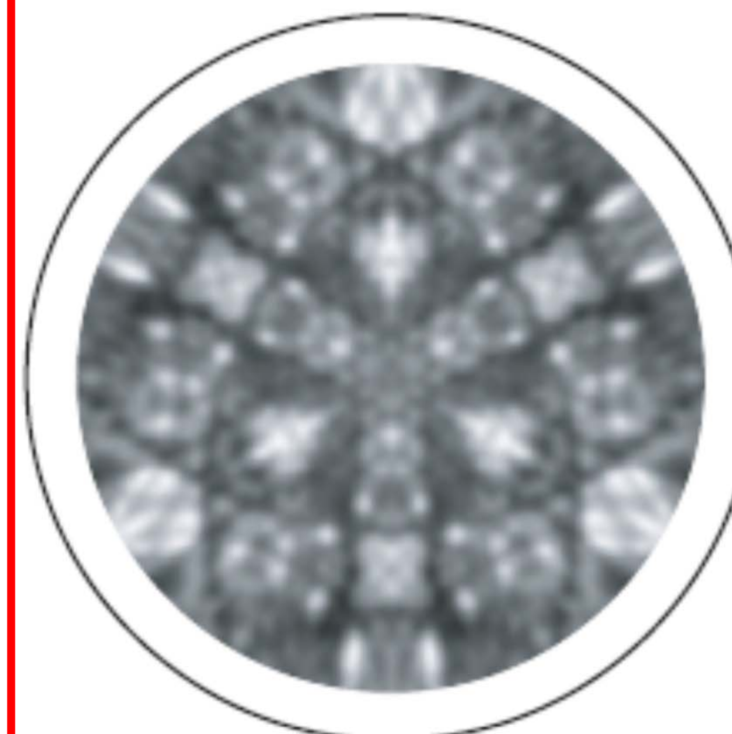

(c) multiple scattering simulation (EDAC)

Most appropriate for higher energies, bulklike emission

A. Winkelmann et al, New J. Phys 10 (2008) 113002

Photoelectron Diffraction with soft and hard x-ray excitation: expt. vs. Kikuchi-band theory

Experiment

STO/LSMO Multilayer
Mn 3p emission
E = 793eV
hv = 833.2 eV

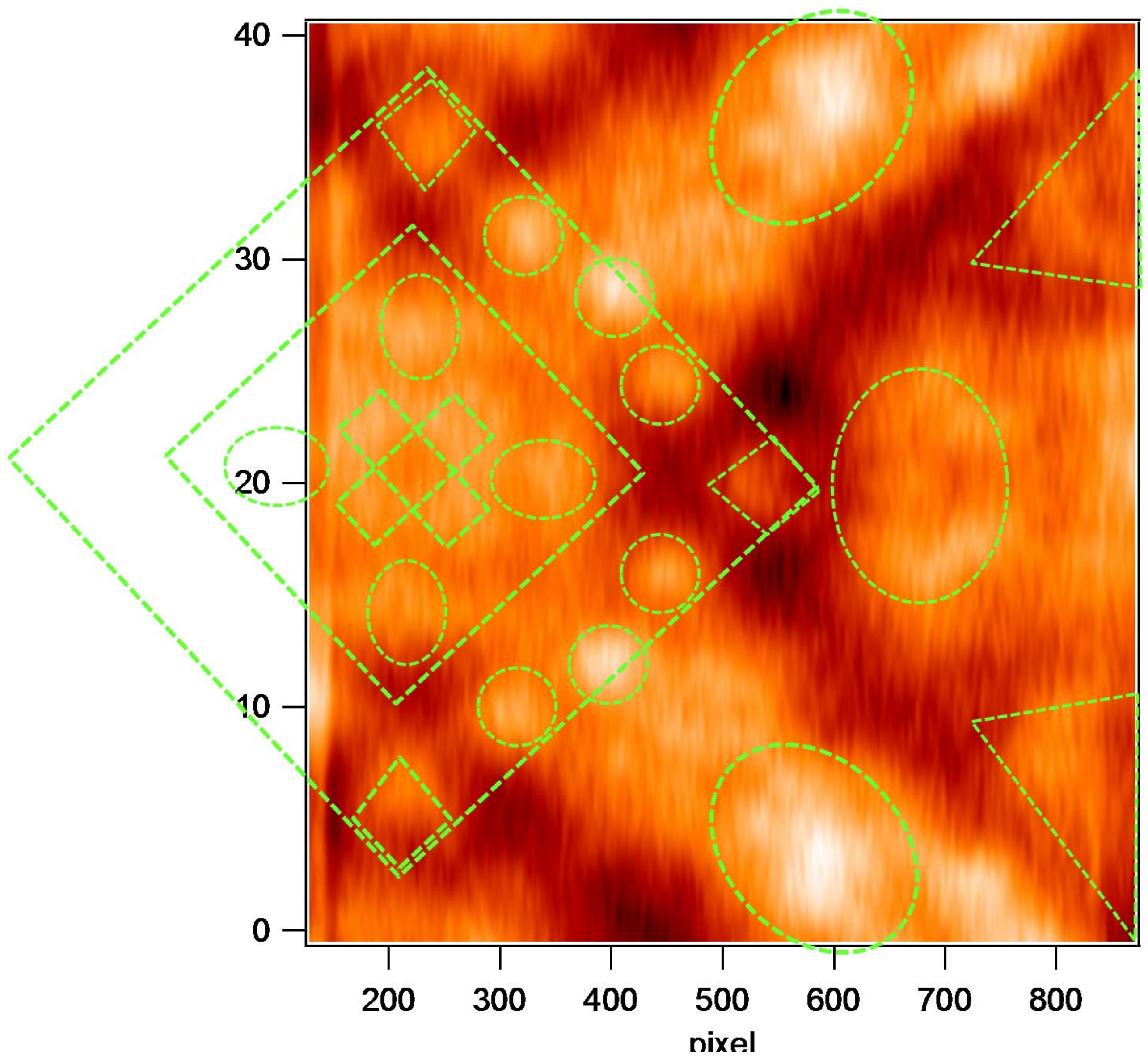

Experiment: Fadley Group-ALS

Photoelectron Diffraction with soft and hard x-ray excitation: expt. vs. Kikuchi-band theory

Experiment

STO/LSMO Multilayer
Mn 3p emission
E = 793eV
hv = 833.2 eV

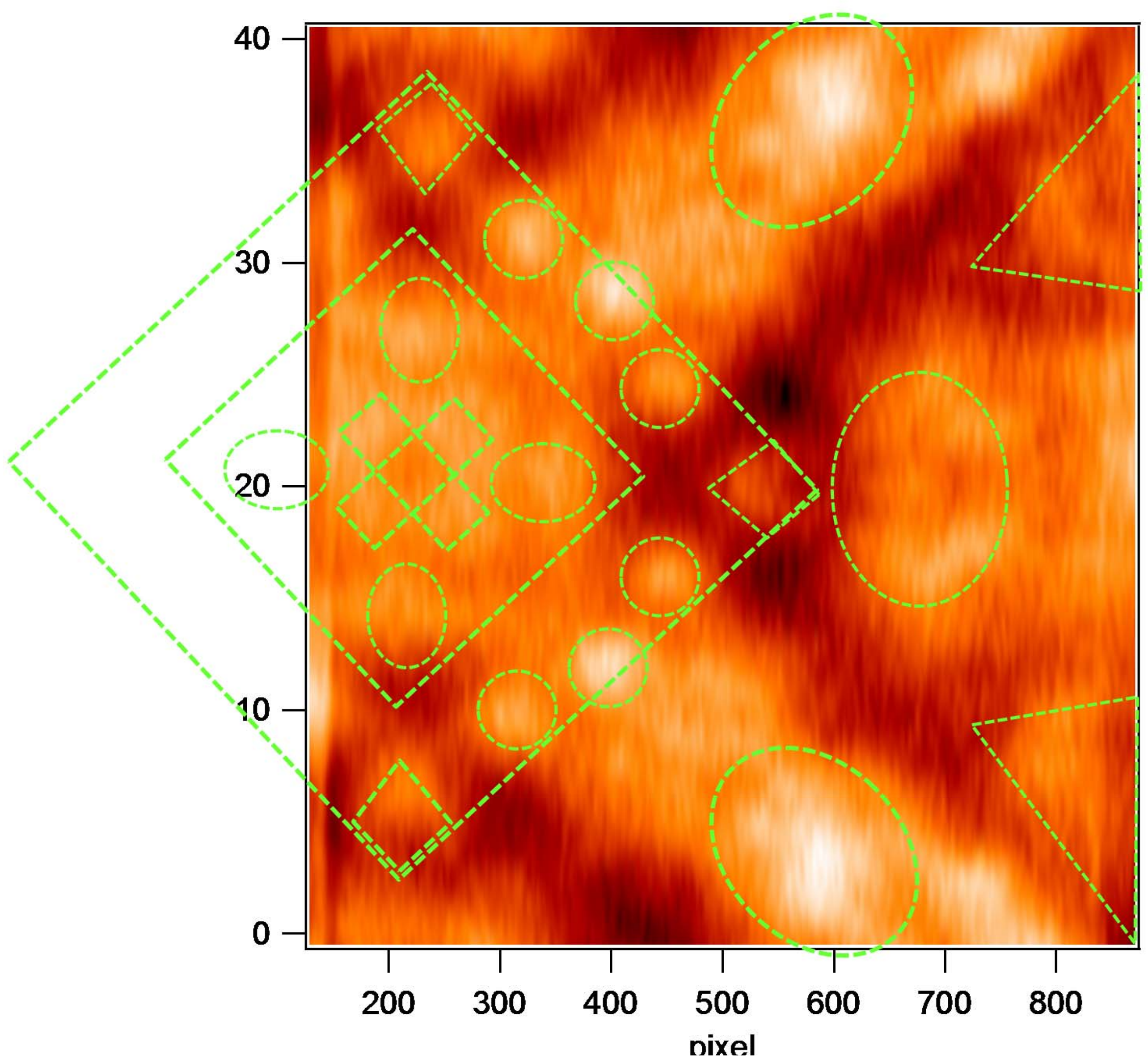

Experiment: Fadley Group

XPD Kikuchi-Band Theory

LSMO 5nm Film „bulk“
Mn emission
E = 793eV
hv = 833.2 eV

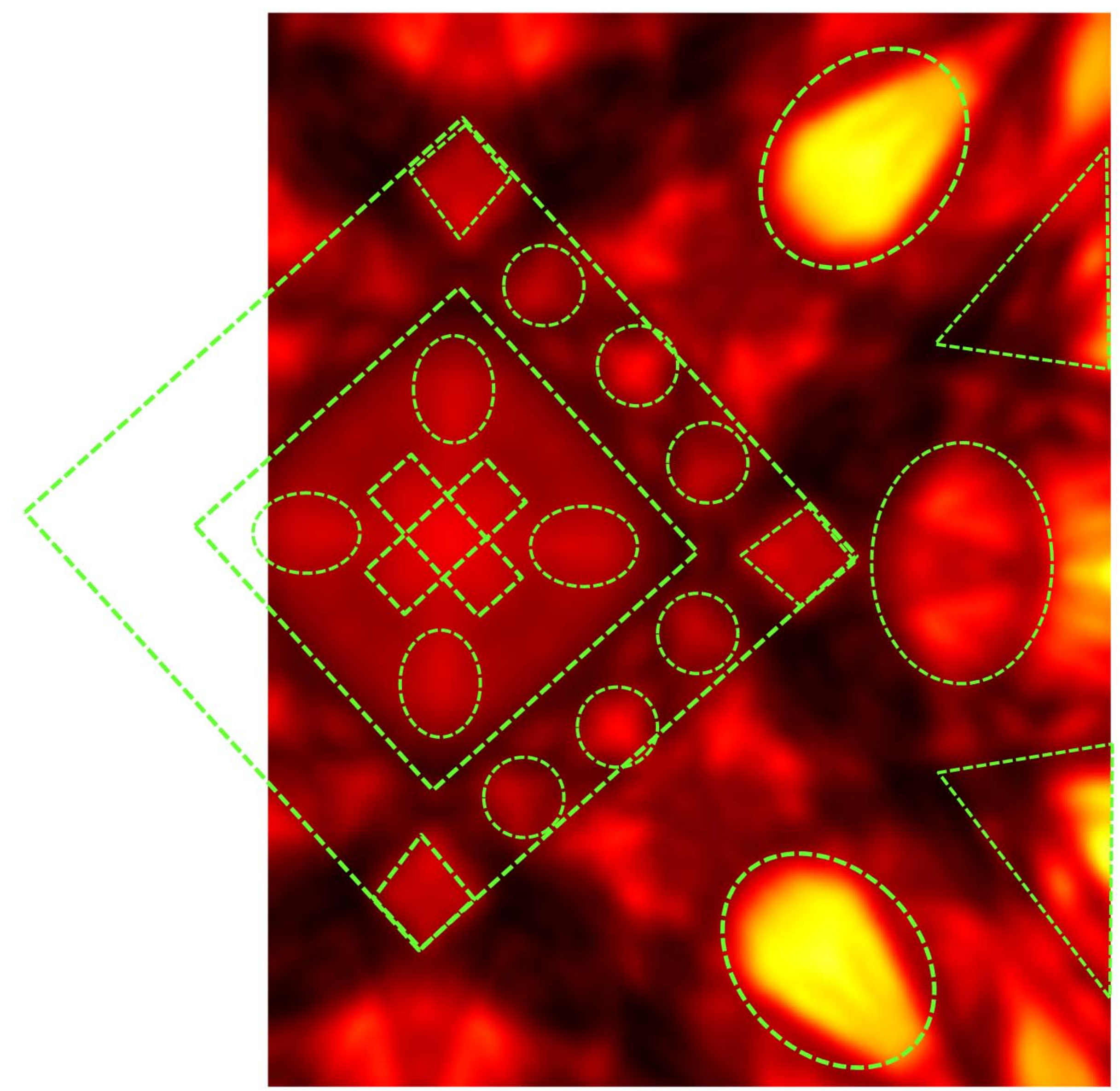

Theory: A. Winkelmann

Hard x-ray photoelectron diffraction--Theory: Sensitivity to lattice distortions and atomic site type?

Si(111)-6 keV: Impurity atom on lattice site (Si) vs. tetrahedral interstitial (T)

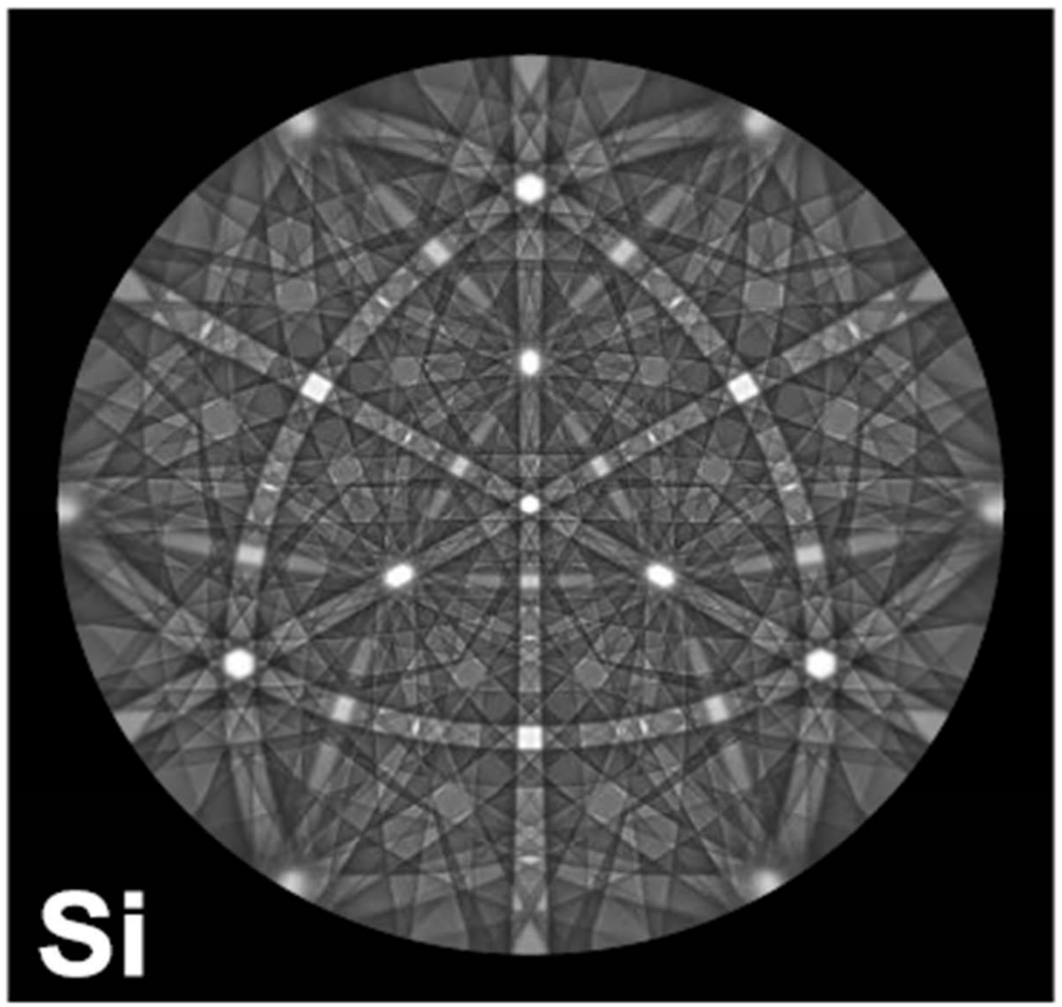

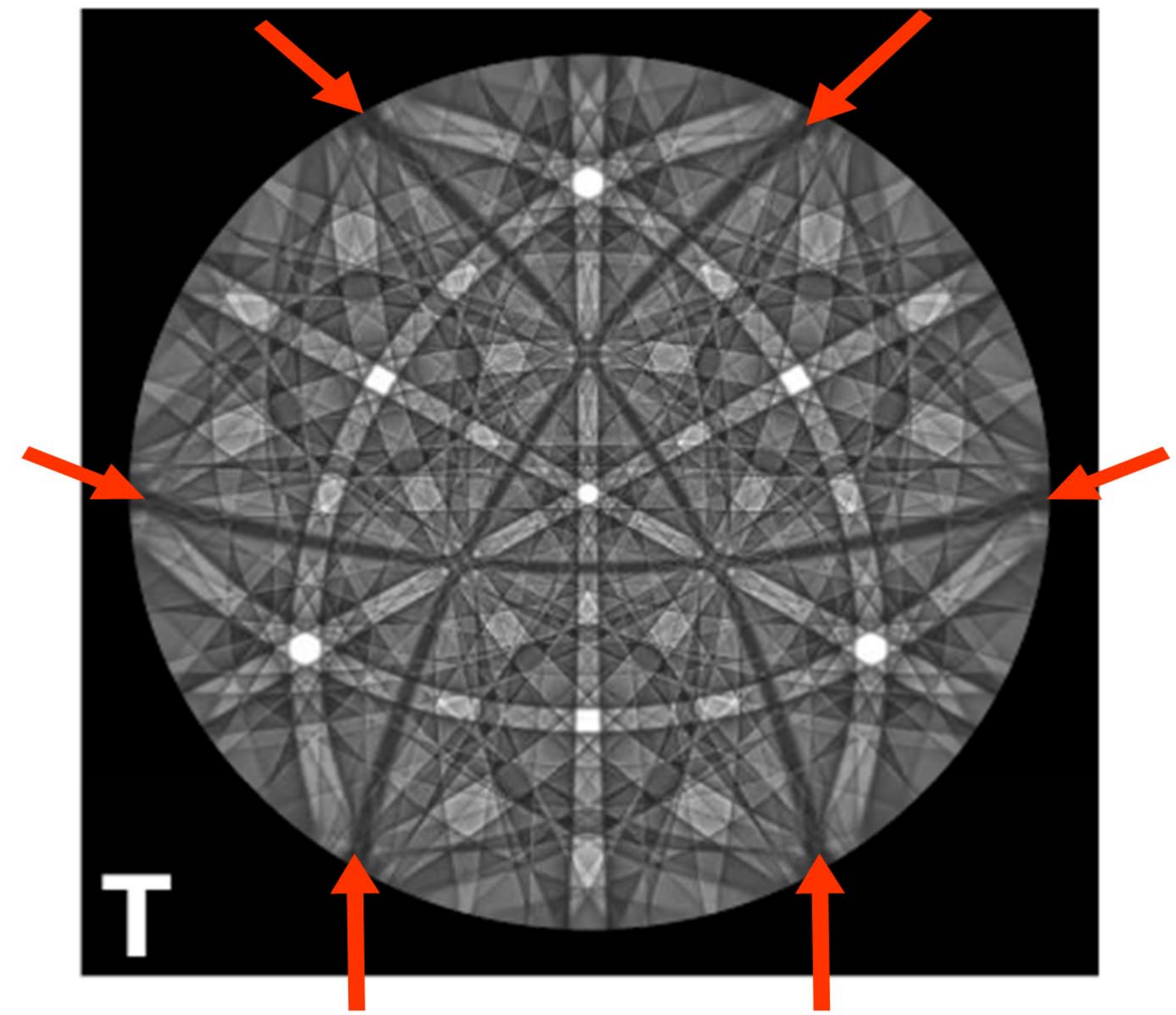

A. Winkelman, J. Garcia de Abajo, MPI Halle, CF, New Journal of Physics 10 (2008) 113002

Missing Kikuchi bands-->”forbidden reflections”

→Future experiment?: Crystal Bragg standing waves for x-rays in plus Kikichi band/standing waves for electrons out

Outline

Photoemission: Some limitations, some new directions

6-8 keV

Hard x-ray photoemission of interesting bulk materials→core and valence spectra:
half-metallic/colossal magnetoresistive $La_{0.67}Sr_{0.33}MnO_3$
semiconducting CrAl alloy
metal-to-insulator transition in thin-film $LaNiO_3$

3.2 & 6 keV

Angle-resolved hard x-ray photoemission→HXPD: Kikuchi-band modeling, and
HARPES for: W, GaAs & the magnetic semiconductor (Ga,Mn)As

833 & 6 keV

Standing-wave photoemission combining soft and hard x-rays, depth-resolved composition, densities of states and ARPES, and magnetization:
$SrTiO_3/La_{2/3}Sr_{1/3}MnO_3$ multilayer
Fe/MgO tunnel junction

500-700 eV

Standing-waves in a photoelectron microscope, adding the third dimension:
multilayers and microdots

Conclusions and Future Outlook

X-ray photoemission: some key elements

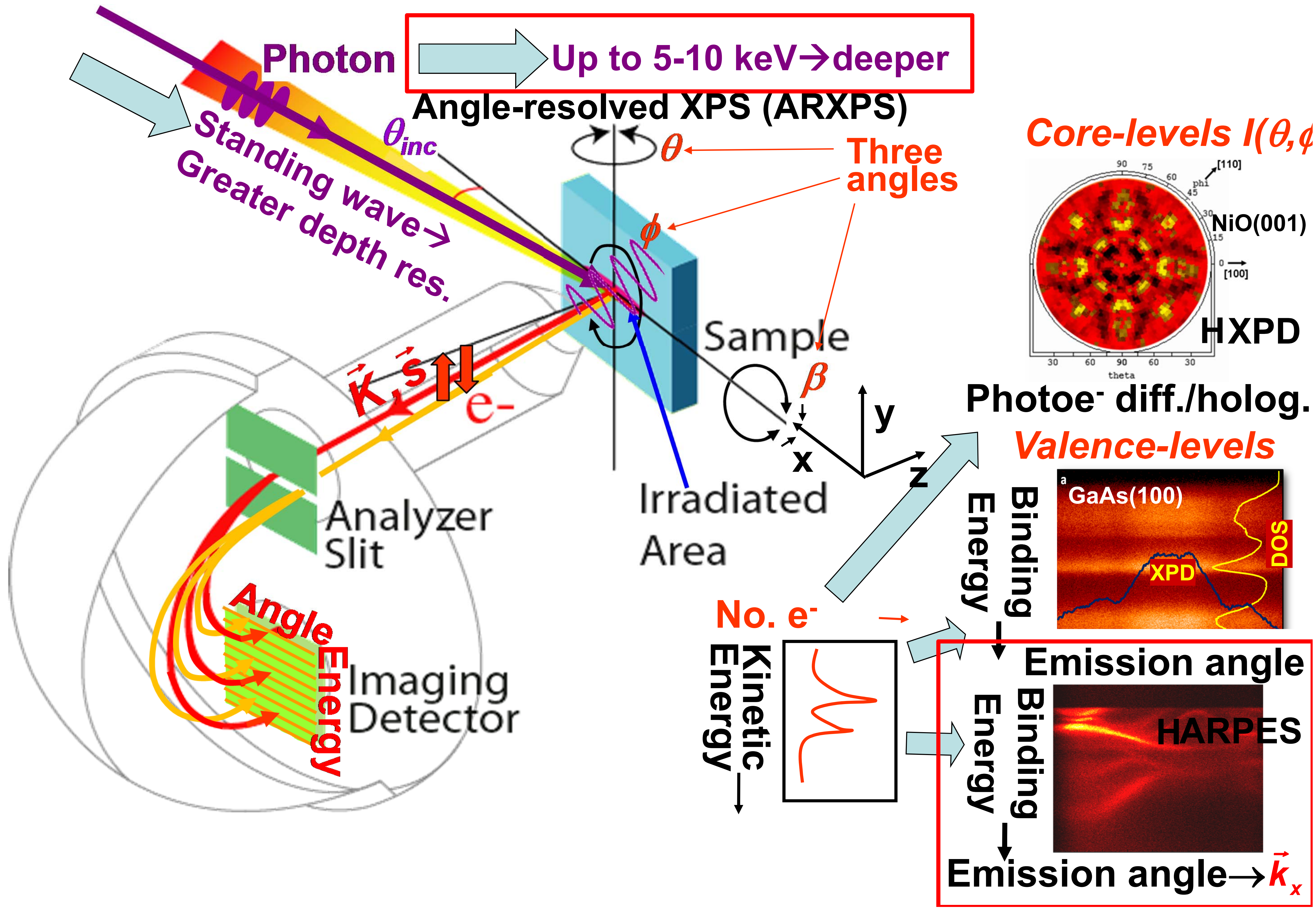

Valence-band photoemission: Angle-Resolved Photoemission (ARPES)

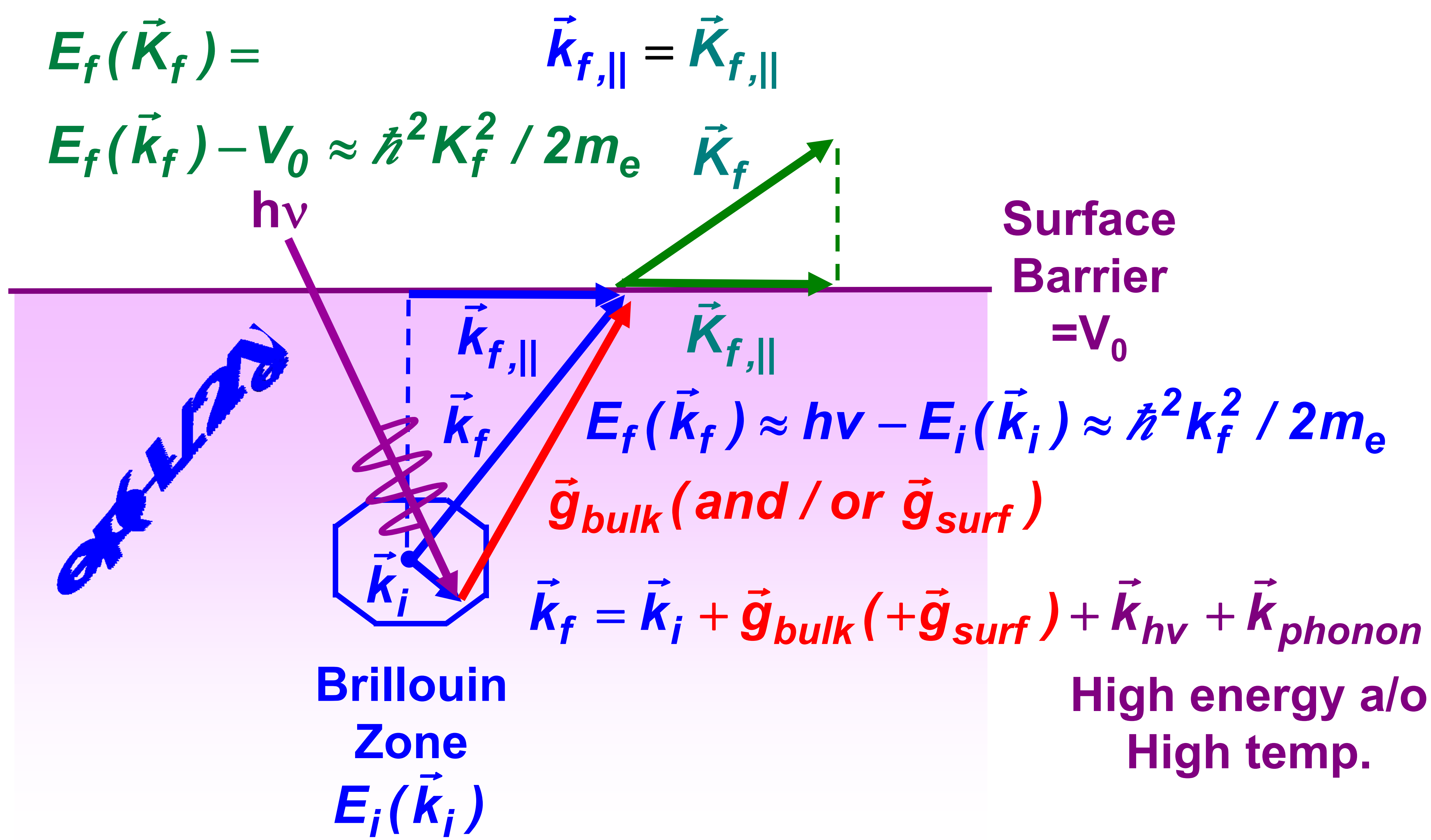

$$I(E_f, \vec{k}_f) \propto \left| \hat{\varepsilon} \bullet \left\langle \varphi_{photoe}(E_f = h\nu + E_i, \vec{k}_f = \vec{k}_i + \vec{g}) \middle| \vec{r} \middle| \varphi(E_i, \vec{k}_i) \right\rangle \right|^2$$

"Direct" or k-conserving transitions

Angle-Resolved Photoemission at High Energy-- How high can we go?:

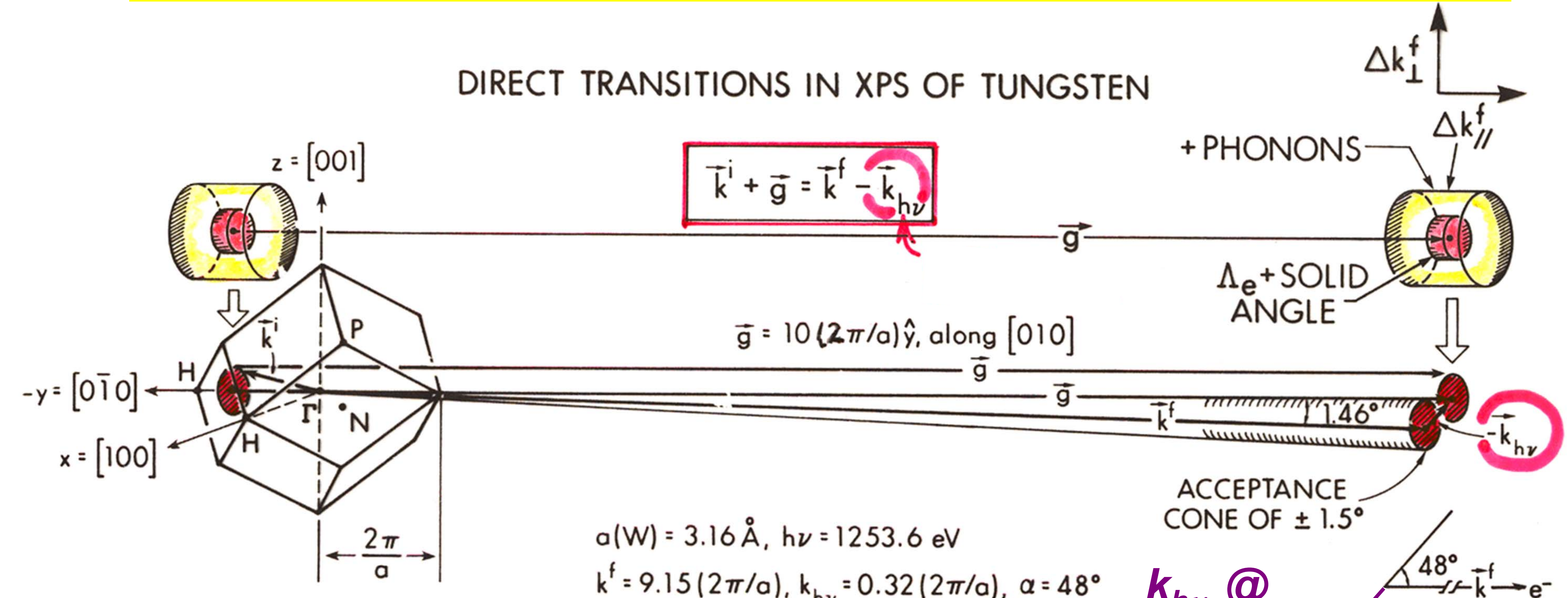

$k_{h\nu}$ @ 1,253 eV

Additional effects at higher energies:

- **Non-dipole--the photon momentum $k_{h\nu}$**
- **Angular acceptance→B.Z. averaging**
- **Lattice recoil→phonon creation→more B.Z. averaging,**

  Fraction DTs ≈ Debye-Waller factor = $W(T) \approx exp[-(k^f)^2 \langle u^2(T)\rangle]$

  $\approx exp[-C_1 (k^f)^2 T/(m\Theta_D^2)] \approx exp(-C_2 E_{kin} T)$

  →the "XPS limit" of full B.Z. averaging and D.O.S. sensitivity

  →core-like photoelectron diffraction

Hussain et al., Phys. Rev. B 22, 3750 (1980)

Takata et al., Phys. Rev. B 75, 233404 (2007)

Alvarez et al., PR*B* 54, 14703 (1996)

- **Recoil leads to peak shifts and broadening:** $E_{recoil}(eV) \approx \left[\frac{m_e}{M}\right] E_{kin} \approx 5.5 \times 10^{-4} \left[\frac{E_{kin}(eV)}{M(amu)}\right]$

Tungsten--Debye-Waller Factor and Recoil Energy

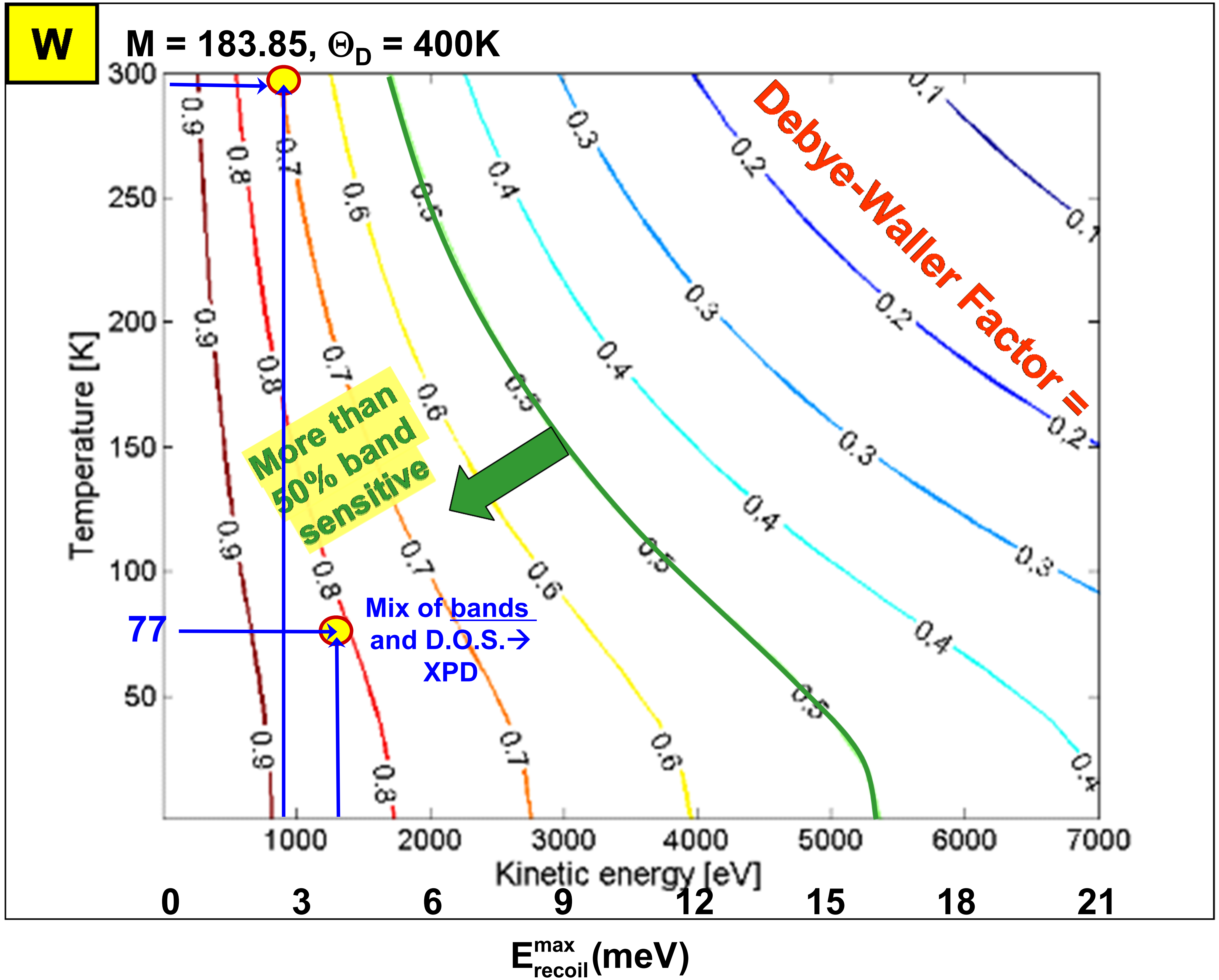

L. Plucinski, et al. PRB 78, 035108 (2008)

Angle-Resolved Photoemission (ARPES) with soft x-rays: W(110) at 860 eV

One-electron, free-electron final-state theory

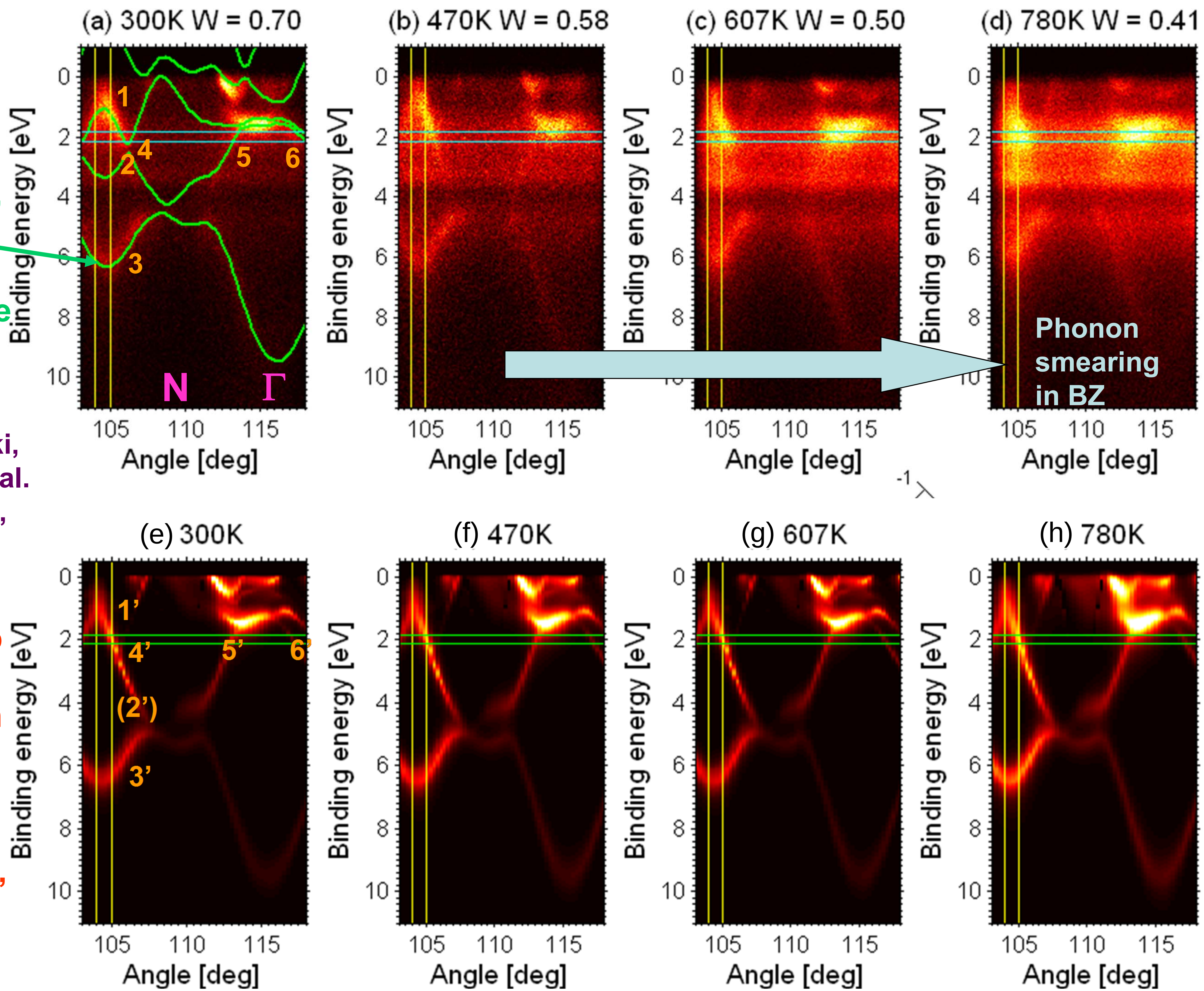

Plucinski, Minar, et al. PRB 78, 035108 (2008)

One-step Photoemission theory, with matrix elements, phonons not proper

ARPES with a non-monochromatized lab. x-ray source: hν = 1253.6 eV, T = ~77K, W = 0.82

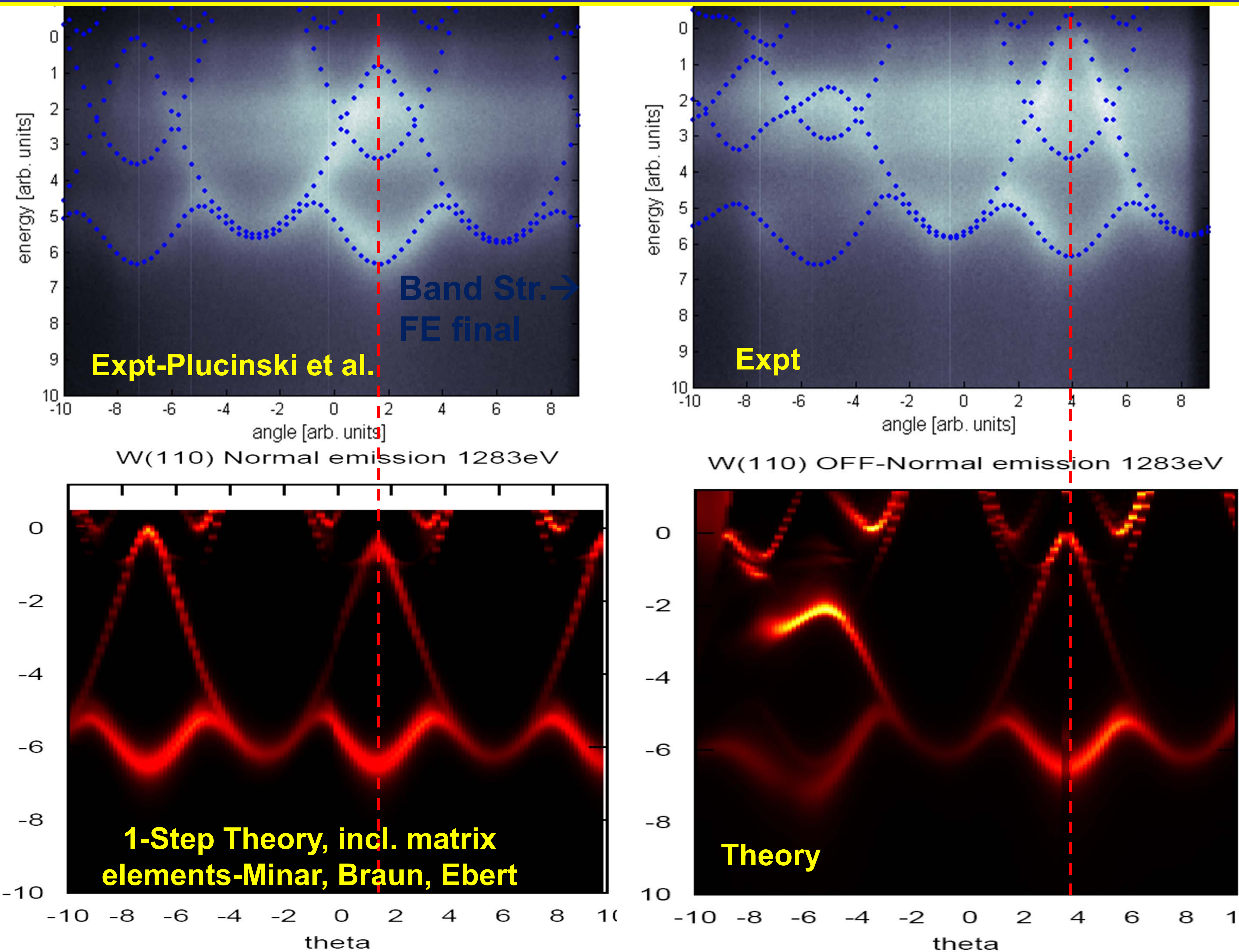

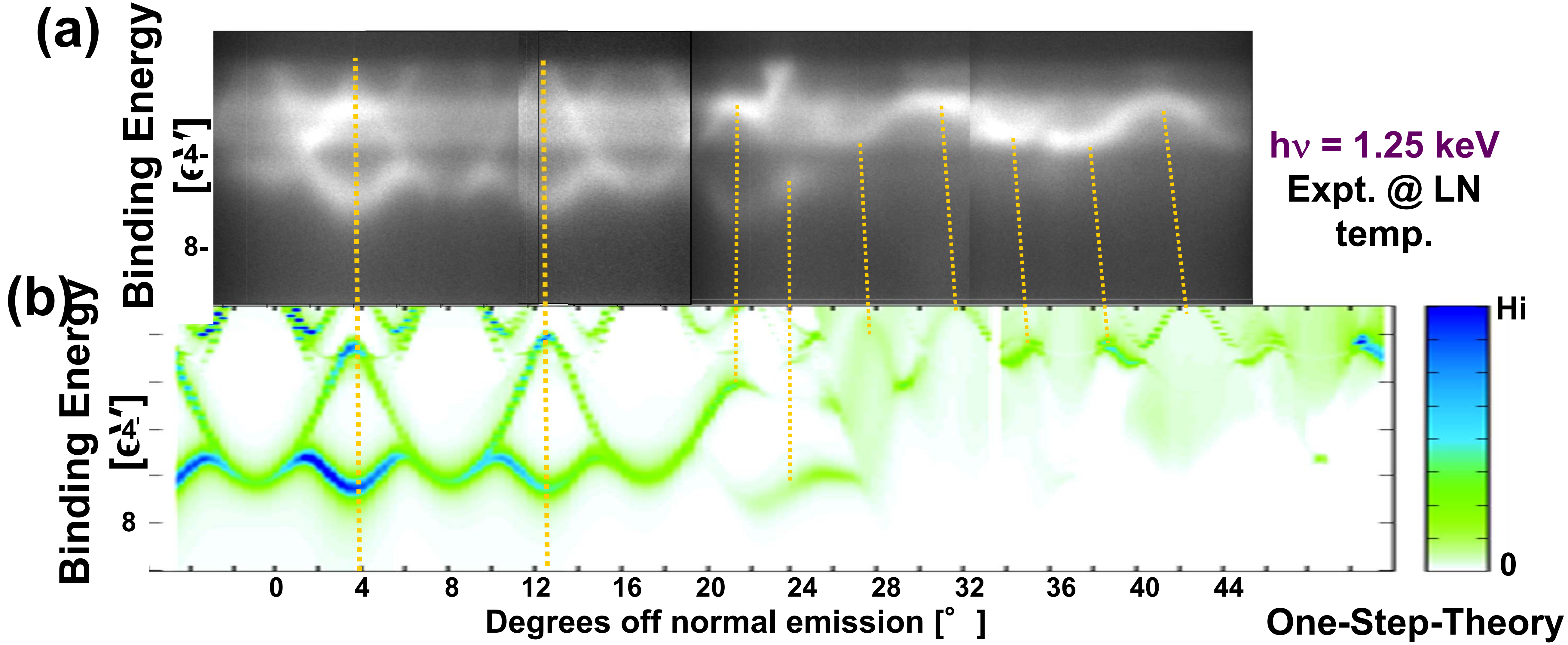

Soft x-ray ARPES from W(110)

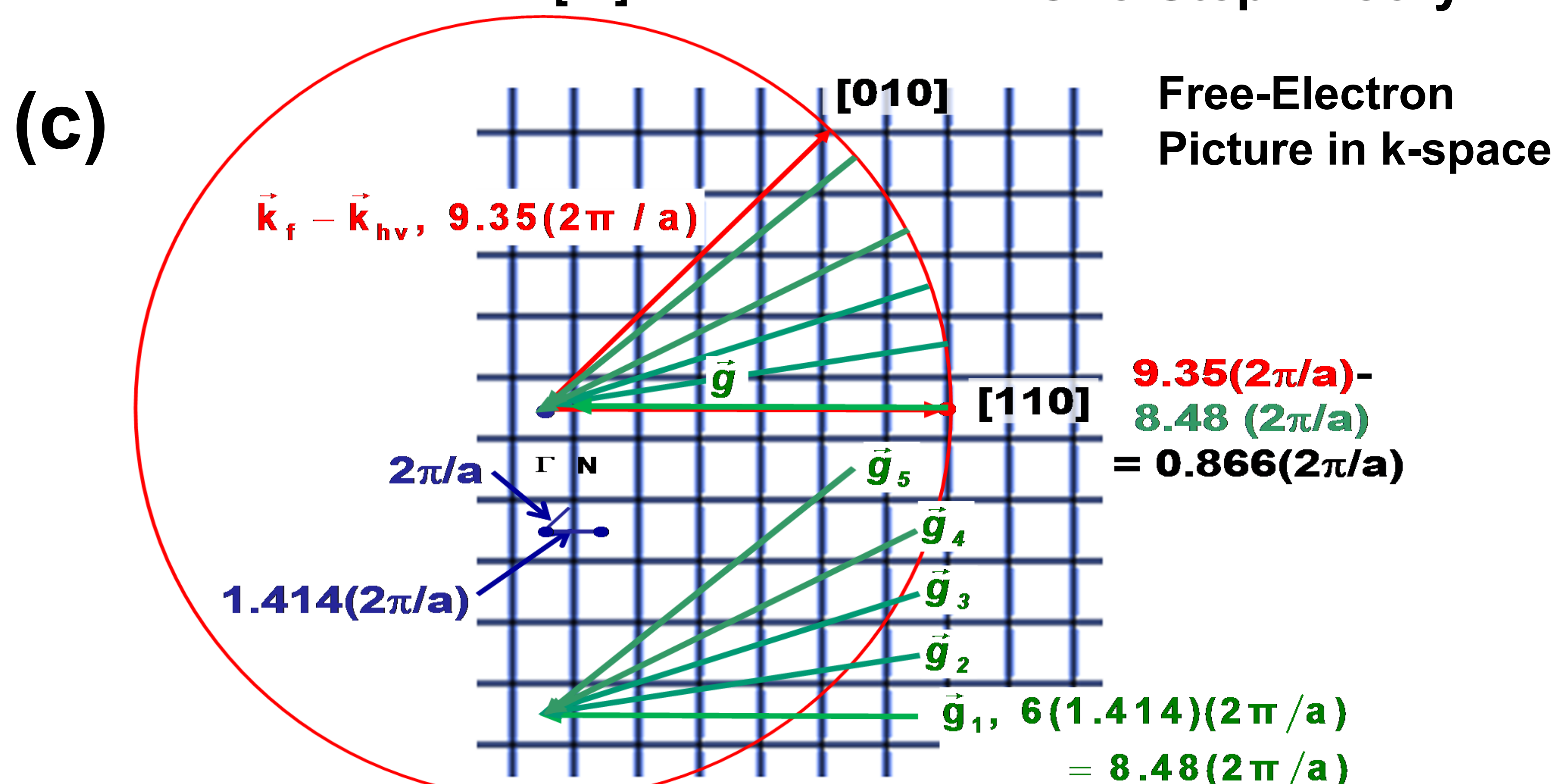

Papp, Plucinski, Minar, Phys. Rev. B, in press- SPring8

Tungsten--Debye-Waller Factor and Recoil Energy

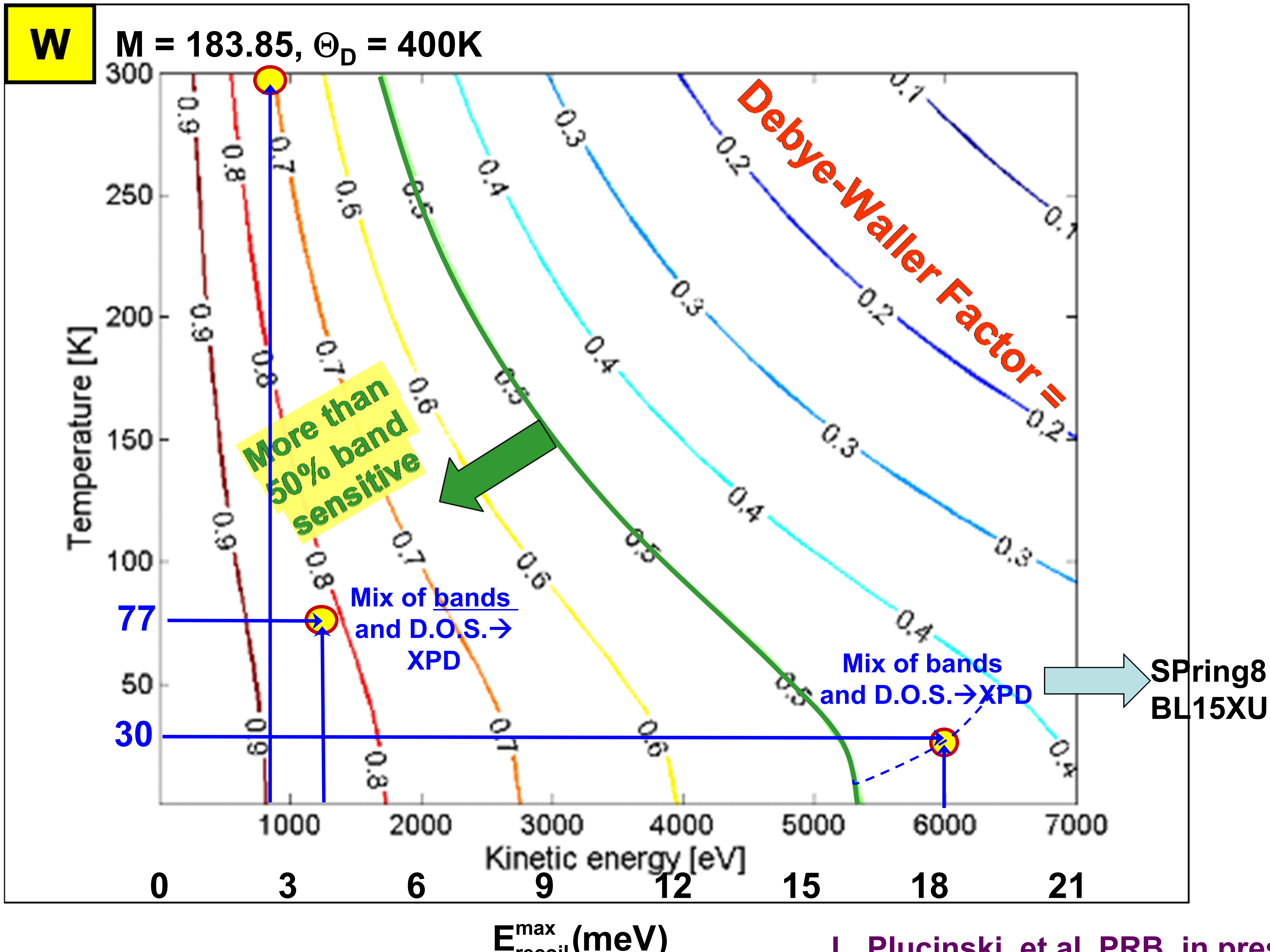

L. Plucinski, et al. PRB, in press

A. Gray et al., Nature Mat., to appear

SPring8

For W(110): hν = 5,946 eV: Where are we in the Brillouin Zone?
Calculation of Photon Momentum Effect on *k* Conservation

The free-electron picture:

$(2\pi / a) = 1.988\ A^{-1}$

hν = 5945 eV

$|\vec{k}_f| = 0.512 E_{kin}^{0.5}(eV) = 39.48\ A^{-1} = 19.85\ (2\pi / a)$

$|\vec{k}_{h\nu}| = 0.000507(h\nu(eV)) = 3.01\ A^{-1} = 1.51\ (2\pi / a)$

$|\vec{k}_f - \vec{k}_{h\nu}| = [39.48^2 + 3.01^2] = 39.59\ A^{-1} = 19.91\ (2\pi / a) --> 14.08\ [1.414((2\pi / a)]$

$|\vec{g}_1| = 14.00\ [1.414((2\pi / a)]$

Angular deflection due to $\vec{k}_{h\nu}$ is : arctan(3.01 / 39.48) = 4.35°

$\Gamma - N - \Gamma$ is 1.414(2π / a), so angular range of this is arctan(1.414/19.19) = 4.21°

Experiment in the Extended Brillouin Zone

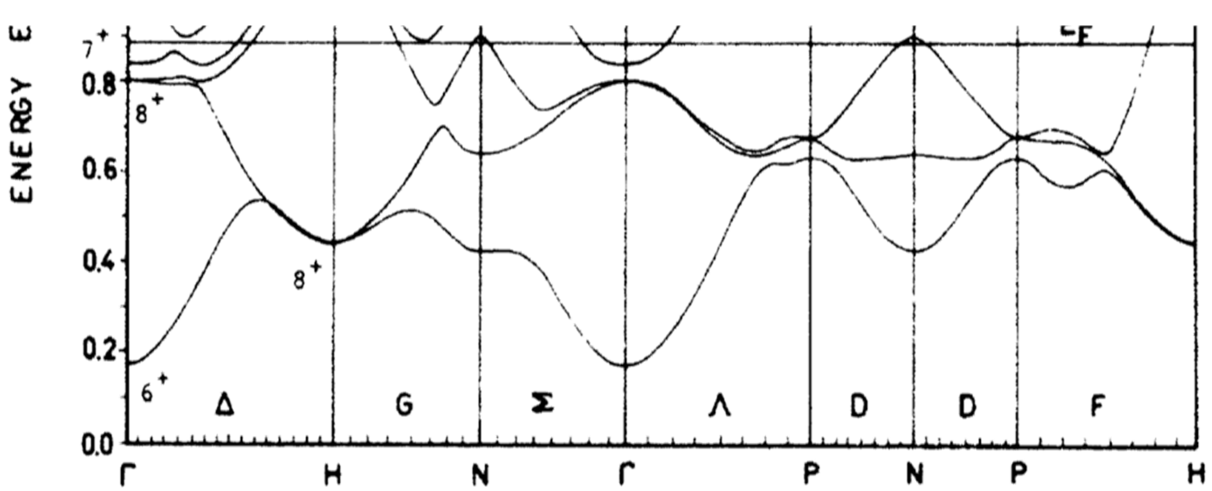

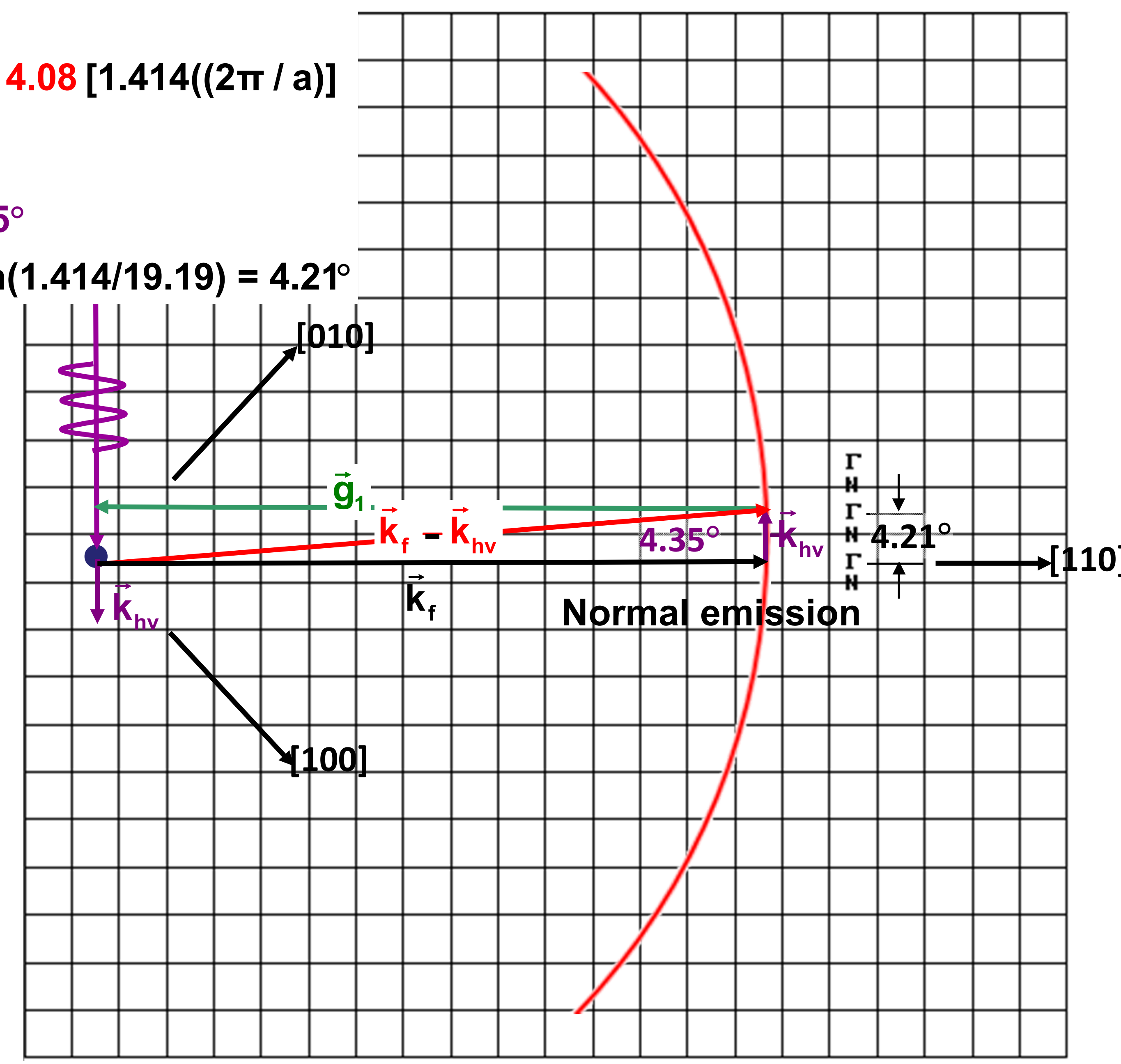

Papp, Gray, Ueda, Minar, Kobayashi, et al., Nature Materials, to appear

For W(110): hν = 5,946 eV: Where are we in the Brillouin Zone?
Calculation of Photon Momentum Effect on *k* Conservation

The free-electron picture:

$(2\pi / a) = 1.988\ \text{A}^{-1}$

$h\nu = 5945\ \text{eV}$

$|\vec{k}_f| = 0.512 E_{kin}^{0.5}(\text{eV}) = 39.48\ \text{A}^{-1} = 19.85\ (2\pi / a)$

$|\vec{k}_{h\nu}| = 0.000507(h\nu(\text{eV})) = 3.01\ \text{A}^{-1} = 1.51\ (2\pi / a)$

$|\vec{k}_f - \vec{k}_{h\nu}| = [39.48^2 + 3.01^2] = 39.59\ \text{A}^{-1} = 19.91\ (2\pi / a) --> 14.08\ [1.414((2\pi / a)]$

$|\vec{g}_1| = 14.00\ [1.414((2\pi / a)]$

Angular deflection due to $\vec{k}_{h\nu}$ is : $\arctan(3.01 / 39.48) = 4.35°$

$\Gamma - N - \Gamma$ is $1.414(2\pi / a)$, so angular range of this is $\arctan(1.414/19.19) = 4.21°$

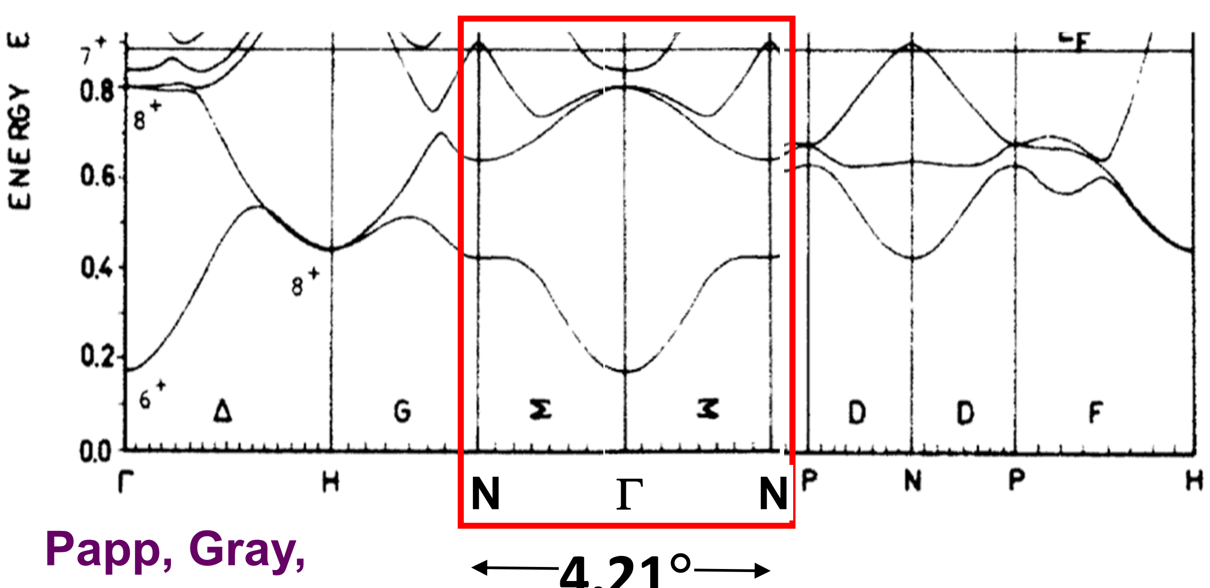

Papp, Gray, Ueda, Minar, Kobayashi, et al., Nature Materials, to appear

Experiment in the Extended Brillouin Zone

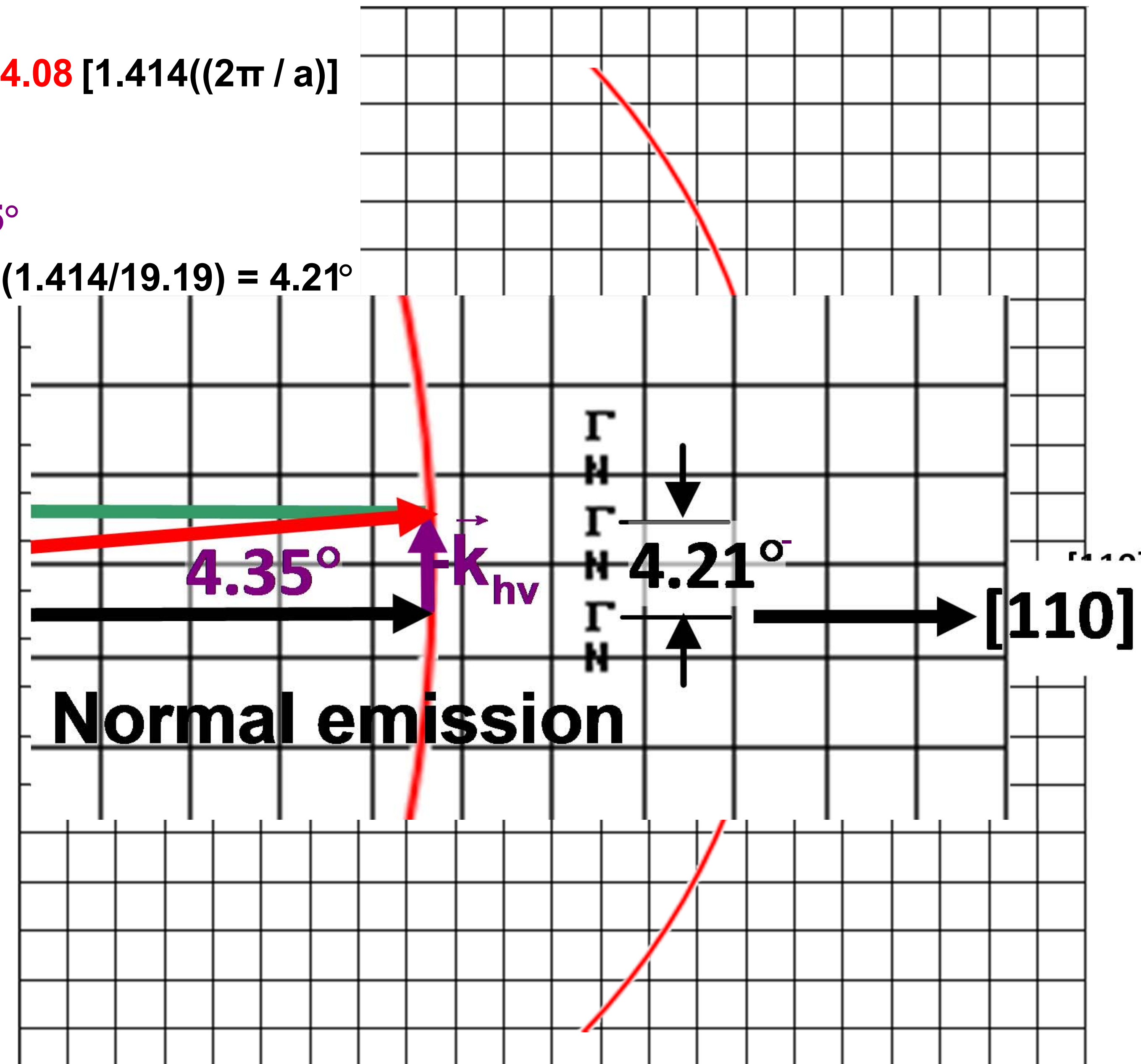

W(110), hν = 5,954 eV, T = 30K: Comparison to one-step theory, matrix elements

W = 0.45

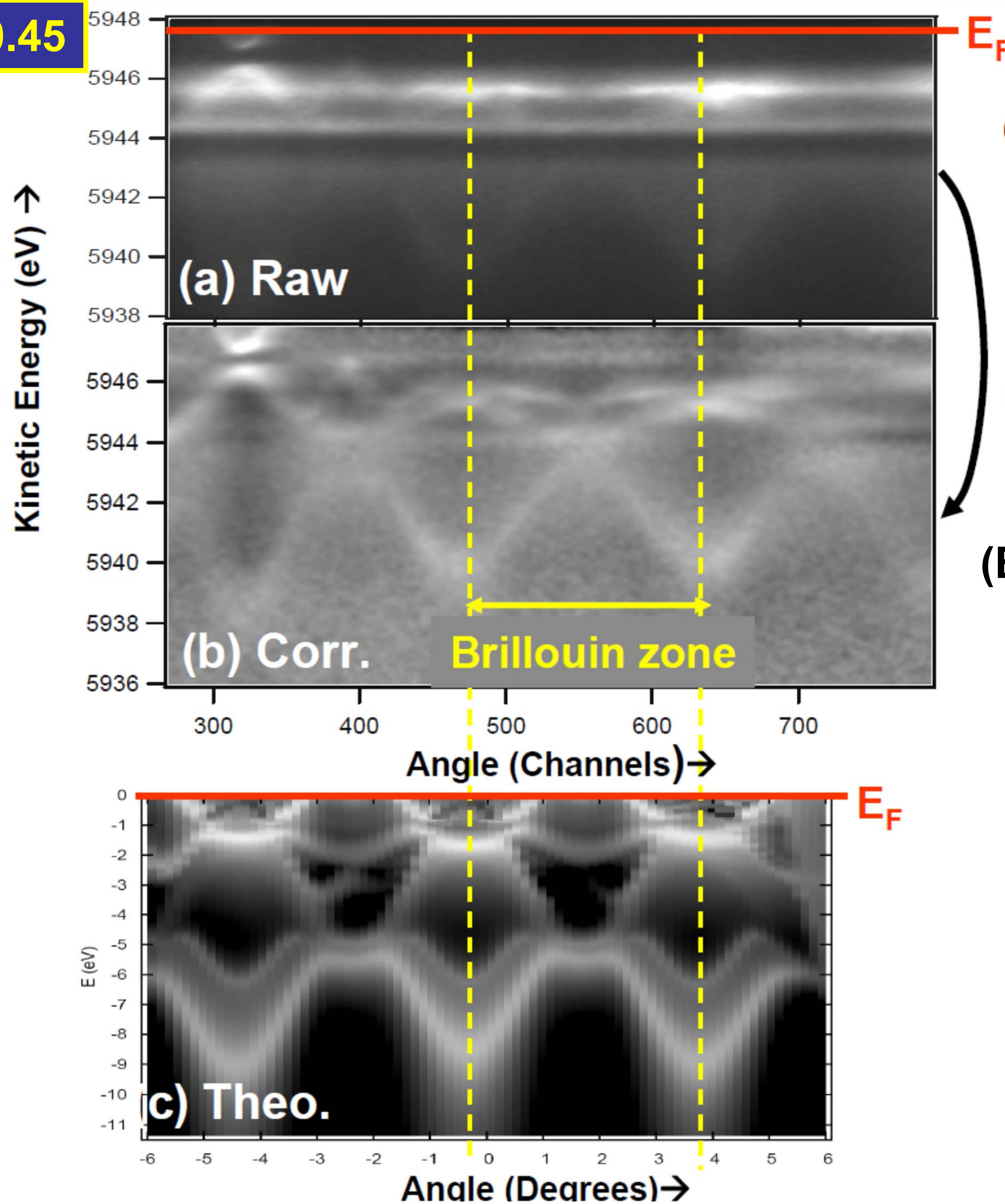

Corrected for phonon-induced density-of-states-like intensity

(Bostwick, Papp)

Expt.-Ueda, Kobayashi, SPring8
Data analysis-Papp, Gray, Plucinski, C.F.
Theory-Minar, Braun, Ebert

Tungsten and Germanium--Debye-Waller Factor and Recoil Energy

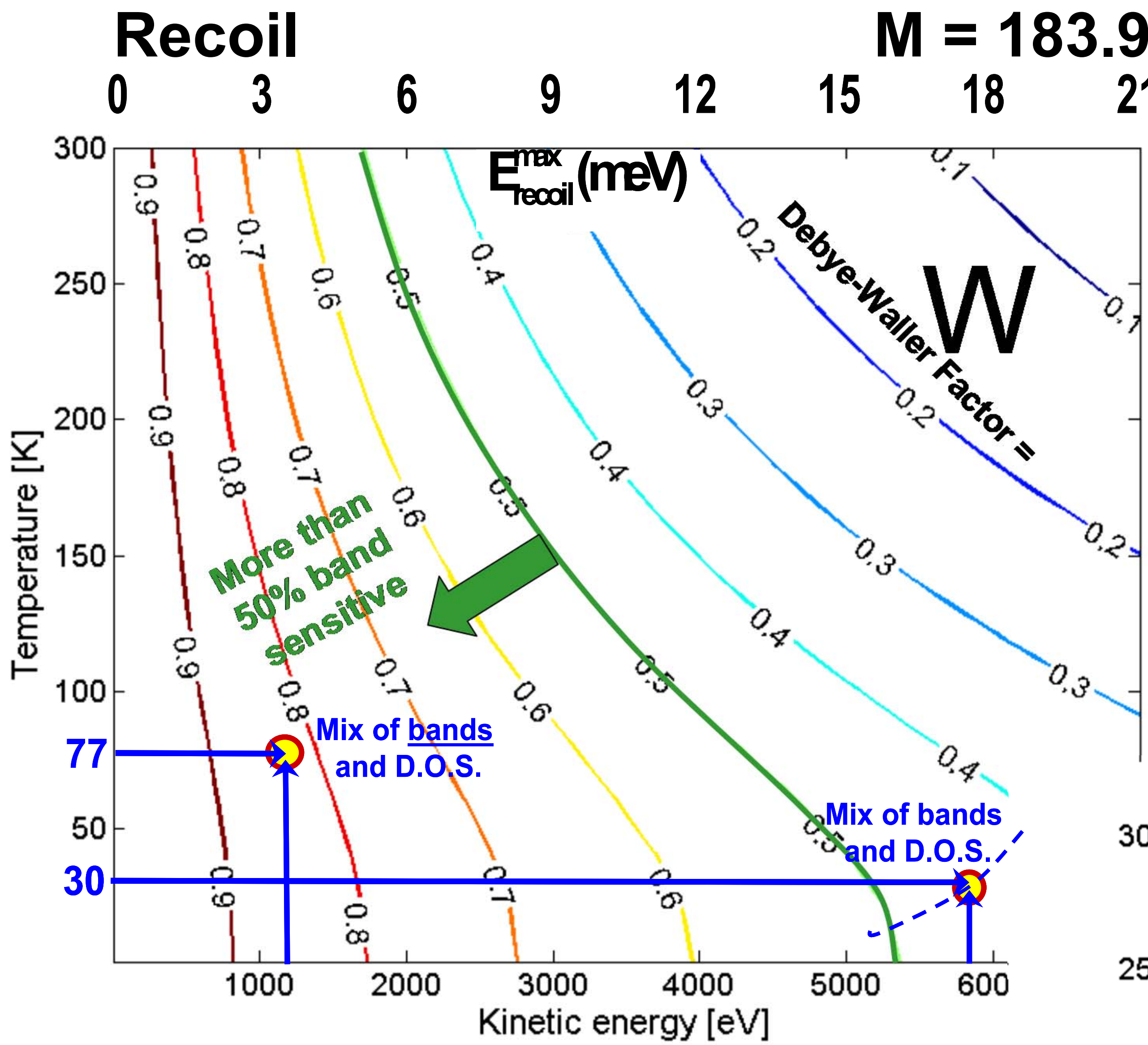

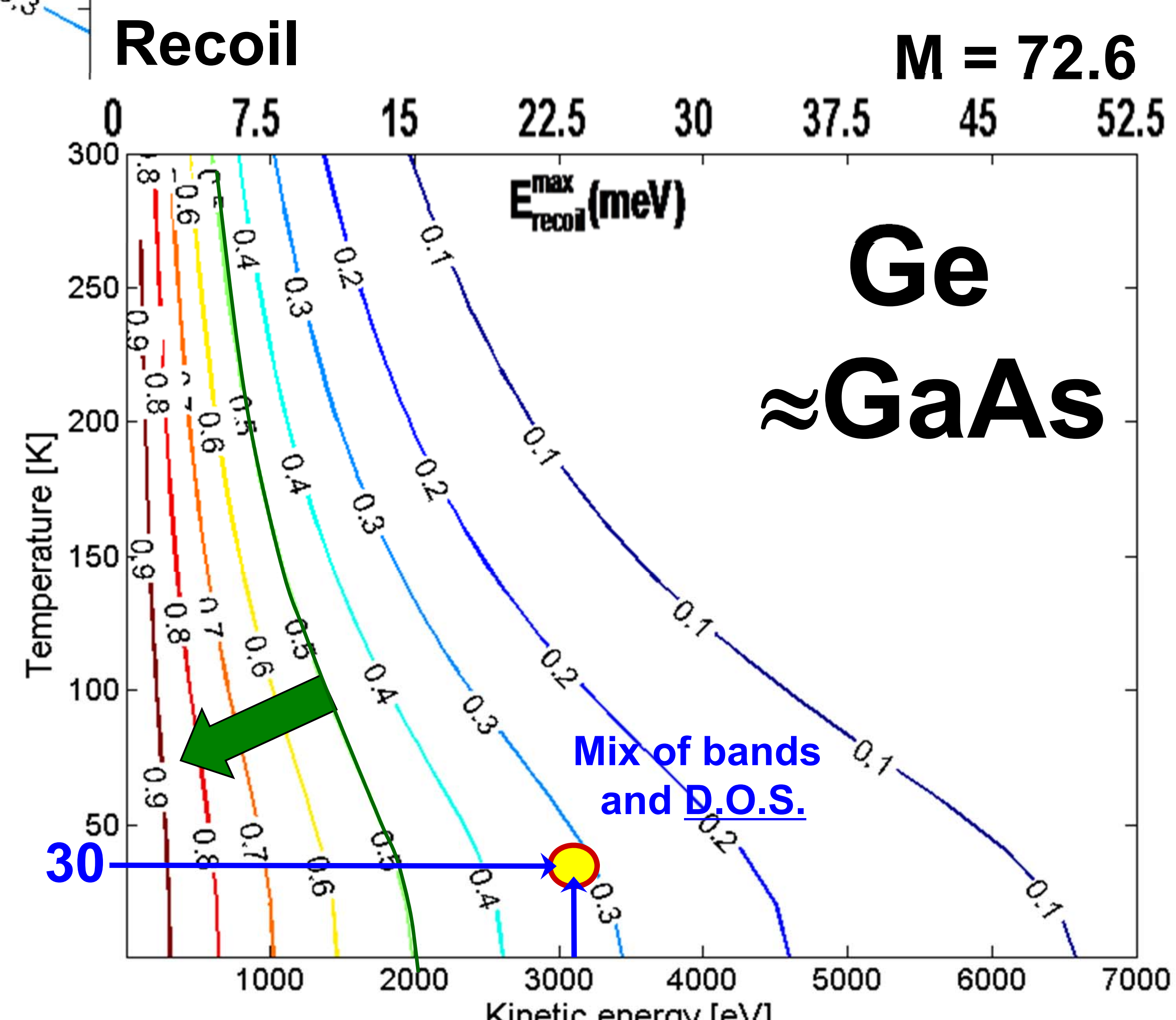

L. Plucinski

GaAs doped with Mn: a magnetic semiconductor $Ga_{0.96}Mn_{0.04}As$--HXPS: T = 20K, Broad Survey

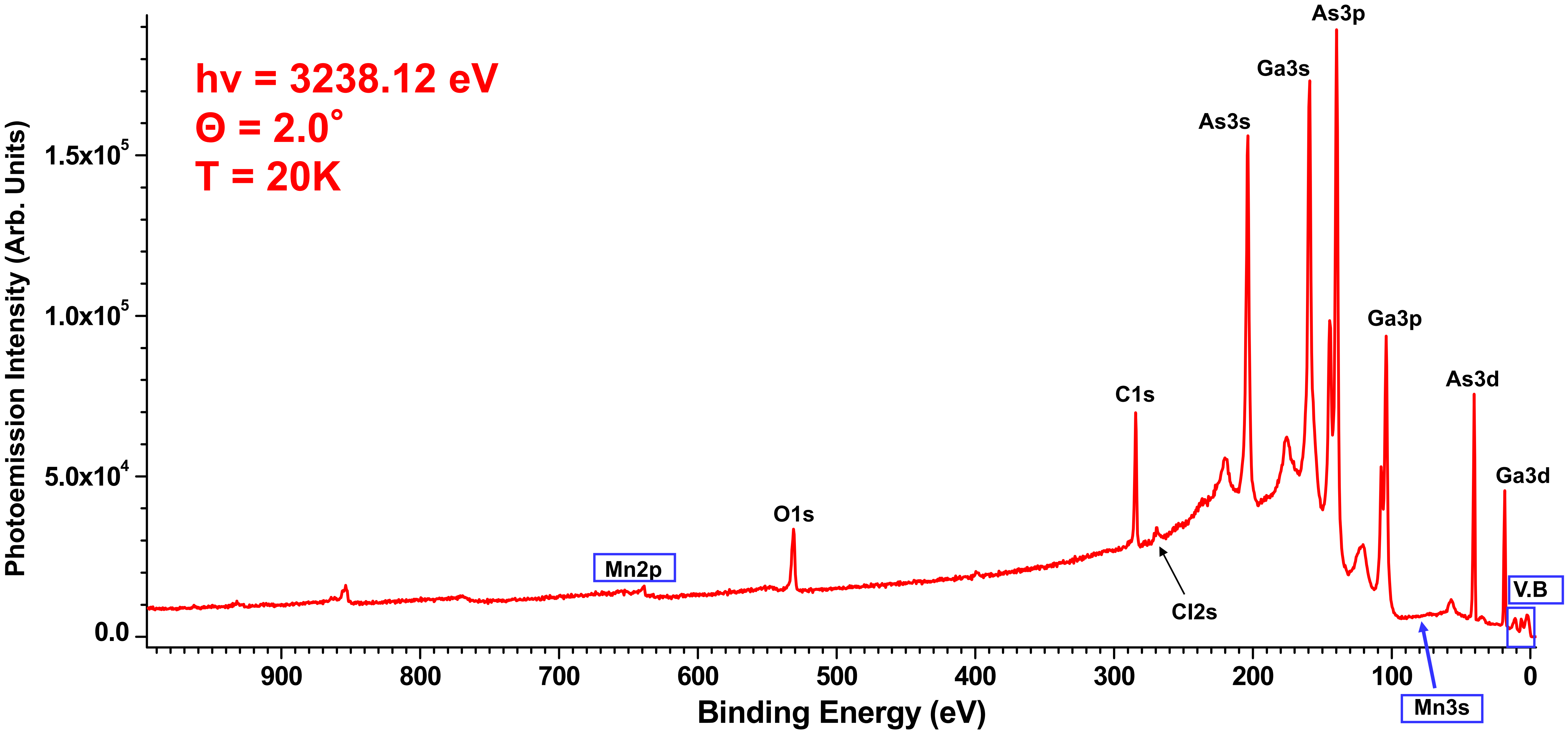

Samples: Stone, Dubon
Expt.-Gray, Papp, Ueda, Yamashita, Kobayashi
Theory- Pickett, Ylvisaker

GaMnAs--HXPS: T = 20K, Mn 2p

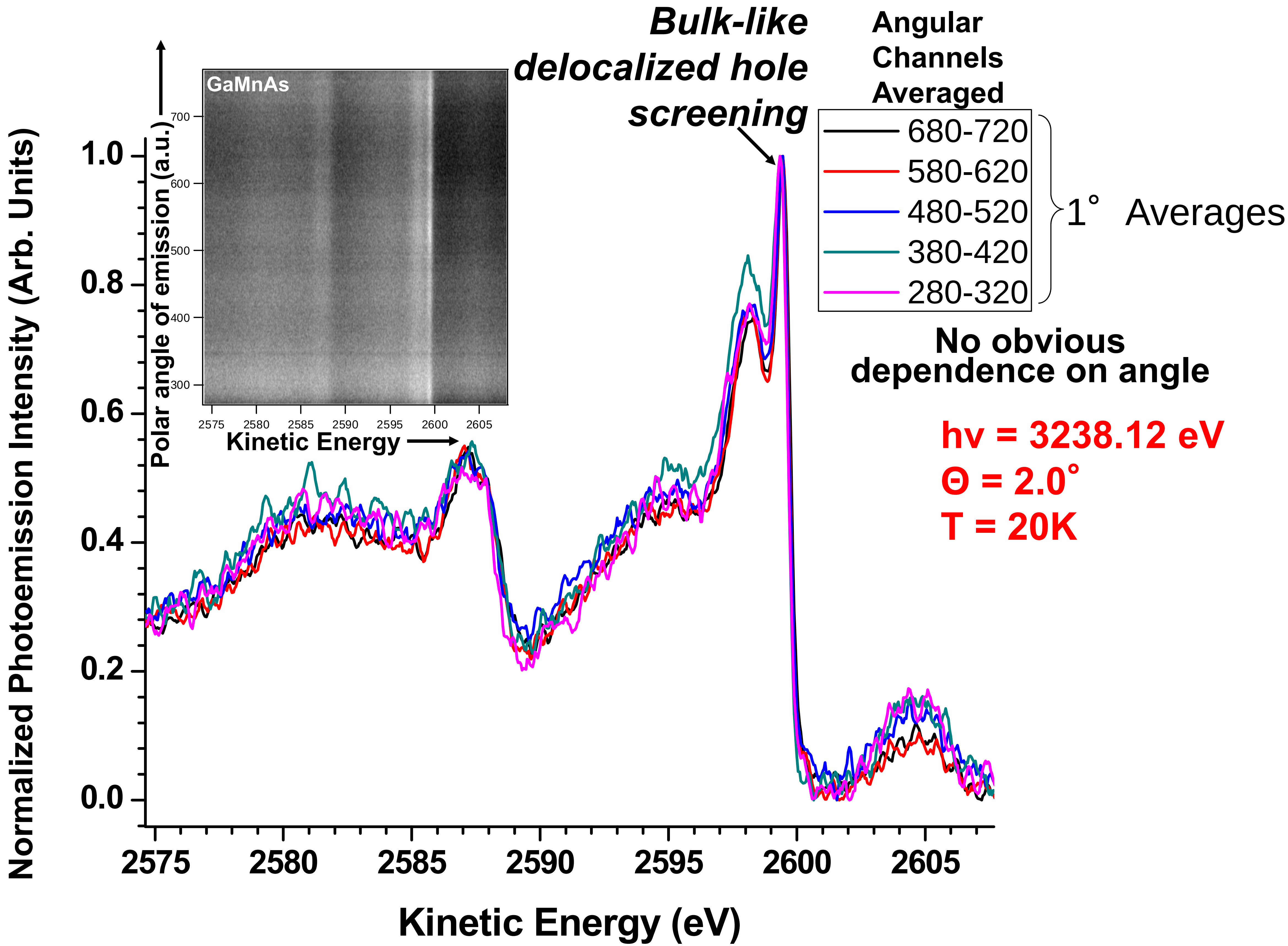

Additional data as a function of concentration from Fujii, Panaccione, et al.

GaMnAs--HXPS: T = 20K, Mn 3s

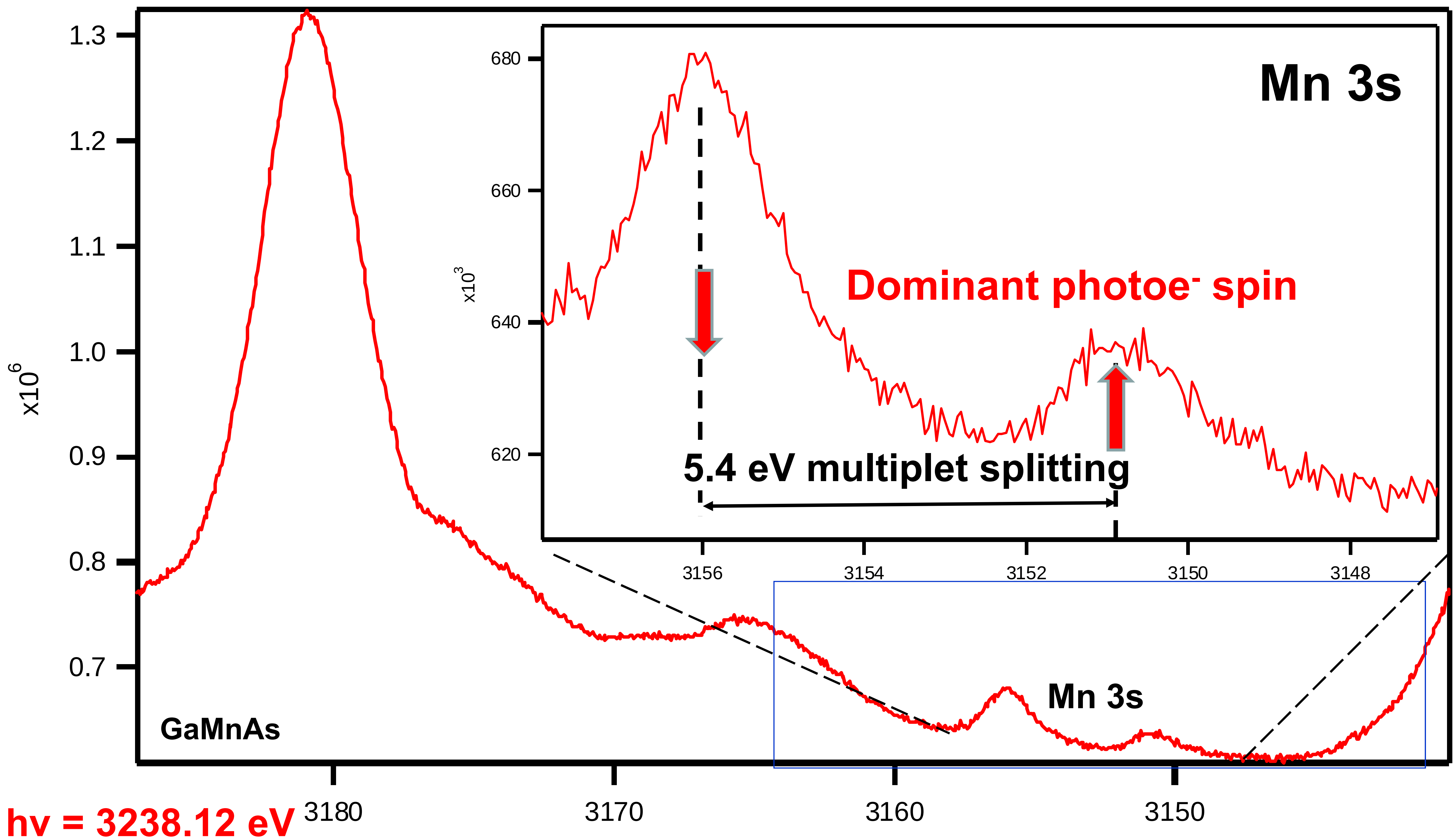

hv = 3238.12 eV
Θ = 2.0°
T = 20K

Calibration collection of Mn 3s splittings for various oxides

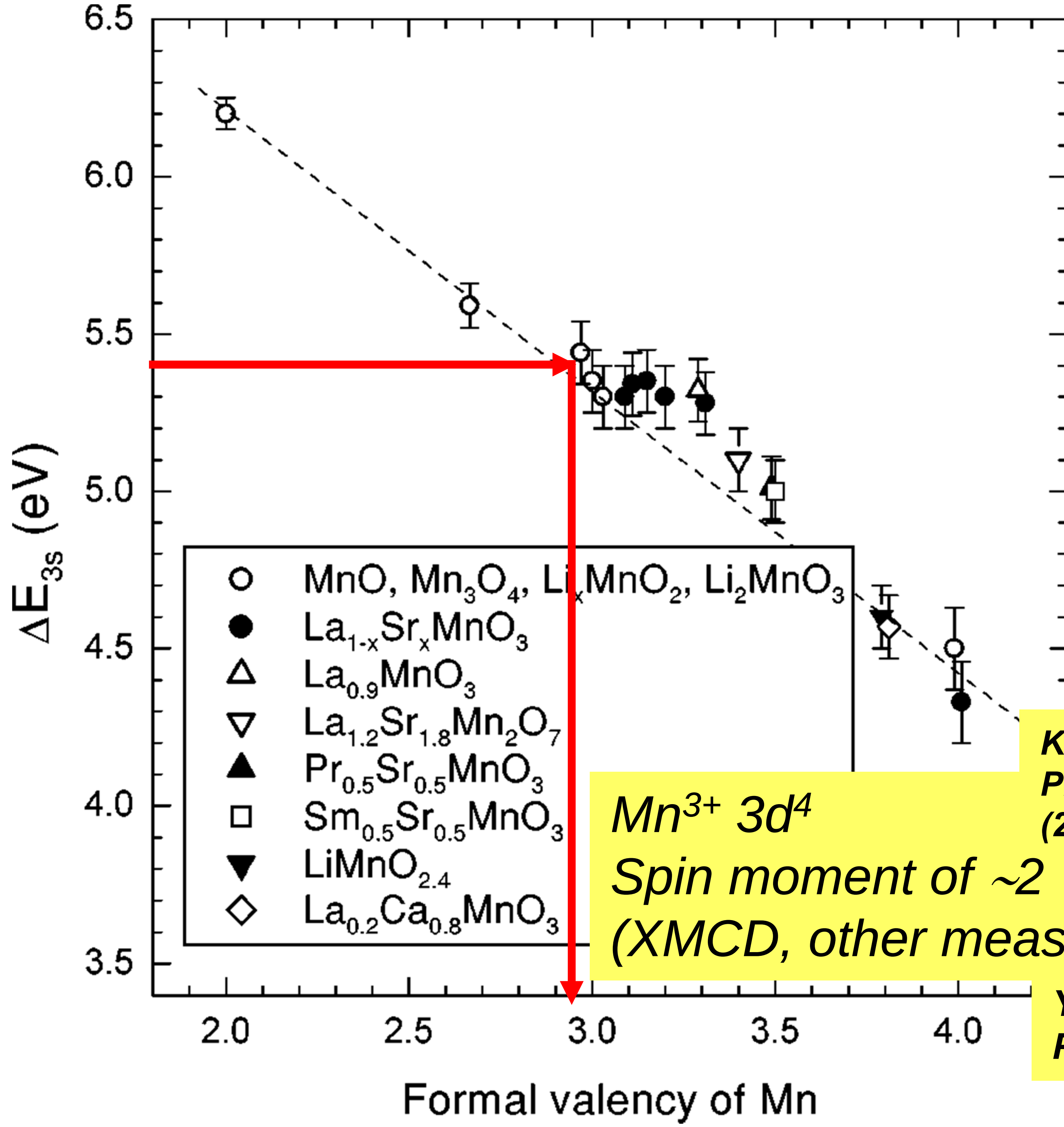

Mn^{3+} $3d^4$
Spin moment of ~2
(XMCD, other meas. yield 2.3-2.5)

K.W. Edmonds et al., Phys. Rev. B 71, 064418 (2005).

Y. Takeda et al. PRL 100, 247202 (2008)

Galakhov et al., PRB 65, 113102 (2002)

Hard x-ray ARPES from GaAs(001)-3.2 keV, 30 K, W = 0.31

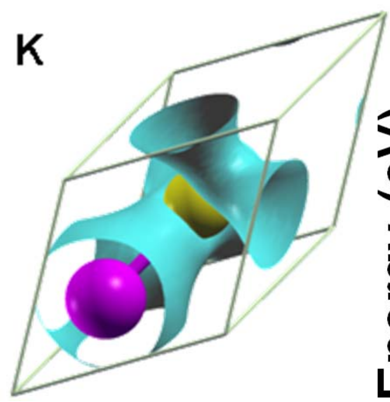

Band-like

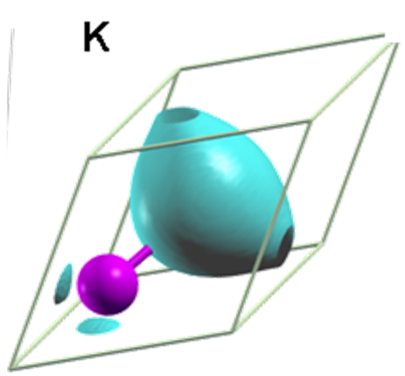

Core-like
As 4s
⇑
Charge densities

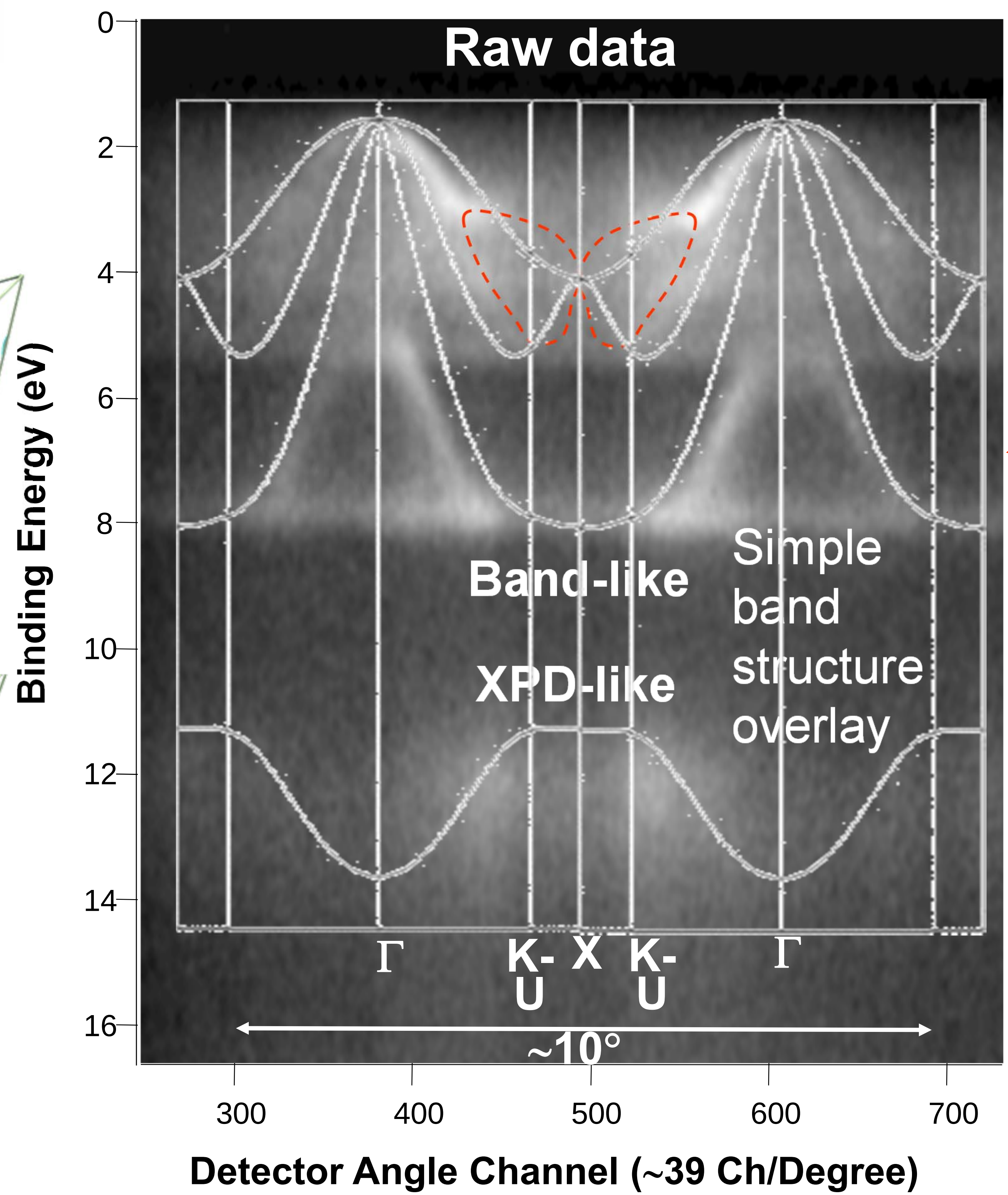

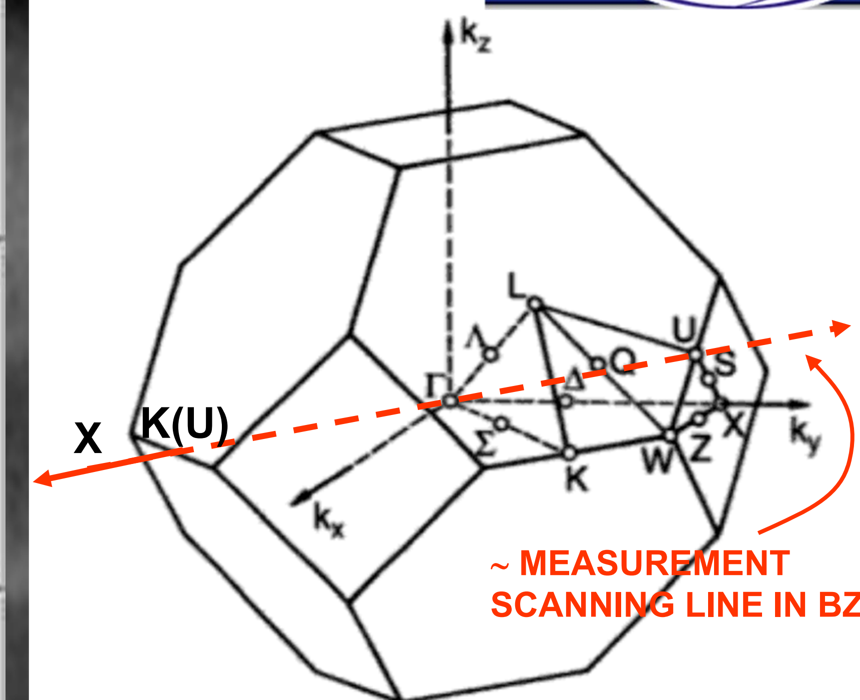

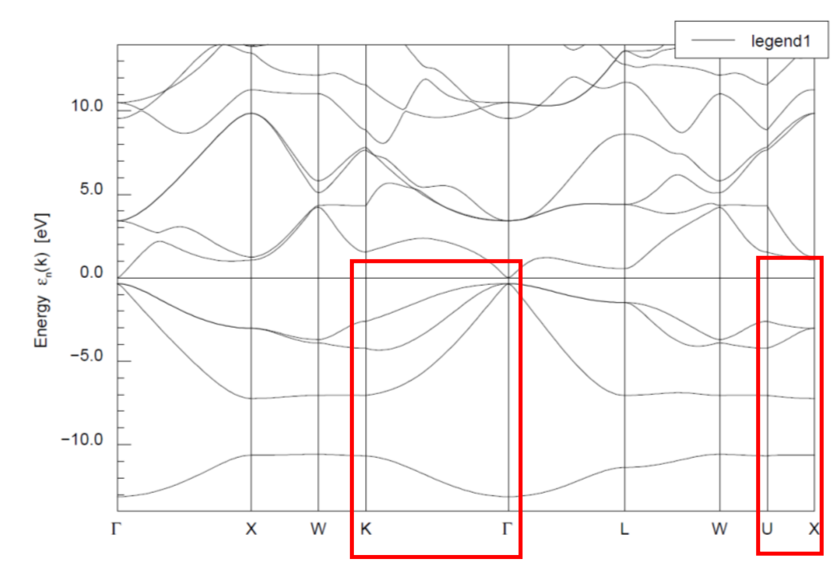

Expt.-Gray, Papp, Ueda, Yamashita, Kobayashi
Theory- Pickett, Ylvisaker

Comparing Experiment and One-Step KKR Theory
GaAs

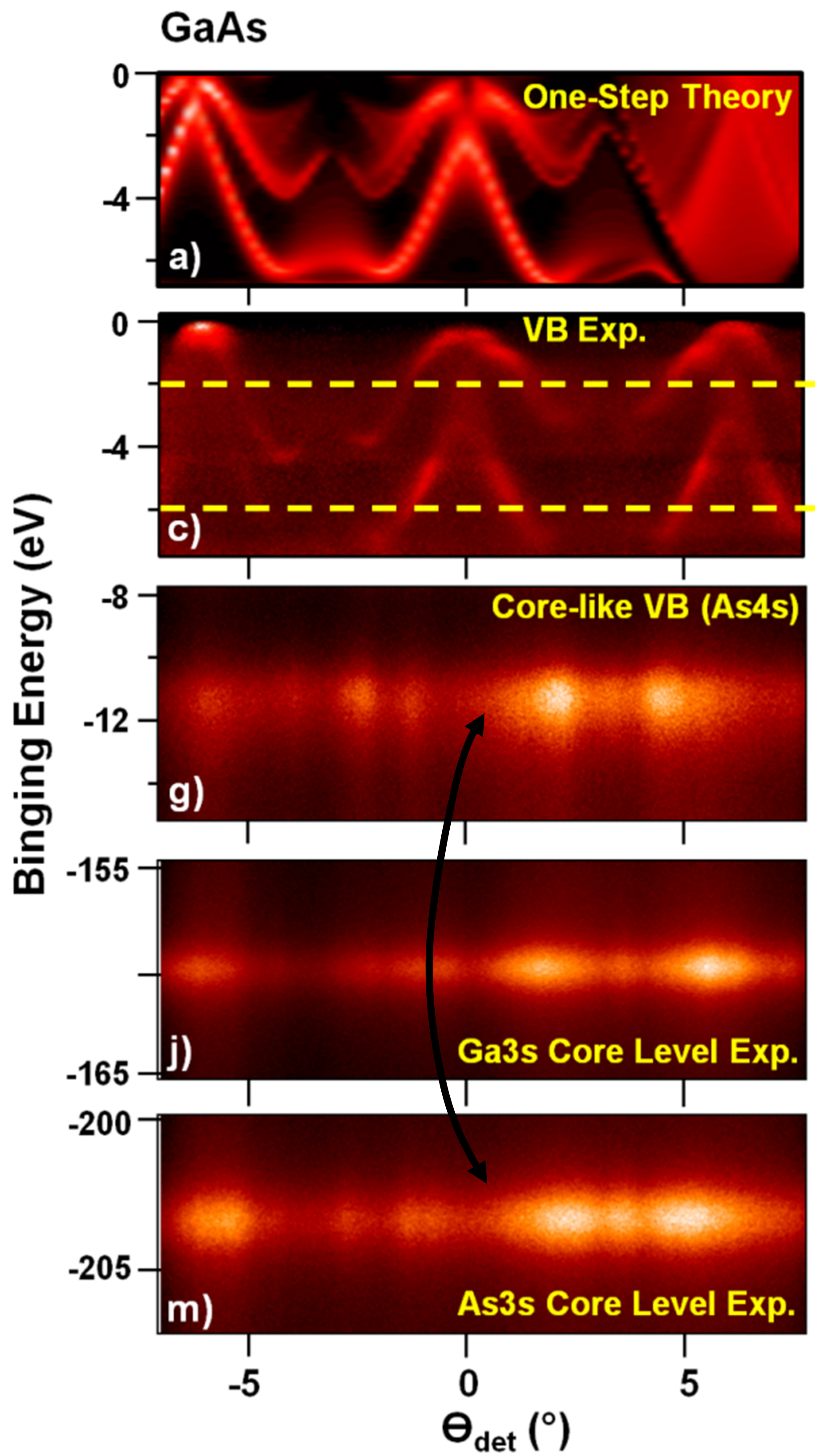

Gray, Papp, Ueda, Minar, Kobayashi, et al.,
Nature Materials, to appear

Comparing Experiment and One-Step KKR Theory
GaAs and $Ga_{0.96}Mn_{0.04}As$

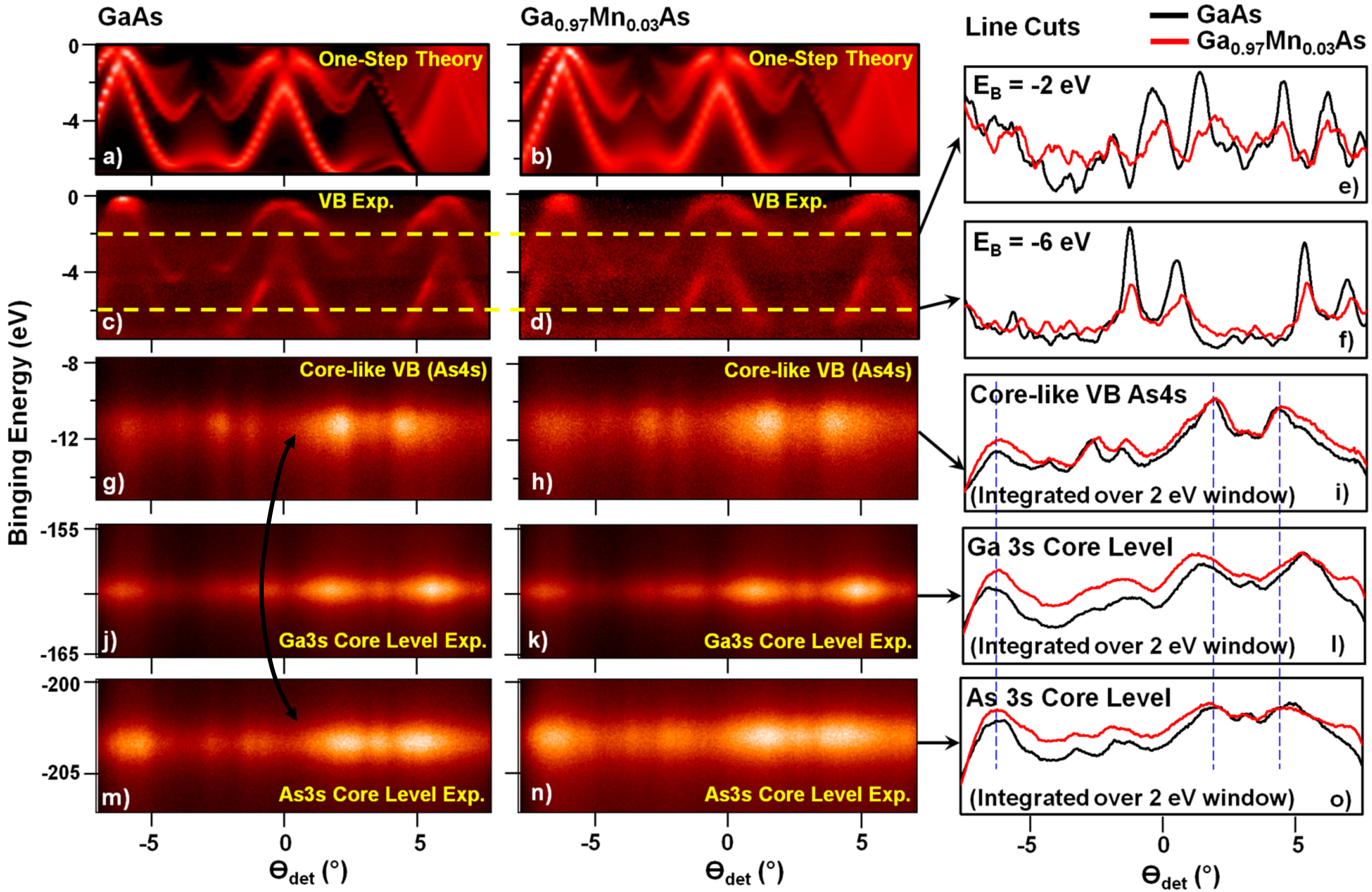

Gray, Papp, Ueda, Minar, Kobayashi, et al.,
Nature Materials, to appear

Photon energy for D-W = O.5 @ 20K

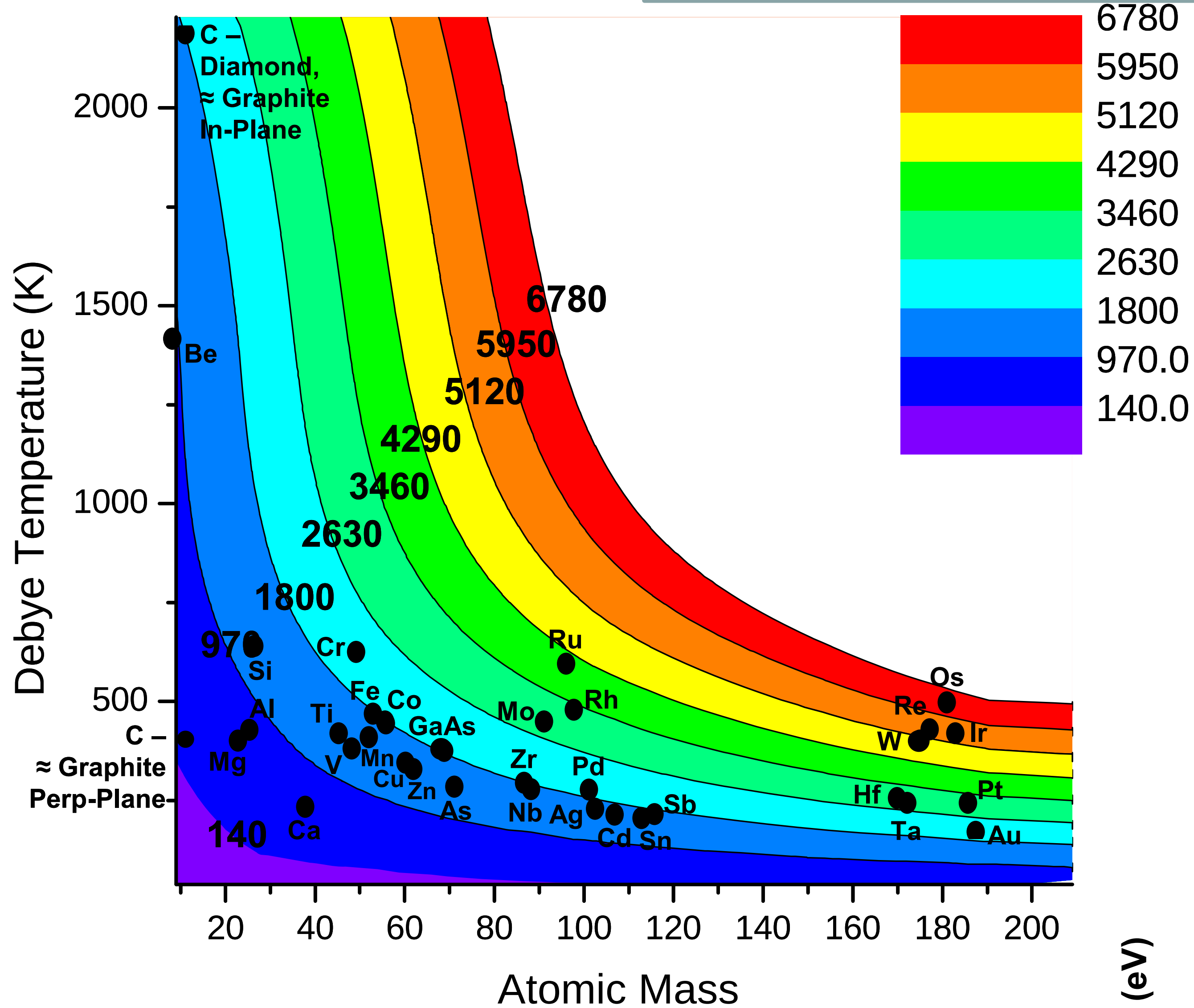

HARPES-How high can we go? Photoemission Debye-Waller Factors and Recoil Energies

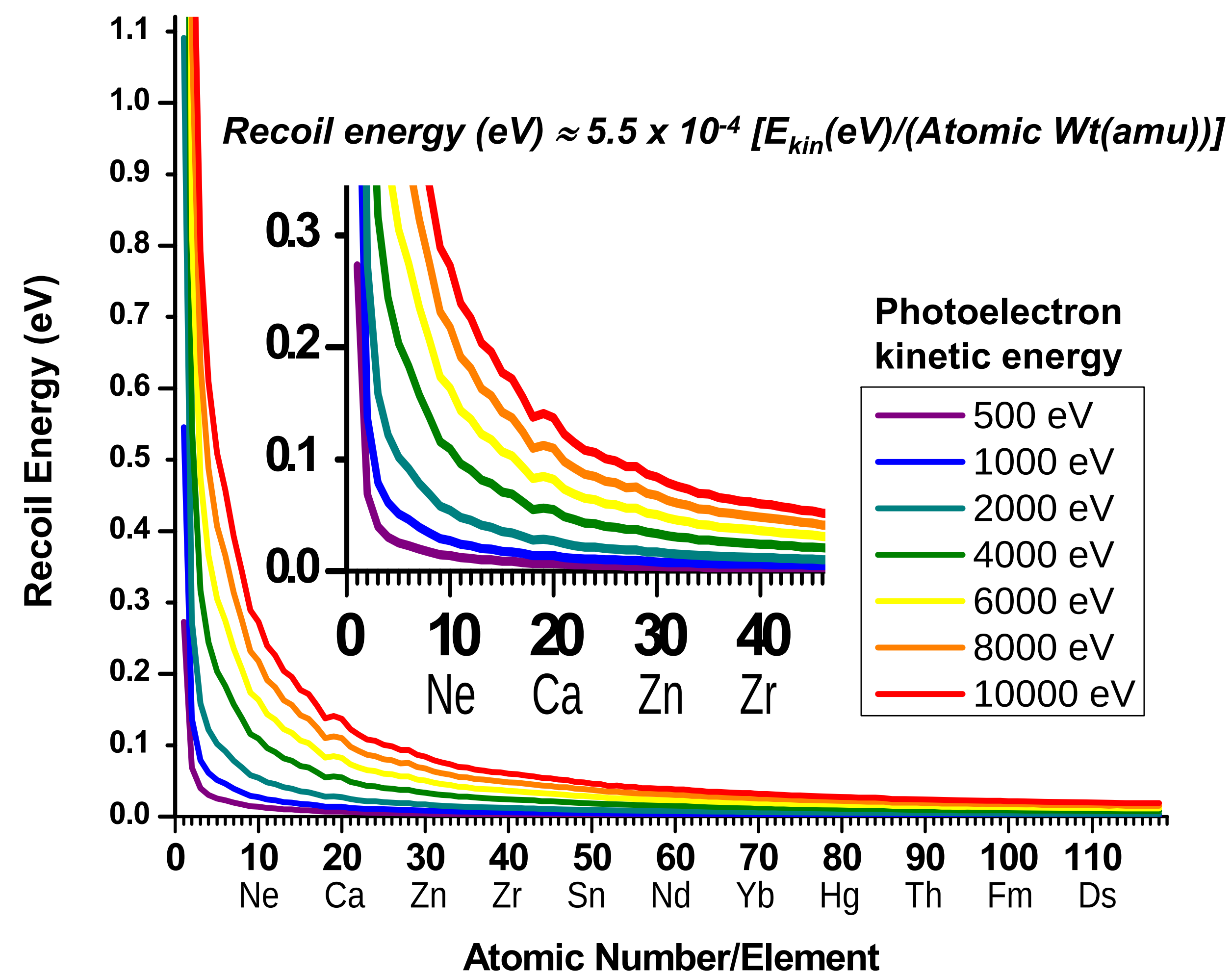

C. Papp. L. Plucinski, et al., Phys. Rev. B, in press

Hard x-ray photoemission—plusses and minusses

•**Plusses**

•More bulk sensitive spectra → a versatile tool for any new material or multilayer nanostructure

•Inelastic background less important & Augers more widely spread, less overlap

•Less radiation damage

•Easier interpretation of angle-resolved data → surface and bulk information

•Easier quantitative analysis via core spectra

•New "bulk fingerprint" satellite effects seen in both core and valence spectra

•Magnetic circular and linear dichroism and spin-resolved spectra for magnetic systems

•Bulk DOS info. at highest energies and temperatures

or

•3d "bulk" band mapping ARPES capability with cryocooling

• Hard x-ray photoelectron diffraction promising: dopants, lattice distortions

•Strong reflectivity and standing wave effects for depth-resolved properties

•Higher pressures possible in ambient pressure experiments, even windowed cell

Minusses

•Cross sections low, need special undulatorbeamline/spectrometer combinations—several solutions→ 1 micron focus and 10 meV resolution

•Intensity calculations must allow for photon wave vector, other non-dipole effects, but easy

•High *n*, low-ℓ cross section components strongly favored, but in VB they can be more involved in transport

•Resolution not as good as VUV PS, but as good/better than SX PS, and down to 50 meV overall, even lower, good enough for many applications

•Phonon effects reduce capability for ARPES at higher energies/temperatures

•Recoil energy limits resolution, esp. for lighter elements; complex systematics, depending on local bond distances/phonon frequencies→Doppler spectroscopy?

Photoemission for properties of bulk materials and complex multilayer heterostructures in spintronics

Core photoemission→XPS, X-ray photoelectron diffraction-XPD,…
Valence photoemission→UPS, SXPS
Higher energy a/o temperature→Densities of states-DOSs
Lower energy a/o temperature→Band mapping, Angle-resolved photoemission-ARPES
are very powerful techniques, but they:

- **are sometimes too strongly influenced by surface effects, if bulk or buried layer/interface properties are to be studied**

- **may not be able to selectively and quantitatively see buried-layer and interface properties**

Two ways to address these limitations:

- **use harder x-ray excitation (HAXPES, HXPS) for deeper probing: core (HXPD) and valence DOSs or hard x-ray ARPES (“HARPES”)**

- **use soft and hard x-ray standing waves to selectively look below the surface, including depth-resolved ARPES**

Outline

Photoemission: Some limitations, some new directions

6-8 keV

Hard x-ray photoemission of interesting bulk materials→core and valence spectra:
half-metallic/colossal magnetoresistive $La_{0.67}Sr_{0.33}MnO_3$
semiconducting CrAl alloy
metal-to-insulator transition in thin-film $LaNiO_3$

3.2 & 6 keV

Angle-resolved hard x-ray photoemission→HXPD: Kikuchi-band modeling, and HARPES for: W, GaAs & the magnetic semiconductor (Ga,Mn)As

833 & 6 keV

Standing-wave photoemission combining soft and hard x-rays, depth-resolved composition, densities of states and ARPES, and magnetization:
$SrTiO_3/La_{2/3}Sr_{1/3}MnO_3$ multilayer
Fe/MgO tunnel junction

500-700 eV

Standing-waves in a photoelectron microscope, adding the third dimension:
multilayers and microdots

Conclusions and Future Outlook

X-ray photoemission: some key elements

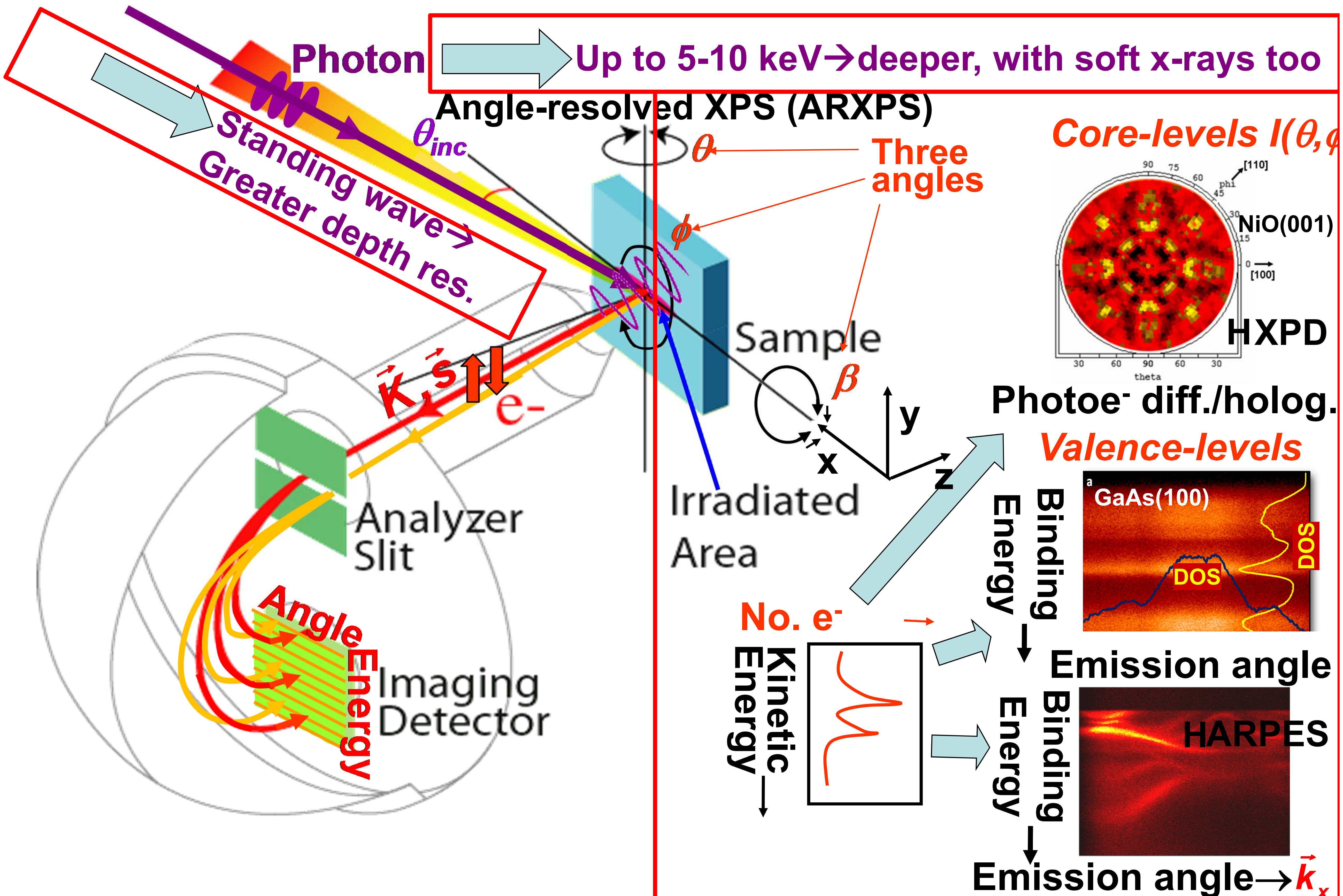

Some x-ray optical effects at 6 keV-theory, exchange bias system

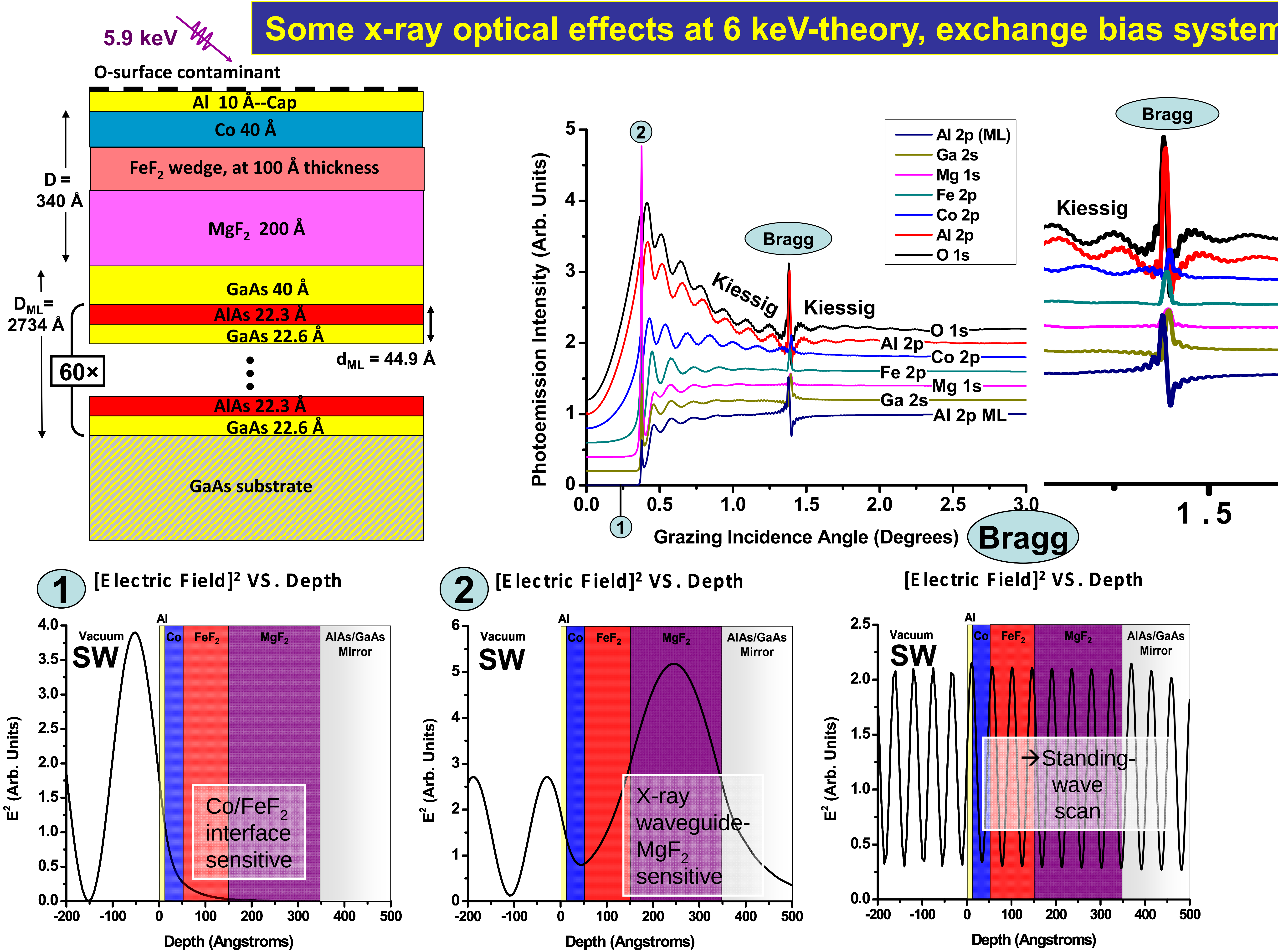

Standing wave formation in reflection from a surface, or single-crystal Bragg planes, or a multilayer mirror

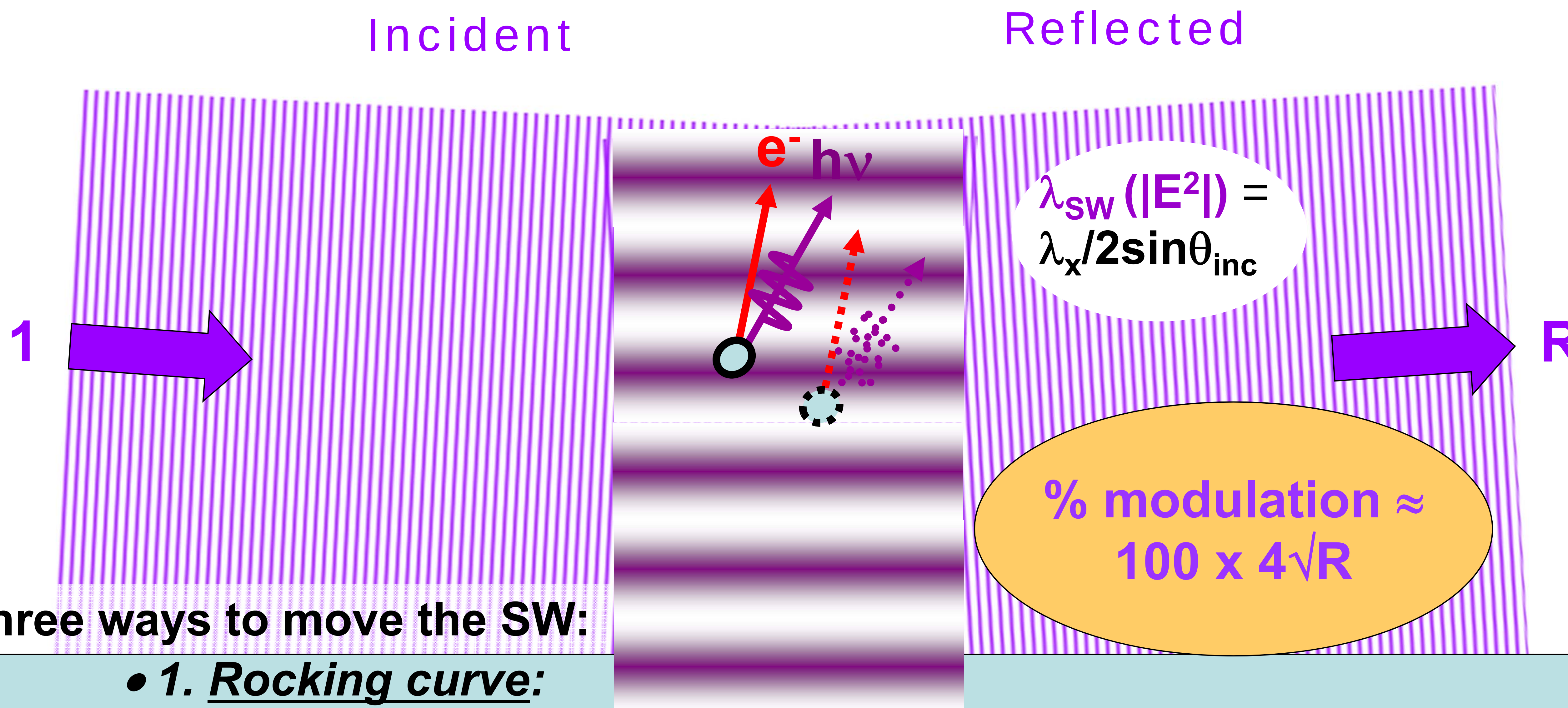

Three ways to move the SW:

- ***1. <u>Rocking curve</u>:***

$$I(\theta_{inc}) \propto 1 + R(\theta_{inc}) + 2\sqrt{R(\theta_{inc})}\, f \cos[\varphi(\theta_{inc}) - 2\pi P]$$

- ***2. <u>Photon energy scan</u>:***

$$I(h\nu) \propto 1 + R(h\nu) + 2\sqrt{R(h\nu)}\, f \cos[\varphi(h\nu) - 2\pi P]$$

with: f = coherent fraction of atoms, P = phase of coherent-atom/layer position

- ***<u>3. Phase scan with wedge-shaped sample ("Swedge" method):</u>***

C.S.F., Journal of Electron Spectroscopy and Related Phenomena 178–179 (2010) 2–32

Standing Wave Behavior During a Rocking Curve Scan

Reflectivity

Relative phase

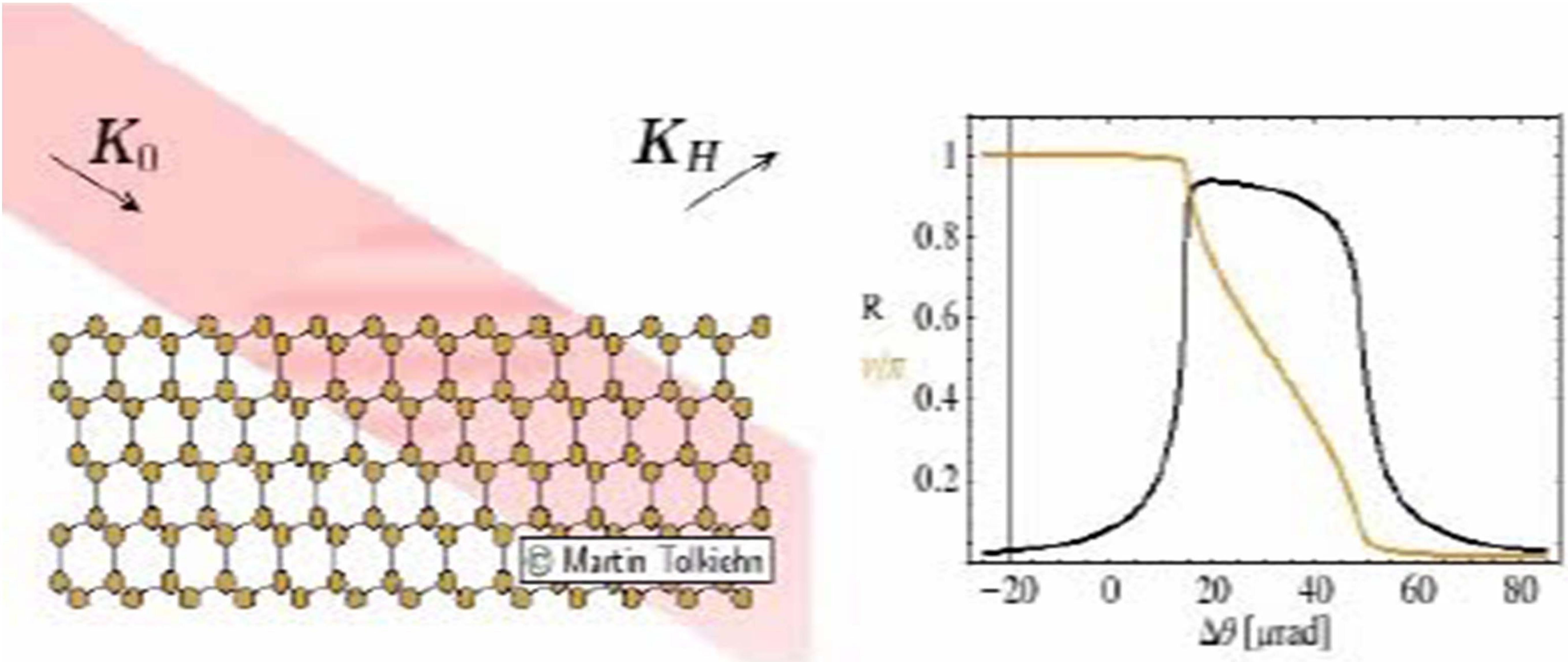

+Same general forms if photon energy is scanned

With thanks to Martin Tolkiehn, Dimitri Novikov, Hasylab

Case study: Standing wave/rocking curve analysis of an epitaxial $SrTiO_3/La_{0.67}Sr_{0.33}MnO_3$ interface: Resonant soft x-ray excitation

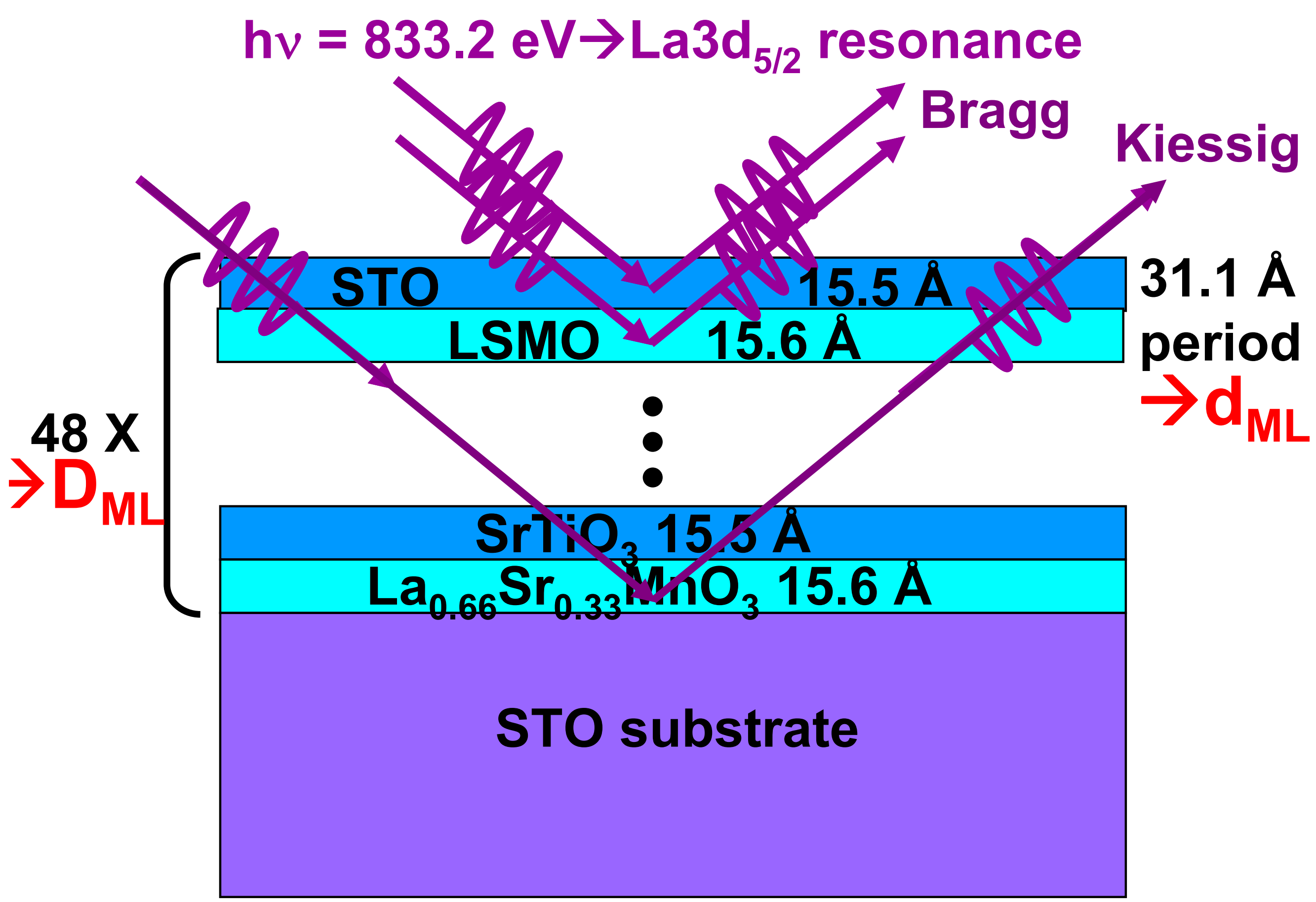

$$\lambda_x = 2d_{ML}\sin\theta_{Bragg}$$

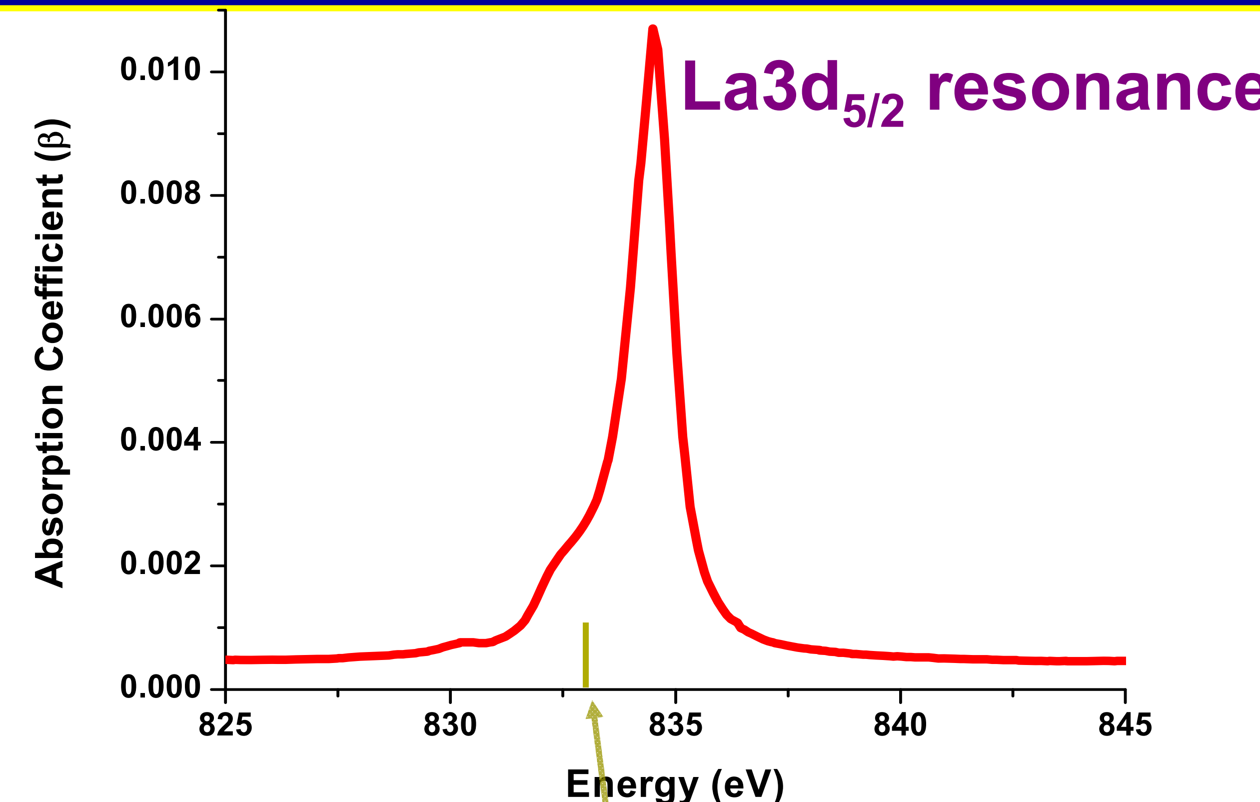

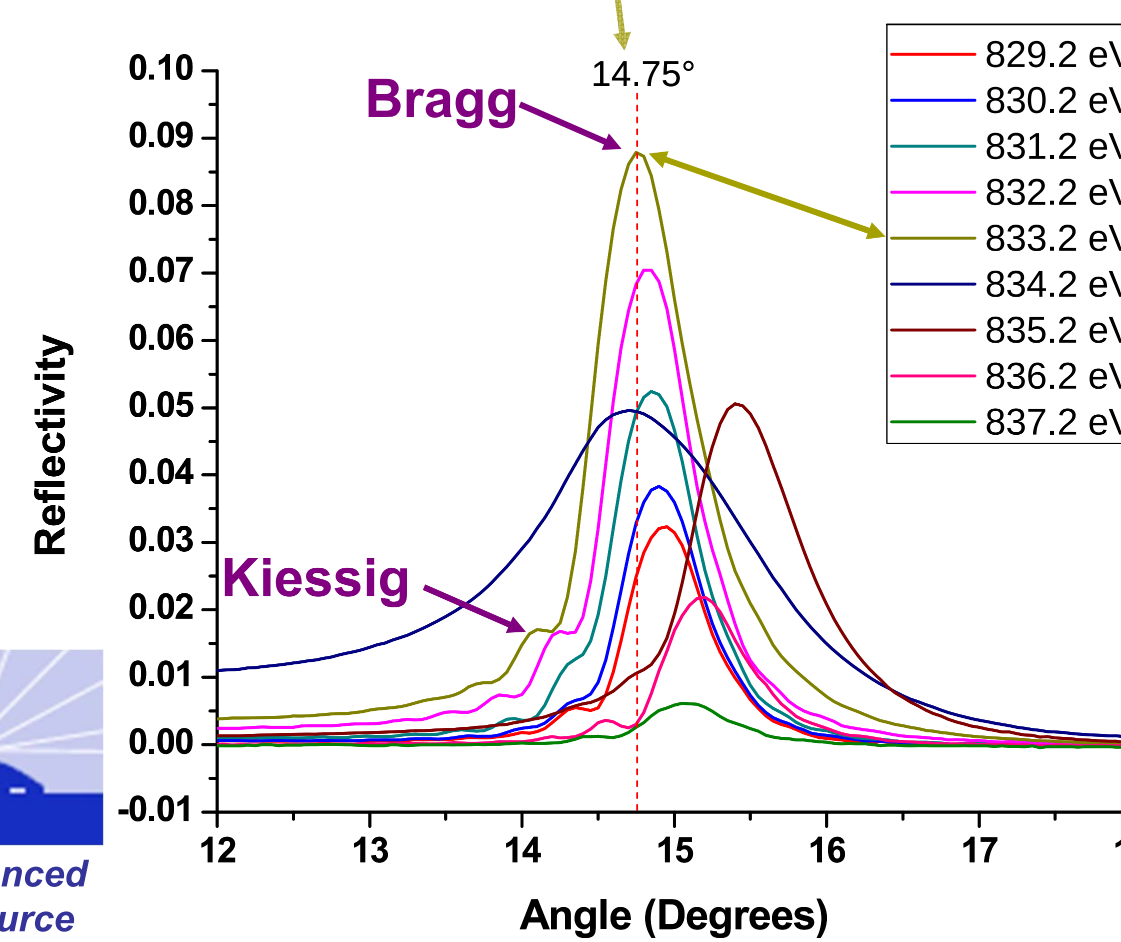

Experiments: A. Gray, C. Papp, A. Bostwick, E. Rotenberg, CF--ALS
Sample: PLD, M. Huijben, R.Ramesh, UCB--Phys. Rev. B 82, 205116 (2010)

The Advanced Light Source

Standing wave/rocking curve analysis of an epitaxial $SrTiO_3/La_{0.67}Sr_{0.33}MnO_3$ interface: hard x-ray excitation

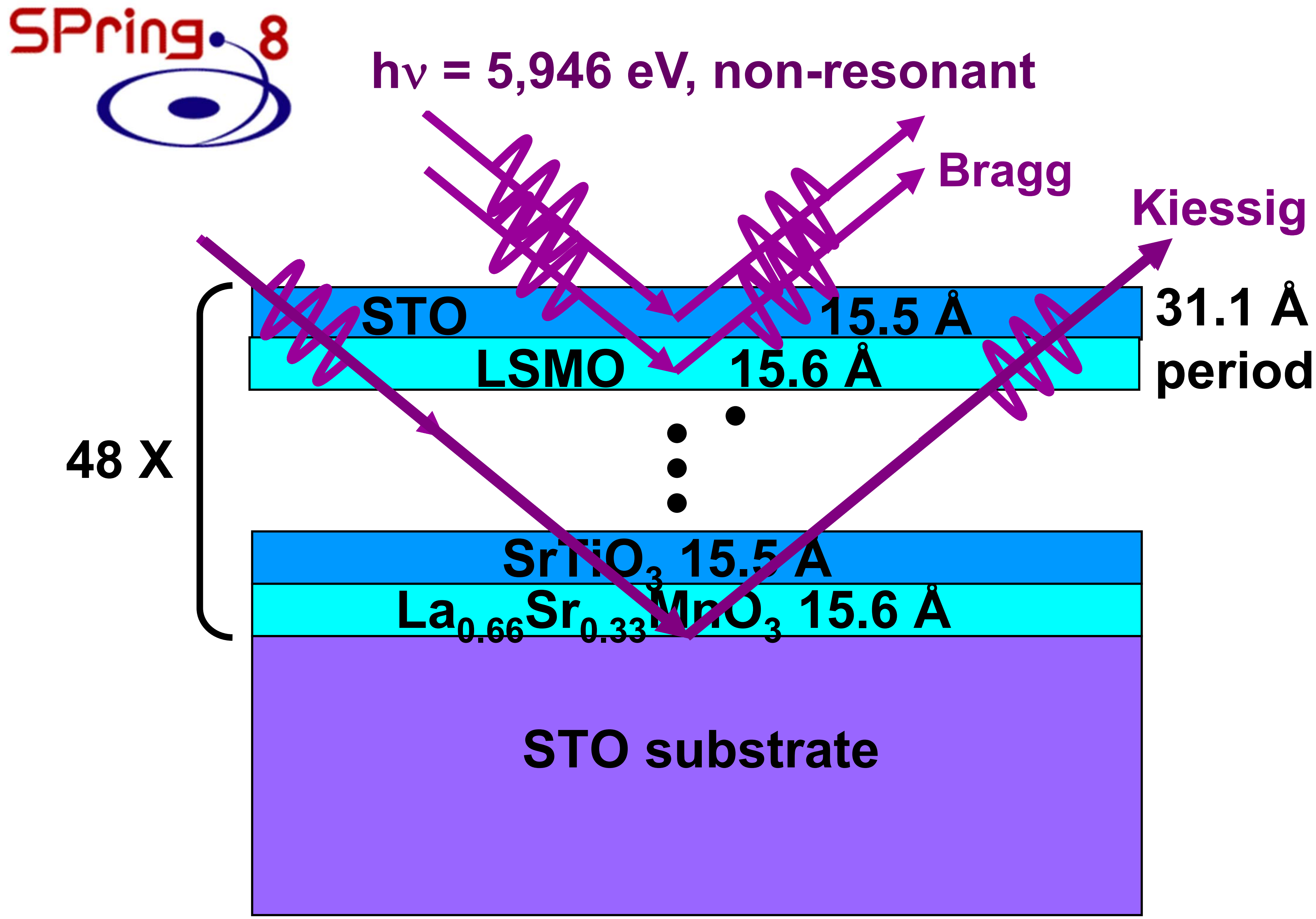

Experiments: A. Gray, C. Papp, S. Ueda, Y. Yamashita, K. Kobayashi, C.F., SPring8

$SrTiO_3$/$La_{0.67}Sr_{0.33}MnO_3$ Multilayer
Analysis of Rocking Curves

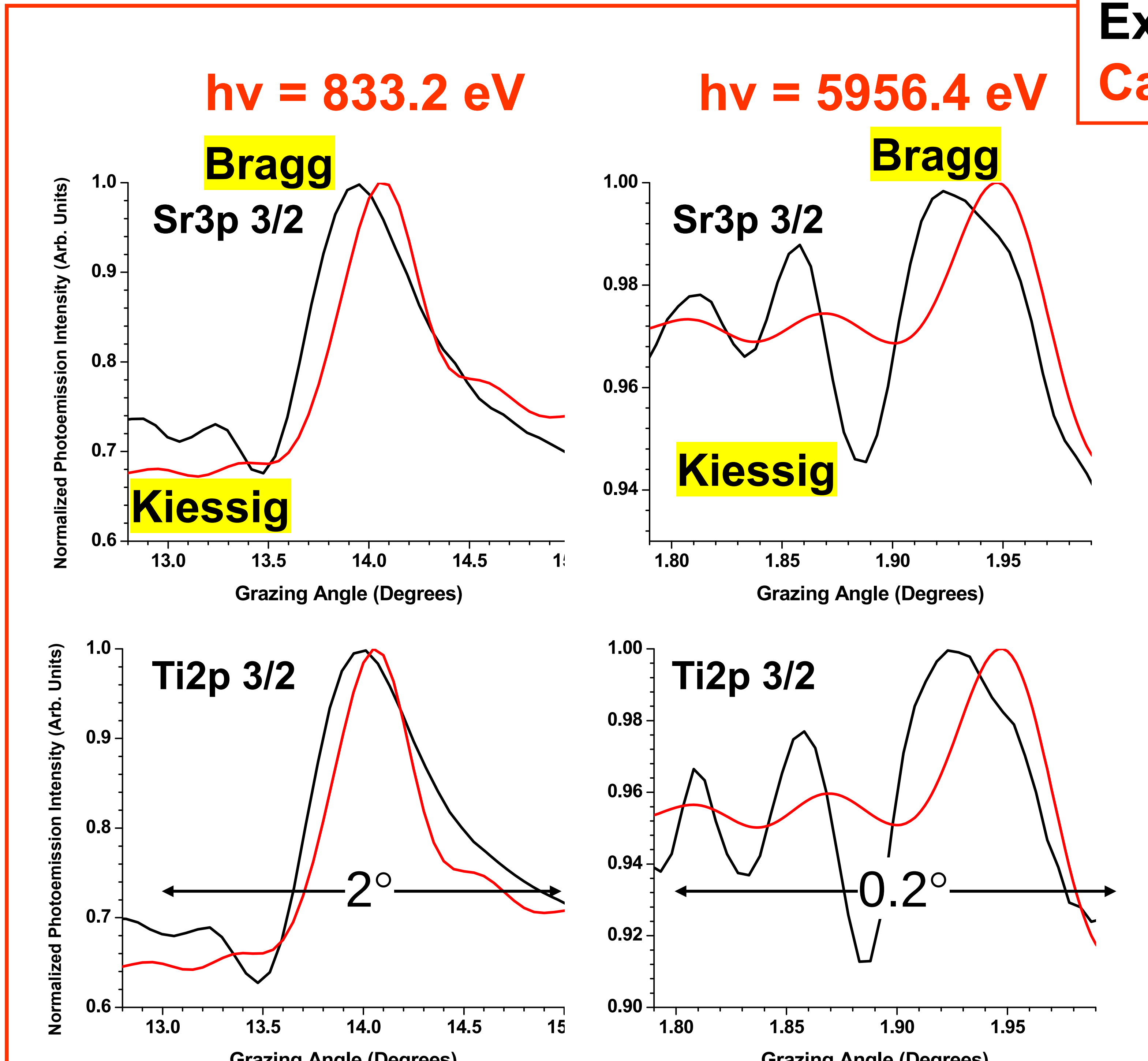

Ideal Bilayer Thickness Gradient Profile

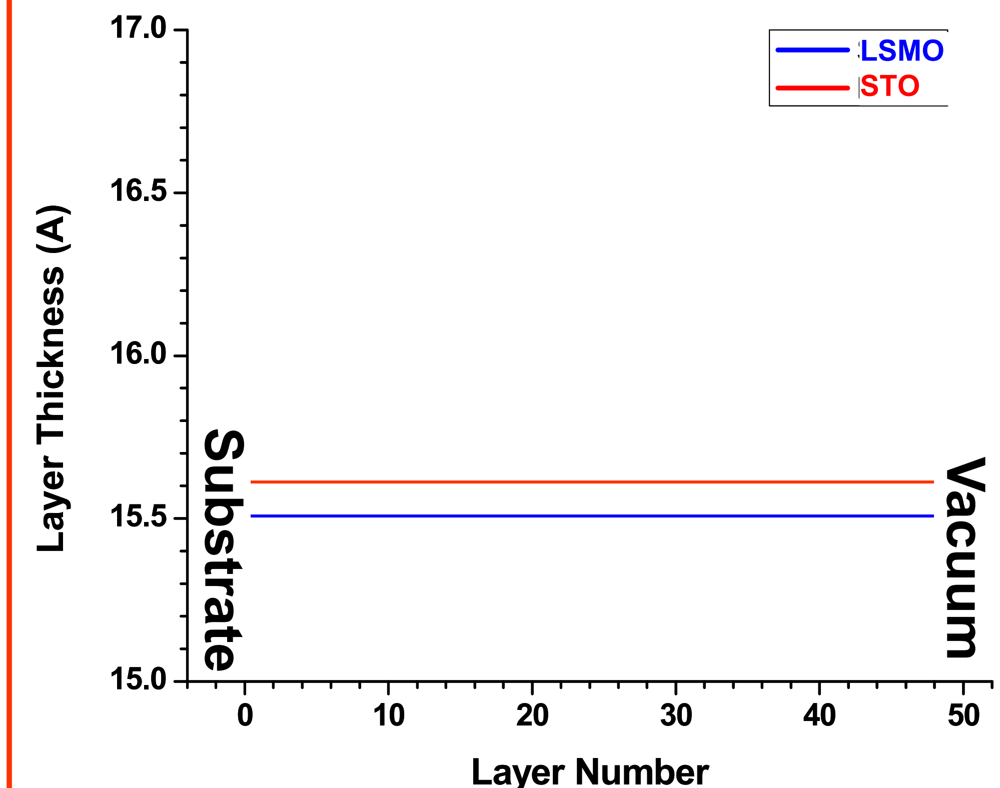

- Relative amplitude of the predicted Kiessig fringes does not agree with experiment
- Strong Kiessig fringes predicted on both sides of the rocking curves, esp. 5.9 keV

A. Gray et al.

The Advanced Light Source

SPring-8

$SrTiO_3/La_{0.67}Sr_{0.33}MnO_3$ Multilayer
Analysis of Rocking Curves

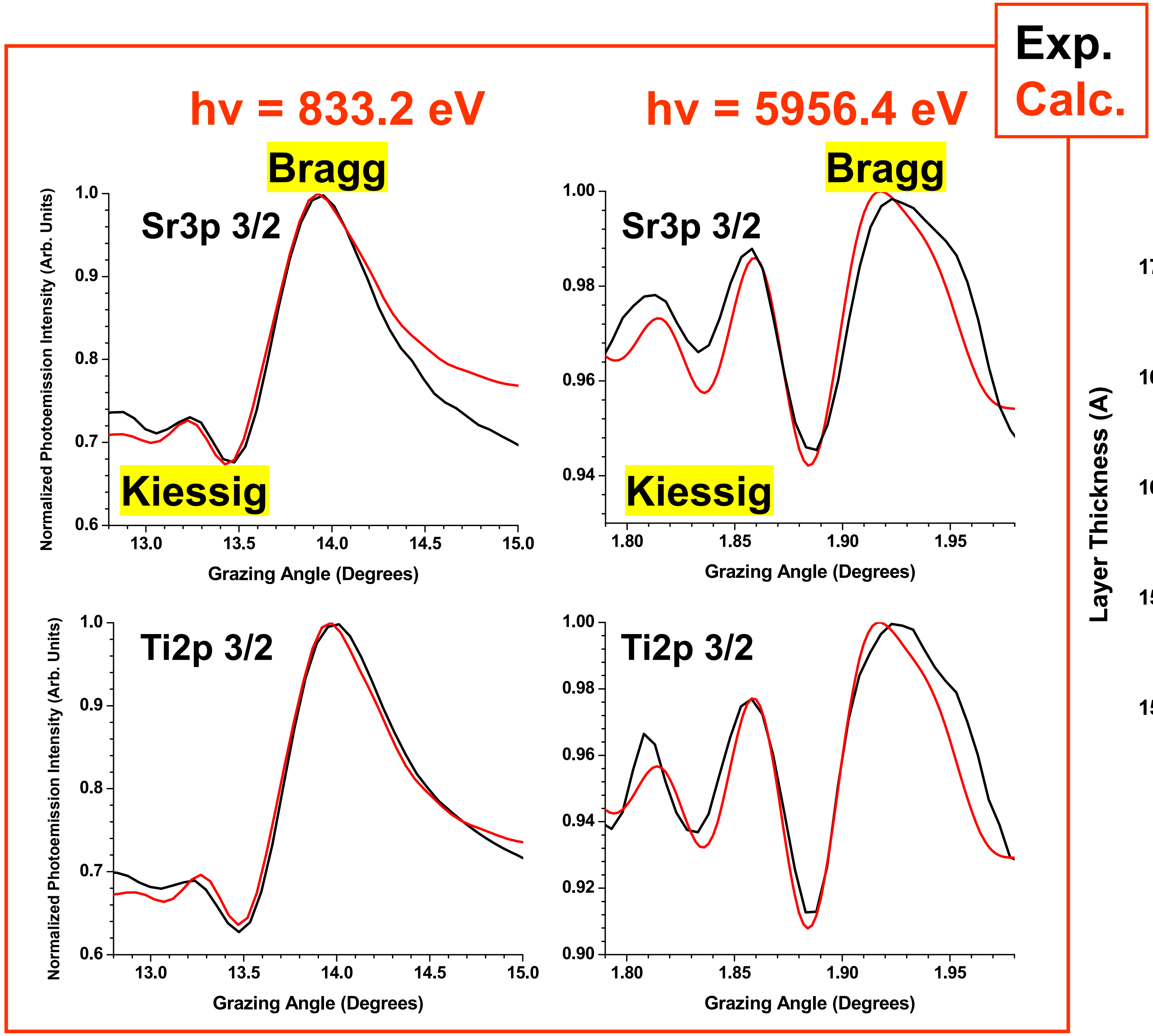

Bilayer Thickness Gradient Profile

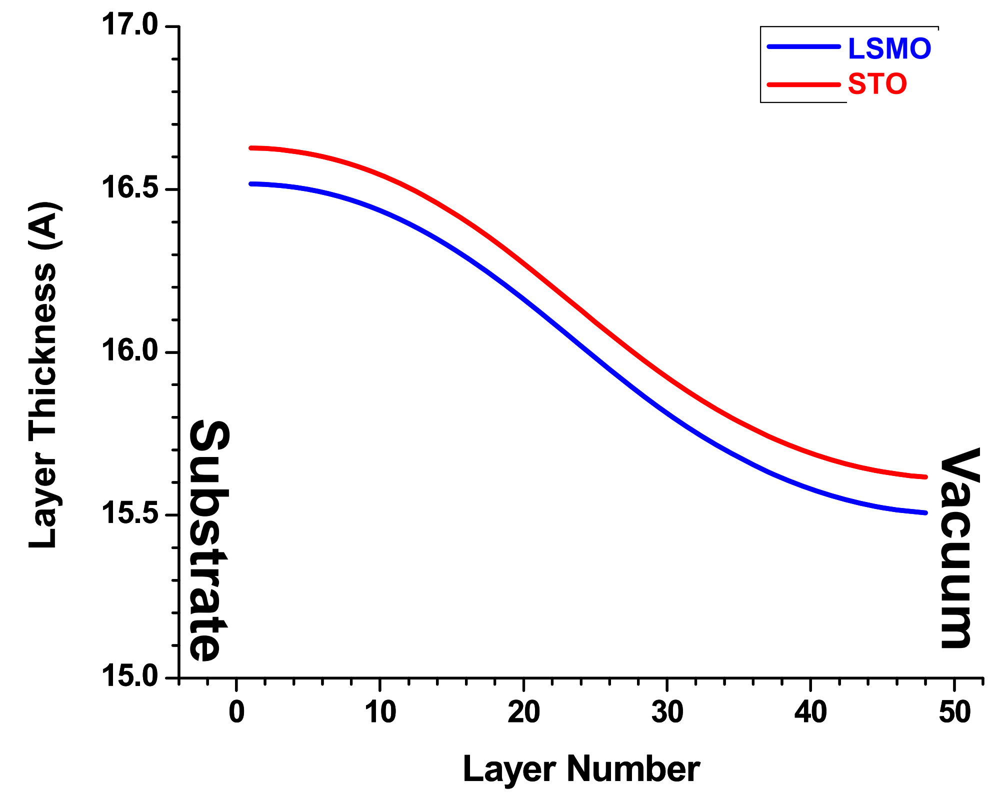

BEST FIT

The Advanced Light Source

SPring-8

→Average multilayer d_{ML} changes by about -1 Å ≈ -6% from top to bottom

A. Gray et al., Phys. Rev. B 82, 205116 (2010)

Fitting of Rocking Curves—All Elements Present, Soft and Hard X-rays

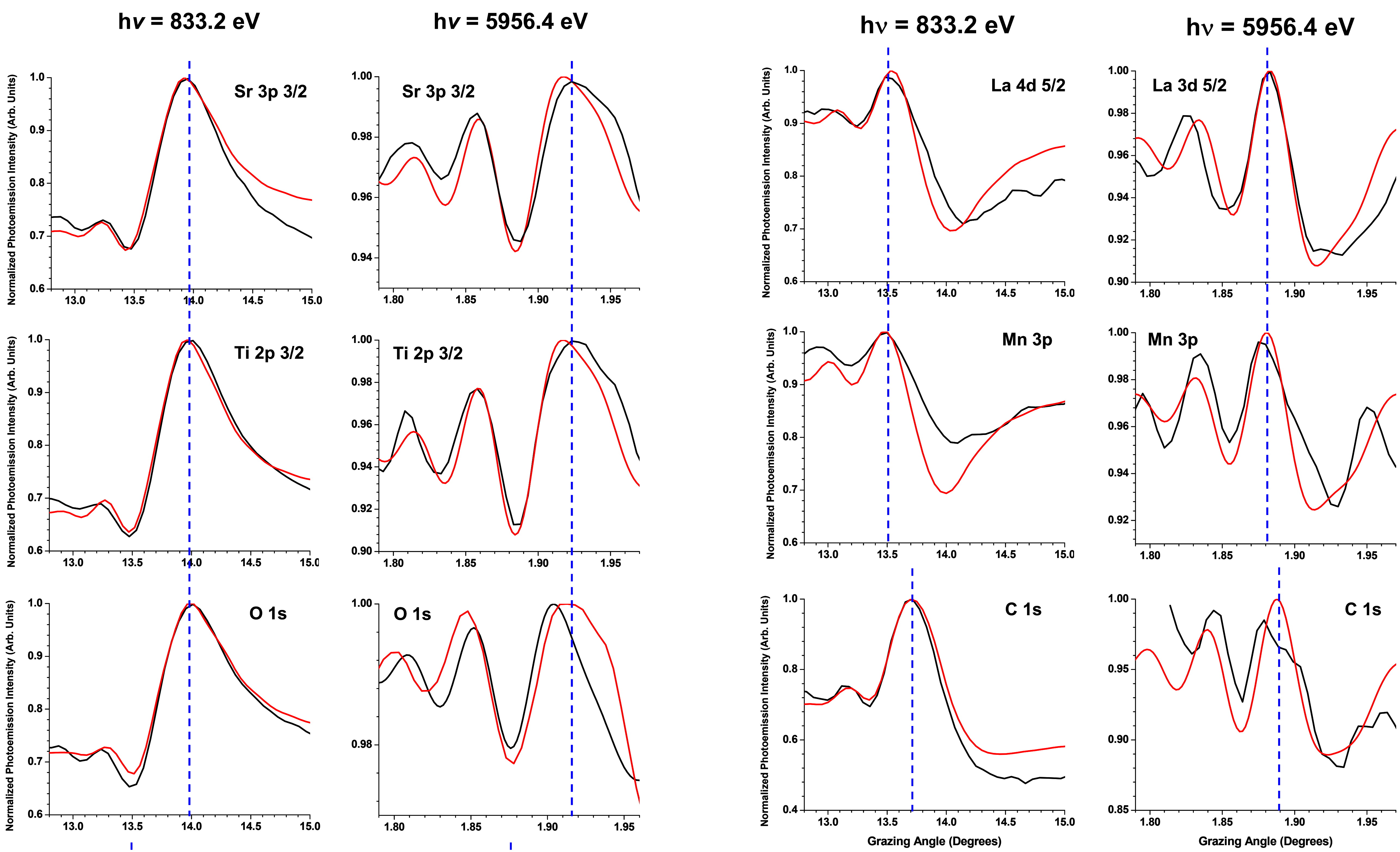

A. Gray et al., Phys. Rev. B 82, 205116 (2010)

Fitting of Rocking Curves—All Elements Present, Soft and Hard X-rays

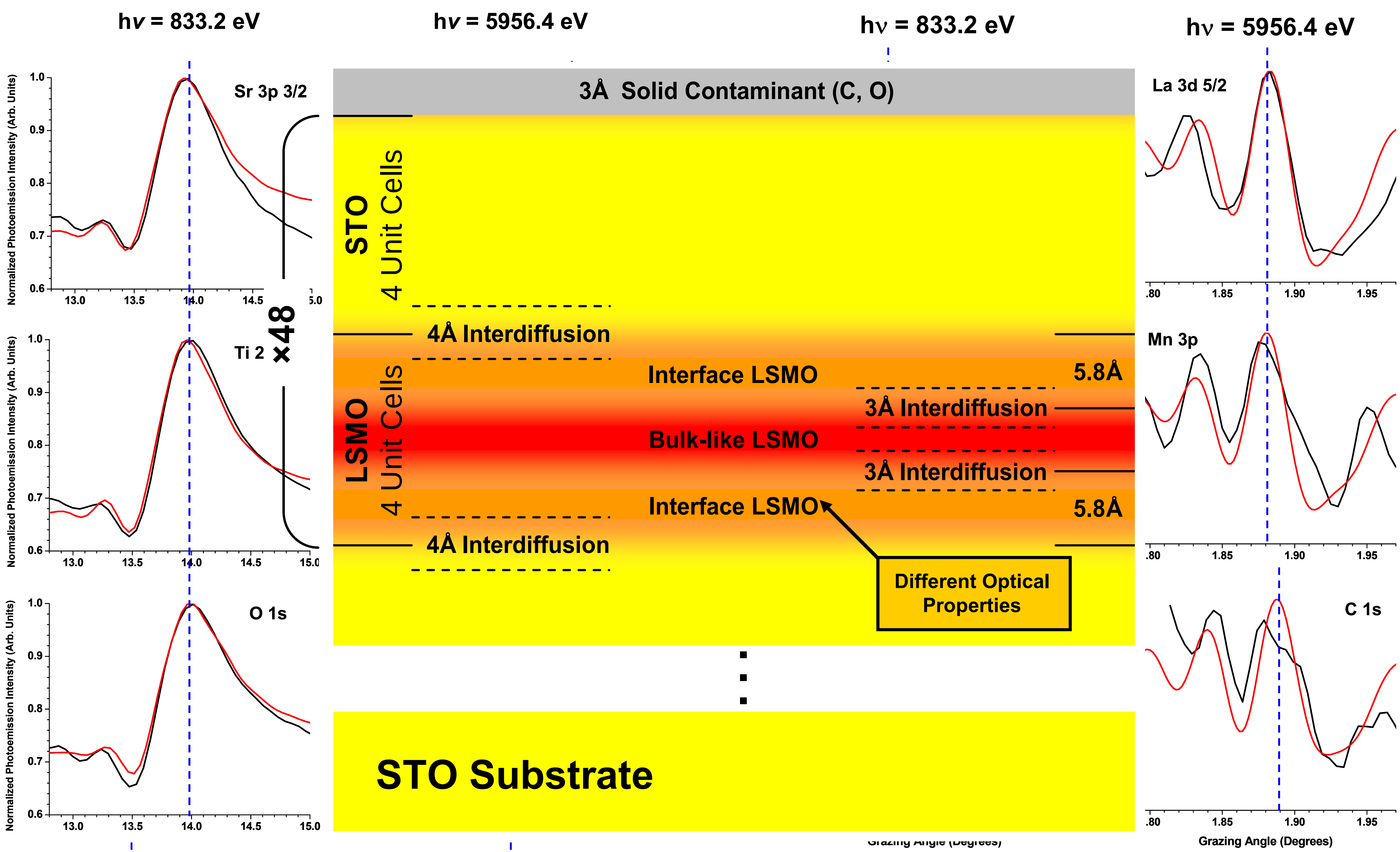

A. Gray et al., Phys. Rev. B 82, 205116 (2010)

Microscopic origins for stabilizing room-temperature ferromagnetism in ultrathin manganite layers

L. Fitting Kourkoutis[a,1], J. H. Song[b,c], H. Y. Hwang[c,d], and D. A. Muller[a,e]

11682–11685 | PNAS | June 29, 2010 | vol. 107 | no. 26

~Consistent with TEM-EELS imaging of other PLD-grown STO/LSMO multilayers

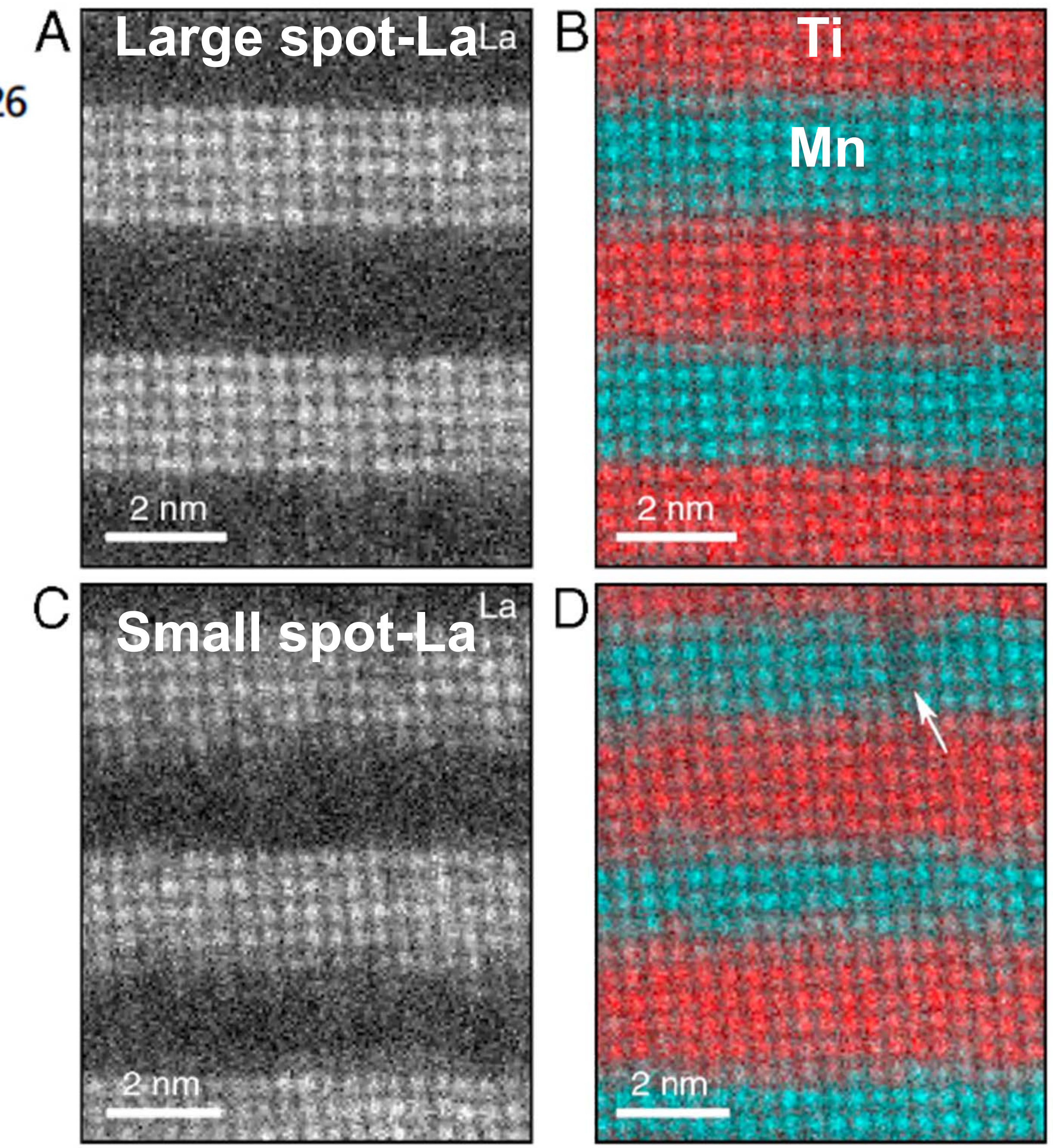

Fig. 2. Spectroscopic-imaging of $La_{0.7}Sr_{0.3}MnO_3/SrTiO_3$ multilayers grown at $P_{O2} = 1$ m torr and at a laser spot size of (*A* and *B*) 7.5 and (*C* and *D*) 1.6×10^{-2} cm^2. (*A* and *C*) La elemental maps and (*B* and *D*) red-green-blue false color B-site maps, obtained by combining the Ti (red) and Mn (green and blue) maps extracted from the spectrum images. The multilayer grown with a smaller laser spot size shows less abrupt interfaces and an extended defect, marked by a white arrow in *D*. The growth direction is from bottom to top.

See also Samet et al.,
Eur. Phys. J. B 34, 179–192 (2003)
DOI: 10.1140/epjb/e2003-00210-8

STO/LSMO-Resonant soft x-ray standing wave/rocking curves at 833 eV: core photoelectron peaks compared to calculated standing-wave field

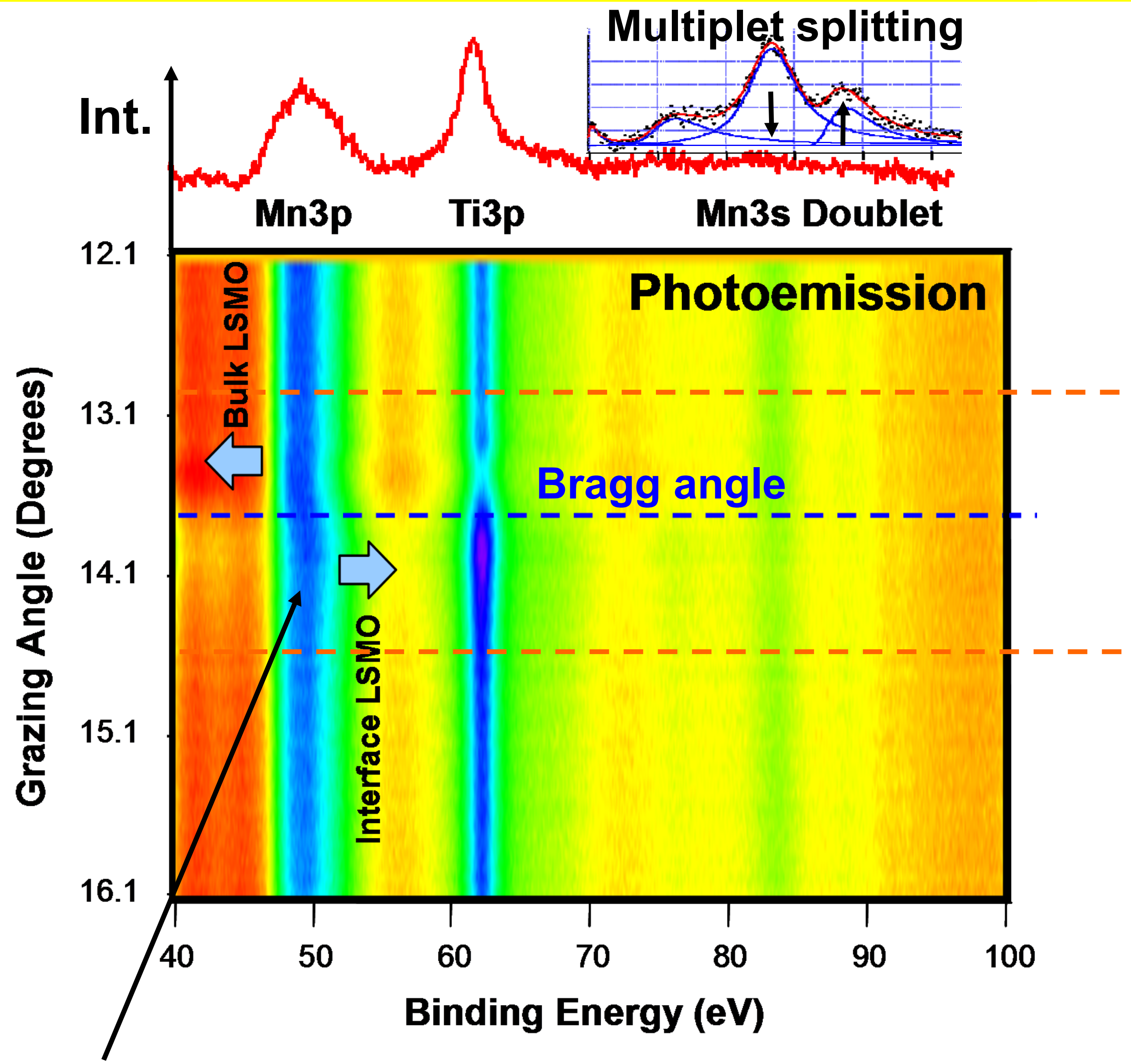

- Clear chemical/final-state shift at interface seen in Mn 3p
- No change in Mn 3s
- No change in Ti 3p—near surface

The Advanced Light Source

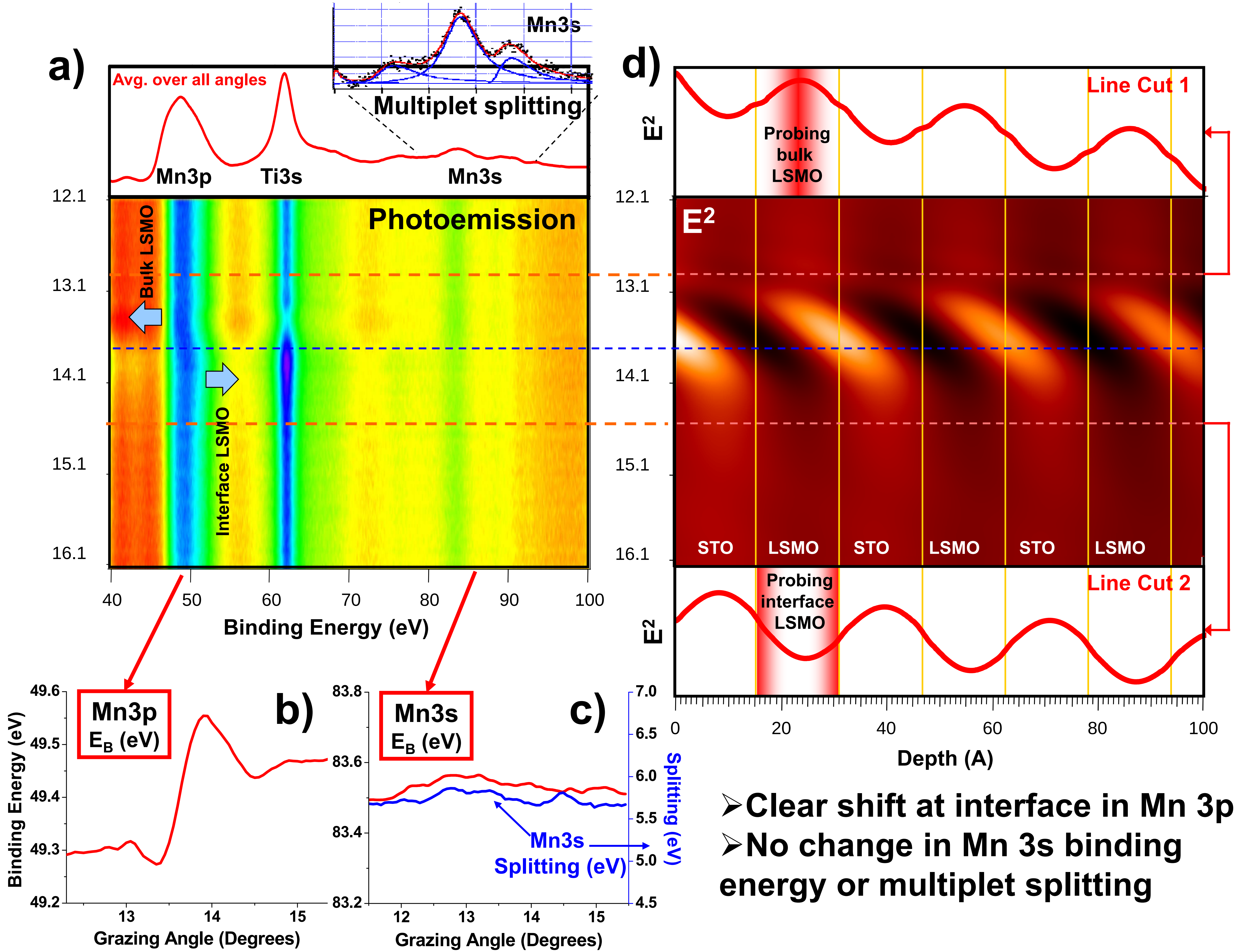

- ➢Clear shift at interface in Mn 3p
- ➢No change in Mn 3s binding energy or multiplet splitting

STO/LSMO-Explaining the Difference Between Mn 3p and Mn 3s behavior

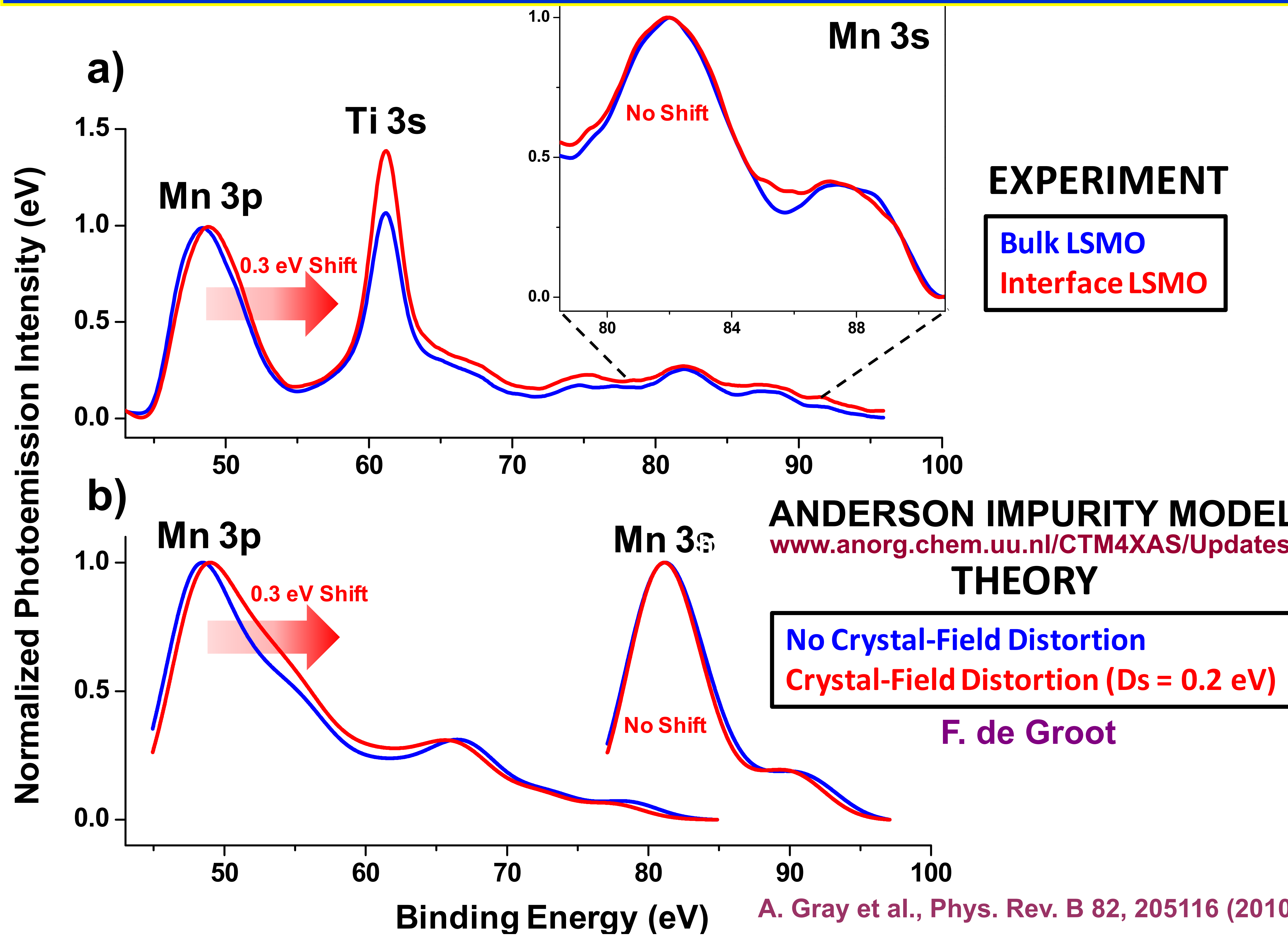

A. Gray et al., Phys. Rev. B 82, 205116 (2010)

$SrTiO_3$ and $La_{0.67}Sr_{0.33}MnO_3$ band structures and DOS

$SrTiO_3$-insulator

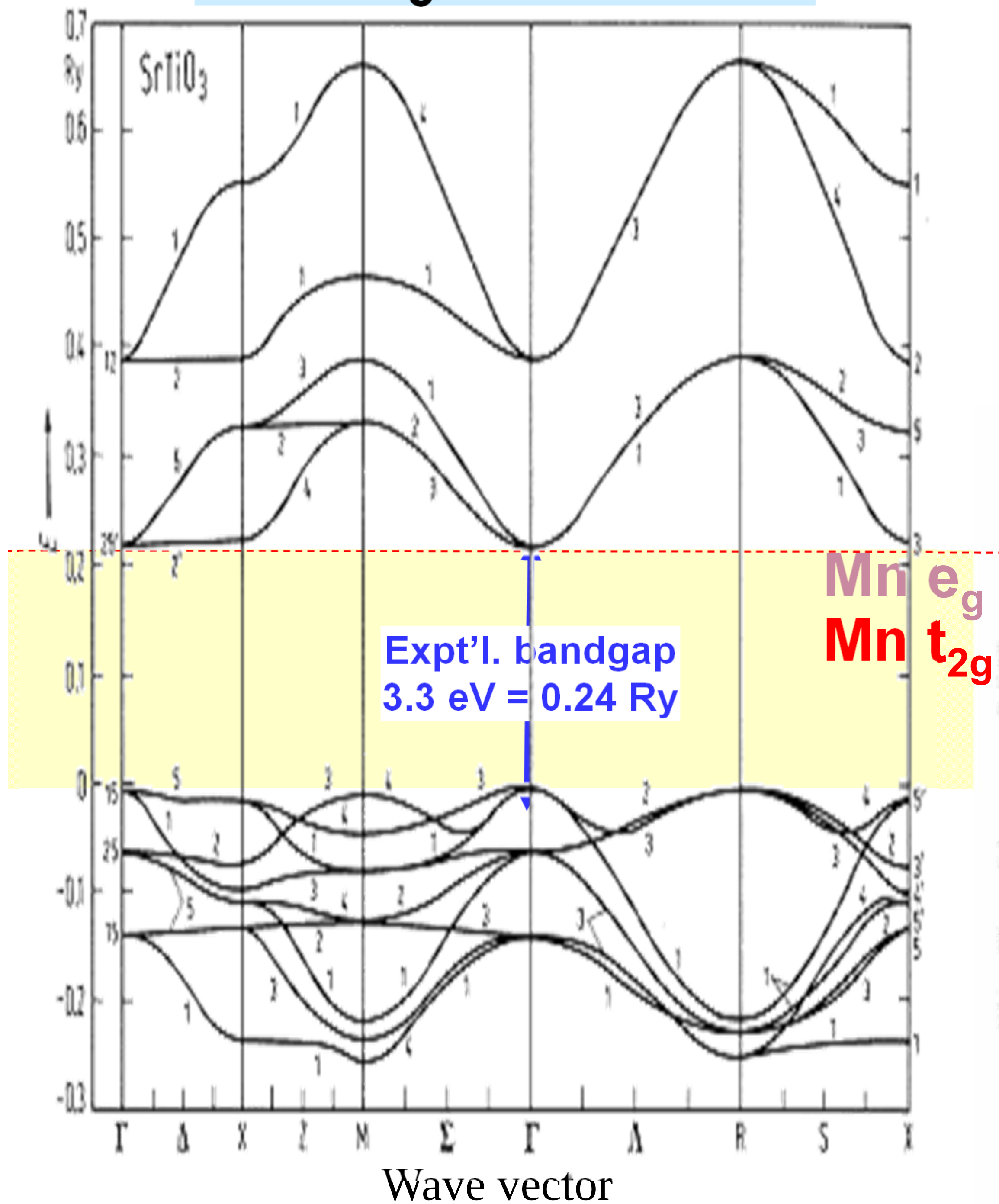

Mattheiss, PRB 6, 4718 (1972)

$La_{0.67}Sr_{0.33}MnO_3$- Half-Metallic Ferromagnetic metal

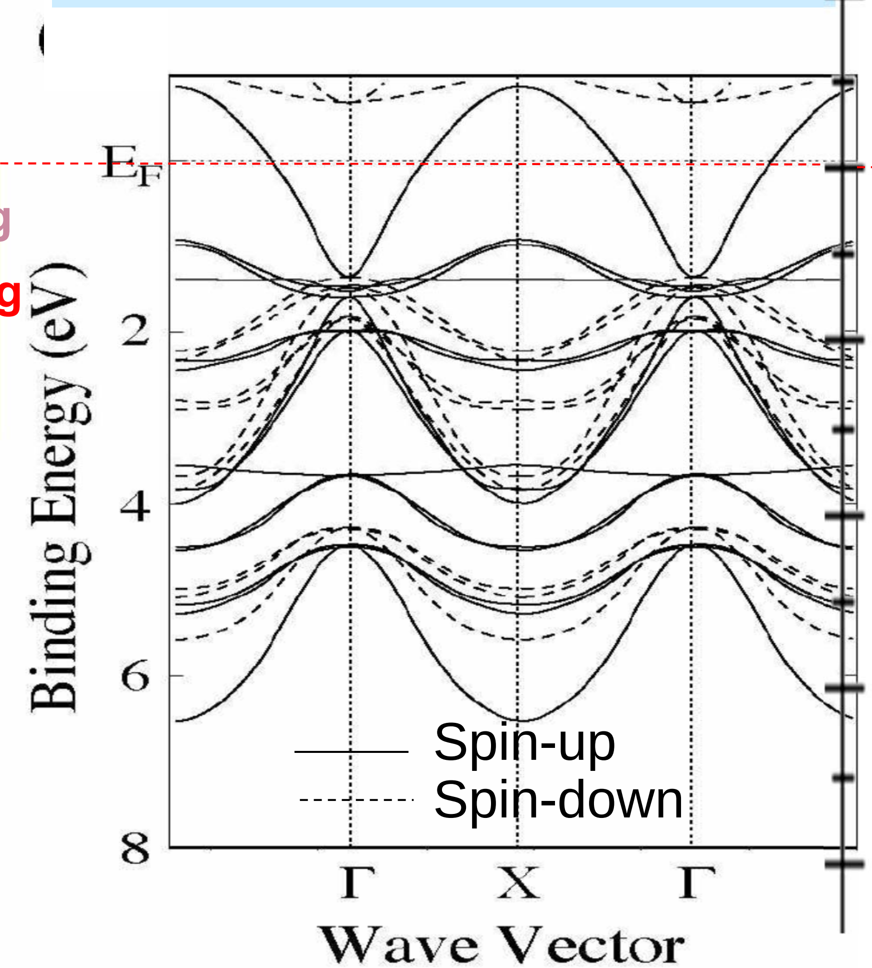

Chikamatsu et al., PRB 73, 195105 (2006)

Zheng, Binggeli, J. Phys. Cond. Matt. 21, 115602 (2009)

Projected DOSs

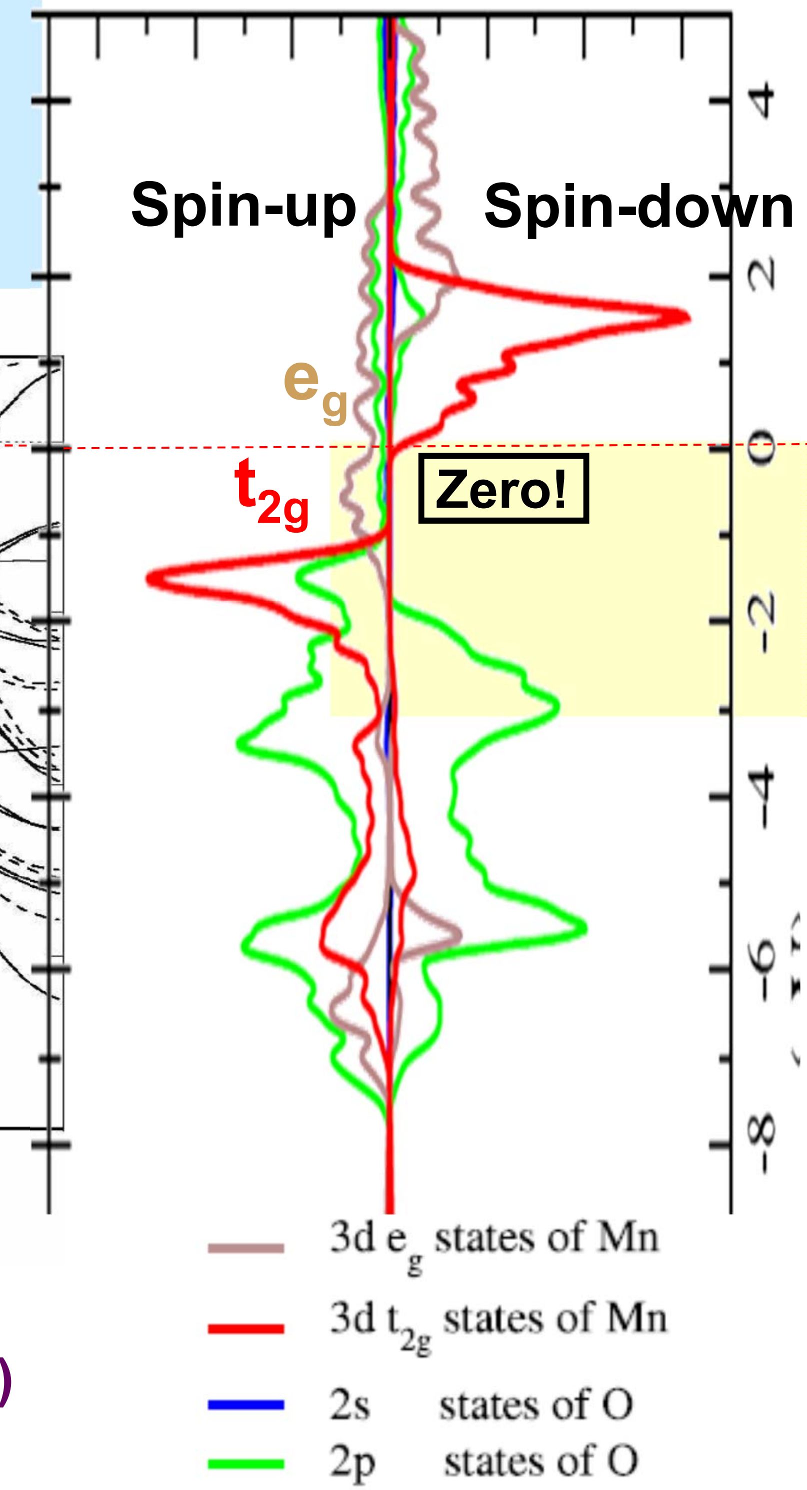

Soft x-ray valence cross sections for Mn and O

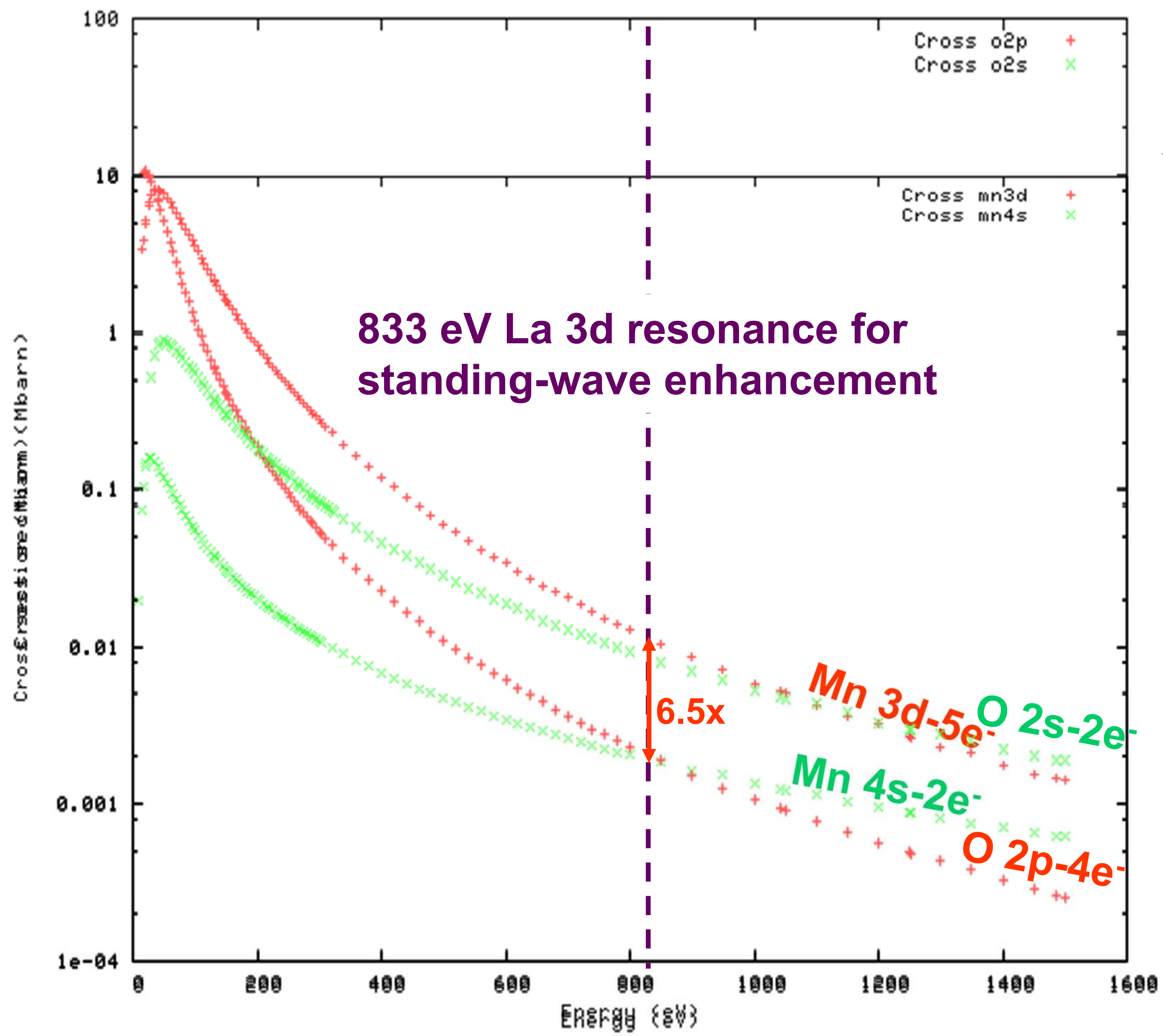

As for $LaNiO_3$, the TM (= Mn) 3d dominates over O 2p in the keV regime

http://ulisse.elettra.trieste.it/services/elements/WebElements.html

STO/LSMO-Standing wave/rocking curves of valence region: 833 eV, 300K

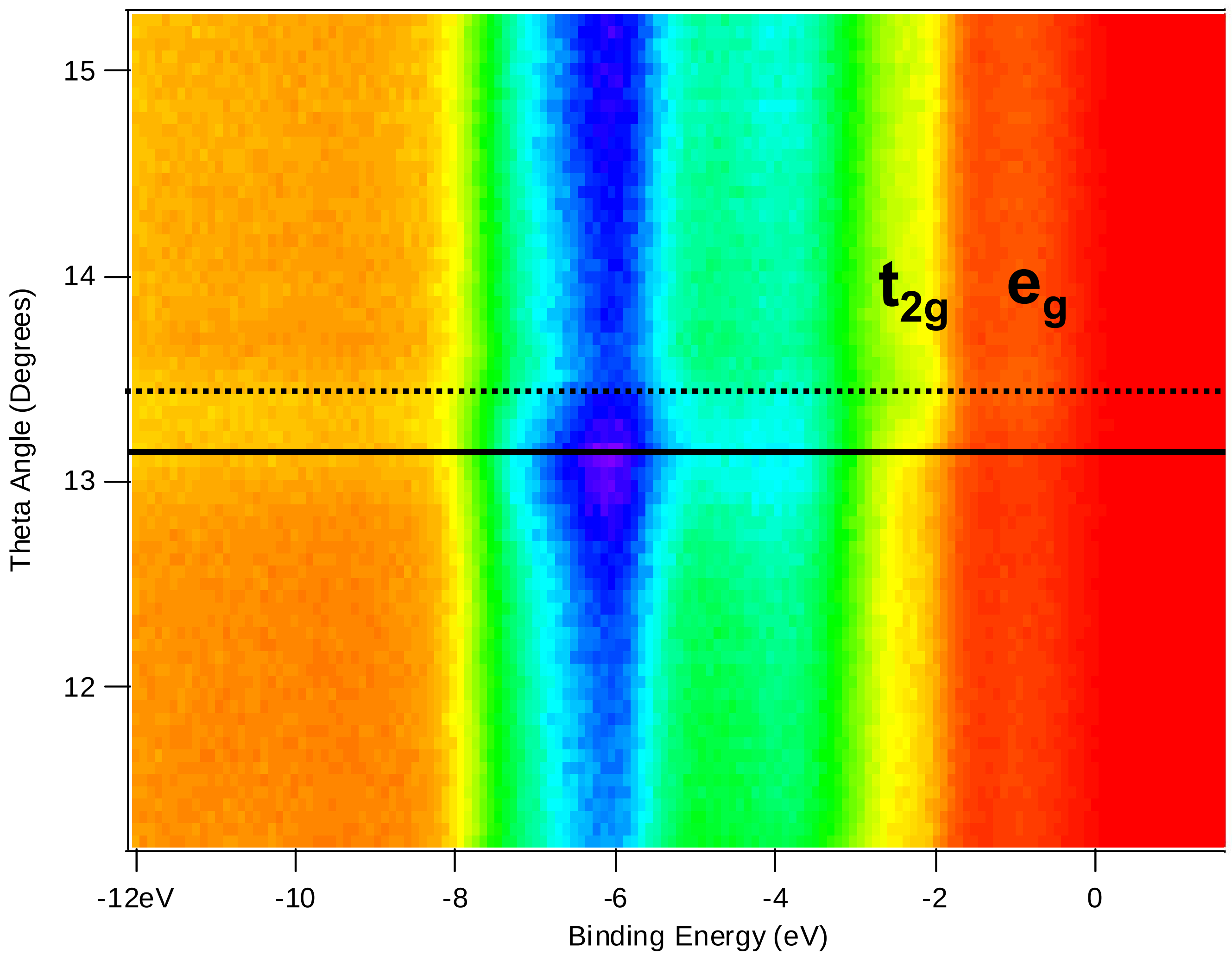

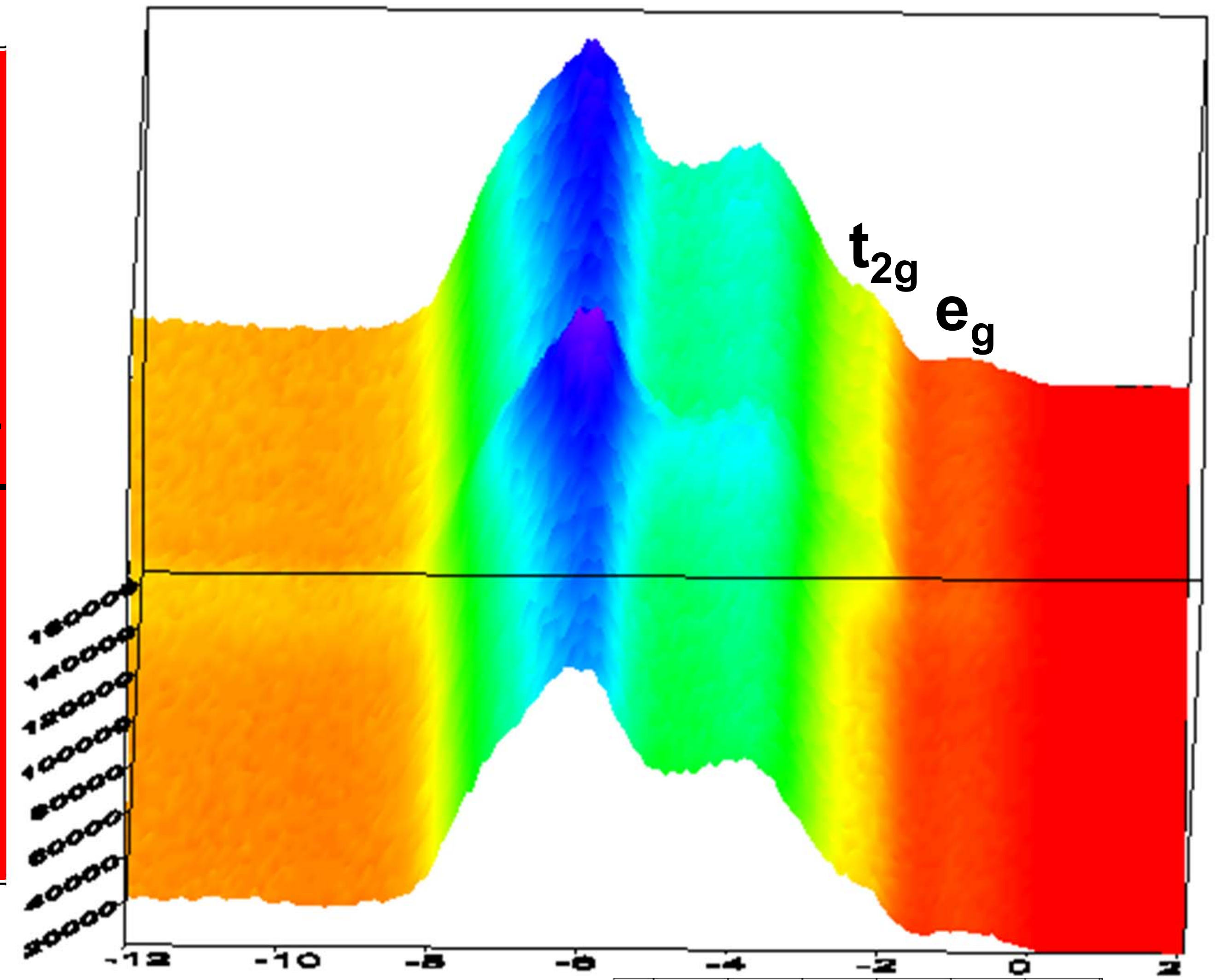

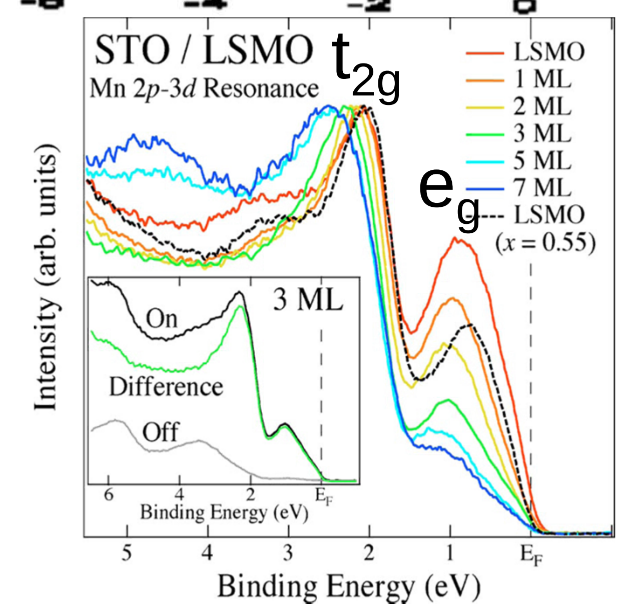

A. Gray et al., Phys. Rev. B 82, 205116 (2010)

The Advanced Light Source

Prior resonant PS: Fujimori et al., J.A.P 99, 08S903 (2006)

Standing-wave angle-resolved photoemission

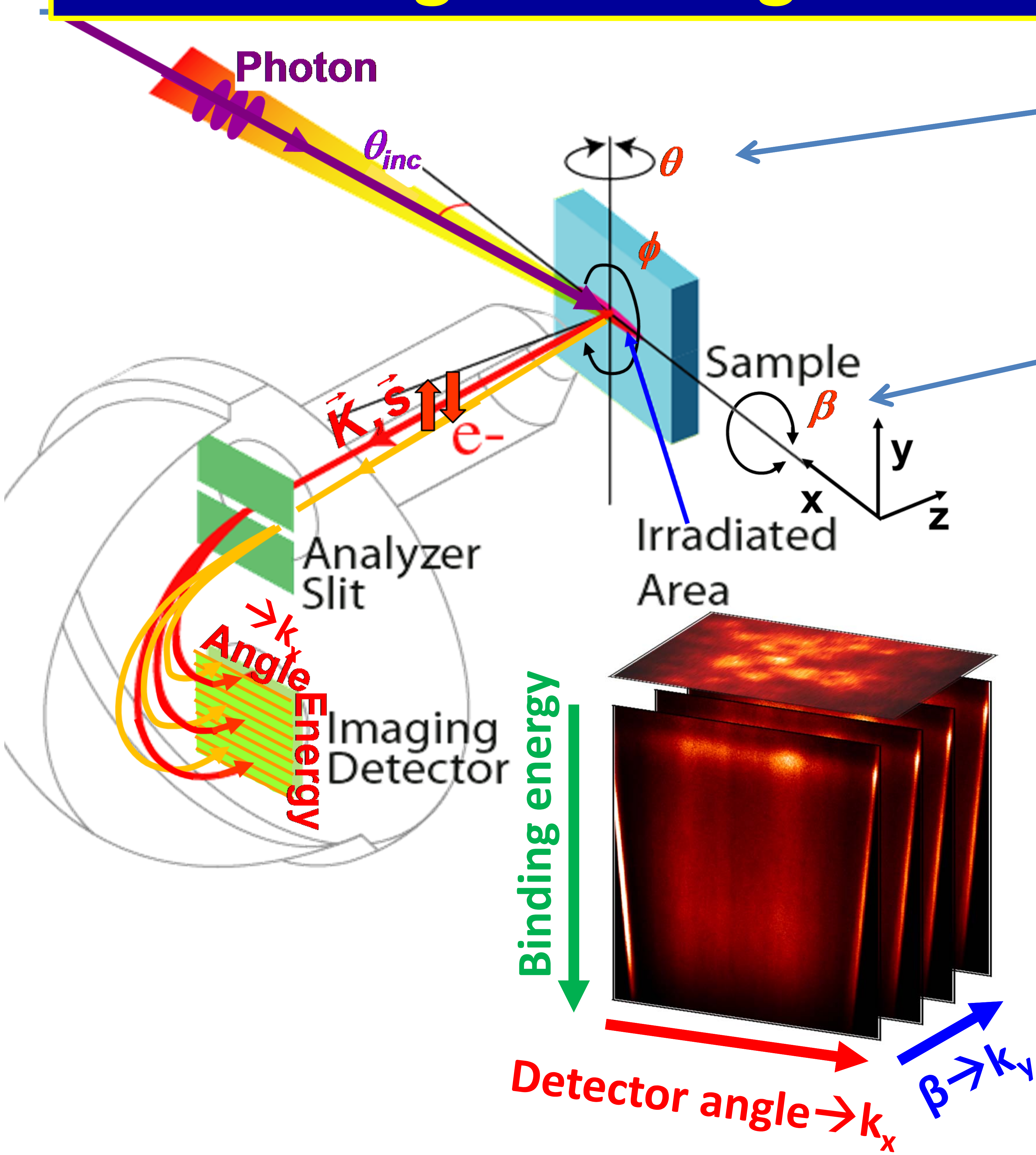

Variation of Θ:
Change of incidence angle
⇨Standing wave effect

Variation of β:
Change of takeoff angle
⇨ measure electrons with different **k**-vector

k-space mapping with scanned standing wave

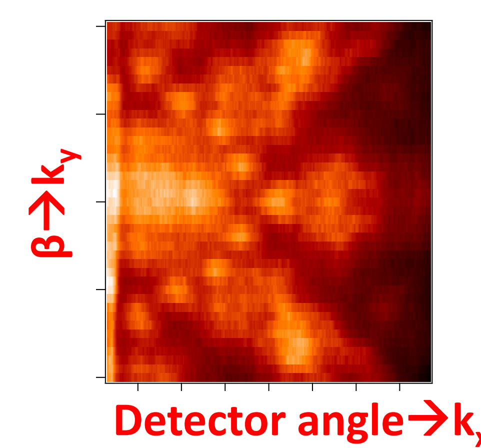

Core levels:
XPD

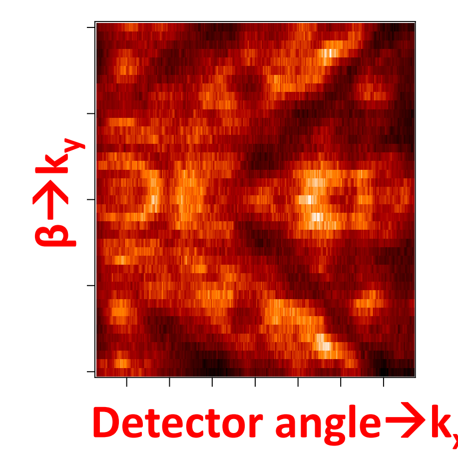

Valence bands:
ARPES

Depth-Resolved ARPES?

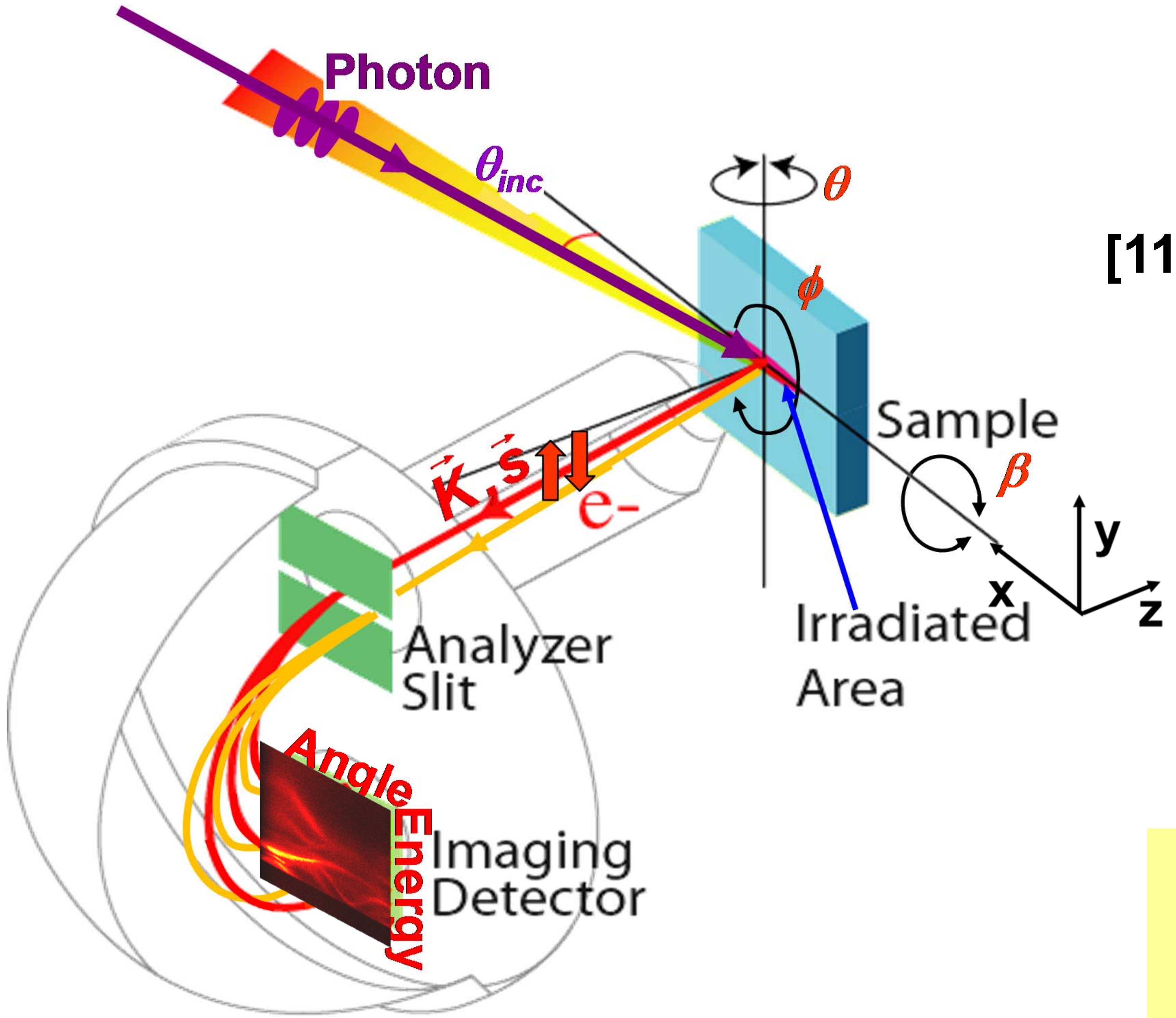

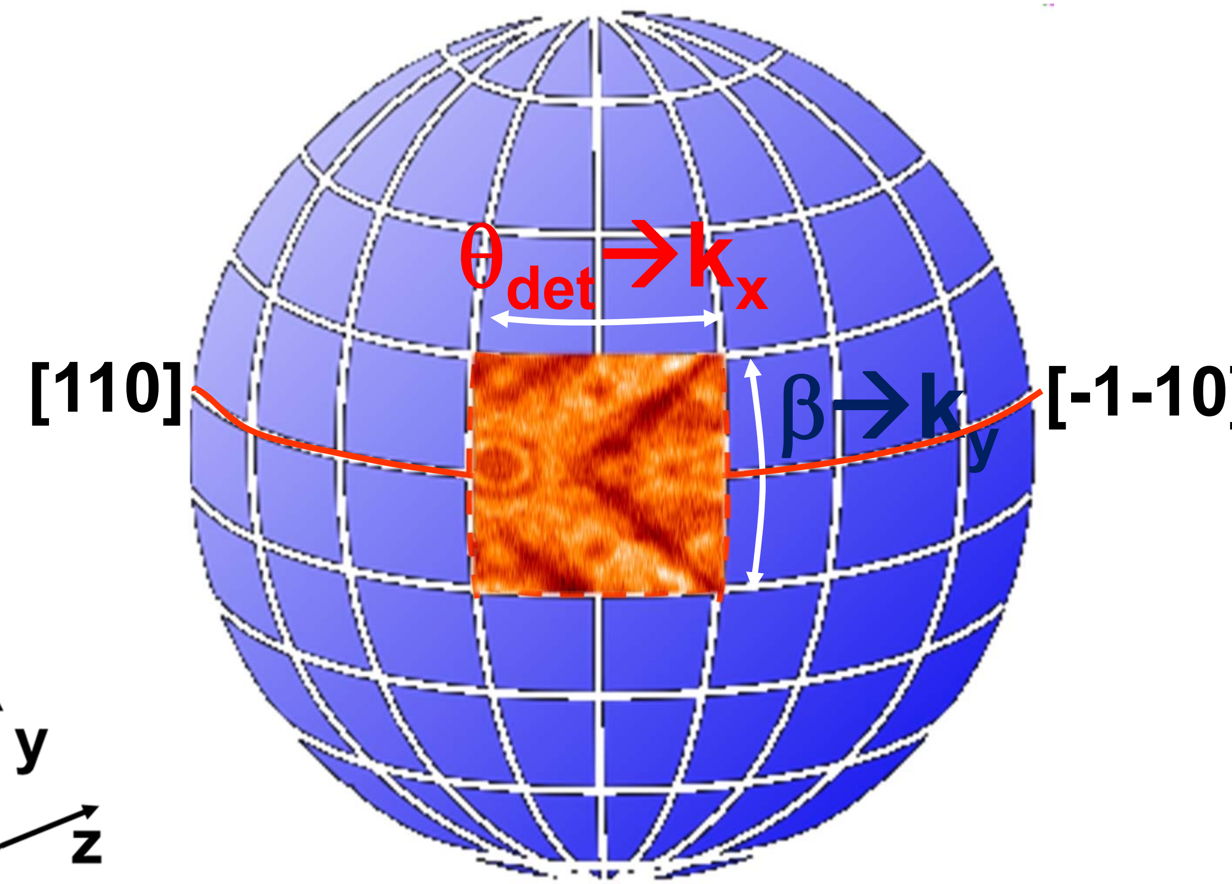

hν = 833.2 eV (still)
T = 20 K
~ARPES limit with
Ca. 75% k-conserving transitions

Beamline 7.0 ALS
With A. Bostwick, E. Rotenberg

Depth-Resolved ARPES?

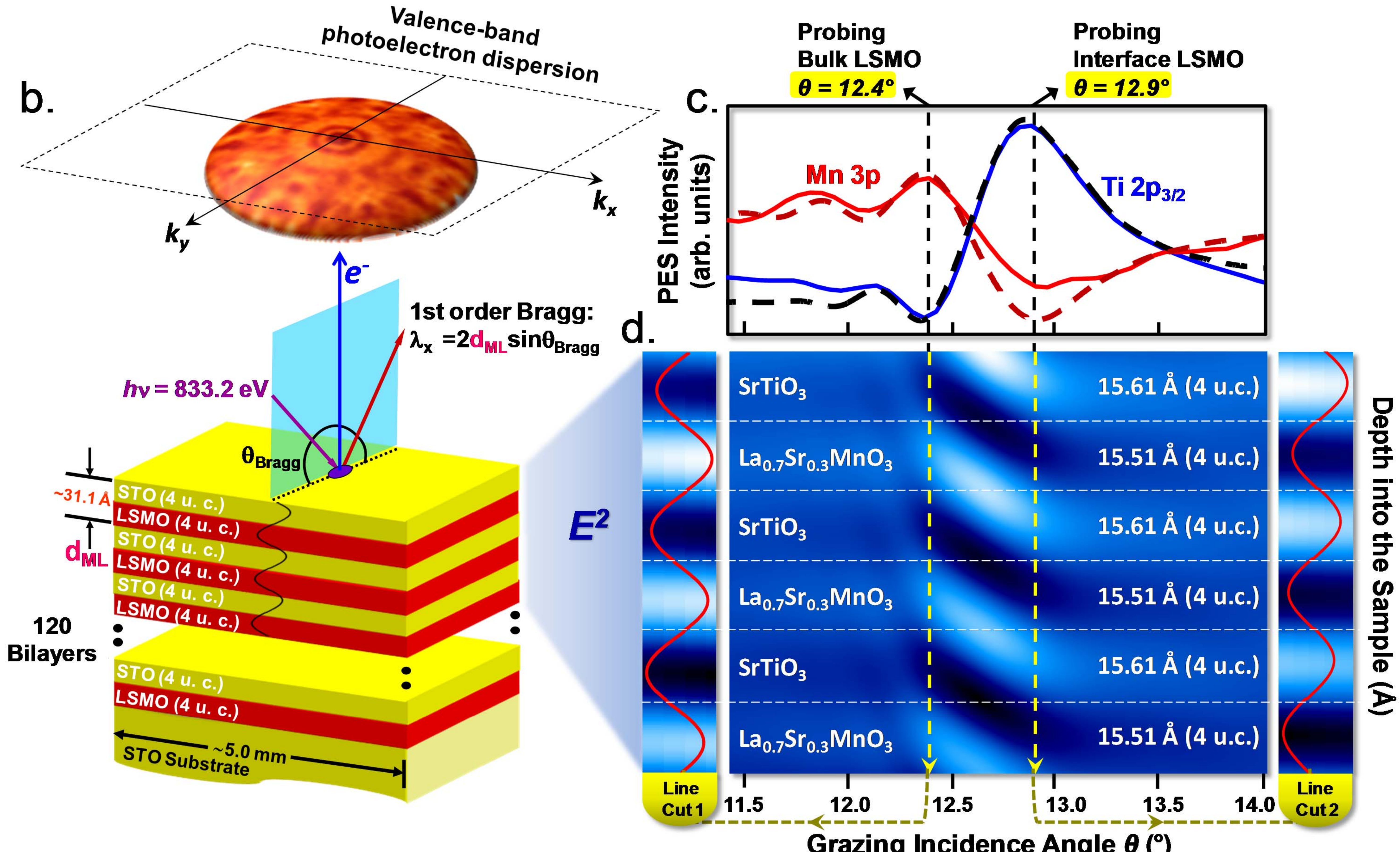

Sample: Huijben, Ramesh

Experiment: Gray, Papp, Rotenberg, Bostwick, Ueda, Yamashita, Kobayashi

Theory: Minar, Braun, Ebert, Plucinski, Yan

STO/LSMO ARPES in k-space: 833 eV, 20K

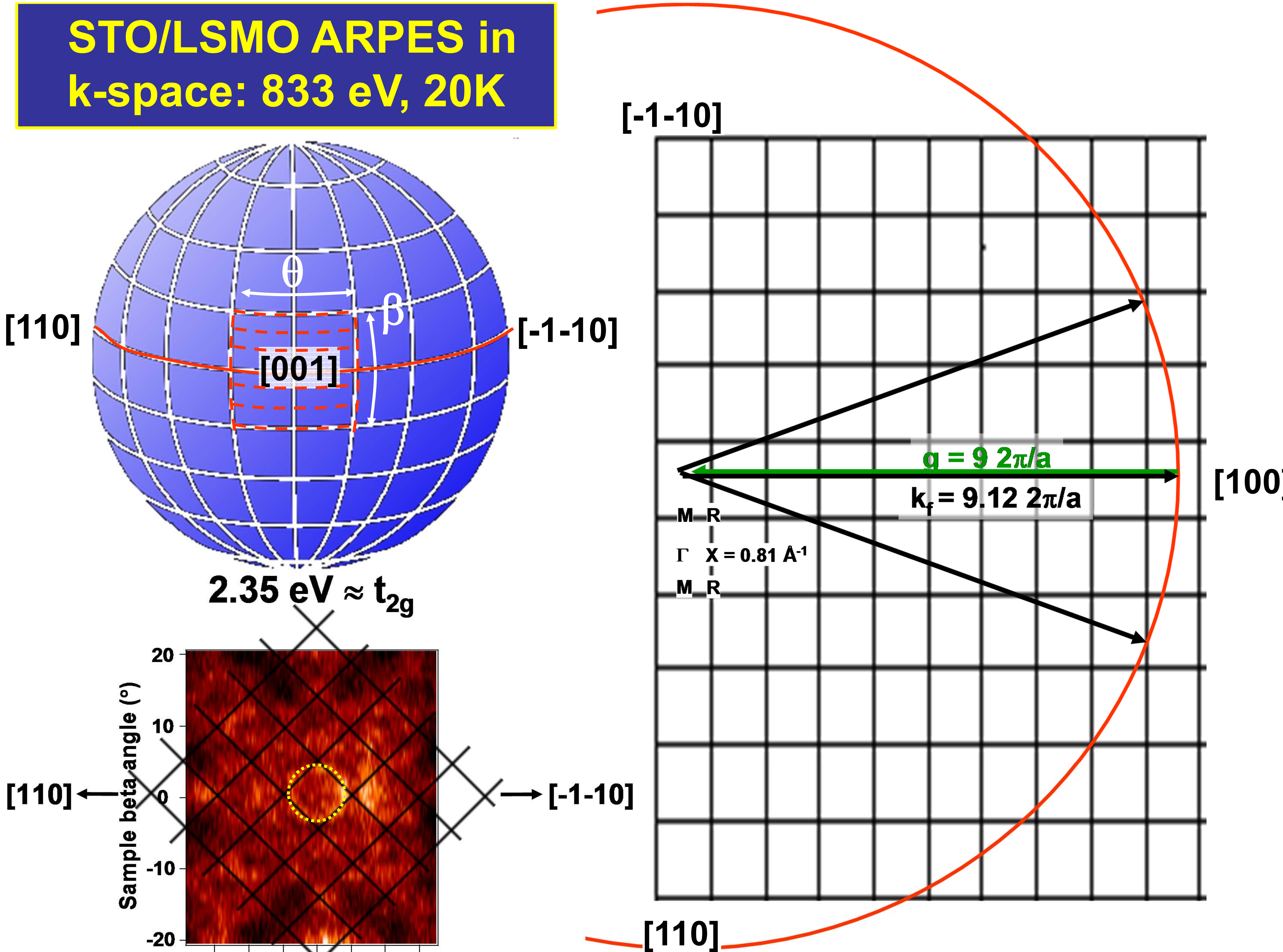

→Depth-resolved/interface band structure?

LSMO Bulk sensitive point E along the rocking curve

Probing
Bulk LSMO
(max. Bulk
sensitivity)

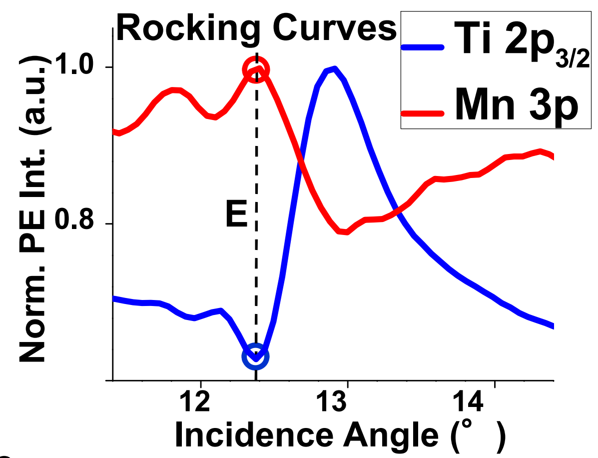

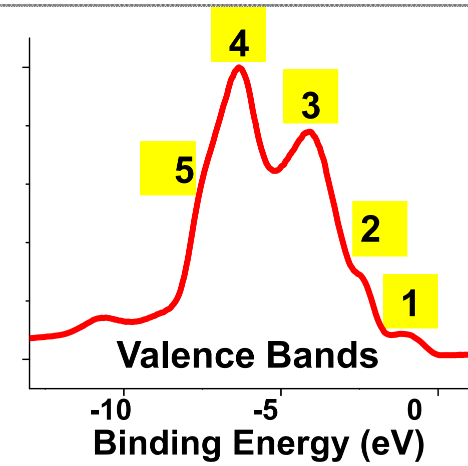

hv = 833.2 eV

RAW DATA

T = 20 K
Debye-Waller ≈ 0.75→
75% DTs +
25% XPD-like

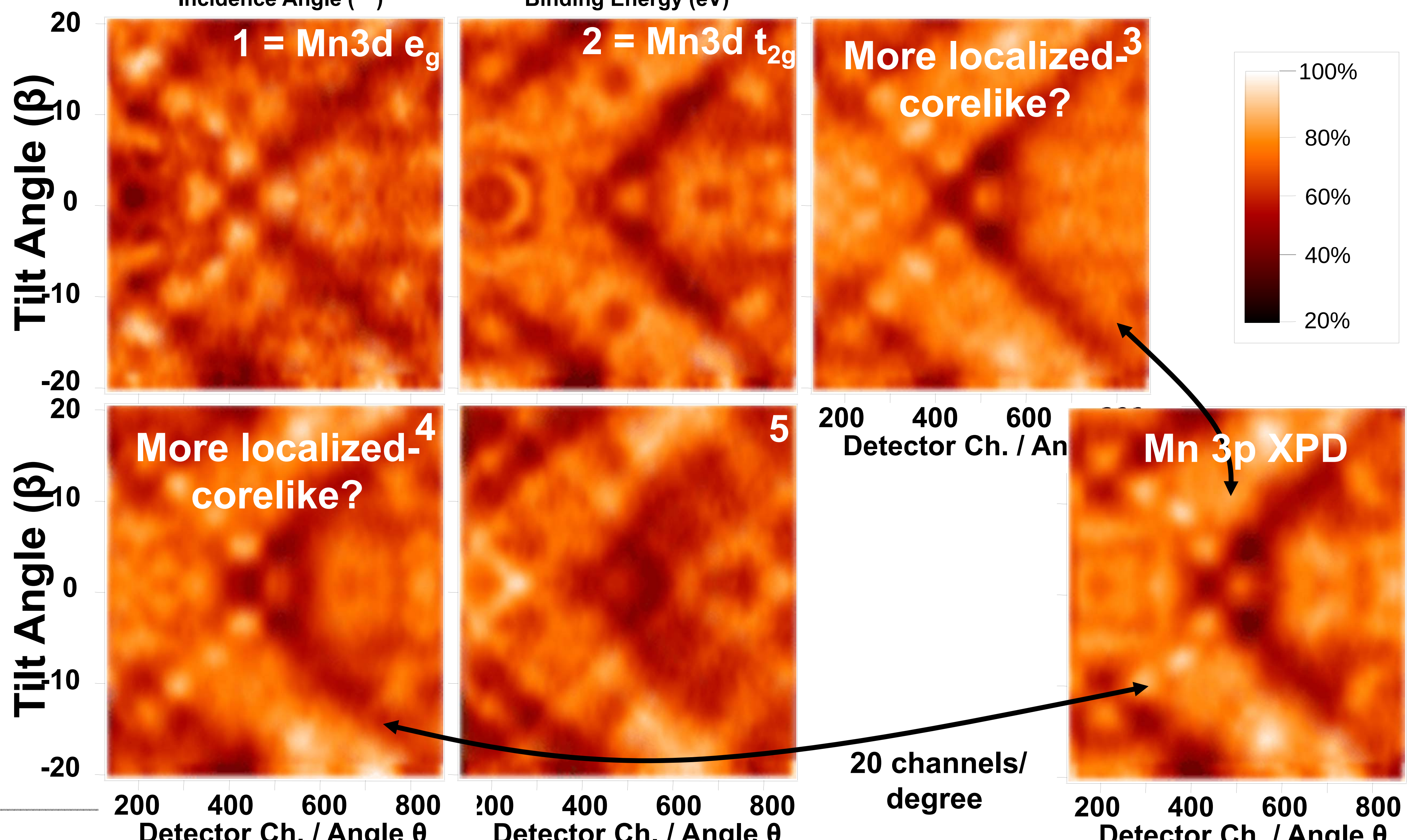

Photoelectron Diffraction with soft and hard x-ray excitation: two viewpoints, expt. vs. theory

Experiment

STO/LSMO Multilayer
Mn 3p emission
E=793eV
hv = 833.2 eV

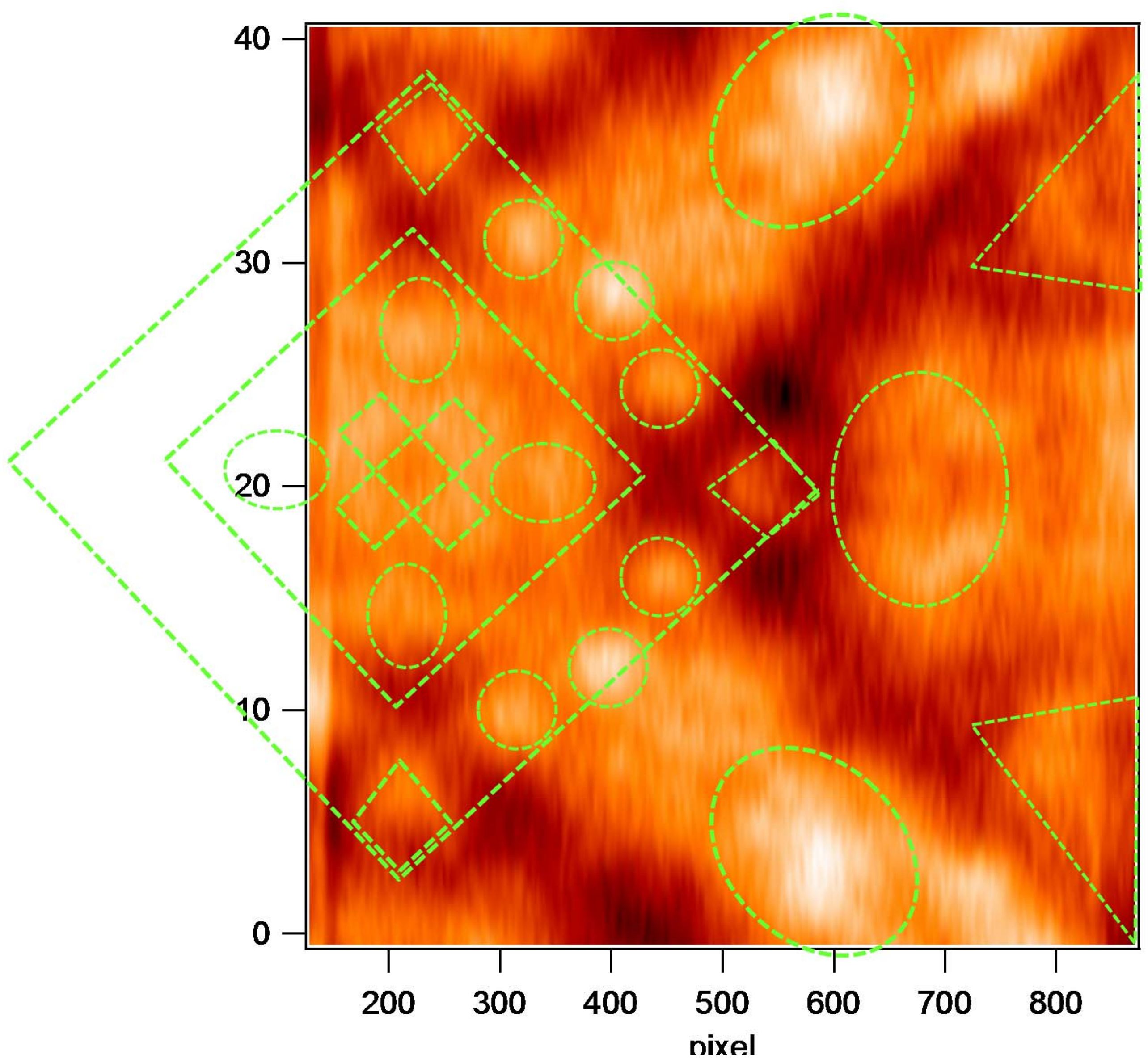

Experiment: Fadley Group-ALS

XPD Kikuchi-Band Theory

LSMO 5nm Film „bulk“
Mn emission
E=793eV
hv = 833.2 eV

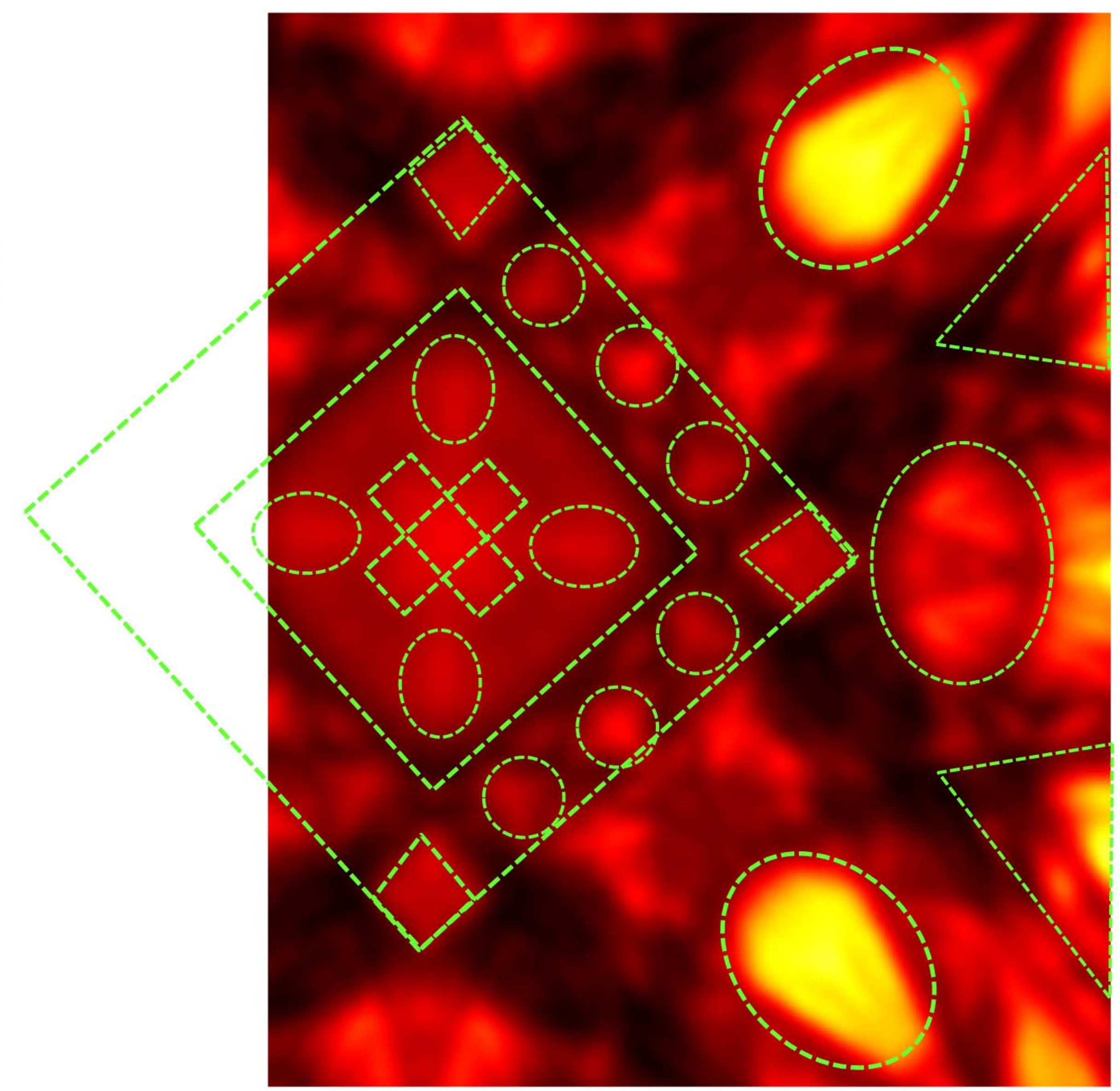

Theory: A. Winkelmann

Correcting buried LSMO layer ARPES for XPD

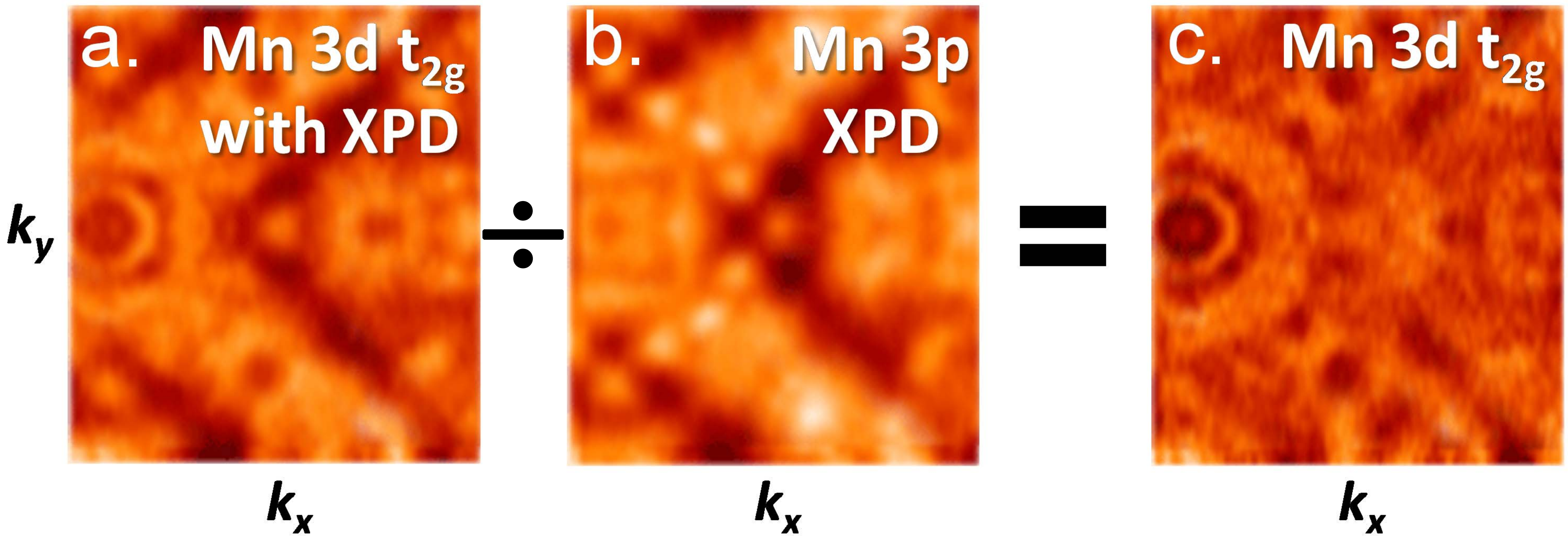

LSMO Bulk sensitive point E along the rocking curve

Probing **Bulk** LSMO (max. Bulk sensitivity)

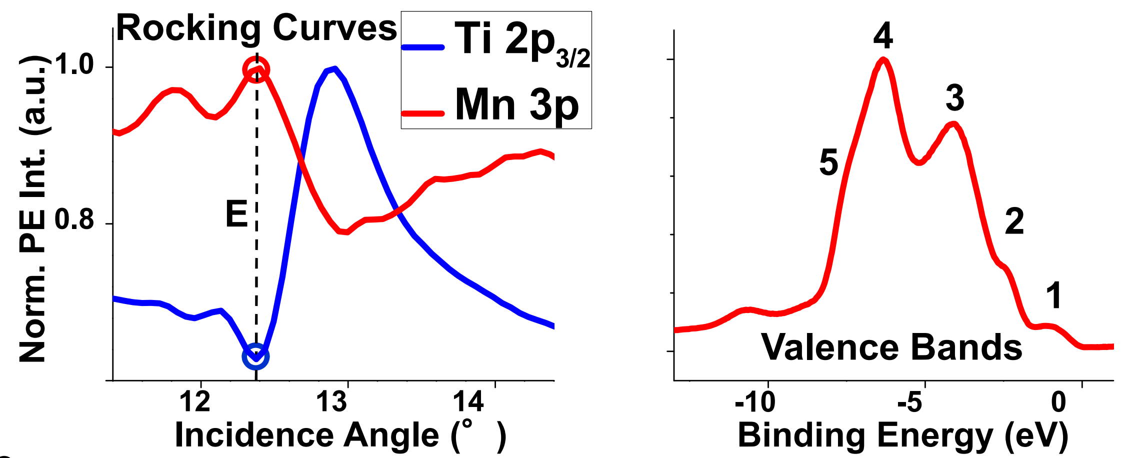

hv = 833.2 eV
T = 20 K
Debye-Waller ≈ 0.75→
75% DTs +
25% XPD-like

CORRECTED FOR XPD

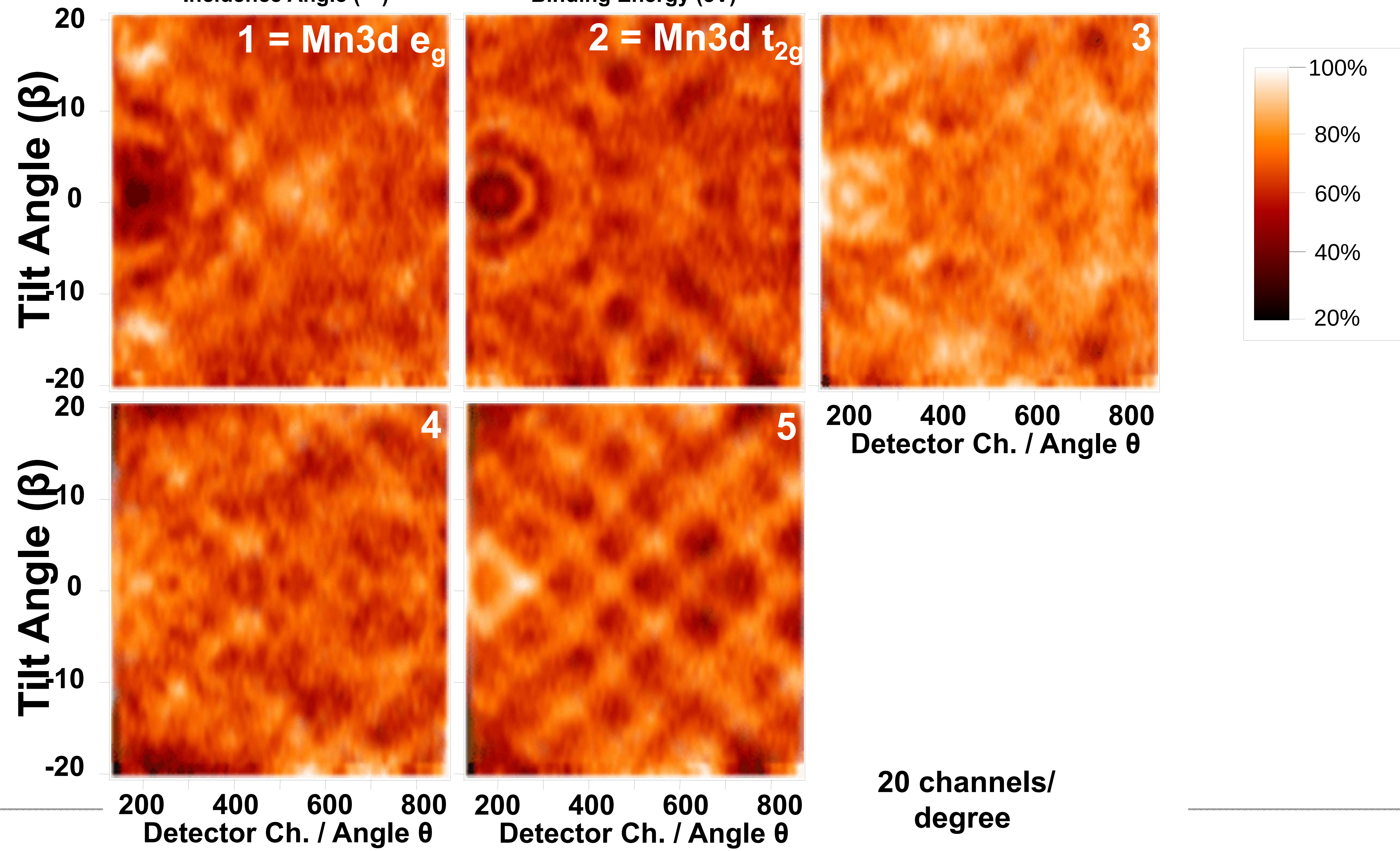

20 channels/ degree

LSMO Bulk sensitive point E along the rocking curve

Probing
Bulk LSMO
(max. Bulk
sensitivity)

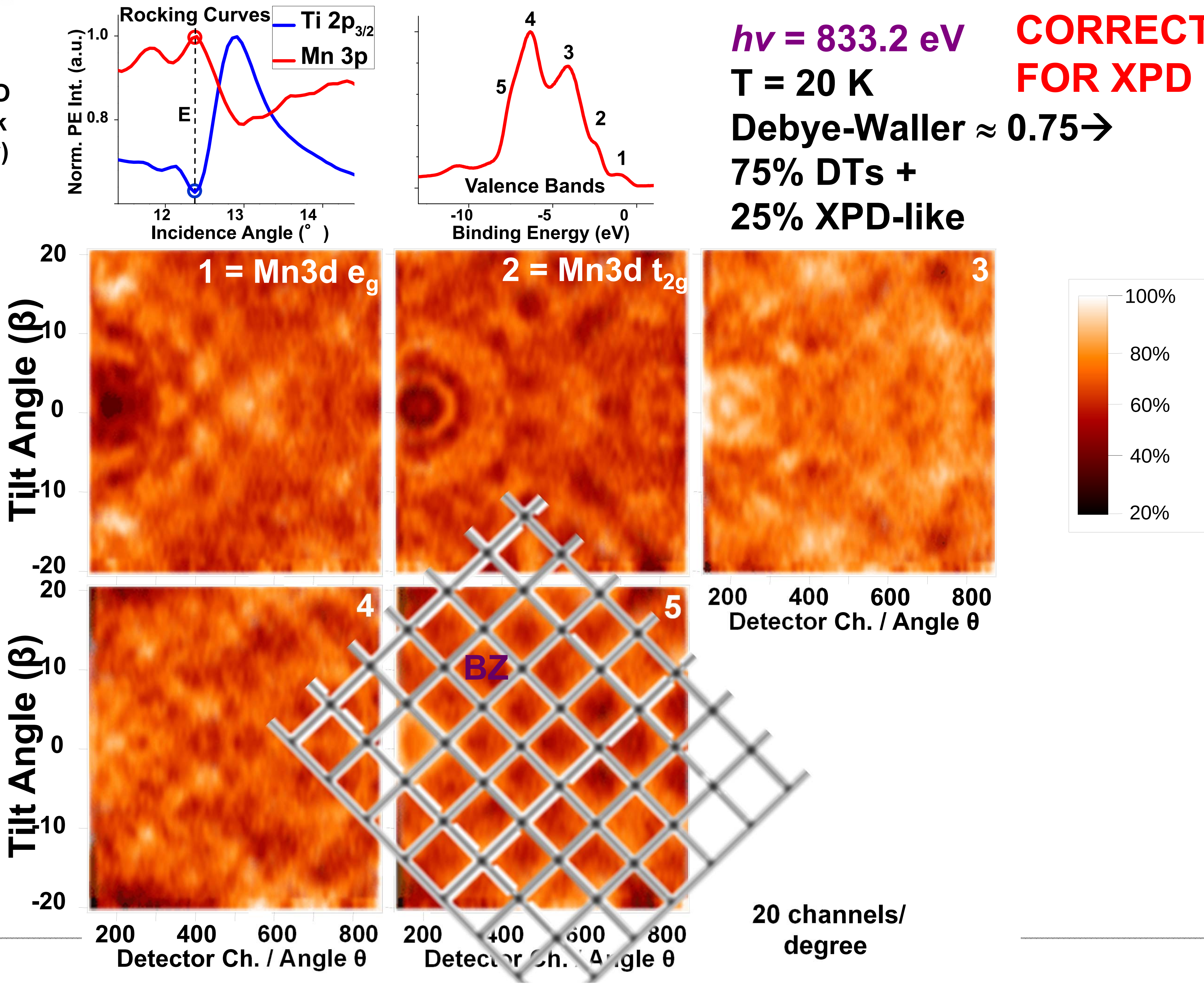

$h\nu$ = 833.2 eV
T = 20 K
Debye-Waller ≈ 0.75→
75% DTs +
25% XPD-like

CORRECTED FOR XPD

20 channels/
degree

First comparison to one-step photoemission theory for LSMO

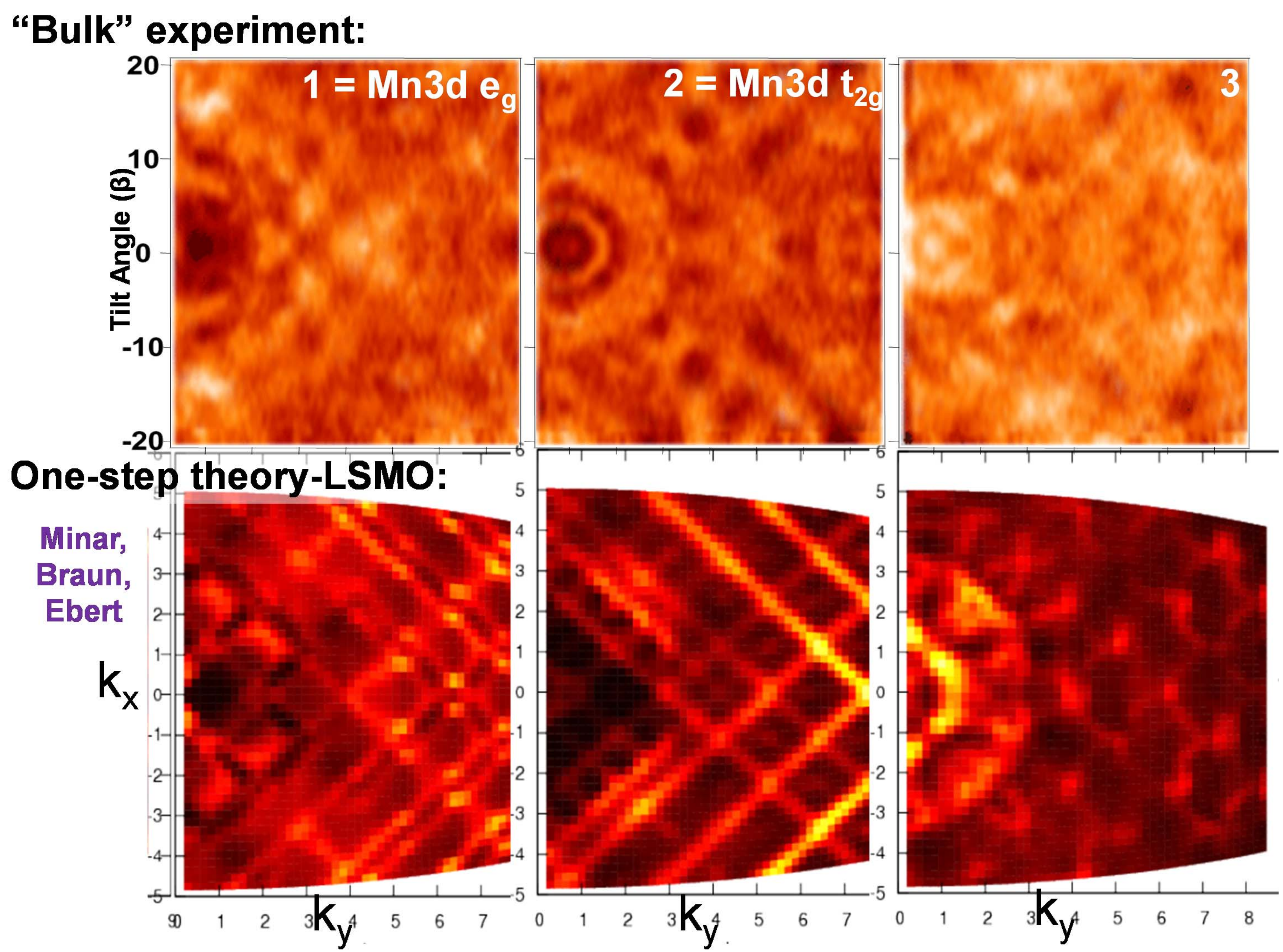

First comparison to one-step photoemission theory for LSMO

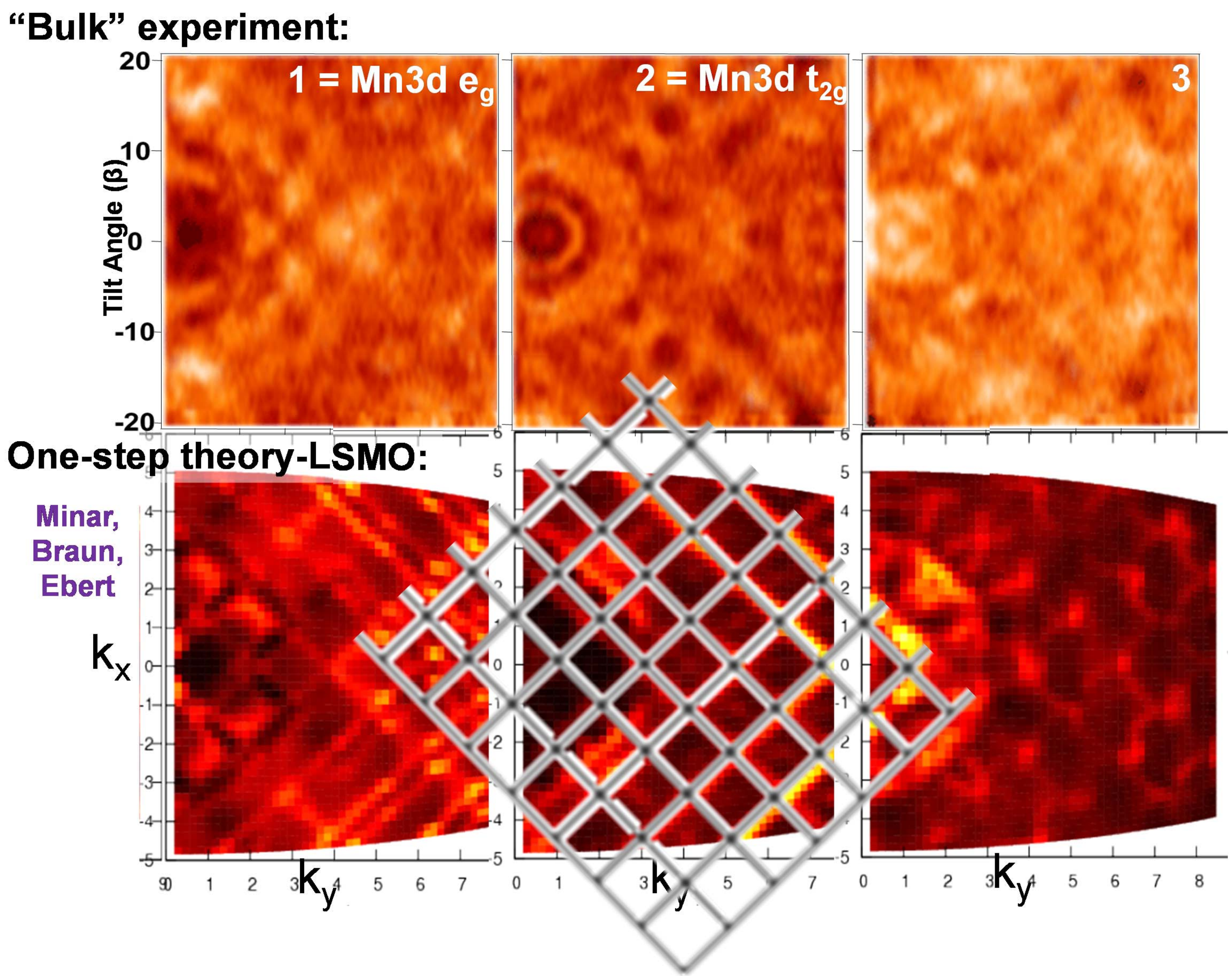

LSMO Bulk sensitive point E along the rocking curve

Probing **Bulk** LSMO (max. Bulk sensitivity)

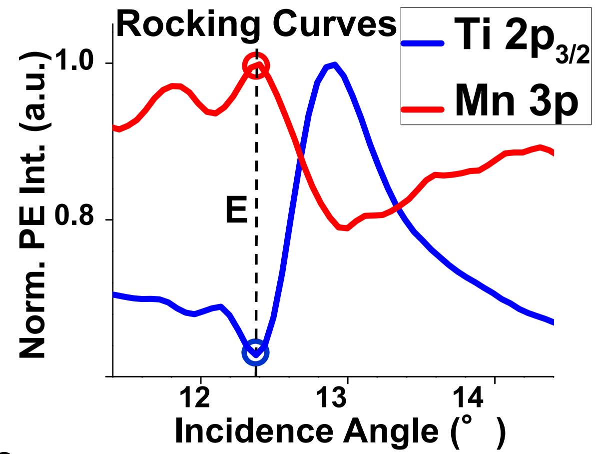

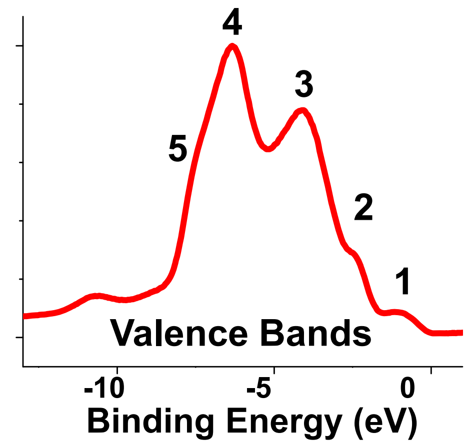

hv = 833.2 eV

T = 20 K

Debye-Waller ≈ 0.75→

75% DTs +

25% XPD-like

CORRECTED FOR XPD

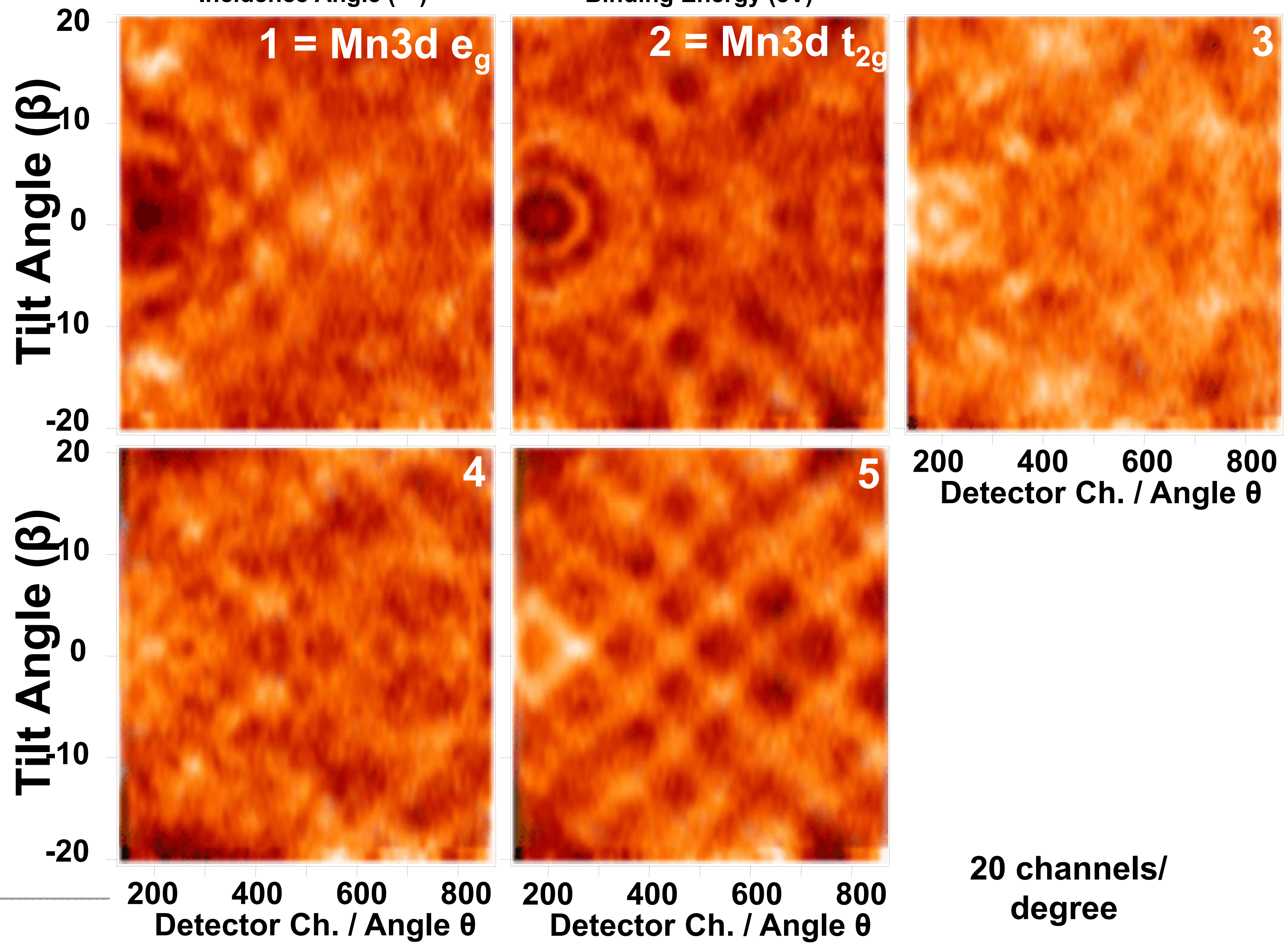

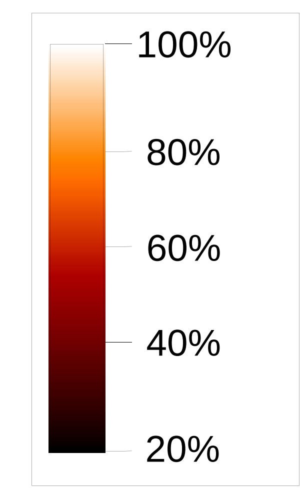

20 channels/ degree

LSMO Interface sensitive point C along the rocking curve

Probing
Interface LSMO
(max. Interface
sensitivity)

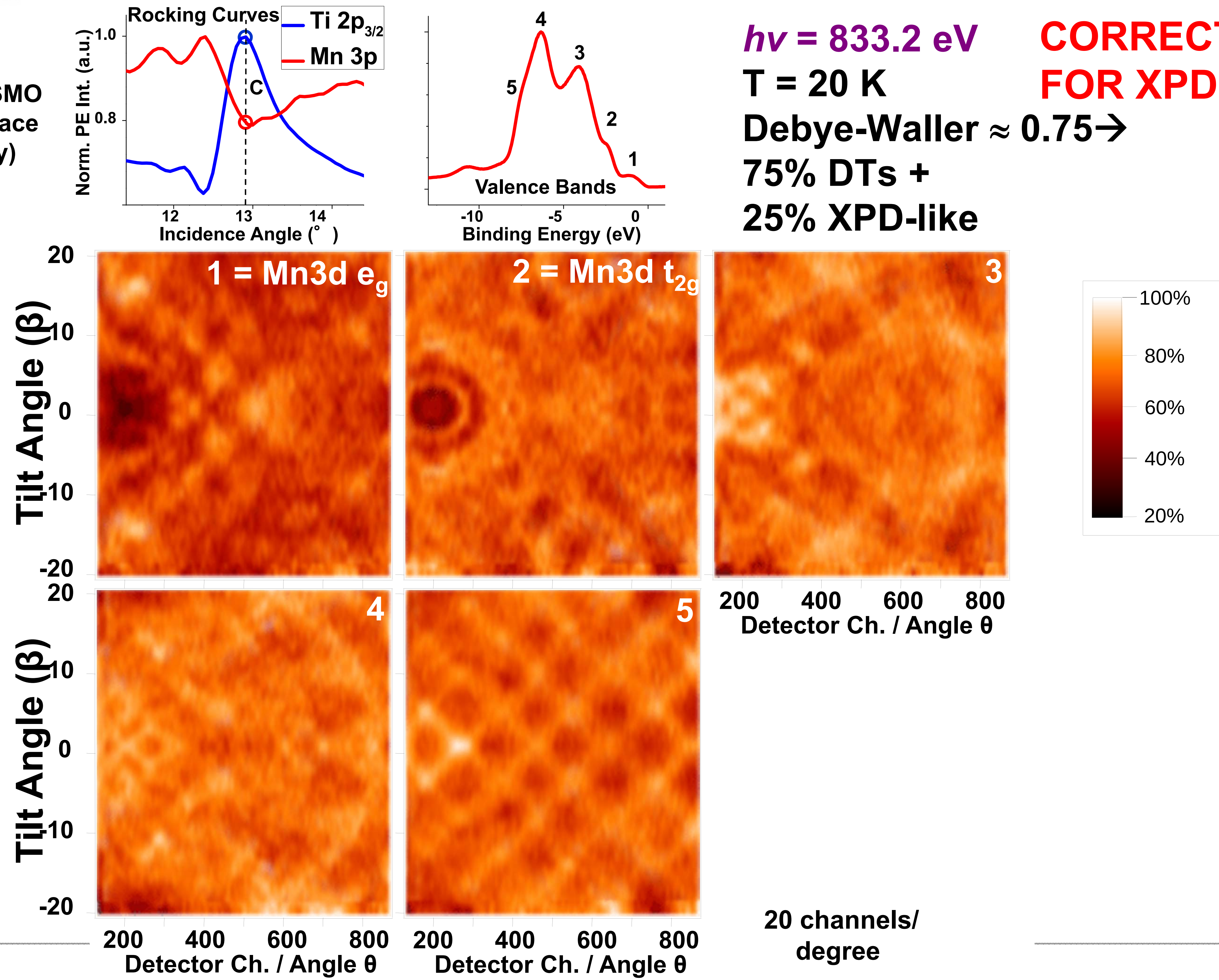

hv = 833.2 eV
T = 20 K
Debye-Waller ≈ 0.75→
75% DTs +
25% XPD-like

CORRECTED FOR XPD

20 channels/
degree

Depth-resolved ARPES- Bulk - Interface

Enhanced Contrast

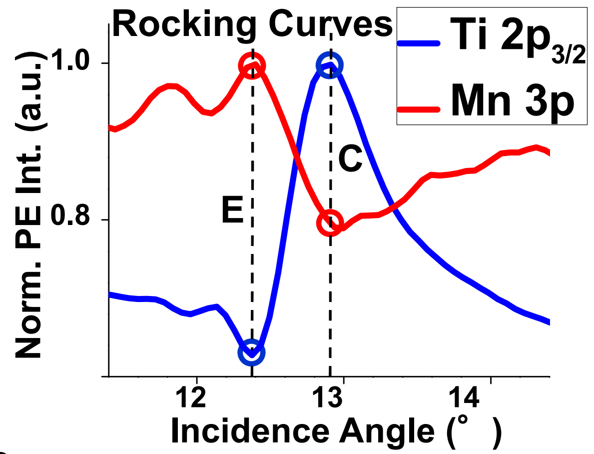

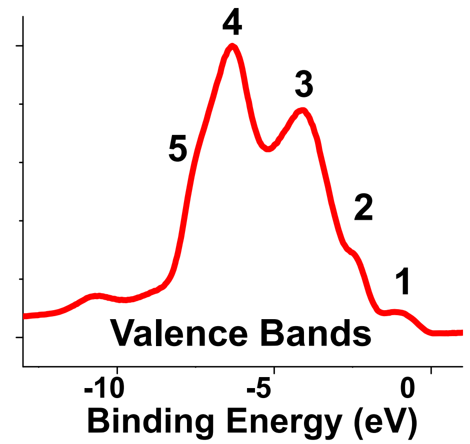

hv = 833.2 eV **RAW DATA**

T = 20 K

Debye-Waller ≈ 0.75→

75% DTs +

25% XPD-like

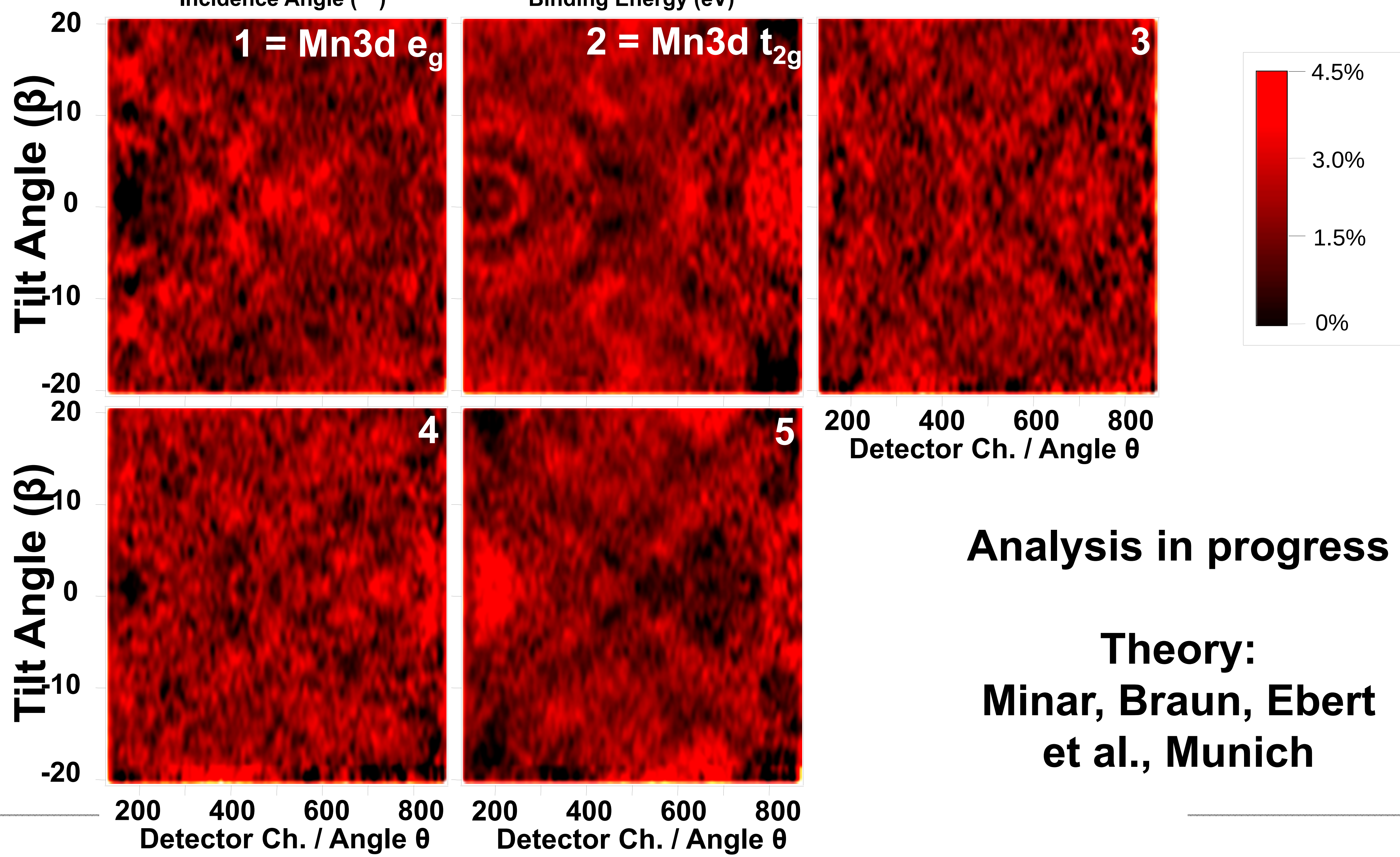

Analysis in progress

Theory:
Minar, Braun, Ebert et al., Munich

Depth-resolved ARPES-Summary

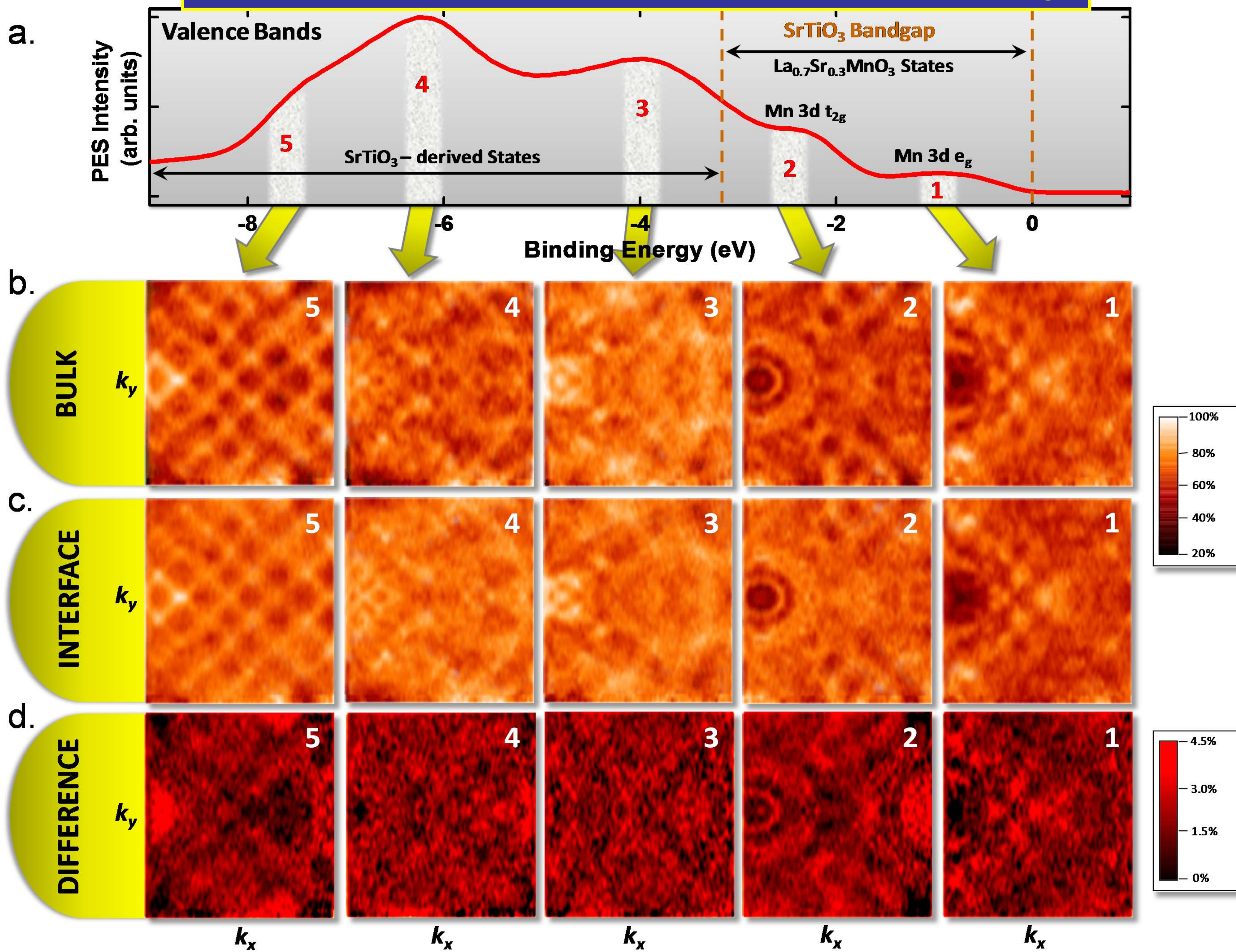

Outline

Photoemission: Some limitations, some new directions

6-8 keV

Hard x-ray photoemission of interesting bulk materials→core and valence spectra:
half-metallic/colossal magnetoresistive $La_{0.67}Sr_{0.33}MnO_3$
semiconducting CrAl alloy
metal-to-insulator transition in thin-film $LaNiO_3$

3.2 & 6 keV

Angle-resolved hard x-ray photoemission→HXPD: Kikuchi-band modeling, and HARPES for: W, GaAs & the magnetic semiconductor (Ga,Mn)As

833 & 6 keV

Standing-wave photoemission combining soft and hard x-rays, depth-resolved composition, densities of states and ARPES, and magnetization:
$SrTiO_3/La_{2/3}Sr_{1/3}MnO_3$ multilayer
Fe/MgO tunnel junction

500-700 eV

Standing-waves in a photoelectron microscope, adding the third dimension:
multilayers and microdots

Conclusions and Future Outlook

Standing wave formation in reflection from a surface, or single-crystal Bragg planes⁺, or a multilayer mirror

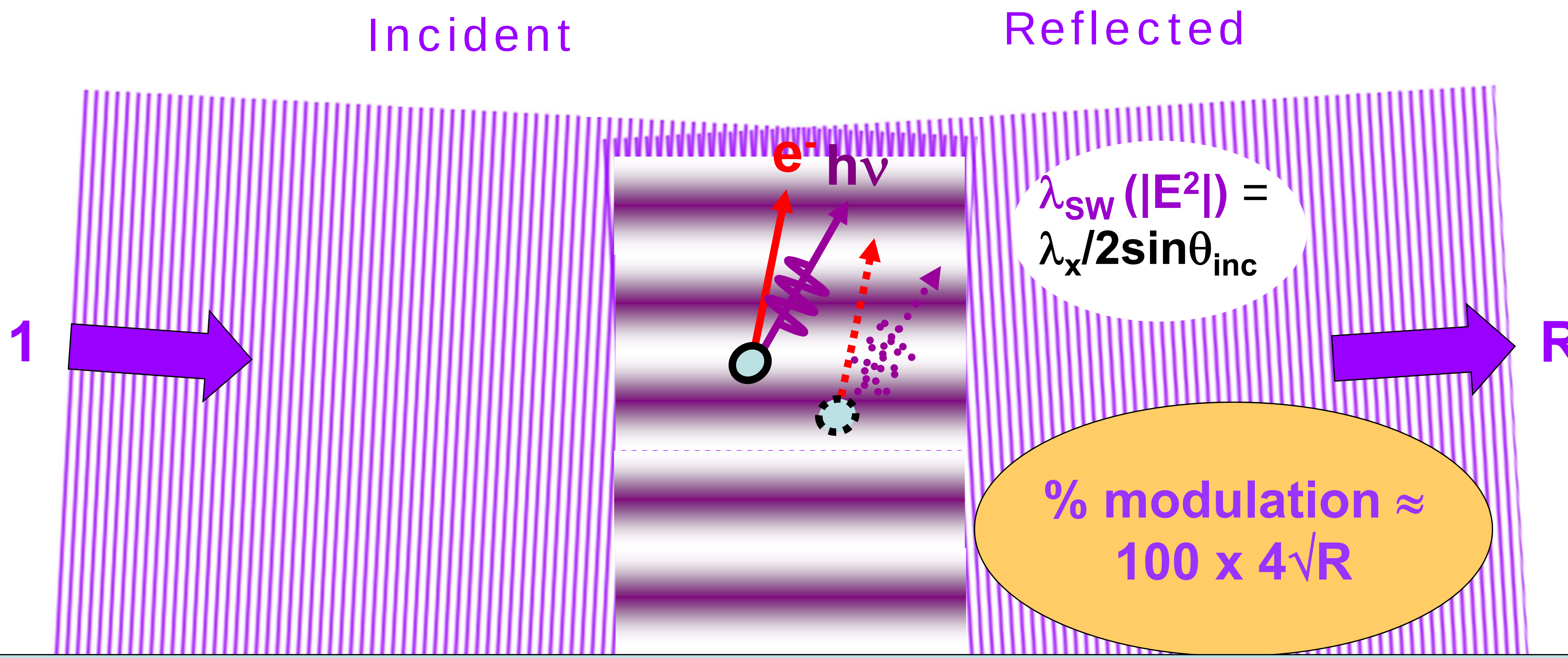

1. *<u>Rocking curve</u>*:

$$I(\theta_{inc}) \propto 1 + R(\theta_{inc}) + 2\sqrt{R(\theta_{inc})}\, f \cos[\varphi(\theta_{inc}) - 2\pi P]$$

2. *Photon <u>energy scan</u>*:

$$I(h\nu) \propto 1 + R(h\nu) + 2\sqrt{R(h\nu)}\, f \cos[\varphi(h\nu) - 2\pi P]$$

with: f = coherent fraction of atoms, P = phase of coherent-atom position

3. *<u>Phase scan with wedge-shaped sample (“Swedge” method)</u>*:

Fe/Cr GMR--Yang, Mun,….,J. Phys. Cond. Matt. 14, L406 (2002); ; **Co/CoFeB/Al_2O_3 TMR**--Yang, Mun,… J. Phys.: Cond. Matt. 18, L259 (2006); **Fe/MgO TMR**— Döring, Balke, Yang—PRB B 83, 165444 (2011) & TBP

Probing Buried Interfaces With X-ray Standing Waves: The standing-wave/wedge (SWEDGE) method

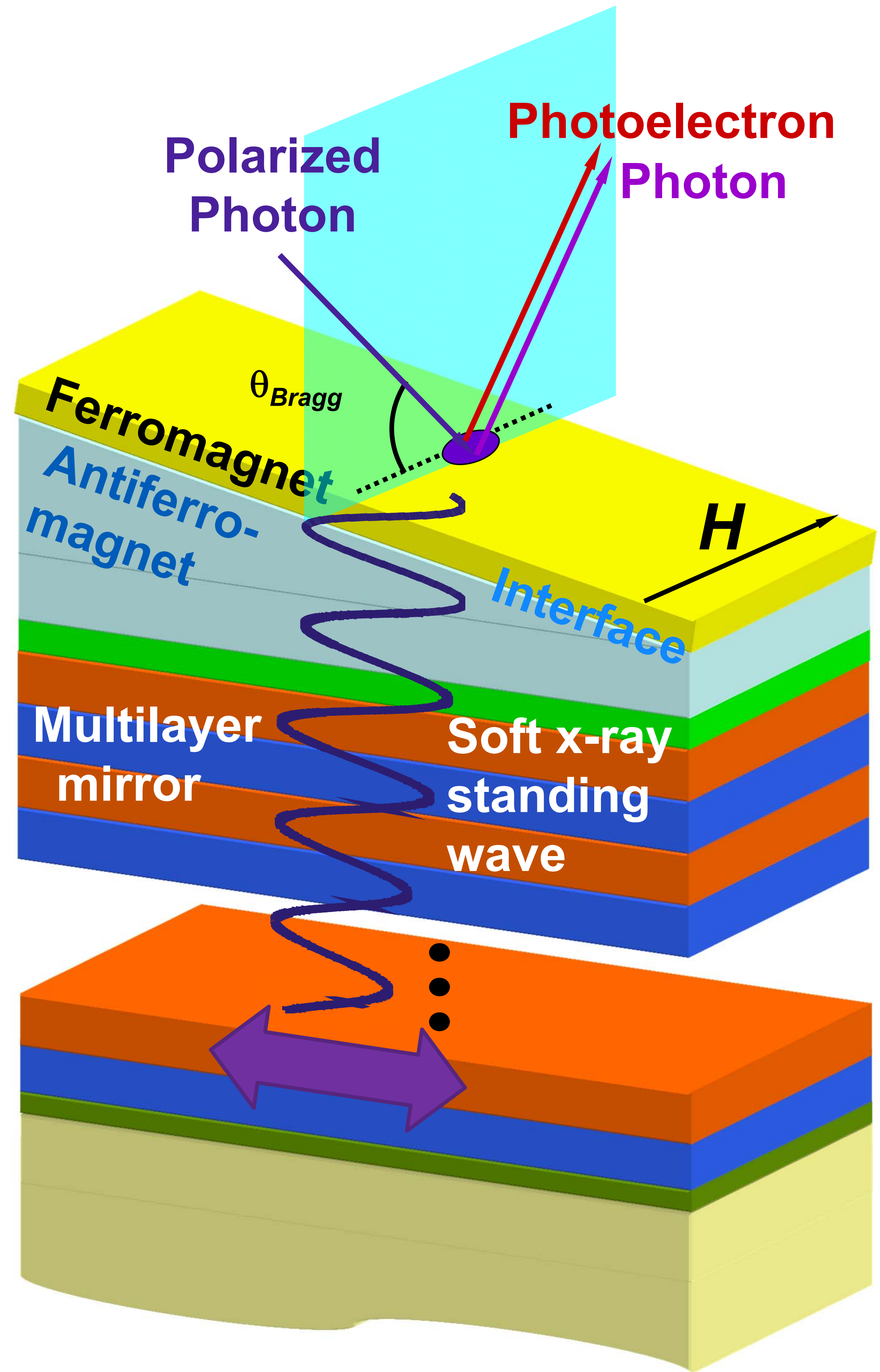

Probing Buried Interfaces: The Standing Wave-Wedge ("Swedge") Method

Example: The MgO/Fe magnetic tunnel junction interface

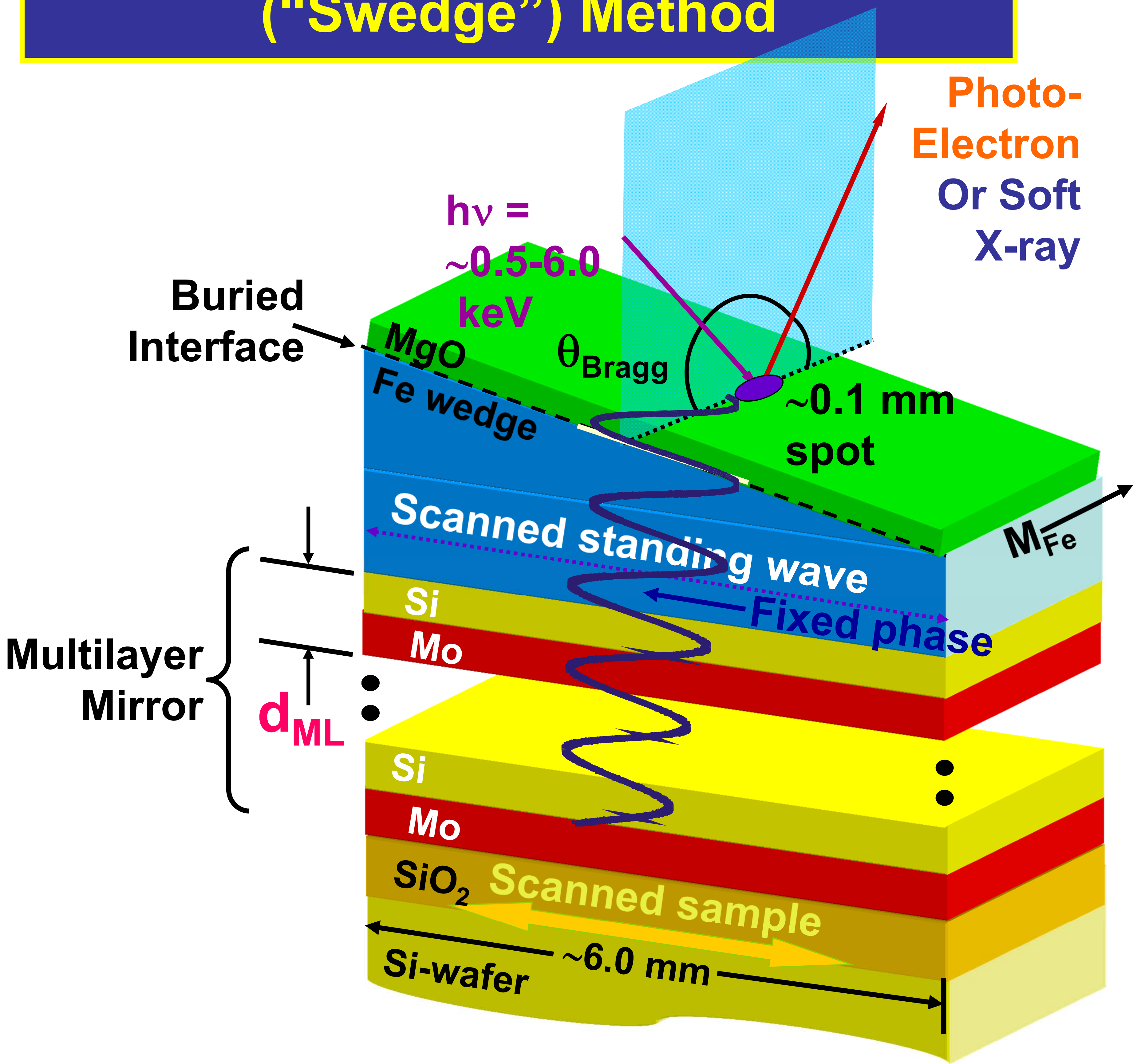

$\lambda_{SW}(|E^2|) = \lambda_x/2\sin\theta_{inc} \approx d_{ML}$

1st order Bragg: $\lambda_x = 2d_{ML}\sin\theta_{Bragg}$

Soft x-ray standing-wave wedge scans through a magnetic tunnel junction

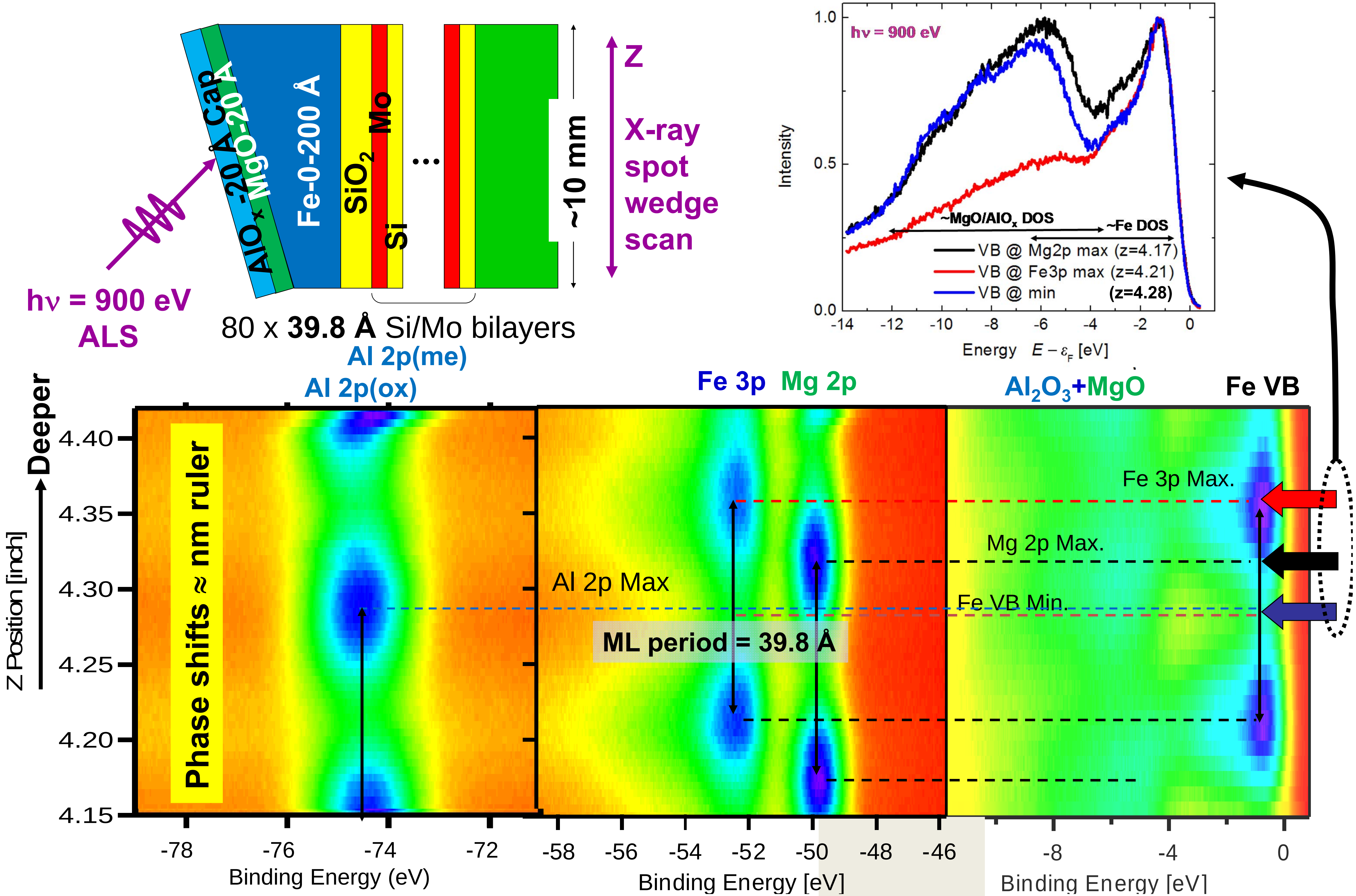

Balke, Yang, Papp, Doring, Berges, Plucinski, PRB, submitted

Hard x-ray wedge scans-BESSY

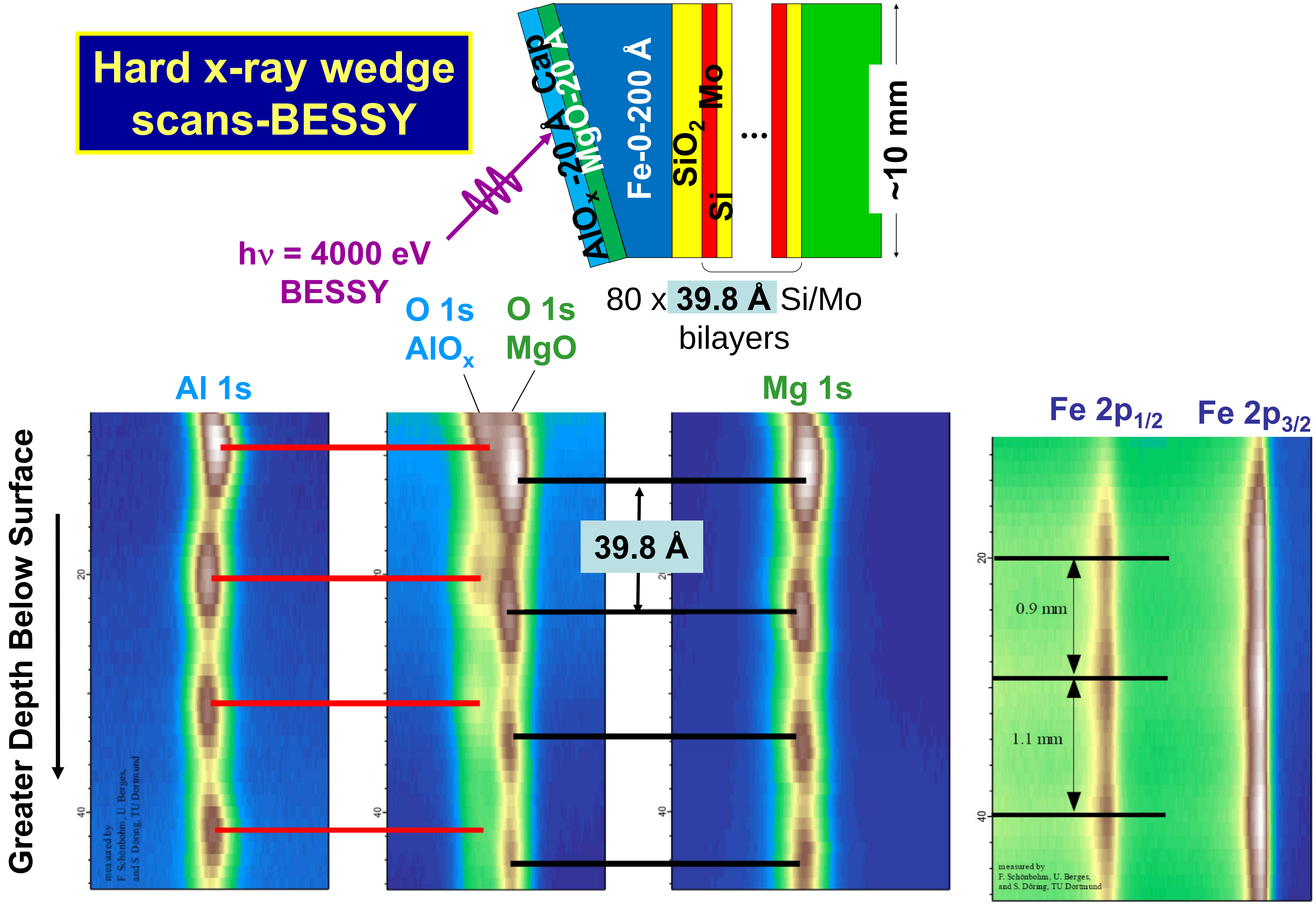

S.Döring, F. Schonbohm, U.Berges, M. Gorgoi, C. Westphal, D. Buergler, C. Schneider, C. Papp, B. Balke, C. Felser, C.F. Phys. Rev. B 83, 165444 (2011)

X-Ray Optical Analysis of Hard X-Ray Wedge Scans--hν = 4.0 keV

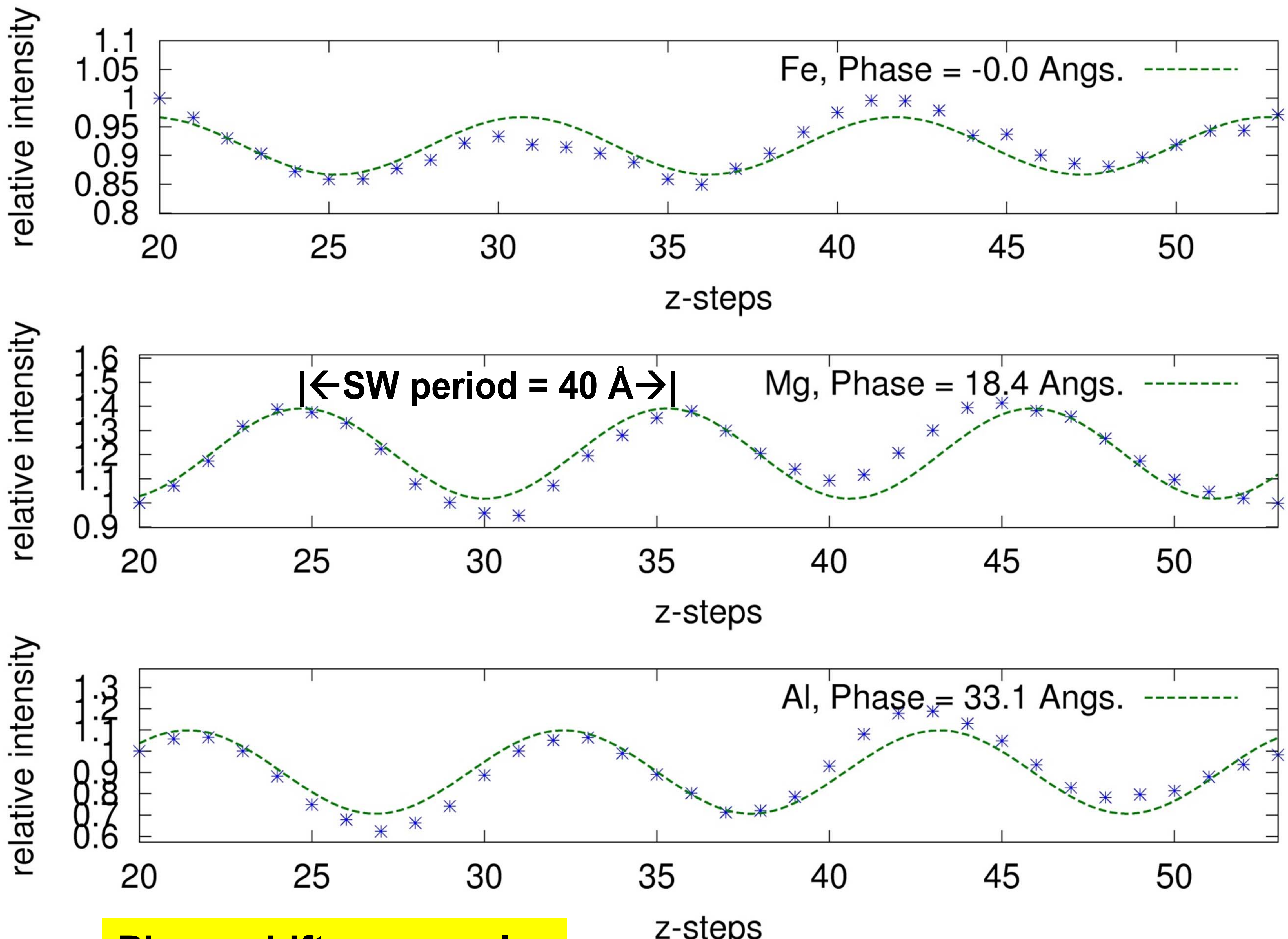

Phase shifts ≈ nm ruler

S. Döring et al., Phys. Rev. B 83, 165444 (2011)

(D) **Magnetic Circular Dichroism with Standing Wave Excitation- MgO/Fe, hν = 900 eV**

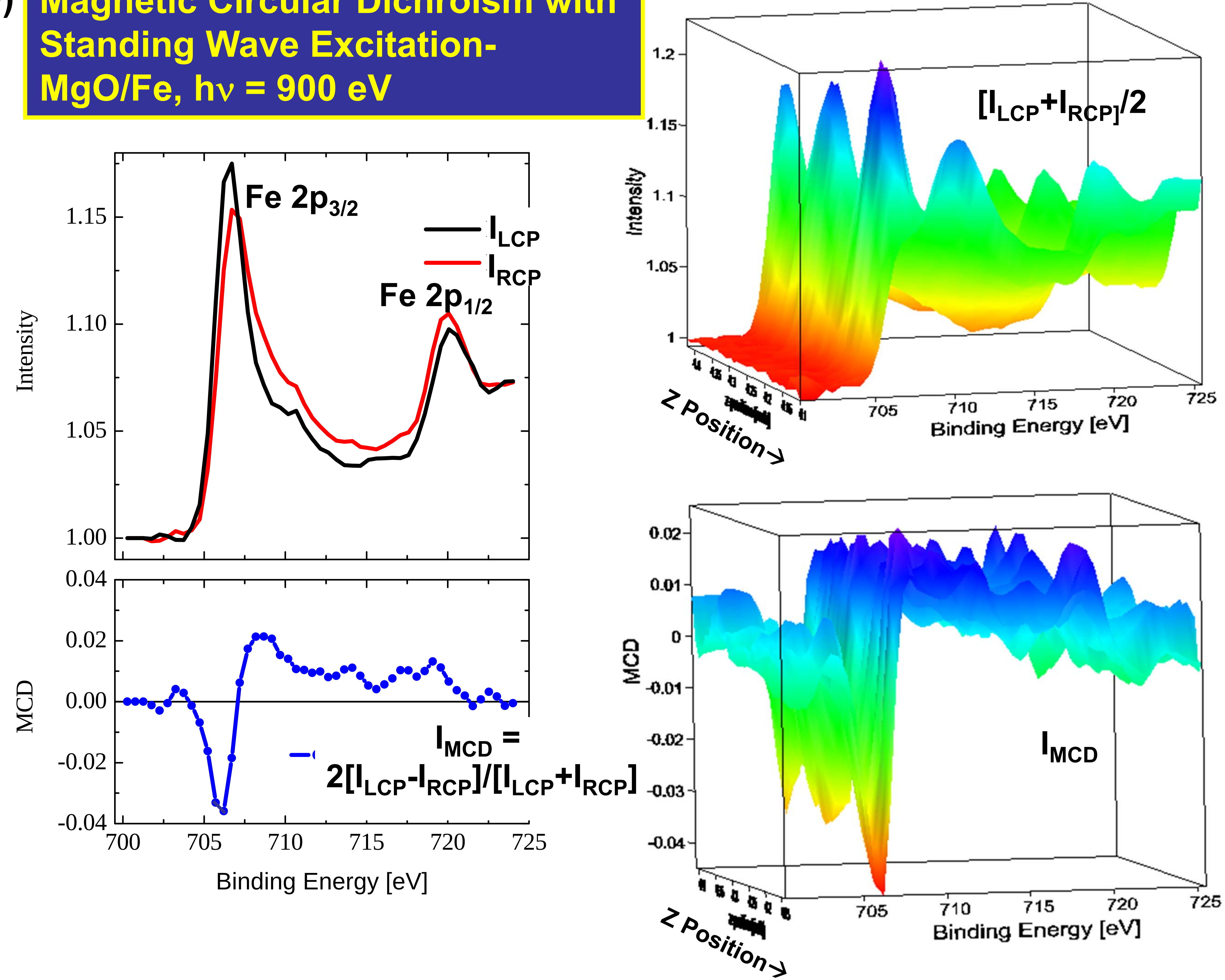

Balke, Yang, et al., PRB, submitted

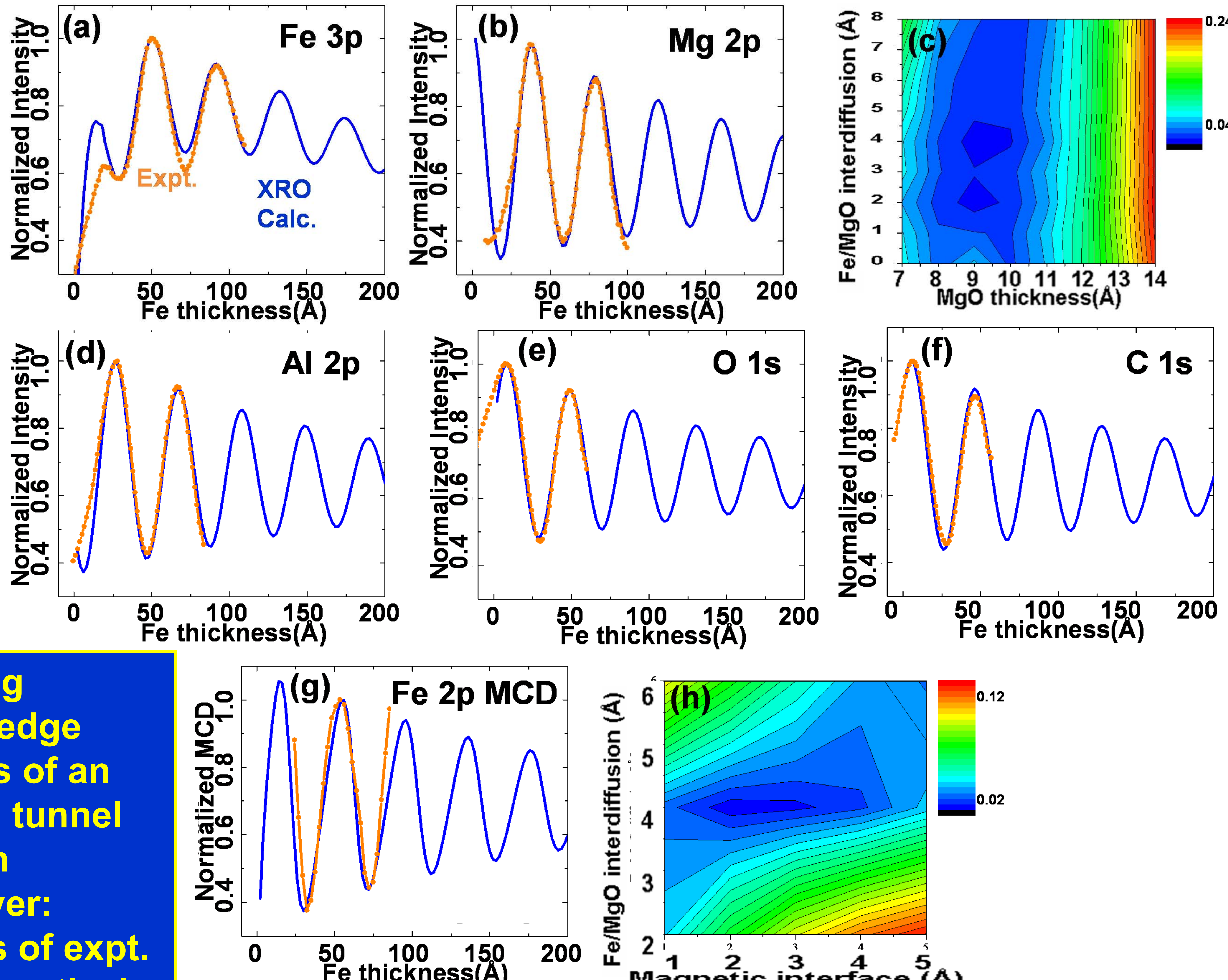

Standing wave/wedge analysis of an Fe/MgO tunnel junction multilayer: final fits of expt. to x-ray optical calcs.

Balke, Yang et al., PRB, submitted

Final profiles of concentration and magnetization

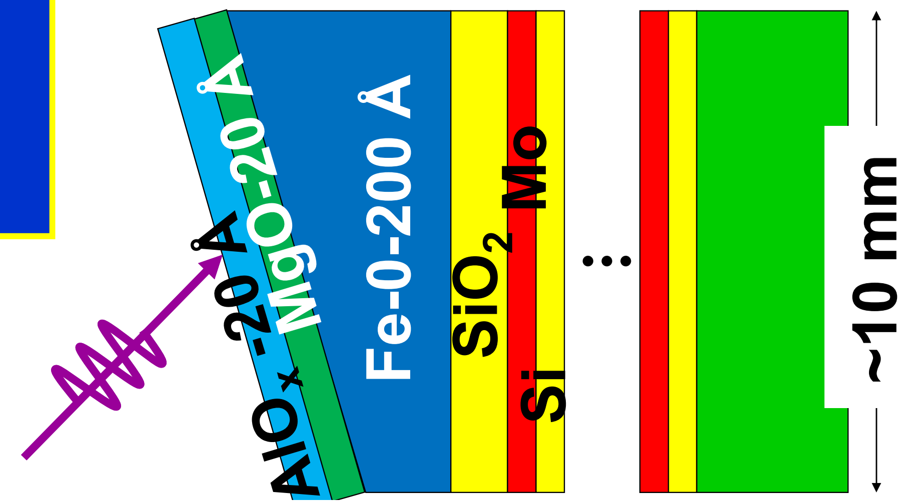

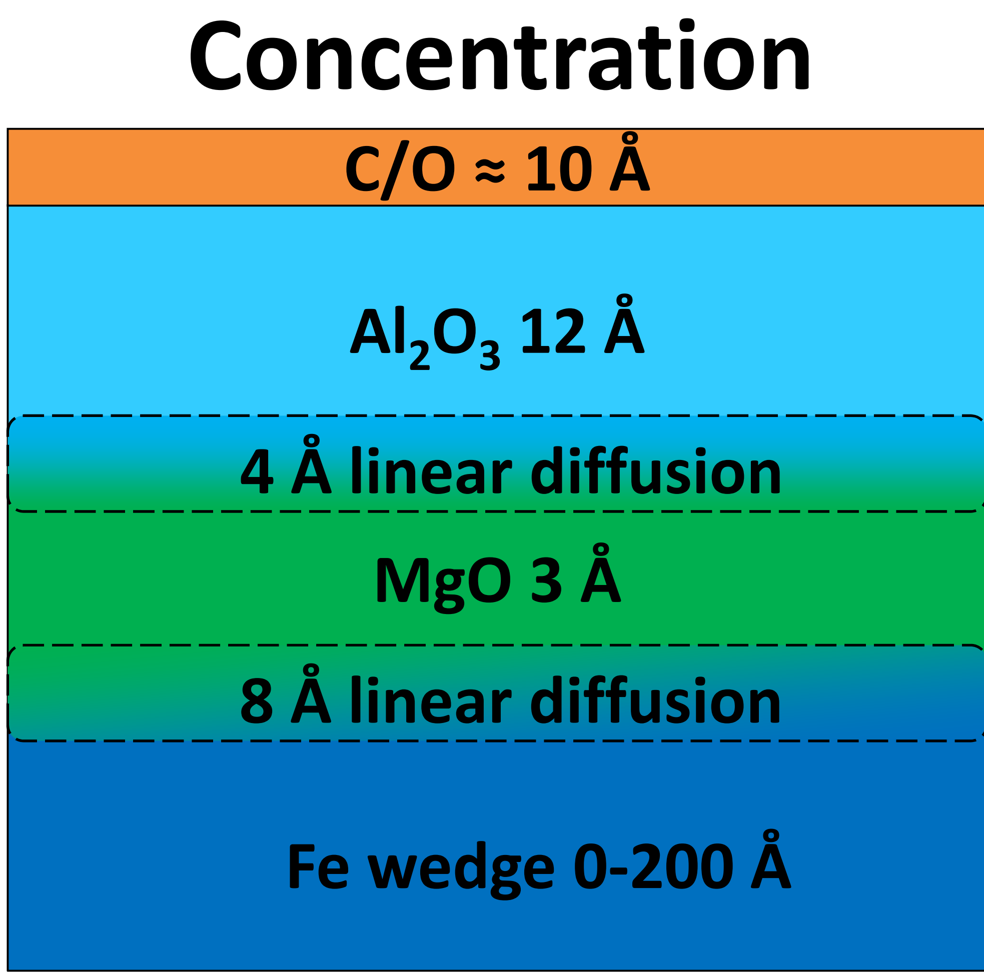

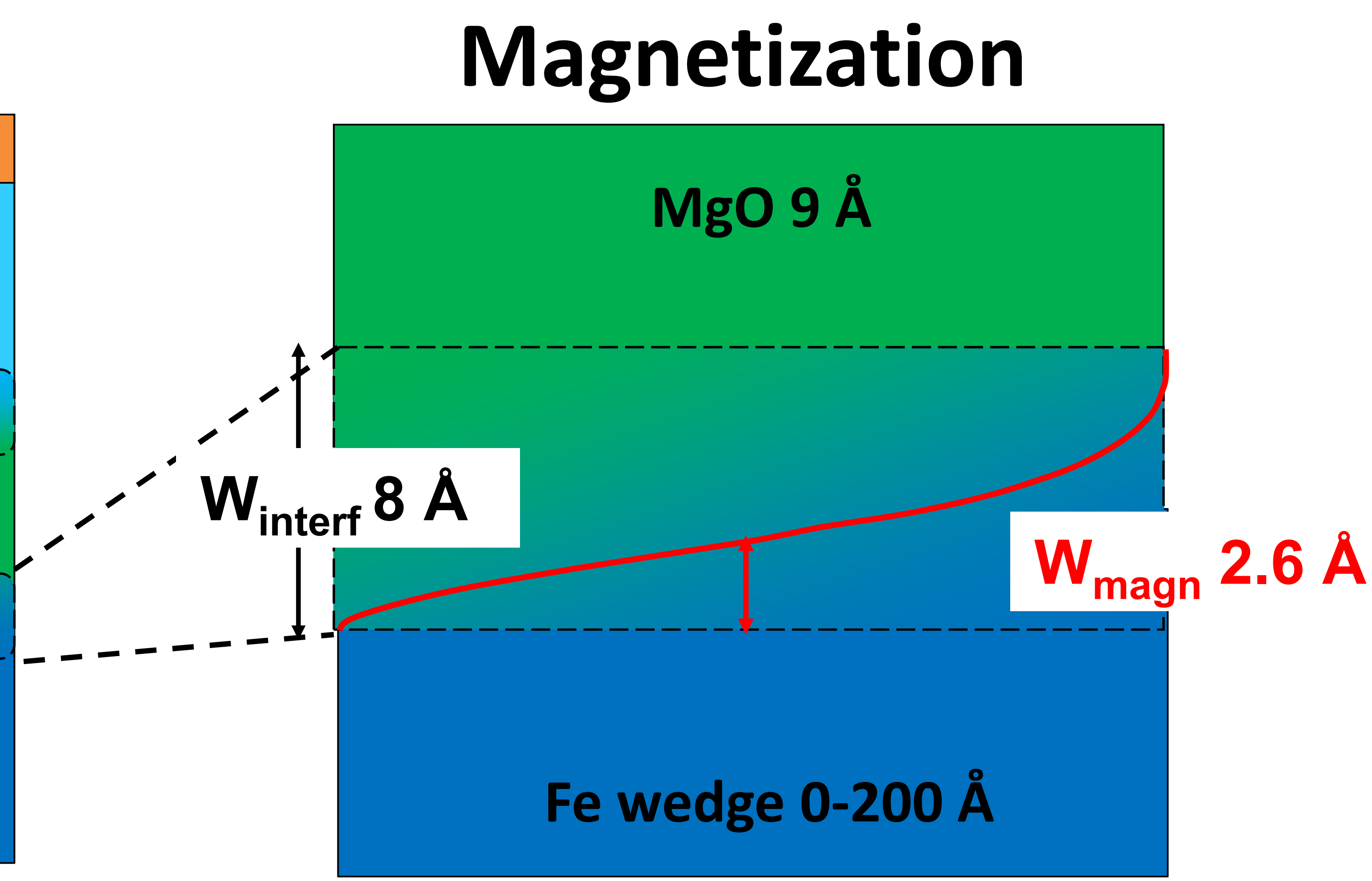

Yang, Balke et al., PRB, submitted

MgO/Fe tunnel junction- the real interface

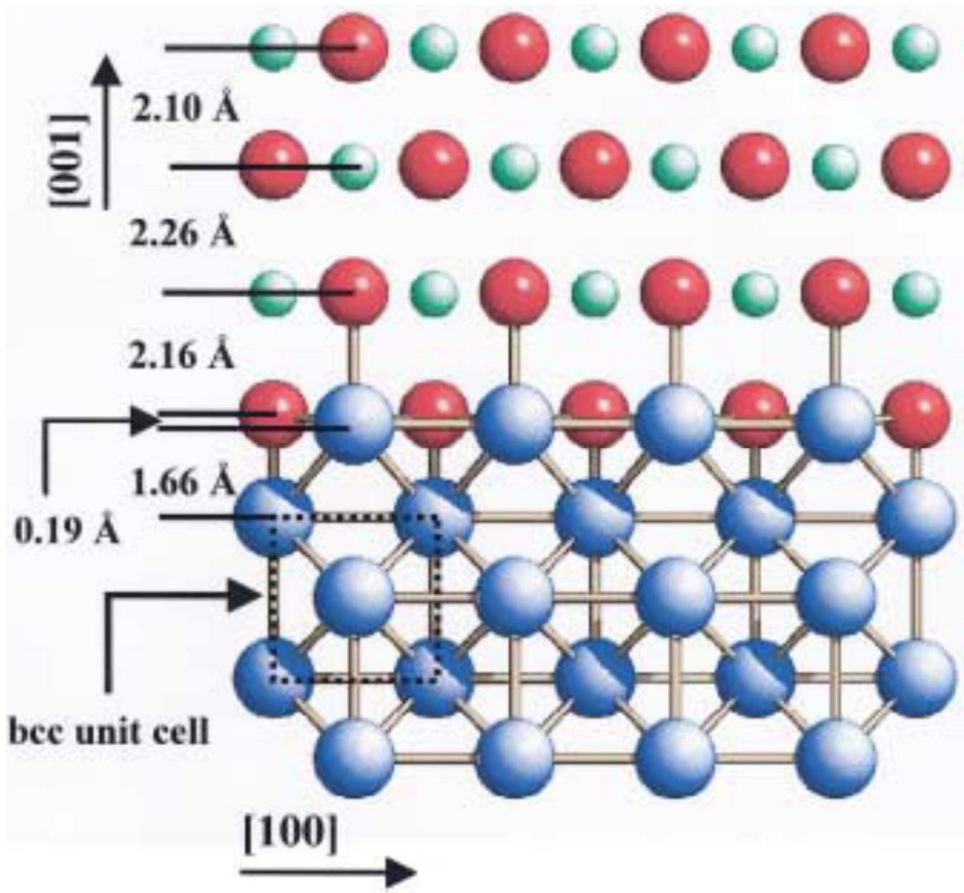

Meyerheim PRL 87, 076102 (2001).

- *Is there FeO at the interface?*
- *What is the density of states at the interface?*
- *Δ_1 controls tunneling? Can we see bands at epitaxial interfaces? (Future project)*

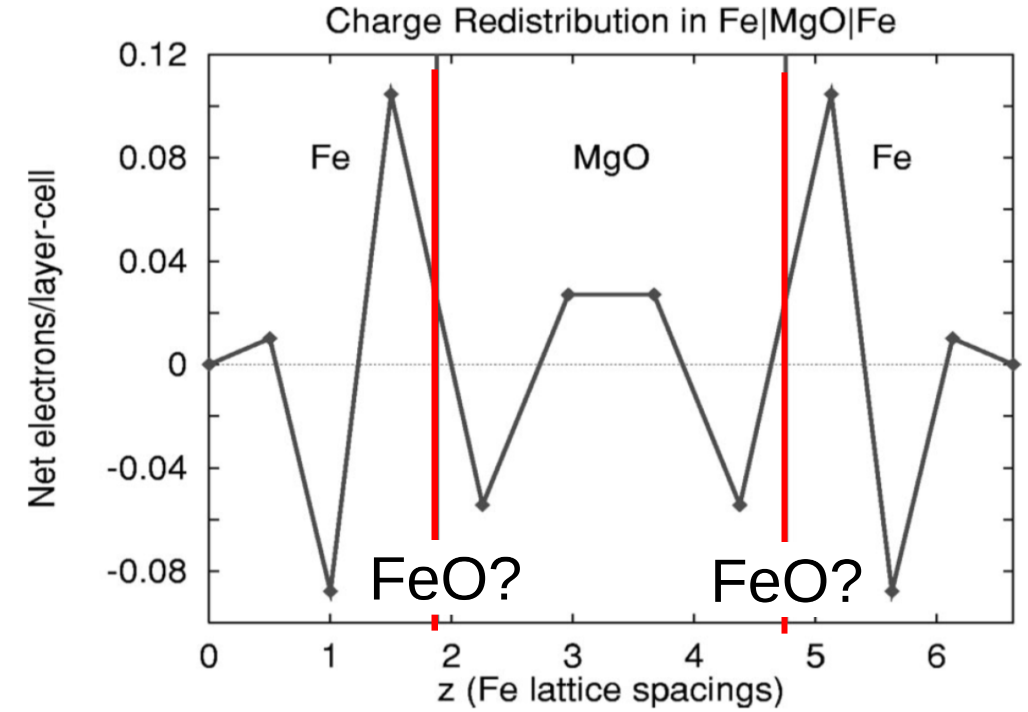

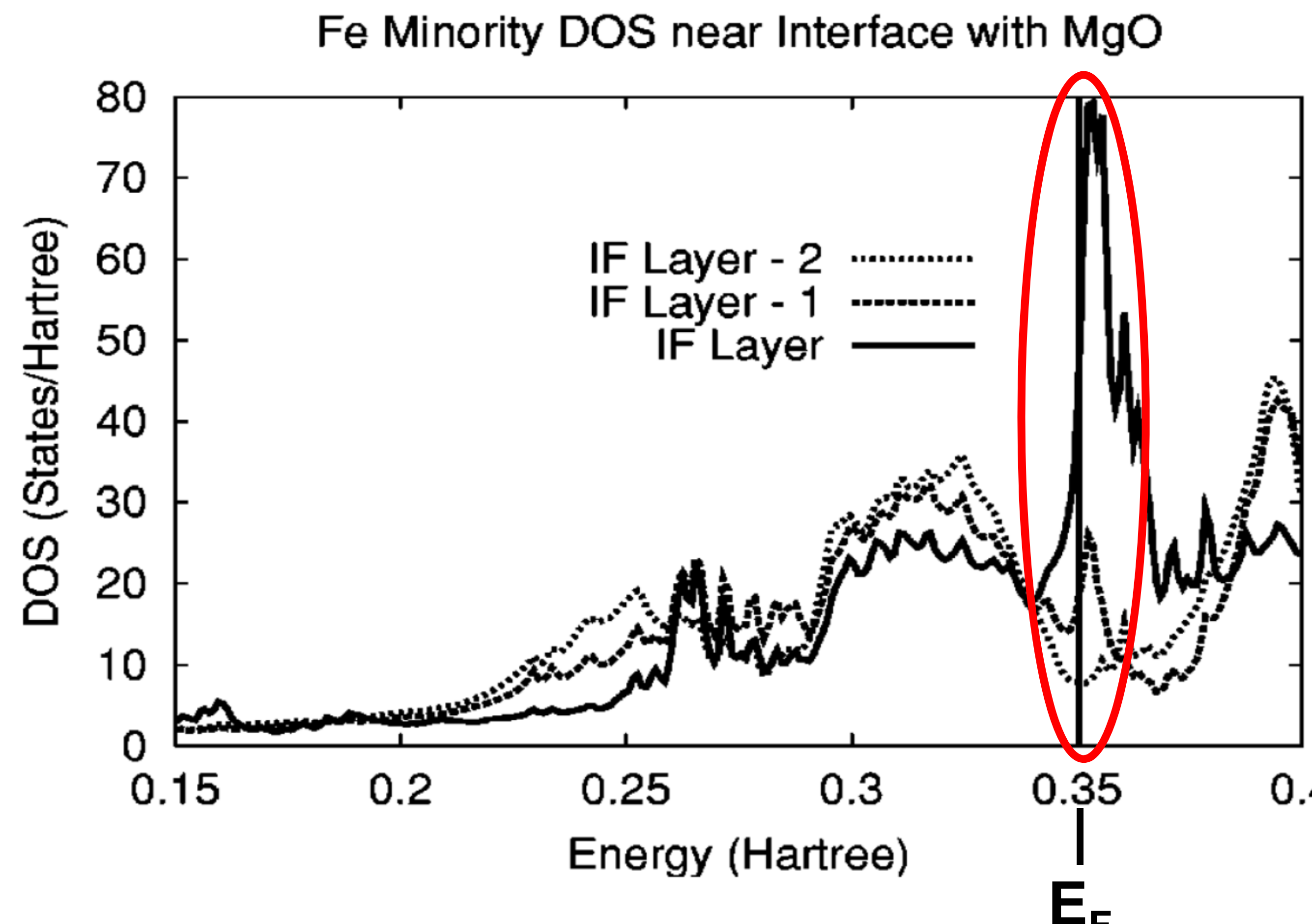

FIG. 3. Density of states for each atomic layer of Fe(100) near an interface with MgO. One hartree equals 27.2 eV.

Butler et al.,PRB 63, 054416 (2001);
Mathon & Umerski, PRB 63, 220403 (2001);
Mertig et al., PRB 73, 214441 (2006)

MgO/Fe tunnel junction-Δ_1 states dominant in tunneling for ideal interface

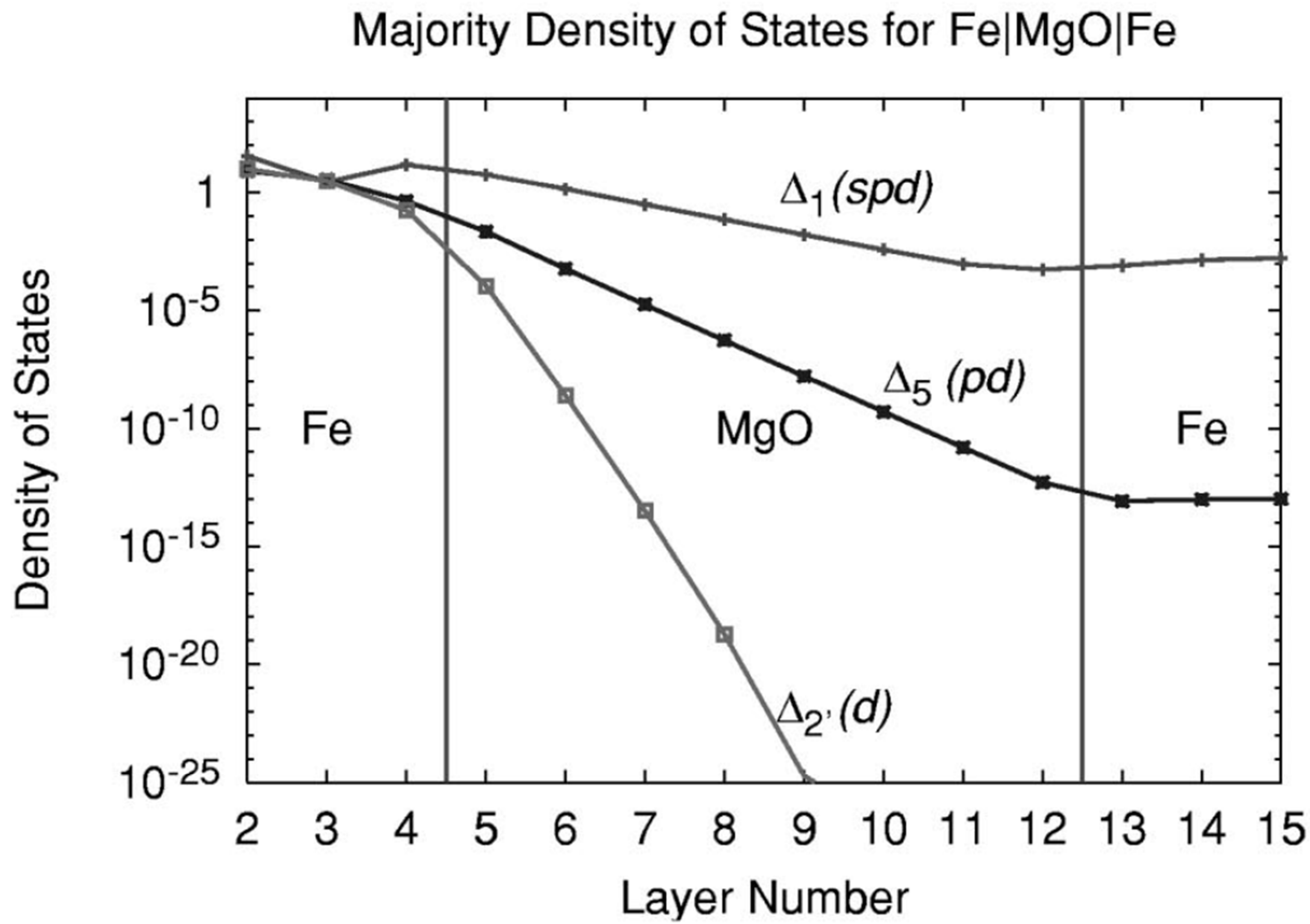

Butler et al.,PRB 63, 054416 (2001)

Self-consistent x-ray optical modeling of layer-resolved valence spectra

$$I_{VB,i=1,2,..N}\left(E_{kin,j},d_{Fe,i}\right)\cong C\sum_{L=layer}\tilde{D}_L\left(E_{kin,j}\right)\int_{z\in L}\left|E\left(z,d_{Fe,i}\right)\right|^2\exp\left[-z/\left(\Lambda_{e,L}\sin\theta_e\right)\right]dz$$

$$=C\sum_L\tilde{D}_L\left(E_{kin,j}\right)\int_0^\infty W_L\left(z,d_{Fe,i}\right)dz$$

$$I_{VB,i}\left(E_{kin},d_{Fe,i}\right)\cong C\sum_L\tilde{D}_L\left(E_{kin}\right)U_L\left(d_{Fe,i}\right)$$

with $\tilde{D}_L\left(E_{kin,j}\right)$ = matrix-element weighted density of states in layer L

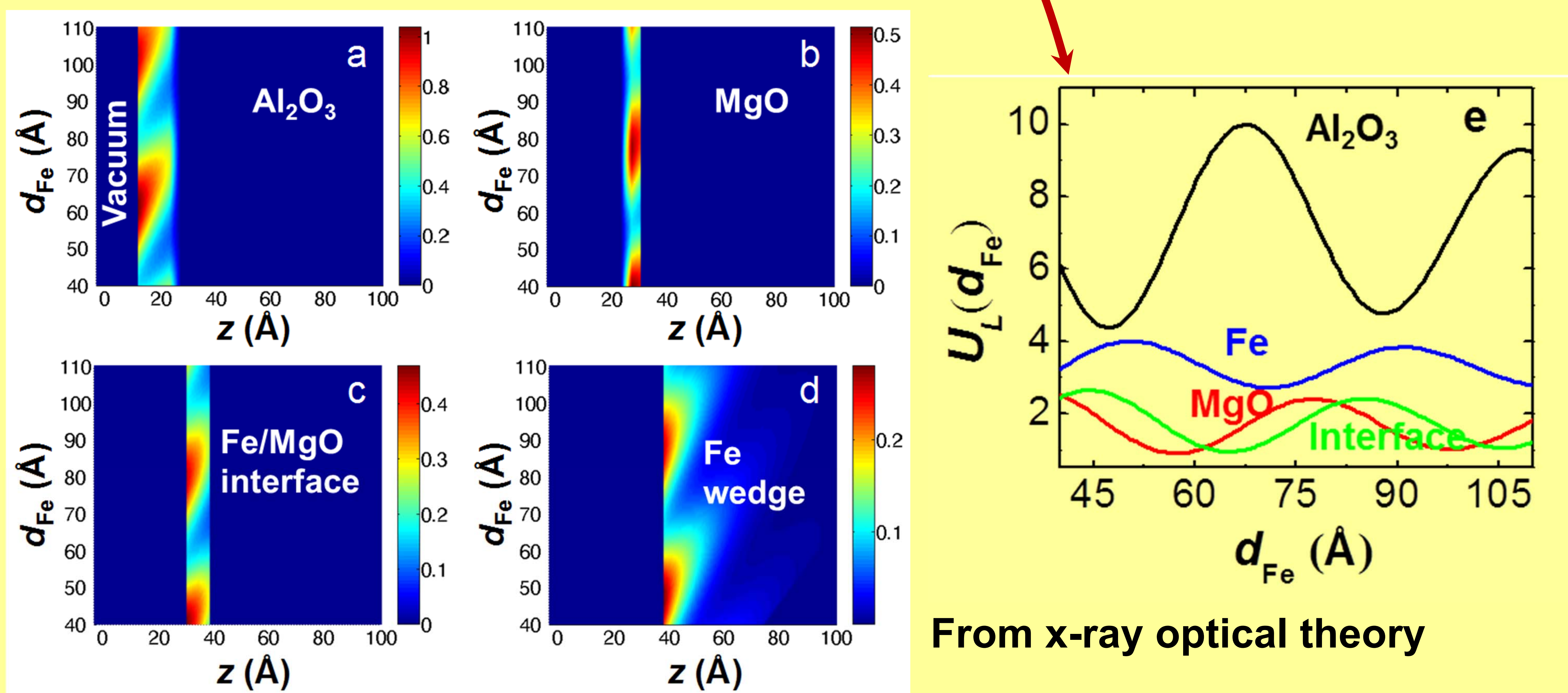

From x-ray optical theory

Standing wave/wedge derivation of depth-dependent densities of states: Fe/MgO tunnel junction

$\tilde{D}_L\left(E_{\text{kin,j}}\right)$ = matrix-element weighted density of states in layer L

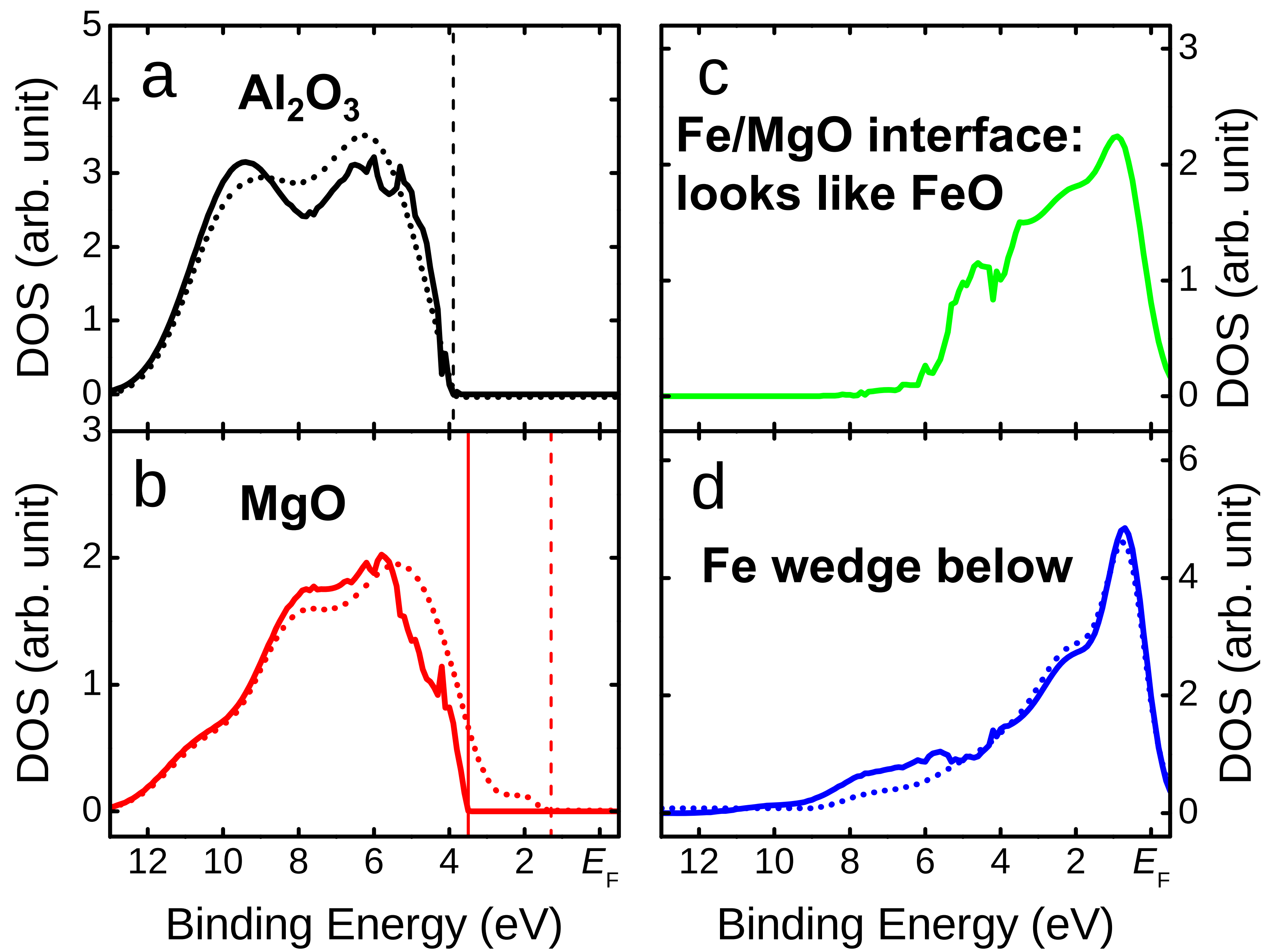

Yang, Balke, et al., PRB, submitted

Standing wave/wedge derivation of depth-dependent densities of states: Fe/MgO tunnel junction

→Oxidation at the Fe/MgO interface

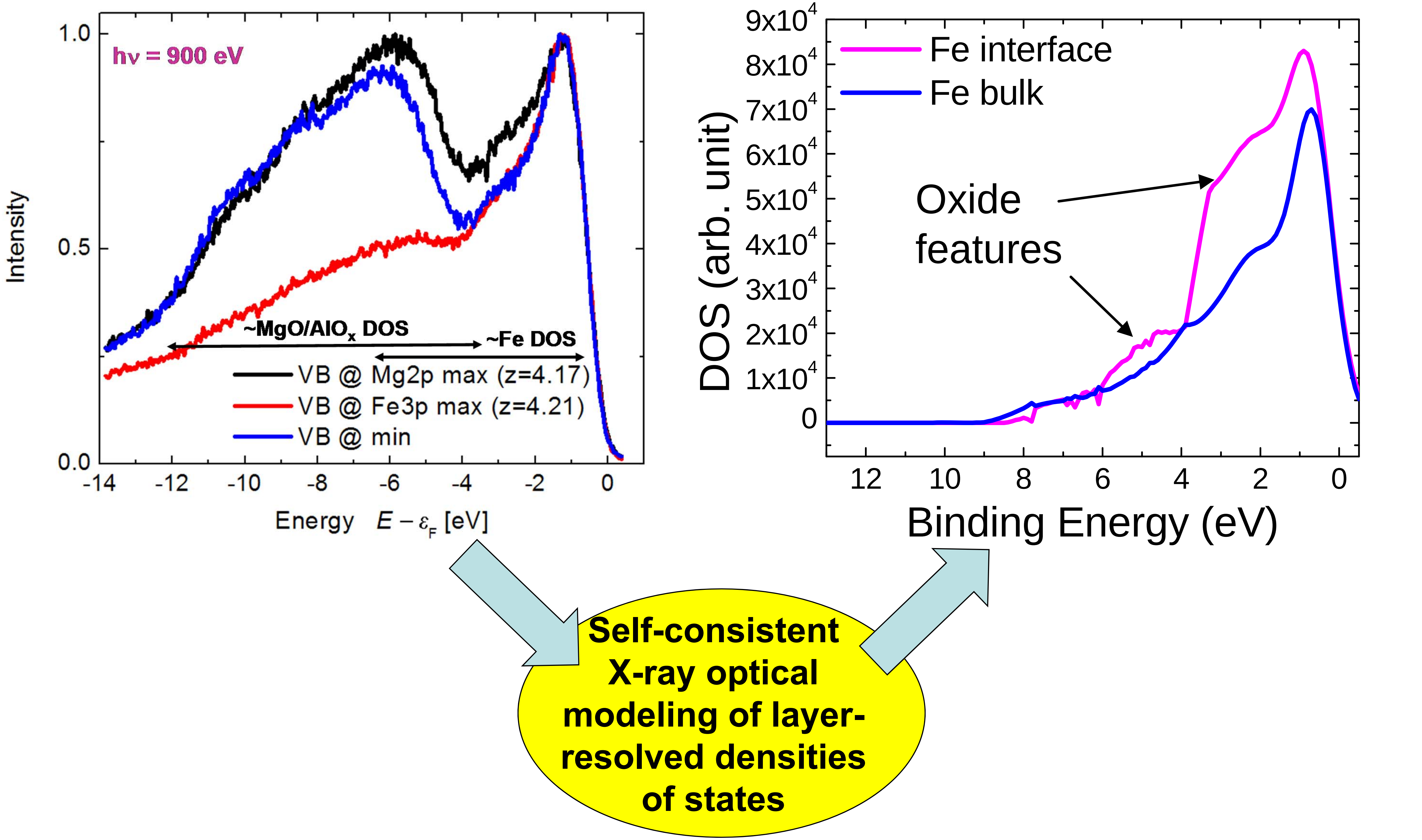

Yang, Balke, et al., PRB, submitted

Outline

Photoemission: Some limitations, some new directions

6-8 keV

Hard x-ray photoemission of interesting bulk materials→core and valence spectra:
half-metallic/colossal magnetoresistive $La_{0.67}Sr_{0.33}MnO_3$
semiconducting CrAl alloy
metal-to-insulator transition in thin-film $LaNiO_3$

3.2 & 6 keV

Angle-resolved hard x-ray photoemission→HXPD: Kikuchi-band modeling, and HARPES for: W, GaAs & the magnetic semiconductor (Ga,Mn)As

833 & 6 keV

Standing-wave photoemission combining soft and hard x-rays, depth-resolved composition, densities of states and ARPES, and magnetization:
$SrTiO_3/La_{2/3}Sr_{1/3}MnO_3$ multilayer
Fe/MgO tunnel junction

500-700 eV

Standing-waves in a photoelectron microscope, adding the third dimension:
multilayers and microdots

Conclusions and Future Outlook

Standing wave formation in reflection from a surface, or single-crystal Bragg planes⁺, or a multilayer mirror

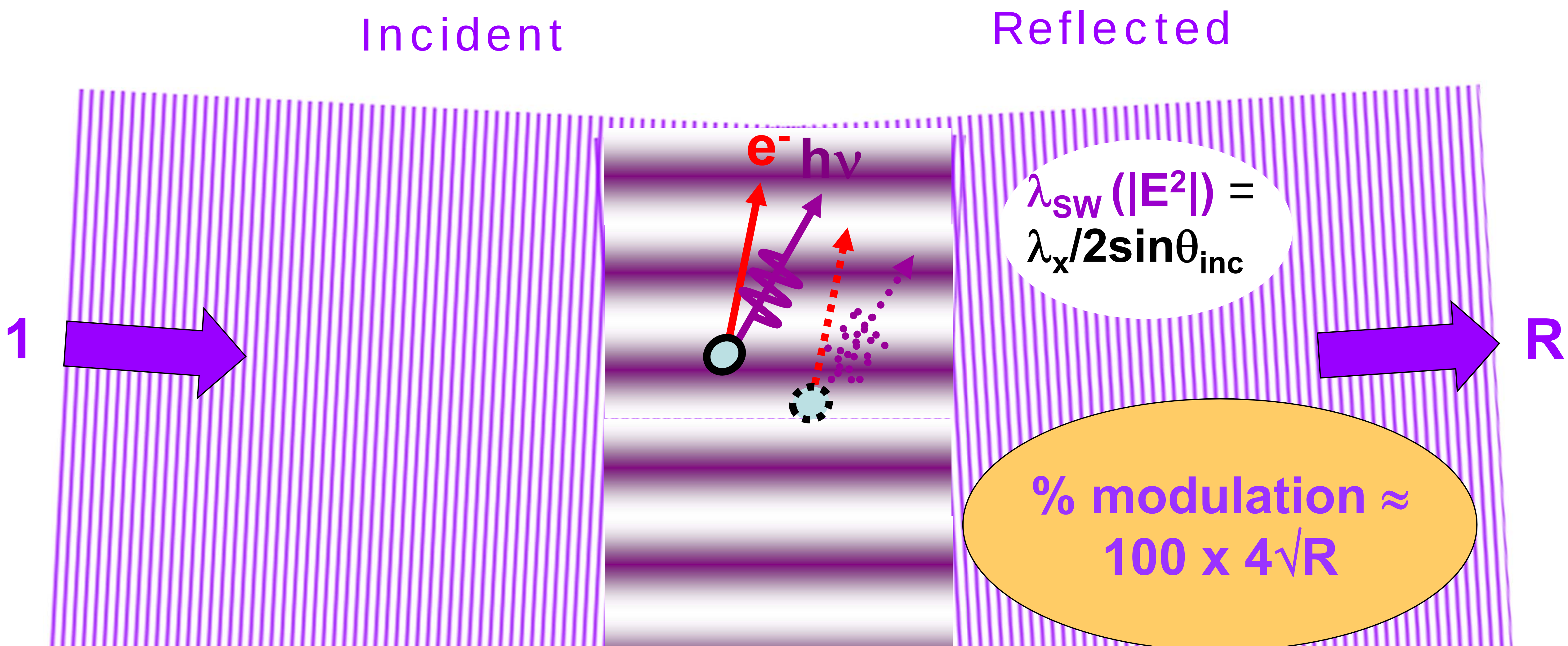

• **Rocking curve:**

$$I(\theta_{inc}) \propto 1 + R(\theta_{inc}) + 2\sqrt{R(\theta_{inc})}\, f \cos[\varphi(\theta_{inc}) - 2\pi P]$$

• **Photon energy scan:**

$$I(h\nu) \propto 1 + R(h\nu) + 2\sqrt{R(h\nu)}\, f \cos[\varphi(h\nu) - 2\pi P]$$

with: f = coherent fraction of atoms, P = phase of coherent-atom position

• ***Phase scan with wedge-shaped sample ("Swedge" method):***

Adding depth resolution to the photoelectron microscope via standing wave excitation

Spin-Polarized Photoelectron Microscope—BESSY, Berlin

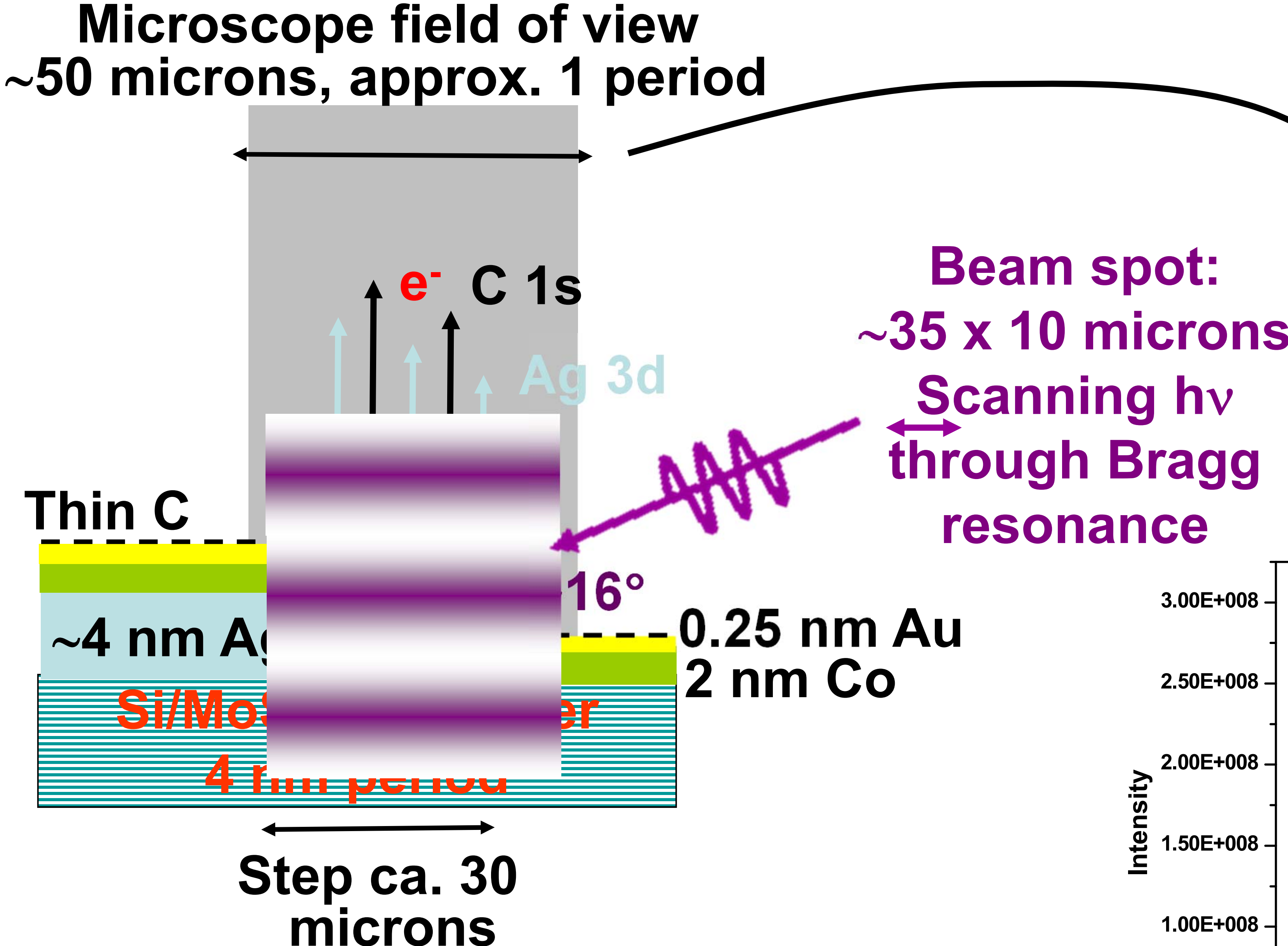

Imaging with element-specific photoelectron peaks

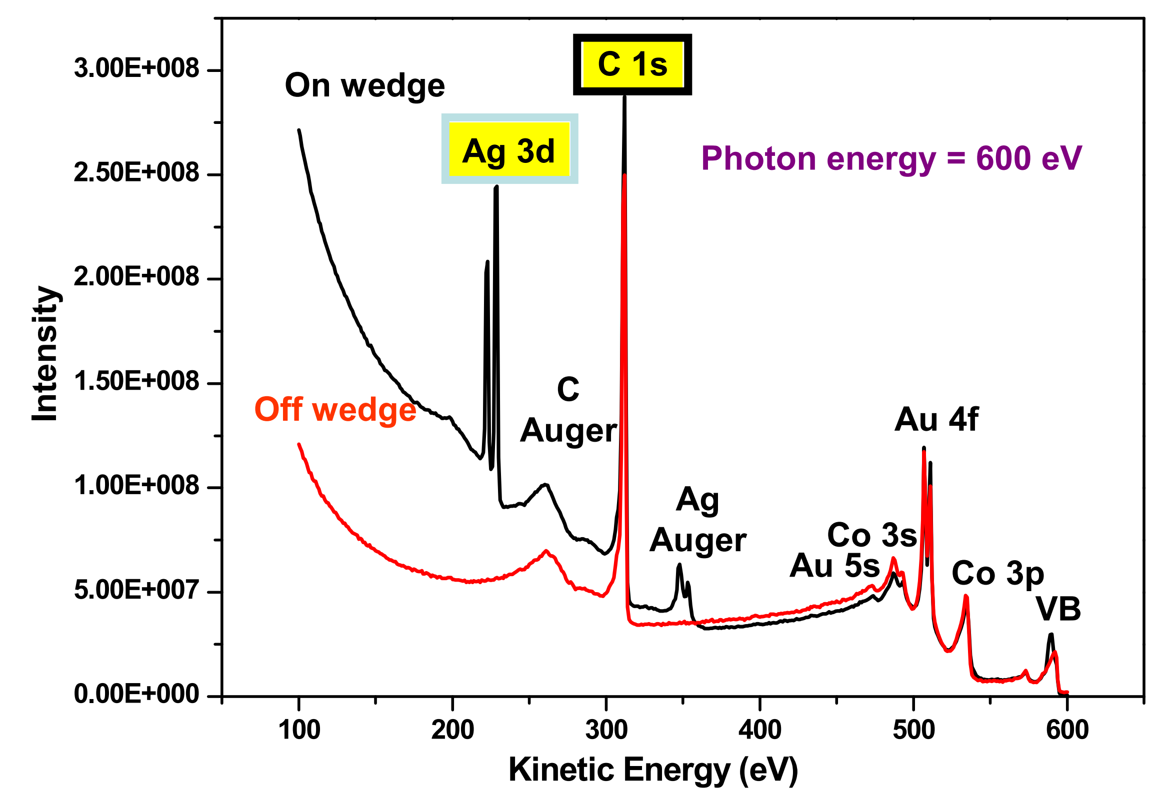

F. Kronast et al., Appl. Phys. Lett. 93, 243116 (2008)

Standing wave effects in a photoelectron microscope

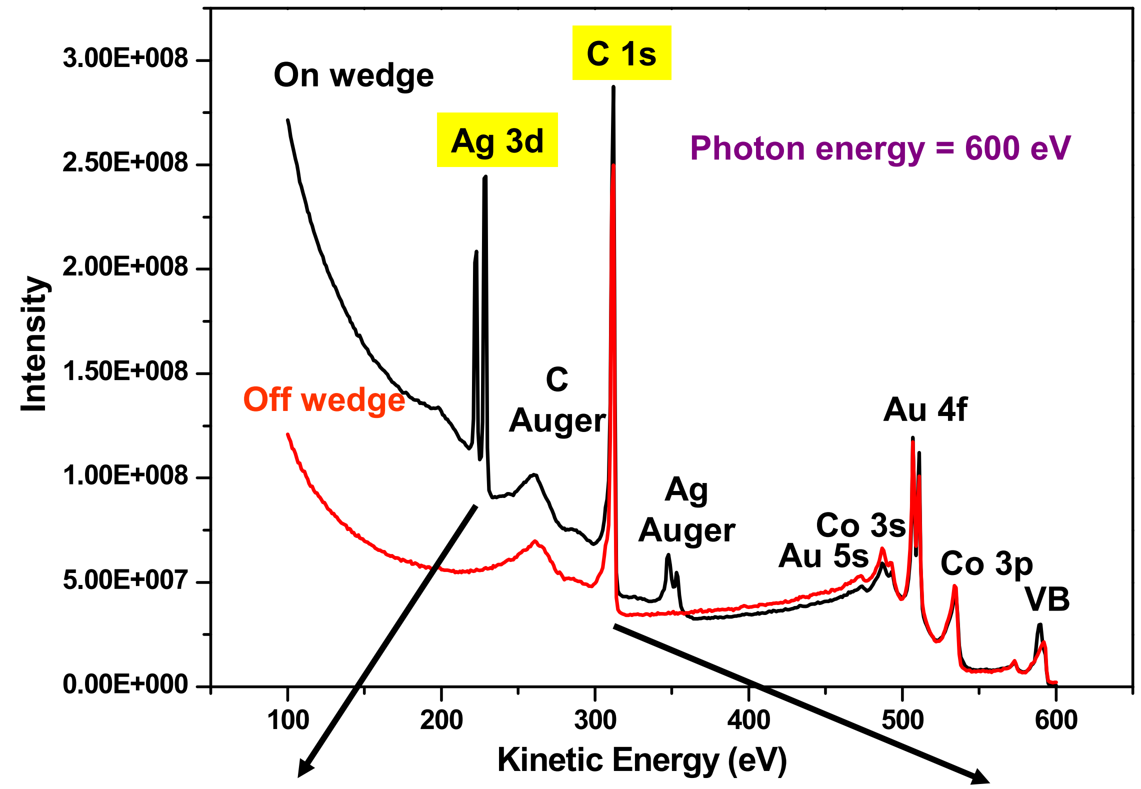

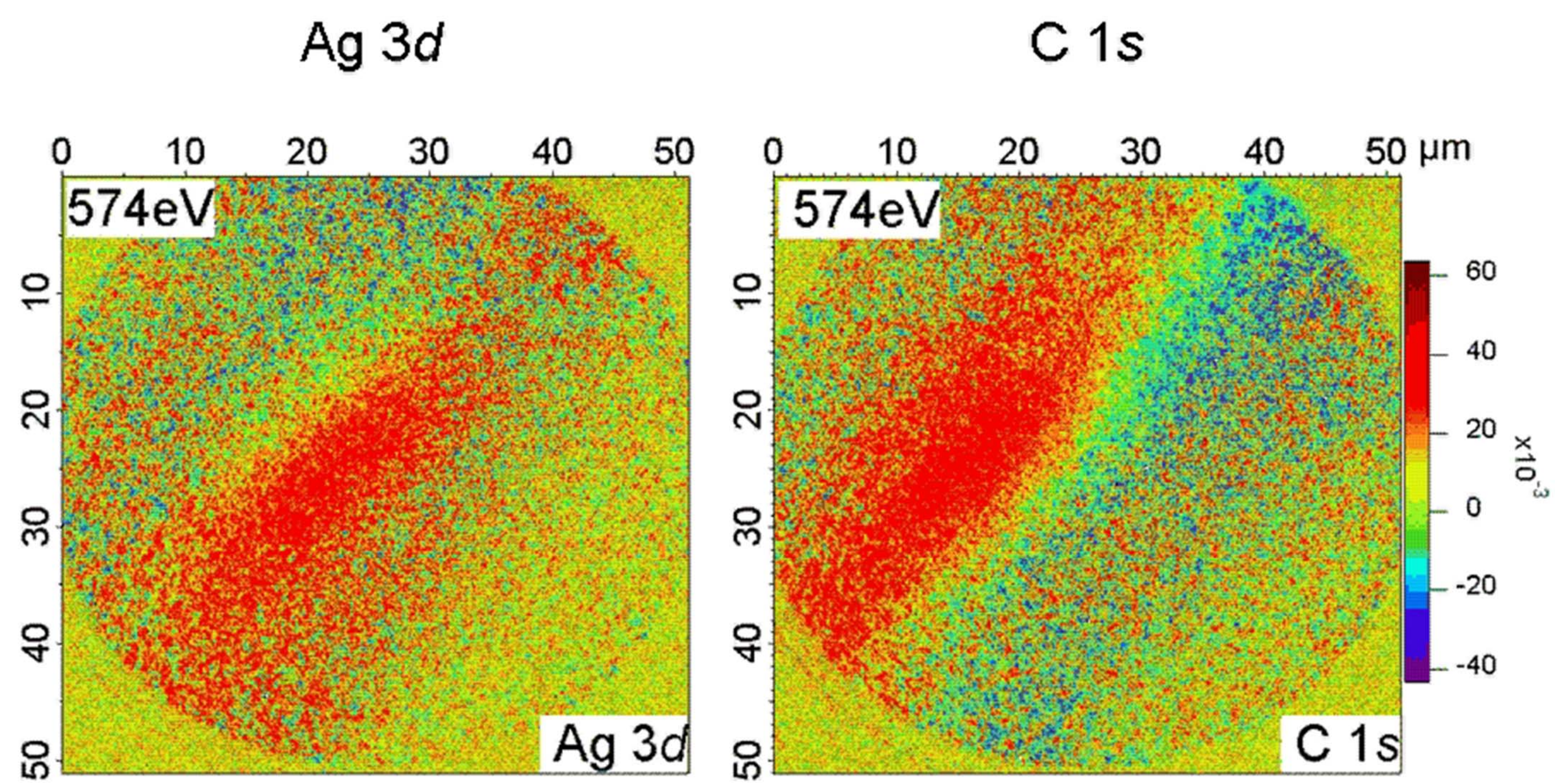

F. Kronast, H. Dürr, BESSY
D. Buergler, R. Scheiber, C. Schneider, Jülich
Yang, IBM, CF,
Appl. Phys. Lett. <u>93</u>, 243116 (2008)

Surfing the waves in a photoelectron microscope-1 μ Co nanodots

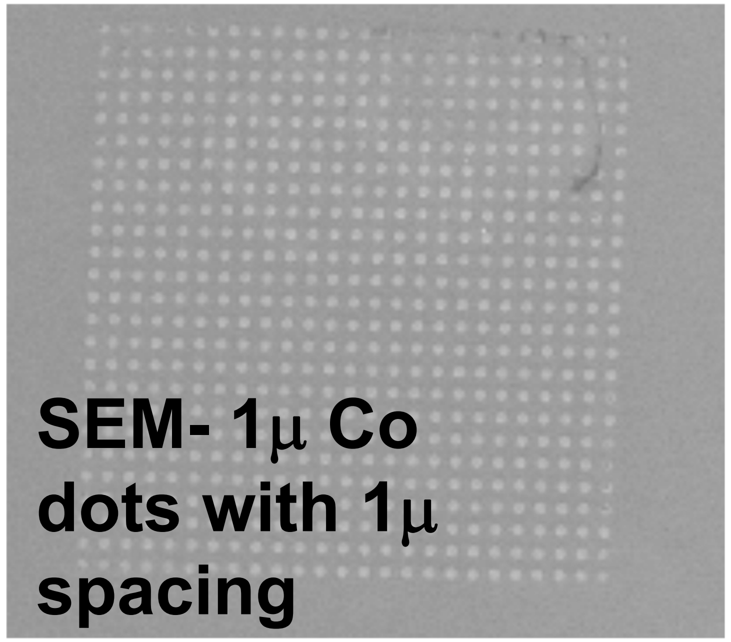

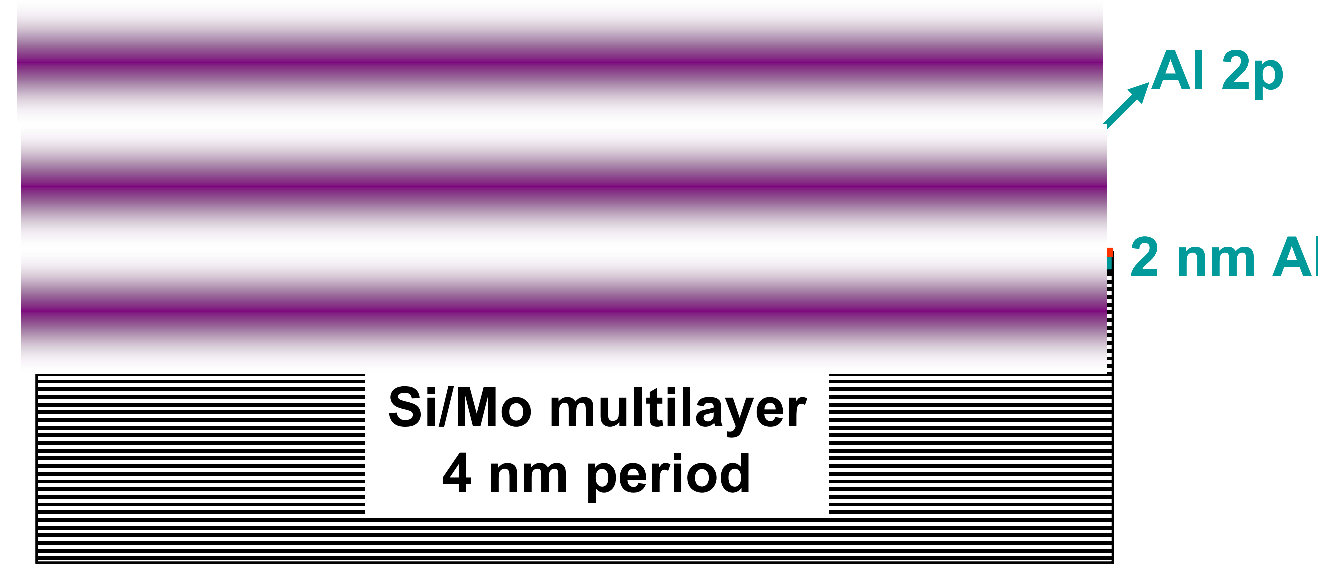

Photon energy scan through Bragg resonance: C 1s, Al 2p, Co 3p, and Si 2p images

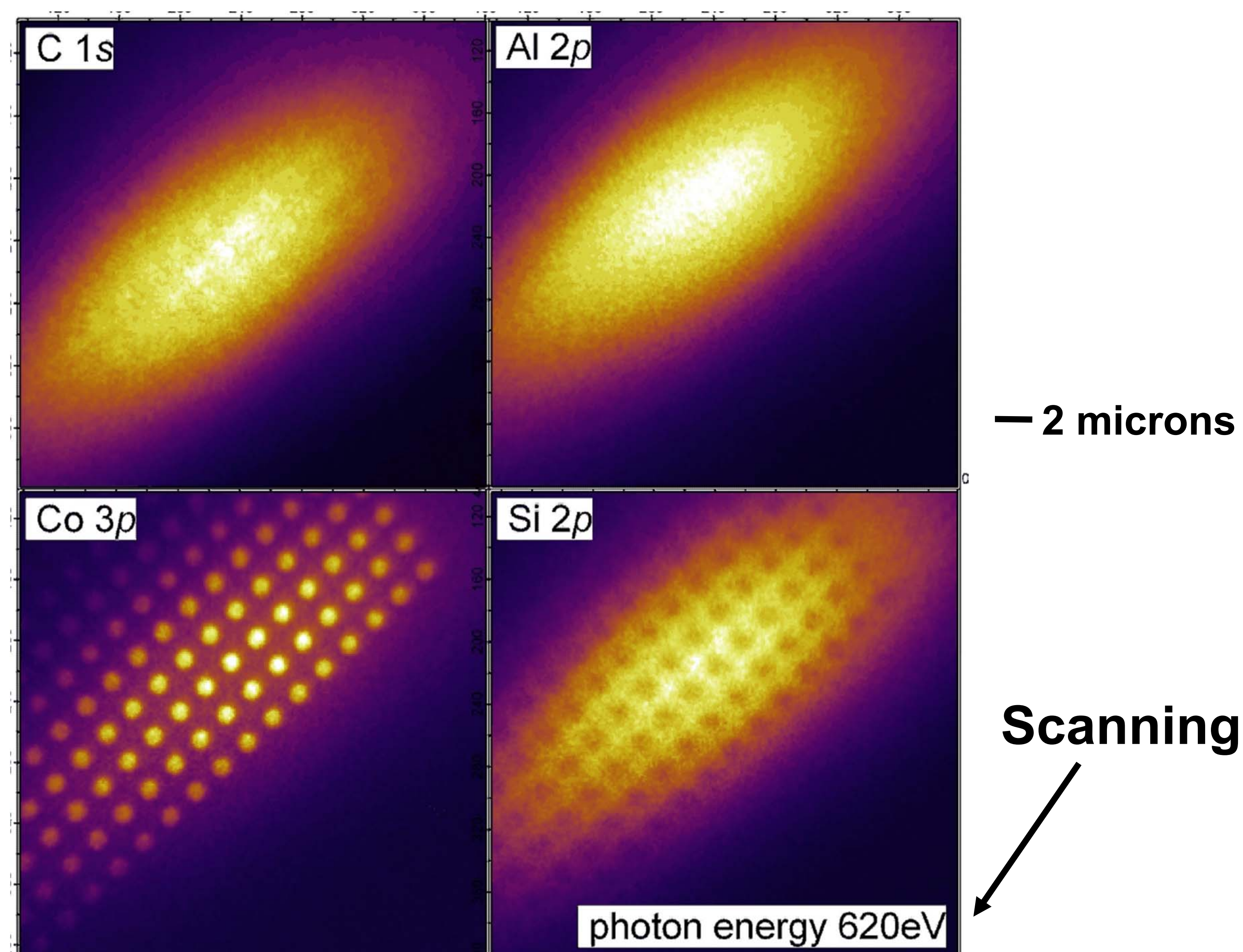

A. Gray, F. Kronast, C. Papp, et al., Appl. Phys. Lett. 97, 062503 (2010)-BESSY

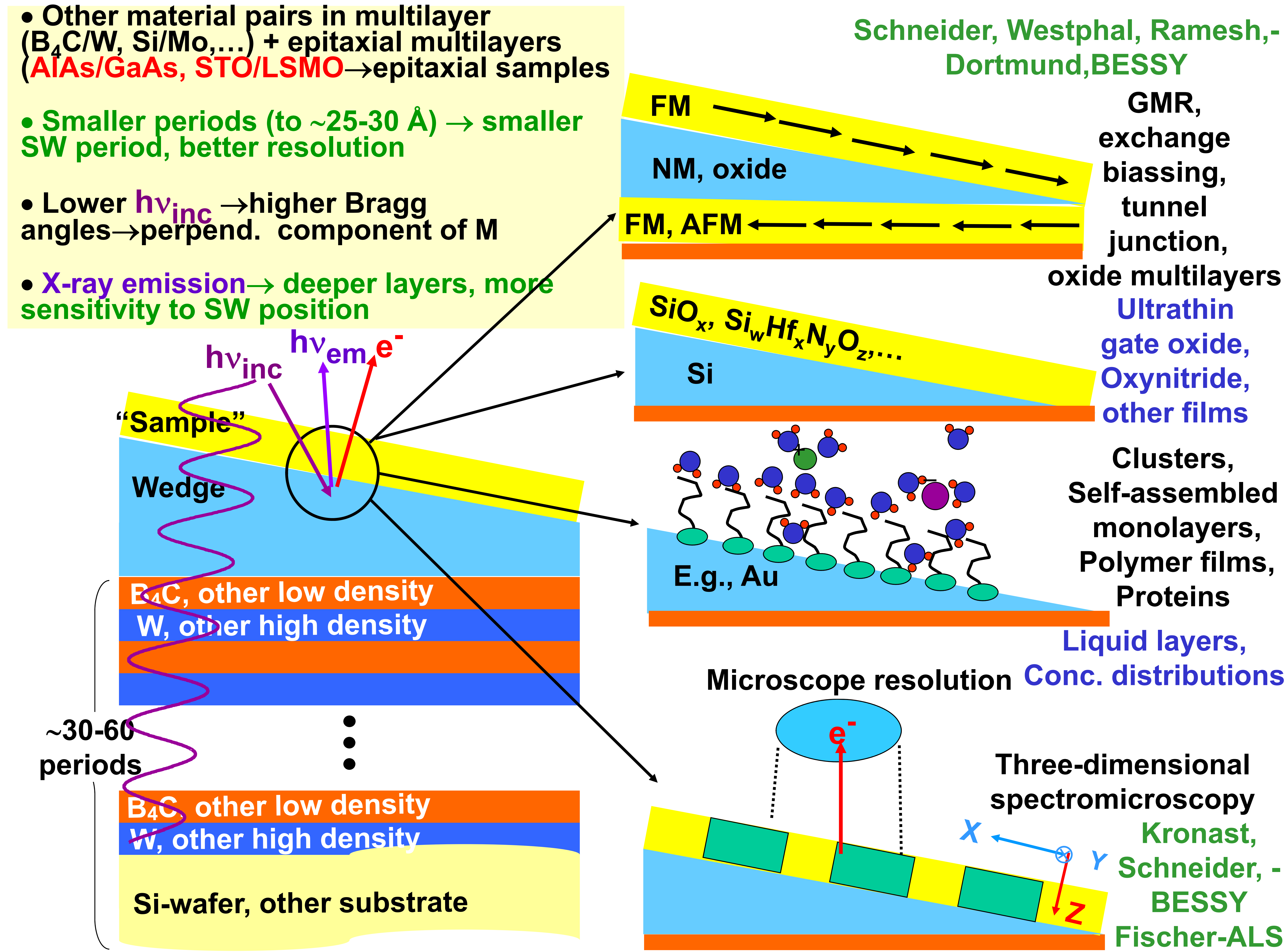
• Other material pairs in multilayer (B_4C/W, Si/Mo,…) + epitaxial multilayers (AlAs/GaAs, STO/LSMO→epitaxial samples
• Smaller periods (to ~25-30 Å) → smaller SW period, better resolution
• Lower $h\nu_{inc}$ →higher Bragg angles→perpend. component of M
• X-ray emission→ deeper layers, more sensitivity to SW position
Schneider, Westphal, Ramesh,- Dortmund,BESSY
FM
NM, oxide
FM, AFM
GMR, exchange biassing, tunnel junction, oxide multilayers
SiO_x, $Si_wHf_xN_yO_z$,…
Si
Ultrathin gate oxide, Oxynitride, other films
$h\nu_{inc}$
$h\nu_{em}$
e^-
"Sample"
Wedge
E.g., Au
Clusters, Self-assembled monolayers, Polymer films, Proteins
Liquid layers, Conc. distributions
B_4C, other low density
W, other high density
~30-60 periods
B_4C, other low density
W, other high density
Si-wafer, other substrate
Microscope resolution
e^-
Three-dimensional spectromicroscopy
X
Y
Z
Kronast, Schneider, - BESSY
Fischer-ALS

Outline

Photoemission: Some limitations, some new directions

6-8 keV

Hard x-ray photoemission of interesting bulk materials→core and valence spectra:
half-metallic/colossal magnetoresistive $La_{0.67}Sr_{0.33}MnO_3$
semiconducting CrAl alloy
metal-to-insulator transition in thin-film $LaNiO_3$

3.2 & 6 keV

Angle-resolved hard x-ray photoemission→HXPD: Kikuchi-band modeling, and HARPES for: W, GaAs & the magnetic semiconductor (Ga,Mn)As

833 & 6 keV

Standing-wave photoemission combining soft and hard x-rays→depth-resolved composition, densities of states and ARPES, and magnetization:
$SrTiO_3/La_{2/3}Sr_{1/3}MnO_3$ multilayer
Fe/MgO tunnel junction

500-700 eV

Standing-waves in a photoelectron microscope→adding the third dimension:
multilayers and microdots

Conclusions and Future Outlook

Conclusions and Future Outlook

→ ***Hard x-ray photoemission (HAXPES, HXPS) probes to average depths of ca. 50-100 Å, up to 10x typical XPS***

- **Bulklike composition and electronic structure, buried layers and interfaces, a rapidly growing aspect of photoemission: $La_{0.67}Sr_{0.33}MnO_3$--T dep. Electronic structure, CrAl semiconducting gap, $LaNiO_3$ thin-film metal-insulator transition**
- **Angle-resolved core-level (HXPD): new element-specific structure probe, with Kikuchi-band modeling, and bulk-sensitive valence-band mapping (HARPES) possible up to several keV: W, GaAs, GaMnAs. Should be applicable to many materials up to a few or more keV**

→ ***Excitation with <u>soft and hard x-ray</u> standing waves from multilayer Bragg reflections:***

- **Additional depth sensitivity in photoemission: ca. ±2-3 Å in concentration, core-level chemical shifts, and magnetization: $SrTiO_3/La_{0.67}Sr_{0.33}MnO_3$, Fe/MgO**
- **Depth-dependent densities of states and band structure (ARPES): $SrTiO_3/La_{0.67}Sr_{0.33}MnO_3$, Fe/MgO**
- **High sensitivity to properties of multilayer mirror: gradient in bilayer thicknesses of only ca. 6%, $SrTiO_3/La_{0.67}Sr_{0.33}MnO_3$**
- **Resonant excitation to enhance reflectivity and standing wave strength: $SrTiO_3/La_{0.67}Sr_{0.33}MnO_3$**
- **Additional depth sensitivity in photoelectron microscopy: Co/Ag bilayer and Co microdots**

→ ***Many future applications of both:*** **Complex and strongly correlated bulk materials, spintronics→tunnel junction-CoFeB/MgO (with Ohno), Mott oxide-$LaNiO_3/SrTiO_3$(with Stemmer), multiferroic- $BiFeO_3/SrTiO_3$ (with Huijben),…**

Recent overviews:

S.-H. Yang, B.C. Sell, and C.S.F., J. Appl. Phys. 103, 07C519 (2008)

C.S.F., Journal of Electron Spectrosc. 178–179, 2 (2010)

X-ray photoemission: some key elements